Synthetic studies of silver and gold complexes containing chalcogen donor ligands

Wiseman, Matthew Robert

Award date:
2001

Awarding institution:
University of Bath

SYNTHETIC STUDIES OF SILVER AND GOLD COMPLEXES CONTAINING CHALCOGEN DONOR LIGANDS

Submitted by ***MATTHEW ROBERT WISEMAN BSc(Hons)***

for the degree of ***DOCTOR OF PHILOSOPHY (PhD)***

At the ***UNIVERSITY OF BATH 2001***

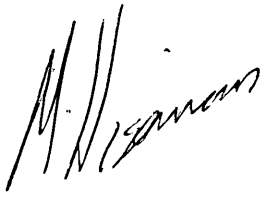

ProQuest LLC
789 East Eisenhower Parkway
P.O. Box 1346
Ann Arbor, MI 48106-1346

To Archibald Frank Mobbs

"Gold is the first of man's follies,

silver is the second"

Virgil's Aeneid 79 A.D.

"Discovery consists not in seeking new landscapes

but in having new eyes."

Marcel Proust

ACKNOWLEDGEMENTS

To Mum and Dad, thank you for your love, friendship and support.

There are many that have influenced and supported me during the course of my postgraduate experience. They have endured the highs and lows of my journey, and enabled me to complete my study in one piece. I will look back on this and remember a happy time.

To everyone from BUSU past and present, thanks for expanding my horizons. To Ruth and Jayne, thanks for listening. To Mike, my brother in all but blood, I miss you man! To Roberto, you have taught me more than you will ever know. To Carys, there is no one I enjoy laughing with more. Amanda, John, Jenny and Nick, you supported me at a time when I needed my friends most, you're the best! To Noel and June for giving me a reason to get up at 7am every Friday.

Specials thanks to Dr. Peter Bishop and Dr. Patsy Marsh at Johnson Matthey Plc. for their time and knowledge. Thanks to the rest of the Brisdon group, Tim, Jim, Mike and Virginie who have made lab and office life more interesting and to the rest of the Inorganic section, staff and students. Gratitude is owed to all the technical and support staff who hold the department together.

There is one person who I must thanks above all others. He has been my advisor, counsel and friend. Without whom this document would have been merely a dream. His integrity and strength have ensured that I, and so many other students have achieved our goals. To Professor Brian Brisdon, Thank you and enjoy your retirement.

ABSTRACT

The work described in this Thesis has focused on the study of the chemistry of silver with oxygen donor ligands and of gold with oxygen and sulphur donors, in order to extend the comparative chemistry of these two metals with hard and soft donor ligands. The properties of the coinage metals and the concepts that have a major influence on their chemistry are outlined early in this Thesis. A survey of the structural chemistry of silver(I) and gold(I) complexes of oxygen and sulphur donor ligands is also included.

The reactions of silver(I) salts, $AgBF_4$, $AgPF_6$, $AgOSO_2CF_3$, $AgNO_3$, AgO_2CMe, AgO_2CCF_3 and AgO_2CPh with the crown-ethers 12-crown-4, 15-crown-5, 18-crown-6, benzo-18-crown-6 and dibenzo-18-crown-6 were investigated. All products, **C1 – C17**, are of the type $[Ag(Y)_a(H_2O)_b(X)]$ (Y= crown-ether, a = 1 or 2, b = 0 or 1, X = counter-ion) and were characterised by characterised by IR and elemental analysis. The solid-state structures of [Ag(15-crown-5)(H_2O)(15-crown-5)][PF_6], **C6**, [Ag(15-crown-5)(OTf)], **C7,** [Ag(15-crown-5)(NO_3)], **C8**, [Ag(18-crown-6)(OTf)], **C11**, [Ag(benzo-18-crown-6)(OTf)], **C13**, and $[Ag(dibenzo\text{-}18\text{-}crown\text{-}6)(OH_2)]^+[OTf]^-.0.5CH_2Cl_2$, **C15,** (OTf = triflate) have been determined by X-ray Crystallography. Selected complexes have also been studied by ^1H and ^{13}C-NMR, and thermal gravimetric analysis (TGA).

Homoleptic gold(I) thiolates, $[Au(SR)]_n$, **G1-G10** were prepared by the reaction of the aryl thiols HSC_6H_4R (R = H, *p*-CMe_3, *o*-CMe_3, *o*-CF_3, *m*-CF_3, *p*-CF_3, *o*-OMe, *m*-OMe, *p*-OMe, and $HSC_{10}H_7$) with $[Au(HO_2CCH(NH_2)(CH_2)_3SCH_3)Cl]$, **R1**. Complexes were characterised by IR, TGA and elemental analysis. $[Au(SC_6H_4\text{-}p\text{-}CMe_3)]_{10}$, **G1**, and $[Au(SC_6H_4\text{-}o\text{-}CMe_3)]_{12}$, **G2**, were studied by Mass Spectrometry, X-ray Crystallography, Raman Spectrometry, ^1H and ^{13}C NMR and were shown to be rare examples of inorganic

[2]catenanes containing multi-auriophilic interactions. Reaction of **G1 – G10** with triphenylphosphine afforded [Au(PPh_3)(SR)], **P1 – P10**, which were isolated and characterised by IR, elemental analysis, TGA, ^1H and ^{13}C-NMR. Solid-state structures of [Au(PPh_3)(SC_6H_4-*p*-CMe_3)], **P1** and [Au(PPh_3)(SC_6H_4-*o*-CF_3)], **P4**, were determined by X-ray Crystallography. Products of the reactions of dipyridyldisulphide, $(PyS)_2$, with gold(III) are also discussed.

The Thesis also includes an account of a brief study of the reactivity of gold(I) and gold(III) derivatives toward anionic and neutral oxygen donor ligands. No reaction occurred between 12-crown-4, 15-crown-5 or 18-crown-6 and either hydrated $H[Au(NO_3)_4]$ or $[(C_5H_{10}S)AuCl]$. Metathetical reactions between Na^+OR^- {R = Me, Et, CMe_3, Ph, C_6H_4-*p*-CMe_3, and C_6H_4-*o*-CMe_3} [Au(PPh_3)Cl], **R3**, were explored. The phenoxide [Au(PPh_3)(OPh)].$0.5H_2O$, **A1**, was an expected product and [Au(PPh_3)(OH)], **A2**, an unexpected product of these reactions. Both were characterised by IR, elemental analysis and ^1H NMR. An unsuccessful attempt to prepare a gold silsesquioxide derivative of $[(Cy)_7Si_7O_9(OH)_3]$ is also summarised.

The experimental techniques and preparative procedures employed during this research, together with publications and presentations given during the course of study, are also noted at the end of the Thesis.

LIST OF ABBREVIATIONS

Aldrithiol	Dithiopyridine, $(H_5C_5NS)_2$
Å	Angstrom
OAc	Acetate
Br	Broad
Bu^n	*n*-butyl, $CH_2CH_2CH_2CH_3$
Bu^t	*tert*-butyl, $C(CH_3)_3$, CMe_3
Cy	Cyclohexyl
d	Doublet
DCM	Dichloromethane
dppf	diphenylphosphinoferrocene
δ	Chemical Shift
Et	Ethyl
FAB	Fast Atom Bombardment
FT	Fourier Transform
HSAB	Hard-Soft Acid-Base Concept
Hz	Hertz
IR	Infra-Red (spectroscopy)
m	Meta
m	Multiplet
m/e	Mass to charge ratio
MS	Mass Spectrometry
Me	Methyl
Naph	Naphthyl

NMR	Nuclear Magnetic Resonance
OTf	Triflate, SO_3CF_3
o	Ortho
p	Para
ppm	Parts per million
Ph	Phenyl
Pr^n	*n*-Propyl
Pr^i	*Iso*-Propyl, $CH_2(CH_3)$
Py	Pyridyl
q	Quartet
R	Alkyl
RMM	Relative Molecular Mass
RTP	Room temperature (298 K) and pressure (1 atm)
TGA	Thermal Gravimetric Analysis
THF	Tetrahydrofuran
THT	Tetrahydrothiophene
TMS	Tetramethylsilane
t	Triplet
wt	Weight

12-crown-4

(1,4,7,10-tetraoxacyclododecane)

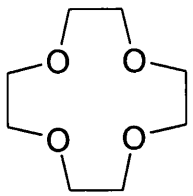

15-crown-5

(1,4,7,10,13-pentaoxacyclopentadecane)

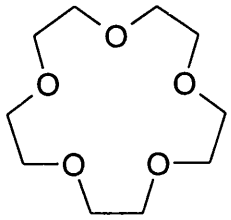

18-crown-6

(1,4,7,10,13,16-hexaoxacyclooctadecane)

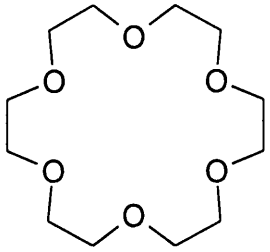

benzo-18-crown-6

(2,3-benzo-1,4,7,10,13,16-hexaoxacycloocta-decane)

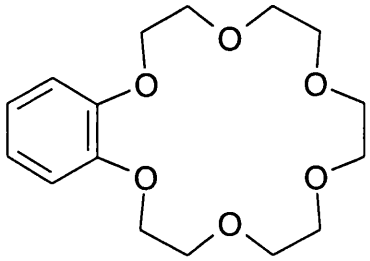

dibenzo-18-crown-6

(2,3,11,12-dibenzo-1,4,7,10,13,16-hexaoxacyclo-octadecane)

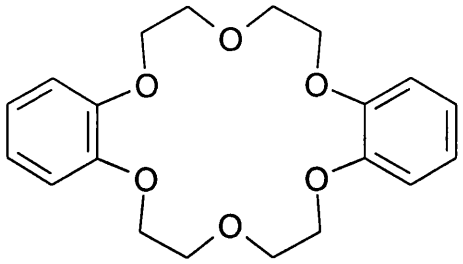

1,1-dimethylsila-11-crown-4

(1,1-dimethyl-1-sila-2,5,8,11-tetraoxacyclo-undecane)

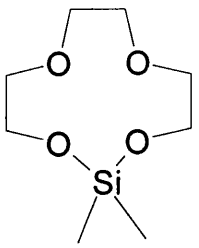

KEY TO COMPOUNDS

R1	$[Au(HO_2CCH(NH_2)CH_2CH_2CH_2SCH_3)Cl]$
R2	[Au(THT)Cl]
R3	$[Au(PPh_3)Cl]$
R4	$[(Cy)_6Si_6O_9]$
R5	$[(Cy)_7Si_7O_9(OH)_3]$
R6	$[(Cy)_7Si_7O_{12}P]$
C1	$[Ag(12\text{-crown-}4)_2][BF_4]$
C2	$[Ag(12\text{-crown-}4)_2][PF_6]$
C3	$[Ag(12\text{-crown-}4)_2][OTf].H_2O$
C4	$[Ag(12\text{-crown-}4)][NO_3].H_2O$
C5	$[Ag(15\text{-crown-}5)][BF_4].H_2O$
C6	$[Ag(15\text{-crown-}5)(H_2O)(15\text{-crown-}5)][PF_6]$
C7	[Ag(15-crown-5)(OTf)]
C8	$[Ag(15\text{-crown-}5)(NO_3)]$
C9	$[Ag(18\text{-crown-}6)][BF_4]$
C10	$[Ag(18\text{-crown-}6)][PF_6].0.5(18\text{-crown-}6)$
C11	[Ag(18-crown-6)(OTf)]
C12	$[Ag(18\text{-crown-}6)(NO_3)]$
C13	[Ag(benzo-18-crown-6)(OTf)]
C14	$[Ag(benzo\text{-}18\text{-crown-}6)(NO_3)]$
C15	[Ag(dibenzo-18-crown-6)(OTf)]
C15a	$[Ag(dibenzo\text{-}18\text{-crown-}6)(H_2O)][OTf].0.5CH_2Cl_2$
C16	$[Ag(dibenzo\text{-}18\text{-crown-}6)][NO_3]$
C17	$[Ag(1,1\text{-dimethylsila-}11\text{-crown-}4)][BF_4]$

G1	$[Au(SC_6H_4\text{-}p\text{-}Bu^t)]_{10}$
G1a	$[Au(SC_6H_4\text{-}p\text{-}Bu^t)]_{10}.0.8C_6H_5OC_2H_5$
G2	$[Au(SC_6H_4\text{-}o\text{-}Bu^t)]_{12}$
G2a	$[Au(SC_6H_4\text{-}o\text{-}Bu^t)]_{12}.2C_6H_5OC_2H_5$
G3	$[Au(SPh)]_n$
G4	$[Au(SC_6H_4\text{-}o\text{-}CF_3)]_n$
G5	$[Au(SC_6H_4\text{-}m\text{-}CF_3)]_n$
G6	$[Au(SC_6H_4\text{-}p\text{-}CF_3)]_n$
G7	$[Au(SC_6H_4\text{-}o\text{-}OMe)]_n$
G8	$[Au(SC_6H_4\text{-}m\text{-}OMe)]_n$
G9	$[Au(SC_6H_4\text{-}p\text{-}OMe)]_n$
G10	$[Au(SNaph)]_n$
G11	"$[AuCl_2SNC_5H_5]$"
P1	$[Au(PPh_3)(SC_6H_4\text{-}p\text{-}Bu^t)]$
P2	$[Au(PPh_3)(SC_6H_4\text{-}o\text{-}Bu^t)]$
P3	$[Au(PPh_3)(SPh)]$
P4	$[Au(PPh_3)(SC_6H_4\text{-}o\text{-}CF_3)]$
P5	$[Au(PPh_3)(SC_6H_4\text{-}m\text{-}CF_3)]$
P6	$[Au(PPh_3)(SC_6H_4\text{-}p\text{-}CF_3)]$
P7	$[Au(PPh_3)(SC_6H_4\text{-}o\text{-}OMe)]$
P8	$[Au(PPh_3)(SC_6H_4\text{-}m\text{-}OMe)]$
P9	$[Au(PPh_3)(SC_6H_4\text{-}p\text{-}OMe)]$
P10	$[Au(Ph_3P)(Snaph)]$
A1	$[Au(PPh_3)(OPh)].H_2O$
A2	$[Au(PPh_3)(OH)]$

TABLE OF CONTENTS

ACKNOWLEDGEMENTS *v*

ABSTRACT *vi*

ABBREVIATIONS *viii*

KEY TO COMPOUNDS *xi*

CONTENTS *xiii*

CHAPTER ONE: INTRODUCTION 1

OVERVIEW 1

SCOPE OF REVIEW 3

SECTION ONE: GENERAL PROPERTIES OF THE COINAGE METALS 4

1.1.1 ATOMIC PROPERTIES 4

1.1.2 OXIDATION STATES AND CO-ORDINATION NUMBERS 5

1.1.3 RELATIVISTIC EFFECTS 8

1.1.4 SECONDARY BONDING 9

1.1.5 HARD-SOFT ACID-BASE PRINCIPLE 13

SECTION TWO: THE STRUCTURAL CHEMISTRY OF SILVER(I) AND GOLD(I) WITH OXYGEN AND SULPHUR DONORS 16

1.2.1 SUMMARY 16

1.2.2 COMPLEXES OF SILVER(I) CONTAINING OXYGEN-DONOR LIGANDS 17

1.2.2.1 ANIONIC OXYGEN DONOR LIGANDS 17

1.2.2.2 NEUTRAL OXYGEN DONOR LIGANDS 23

1.2.3 COMPLEXES OF GOLD(I) CONTAINING OXYGEN-

DONOR LIGANDS 29

1.2.4 COMPLEXES OF SILVER(I) CONTAINING SULPHUR-DONOR LIGANDS 33

1.2.4.1 ANIONIC SULPHUR DONOR LIGANDS 34

1.2.4.2 NEUTRAL SULPHUR DONOR LIGANDS 36

1.2.5 COMPLEXES OF GOLD(I) CONTAINING SULPHUR-DONOR LIGANDS 38

1.3 CONCLUSIONS 46

1.4 REFERENCES 47

CHAPTER TWO: CROWN-ETHER COMPLEXES OF SILVER(I) SALTS 54

2.1 INTRODUCTION 54

2.2 SYNTHESIS AND PROPERTIES 56

2.3 CHARACTERISATION 58

2.3.1 ^{1}H-NMR AND ^{13}C-NMR SPECTROSCOPY 60

2.3.2 THERMAL GRAVIMETRIC ANALYSIS 61

2.3.3 SOLID-STATE STRUCTURAL STUDIES 63

2.3.3.1 STRUCTURAL COMPARISON OF 15-CROWN-5 DERIVATIVES OF THREE SILVER SALTS 63

2.3.3.2 STRUCTURAL COMPARISON OF CROWN-ETHER DERIVATIVES OF SILVER TRIFLATE 77

2.4 CONCLUSIONS 88

2.5 REFERENCES 90

CHAPTER THREE: HOMOLEPTIC GOLD(I) THIOLATES AND THEIR TRIPHENYLPHOSPHINE DERIVATIVES 92

3.1 INTRODUCTION 92

3.2 HOMOLEPTIC GOLD(I) THIOLATES 94

3.2.1 SYNTHESIS AND PROPERTIES 94

3.2.2 CHARACTERISATION 96

3.2.2.1 SOLID-STATE STUDIES 97

3.2.2.2 ^{1}H AND ^{13}C NMR SPECTROSCOPY 107

3.2.2.3 MASS SPECTROMETRY 112

3.2.2.4 RAMAN SPECTROSCOPY 114

3.2.2.5 THERMAL GRAVIMETRIC ANALYSIS 116

3.3 TRIPHENYLPHOSPHINE GOLD(I) THIOLATES 119

3.3.1 SYNTHESIS AND PROPERTIES 119

3.3.2 CHARACTERISATION 121

3.3.2.1 SOLID-STATE STUDIES 121

3.3.2.2 THERMAL GRAVIMETRIC ANALYSIS 130

3.4 2,2'-DITHIOPYRIDINE REACTIONS 132

3.5 CONCLUSIONS 133

3.6 REFERENCES 134

CHAPTER FOUR: CHEMISTRY OF GOLD WITH OXYGEN DONOR LIGANDS 136

4.1 INTRODUCTION 136

4.2 ATTEMPTED PREPARATIONS OF CROWN-ETHER COMPLEXES OF GOLD 139

4.3	**GOLD(I) COMPLEXES OF ANIONIC OXYGEN DONORS**	**141**
	4.3.1 ATTEMPTED PREPARATIONS OF HOMOLEPTIC GOLD(I) COMPLEXES	**141**
	4.3.2 PREPARATIONS OF TRIPHENYLPHOSPHINE GOLD(I) ALKOXIDES AND PHENOXIDES	**141**
4.4	**REACTIONS OF GOLD(I) AND GOLD(III) WITH A SILASESQUIOXANES**	**143**
4.5	**CONCLUSIONS**	**145**
4.6	**REFERENCES**	**146**
CHAPTER FIVE: EXPERIMENTAL		**148**
5.1	**INTRODUCTION**	**148**
5.2	**SYNTHETIC TECHNIQUES**	**148**
	5.2.1 SAFETY	**148**
	5.2.2 GENERAL REACTION PROCEDURES	**148**
	5.2.3 REAGENTS	**149**
	5.2.4 SOLVENTS	**149**
	5.2.5 ANALYTICAL TECHNIQUES	**149**
5.3	**PREPARATIONS OF CROWN ETHER CONTAINING SILVER(I) COMPLEXES**	**151**
	5.3.1 GENERAL PROCEDURE	**151**
	5.3.2 CHARACTERISATION	**153**
5.4	**HOMOLEPTIC GOLD(I) THIOLATES AND THEIR TRIPHENYLPHOSHINE DERIVATIVES**	**159**

5.4.1 STARTING MATERIALS 159

5.4.2 HOMOLEPTIC GOLD(I) THIOLATES 160

5.4.3 TRIPHENYLPHOSPHINE GOLD(I) THIOLATES 165

5.4.4 GOLD – 2,2'-DITHIODIPYRIDINE REACTIONS 170

5.5 CHEMISTRY OF GOLD WITH OXYGEN DONOR LIGANDS 171

5.5.1 SUMMARY 171

5.5.2 STARTING MATERIALS 171

5.5.3 ATTEMPTED PREPARATIONS OF CROWN-ETHER COMPLEXES OF GOLD 173

5.5.4 GOLD(I) COMPLEXES OF ANIONIC OXYGEN DONORS 174

5.5.4.1 ATTEMPTED PREPARATIONS OF HOMOLEPTIC GOLD(I) COMPLEXES 174

5.5.4.2 PREPARATION OF TRIPHENYLPHOSPHINE GOLD(I) ALKOXIDES AND PHENOXIDES 174

5.5.5 ATTEMPTED REACTIONS OF GOLD WITH A SILSESQUIOXANE 177

5.6 REFERENCES 178

CHAPTER SIX: CONCLUSIONS AND FUTURE STUDY 179

6.1 INTRODUCTION 179

6.2 CROWN ETHER COMPLEXES OF SILVER(I) SALTS 179

6.3 HOMOLEPTIC GOLD(I) THIOLATES AND THEIR TRIPHENYLPHOSPHINE DERIVATIVES 181

6.4 CHEMISTRY OF GOLD WITH OXYGEN DONOR LIGANDS 182

APPENDIX ONE: X-RAY CRYSTALLOGRAPHIC DATA ON COMPOUNDS C6, C7, C8, C11, C13, AND C15 **183**

APPENDIX TWO: X-RAY CRYSTALLOGRAPHIC DATA ON COMPOUNDS G1, G2, P1 AND P4 **198**

APPENDIX THREE: PUBLICATIONS AND PRESENTATIONS **214**

CHAPTER ONE: INTRODUCTION

OVERVIEW

From the beginning to the end of the first millennium only four transition metals were known, copper, iron, silver and gold. Indeed it was not until the 18th century that more were isolated. The significance of these four metals not only in chemistry but also in the development of our society cannot be underestimated. Each element has performed an important role ever since.

Iron and copper have many essential uses, from the iron in the steel that is used in almost every car, ship and aeroplane, to the copper that carries the gas around our houses and the electricity to our computers. These two elements have been crucial to the development of technology, transport and communication.

Yet it is silver and gold that the average person would hold in much higher esteem; but not because of the vital role that they play in our lives. The reverse is true. The majority of gold that has been mined is stored as bullion in vaults under Manhattan Island or in countless other banks around the globe. Gold immediately creates an image of glamour, wealth and prosperity. Silver and gold are considered "precious metals" and held symbolically within most societies as elements to be cherished, and in some cases worshiped. The ownership of these elements is still a measure of great personal and national prestige.

Figure 1.1 The diamond encrusted gold wedding band. A symbol of love and commitment, or a simple combination of Au and C?

All three coinage metals (copper, silver and gold) were known to ancient civilisations. Copper was first extracted as an ore 5500 years ago, and it was soon discovered that it could be hardened with a little tin to form bronze. Silver was being mined in Asia Minor in 3000 BC and was used primarily as coinage. The use of gold dates back to before 3400 BC when the Egyptians introduced the first gold coins. Even in 2500 BC the Chinese were using gold "medicines". The current names of these three elements are derived from their ancient names; copper from 'cuprum', the Latin name for Cyprus, silver from the Anglo-Saxon 'seolfur' meaning silver, and gold from the same Anglo-Saxon word for the metal.

Copper is a reddish-gold colour and it is the most common (50 ppm of the earth's crust) and least valued of the coinage metals. Silver is white and metallic in colour, and its many uses include jewellery, tableware, and photography. Gold, the "king" of metals, has a characteristic yellow colour, is chemically unreactive and is used in jewellery, electronics and to decorate ceramics. All three metals are highly conducting and silver is the most conducting of all metals (429 $Wm^{-1}K^{-1}$ at 300 K) and has the least electrical resistance (1.59 x 10^{-8} Ωm at 293 K). Each metal is malleable and gold is the most malleable of the transition metals.

Figure 1.2 The visual representations of Cu, Ag and Au. (Images © Murray Robertson 1999)

The chemistry of copper and silver is well established, yet that of gold had been comparatively neglected until the mid 20th century. In recent times we have seen the

science of gold, described as "the sleeping beauty" by H. Schmidbaur, develop in catalysis[1ab], and medicine[2abc].

SCOPE OF REVIEW

The majority of the literature coverage and practical research carried out in this project has been devoted to the chemistry of silver(I) and gold(I) with oxygen and sulphur donor ligands. However an understanding of the differences in the chemistry of these two metals cannot be achieved without first appreciating some basic concepts as well as the properties of the elements themselves.

In **Section One** of this chapter the atomic properties of the coinage metals (Cu, Ag and Au) will be introduced and rationalised by consideration of a number of chemical concepts, including the Hard-Soft Acid-Base principle first elucidated by Pearson[3], and the relativistic effect which is of particular importance for gold.

Section Two of this chapter provides an introduction to the structural chemistry of Ag(I) and Au(I) with oxygen and sulphur donor ligands.

SECTION ONE: THE GENERAL PROPERTIES OF THE COINAGE METALS

1.1.1 ATOMIC PROPERTIES

Copper, silver and gold each possess a single valence *s* electron and a completed *d* shell, but there are major differences between the chemistries of these elements that arise primarily from their different electronic configurations, Table 1.1 and Figure 1.3

Atomic Properties		Cu	Ag	Au
Atomic Number		*29*	*47*	*79*
R.A.M		*63.55*	*107.87*	*196.97*
Electronic Configuration		*$[Ar]3d^{10}4s^1$*	*$[Kr]4d^{10}5s^1$*	*$[Xe]4f^{14}5d^{10}6s^1$*
Effective Nuclear Charge (Clementi)		*5.8*	*8.0*	*10.9*
Ionisation Energy ($kJ\ mol^{-1}$)	*1^{st}*	*746*	*731*	*890*
	2^{nd}	*1958*	*2073*	*1980*
	3^{rd}	*3554*	*3361*	*2900*
Reduction Potential, E° (V)	*0 - I*	*0.52*	*0.7991*	*1.83*
	I - III		*1.670*	*1.36*
	0 - III			*1.52*
Electron Affinity ($kJ\ mol^{-1}$)		*119*	*126*	*223*
Electronegativity (Pauling)		*1.9*	*1.9*	*2.4*
Isotopic Composition (% abundance)		*^{63}Cu (69.17)*	*^{107}Ag (51.83)*	*^{197}Au (100)*
		^{65}Cu (30.83)	*^{109}Ag (48.17)*	
Nuclear Spin (I)		*^{63}Cu – 3/2*	*^{107}Ag - 1/2*	*^{197}Au - 3/2*
		^{65}Cu – 3/2	*^{109}Ag - 1/2*	
Atomic Radius (Å)		*1.28*	*1.44*	*1.44*
Covalent Radius (Å)		*1.17*	*1.34*	*1.34*
Ionic Radius (Å)	*M^+*	*0.96*	*1.13*	*1.37*

Table 1.1 The atomic properties of the Group 11 metals[4]

All three metals are stable in pure dry air and occur naturally in the metallic state. There is little difference in the first ionisation energies of copper and silver, whereas that of gold is appreciably larger. This is an important factor in explaining the relative inertness of Au metal compared with that of Cu, which forms Cu_2O in air at elevated temperature, and that of both Cu and Ag which are attacked by sulphur. The effective nuclear charges increase steadily down the group; the electron affinity and electronegativity of Au are the highest of all the metals and Au has a comparable electronegativity to that of iodine ($E.N._{.pauling}$ (I) = 2.5). Thus gold can be reduced to Au(-1) in liquid ammonia to form $[Au(NH_3)]_n^-$. In addition Cs^+Au^- is well known and adopts the CsCl structure, in which Au^- acts as a pseudohalogen and has eight near neighbour Cs^+ ions.

Both the atomic and covalent radii of Ag and Au are extremely similar and significantly larger than those of Cu. The similarity in the atomic sizes of these 2nd and 3rd row metals is a consequence of the relativistic effect, which will be discussed in more detail later. Only Ag, with both of its naturally abundent isotopes having a spin of I = 1/2 is NMR active. The isotopes of Cu and Au have a nuclear spin I = 3/2, and due to quadrupolar relaxation neither metal is used in NMR.

1.1.2 OXIDATION STATES AND CO-ORDINATION NUMBERS

Copper exhibits five formal oxidation states (IV, III, II, I, O), but its chemistry is dominated by Cu(I) and Cu(II). Silver forms compounds in which it has the four formal oxidation states III, II, I and 0, but Ag(I) dominates. Gold exhibits seven possible formal oxidation states (VII, V, III, II, I, 0, -I), although its chemistry is dominated by Au(I) and Au(III). For metals in these dominant oxidation states some generalisations can be made about the common co-ordination numbers and geometries of their complexes.

Figure 1.3 shows the variations in the energies of the atomic orbitals with increasing atomic number of the neutral atoms (Z = 1 - 100). It can be seen from this plot that there are small differences in energy between the valence *d* and *s* orbitals for the neutral elements Cu, Ag, and Au, which permit the formation of $d(z^2)$-*s* hybrid orbitals and hence linear co-ordination for all three M(I) ions.

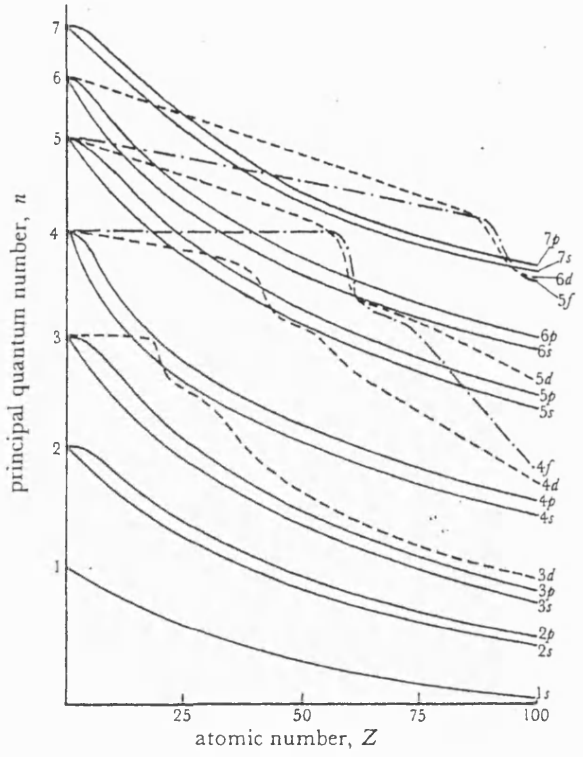

Figure 1.3 The variation of the relative energies of atomic orbitals with increasing atomic number in neutral atoms (not to scale)[5]

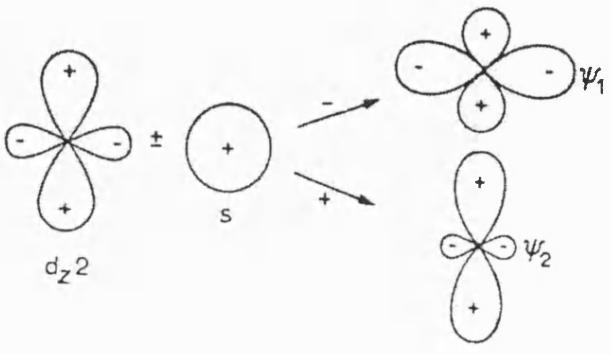

Figure 1. 4 Mixing of $d(z^2)$ and *s* orbitals to give hybrid *sd* orbitals

In the case of Cu(II) (d^9), the effect of Jahn-Tellar distortion is significant with many known examples of distorted octahedral and square planar complexes, Figure 1.5.

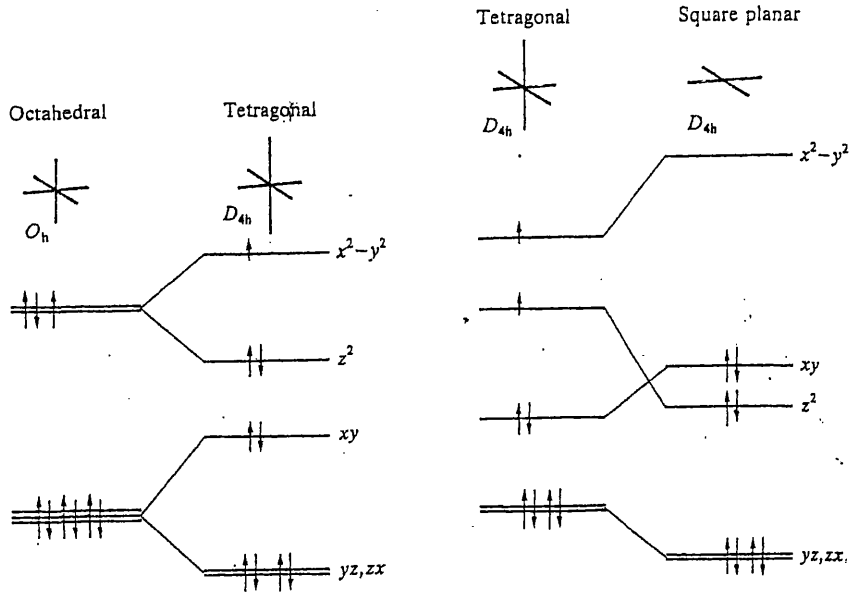

Figure 1. 5 The crystal field *d*-orbital splitting patterns of d^9 and d^8 ions[6]

Finally, the d^8 configuration of M(III) ions favours the formation of diamagnetic square planar complexes. The common stereochemistries of M(I-III), M = Cu, Ag , Au, complexes are summarised and exemplified in Table 1.2.

Oxidation State	C.N.	Stereochemistry	Cu	Ag	Au
+1 (d^{10})	2	linear	Cu_2O	$[AgSCN]_n$	$[Au(PPh_3)Cl]$
	3	trigonal	$[Cu(CN)_3]^{2-}$	$[AgI(PEt_2Ph)_2]$	$[Au(PCy_3)SCN]_n$
	4	tetrahedral	$[Cu(py)_4]^+$	$[Ag(diars)_2]^+$	$[Au(PMePh_2)_4]^+$
	6	octahedral	-	AgX X=F, Cl, Br	-
+2 (d^9)	4	tetrahedral	$Cs_2[CuCl_4]$	-	-
		square planar	CuO	$[Ag(py)_4]^{2+}$	$[Au(S_2C_2(CN)_2)_2]^{2-}$
	5	trigonal bipyramidal	$[Cu(bipy)_2I]^+$	-	-
		square pyramidal	$[Cu(dmg)_2]_2$*		
	6	octahedral	$K_2Pb[Cu(NO_2)_6]$		
+3 (d^8)	4	square planar	$CuBr_2(S_2CNBu^t_2)$	$[AgF_4]^-$	$[AuCl_4]^-$
	6	octahedral	$[CuF_6]^{3-}$	$[AgF_6]^{3-}$	$[AuI_2(diars)_2]^+$

Table 1.2 Common co-ordination geometries of Cu, Ag and Au complexes *(dmg = dimethylglyoxime)

1.1.3 RELATIVISTIC EFFECTS

As nuclear charge becomes larger all the *s* (and to a lesser extent, *p*) electrons close to the nucleus are accelerated, and for elements with Z > 70 their speed will become a significant fraction of the speed of light. For example, the speed of a 1*s* electron of mercury (Z = 80) [7] has been calculated to be 60 % of the speed of light. At these speeds the theory of relativity shows that the mass increases by 20 % and the *s* orbital radius contracts by 20 %. The contracted orbitals become more stable and shield the less polarisable outer orbitals more effectively from the nuclear charge, resulting in an expansion and destabilisation of the outermost *d* orbitals.

In the case of gold (Z = 79), the stabilisation and lowering in energy of the outer 6*s* orbital is more pronounced than for all other metals (Figure 1.6), with the 6*p* orbitals affected to a lesser extent. The resultant increased shielding of the 5*d* orbitals results in their expansion and an increase in their relative energy. Thus a small 5*d*-6*s* energy separation and a larger 6*s*-6*p* separation results. This is a significant factor in causing the high 1st ionisation energy of gold, which involves removal of the single electron from the 6*s* orbital, compared to the relatively lower 2nd and 3rd ionisation energies as electrons are lost from the 5*d* orbitals.

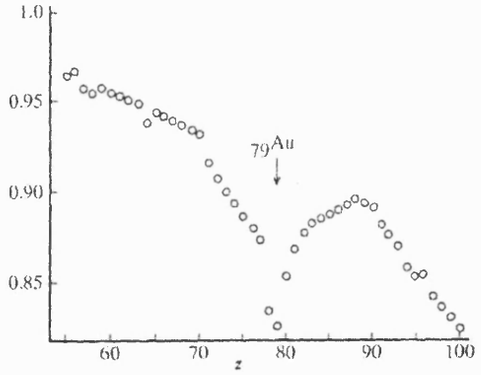

Figure 1. 6 Relativistic contraction ($r_{rel}/r_{non\text{-}rel}$) of the 6*s* orbital as a function of atomic number (Z = 55 - 100)[8]

This effect also explains why the Au...Au distance in metallic gold (2.884 Å) is if anything very slightly shorter than the separations of silver atoms in metallic silver (2.889 Å)[9]. It also accounts for the density of gold being higher (by 18 %)[6] than that expected based on non-relativistic calculations.

1.1.4 SECONDARY BONDING

A property that is very significant in the chemistry of gold, and to a lesser extent silver and copper, is secondary metal-metal bonding. These metal-metal contacts are defined throughout this Thesis as contacts less than the combined van der Waals radii, Ag...Ag < 3.20 Å and Au...Au < 3.50 Å, and they are comparable in strength to other weak interactions such as hydrogen bonds and π-π interactions. Secondary metal interactions are not unique to the coinage metals and are observed in the chemistry of, for example, thallium, lead, platinum and tin[10], but these interactions are particularly common for d^{10} metal ions, such as Hg(II) and Au(I). In the case of Au(I) it has been suggested[11] that the filled non-bonding $6s$-$5d(z^2)$ hybrid orbital donates electrons to the vacant $6p_x,p_y$ orbitals on an adjacent Au atom. Another study of $[ClAuPH_3]_2$ using *ab initio* calculations suggests that the effect is caused by ligand dipole-dipole forces combined with the relativistic effect[12].

In Au(I) compounds these interactions are enhanced by the relativistic effect. In a recent study[13] of the oligomeric dicyanoargentate(I), $[Ag(CN)_2]_n^-$, and dicyanoaurate(I), $[Au(CN)_2]_n^-$ ions, the average argentophilic and auriophilic bond strengths were calculated from absorption spectra data to be 25.3 and 31.5 kJ mol^{-1}, respectively. A recent extensive review[10] of secondary metal interactions reports the average auriophilic bond strength to be 34.0 kJ mol^{-1}.

Argentophilic interactions are less common than auriophilic interactions, and are very often bridging ligand assisted. For example, reaction of $[Ag(MeCN)_4][ClO_4]$ with 3.6-bis-(diphenylphosphino)pyridazine, (L), in acetonitrile yields the polymer $\{[Ag_2(MeCN)_2(L)]\}_n[ClO_4]_{2n}$[14]. The Ag-Ag separations in this polymer are 3.00 and 3.18 Å, and are at least partially a consequence of the geometry of the ligand combined with linear two-co-ordination about Ag(I).

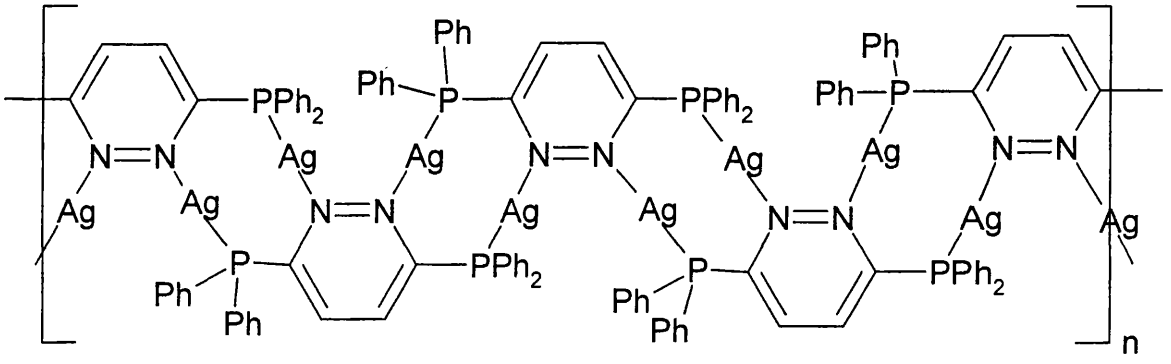

Figure 1. 7 $\{[Ag_2(MeCN)_2(L)]\}_n[ClO_4]_{2n}$

It is widely recognised[15abc] and accepted that small and non-stereochemically inhibited mononuclear gold complexes frequently undergo intermolecular aggregation via short sub van der Waals Au-Au contacts typically (2.5 - 3.5 Å).

The contrasting abilities of Cu, Ag and Au to exhibit M-M bond formation is also evident in the cluster chemistry of these three metals. Gold forms a wide range of Au_n clusters, ranging from n = 4 to n = 55, in which the average oxidation state of the gold is less than one. They can be formed by reduction of gold(I) phosphine complexes for example, as illustrated below[11,16] in Figure 1.8 and 1.9. Copper and silver do not generally form comparable compounds.

$$[Au_{11}(PMe_2Ph)_{10}]^{3+} \xrightarrow{Cl^-} [Au_{13}Cl_2(PMe_2Ph)_{10}]^{3+}$$

$$[AuCl(PPh_3)] \xrightarrow{NaBH_4} [Au_{11}Cl_2(PPh_3)_8]^{+}$$

$$[AuCl(PPh_2Cy)] \xrightarrow{NaBH_4} [Au_6(PPh_2Cy)_6]^{2+}$$

Figure 1. 8 Some routes to gold cluster compounds

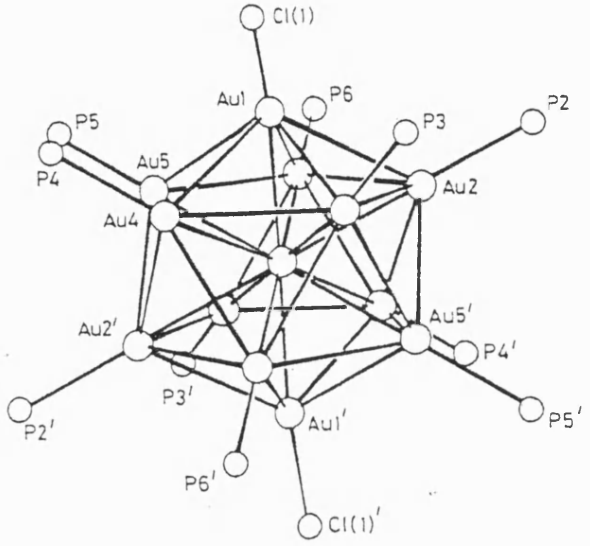

Figure 1.9 The core structure of $[Au_{13}Cl_2(PMe_2Ph)_{10}][PF_6]_3$[17]

Properties such as steric size and the number and type of co-ordinated ligand are relevant in determining intermolecular interactions. A recent study[18] of gold(I) dithiocarbamates and thiolates illustrates this point. Reaction of sodium tetrachloroaurate with the dithiocarbamate $K[S_2CN(C_2H_4OMe)_2]$ yields $[Au_2(S_2CN(C_2H_4OMe)_2)]_n$ which aggregates through Au...Au interactions to form a polymeric structure.

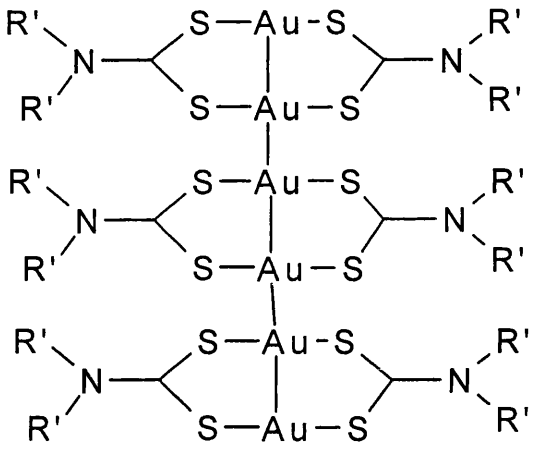

Figure 1. 10 $[Au_2(S_2CN(C_2H_4OMe)_2)]_n$, [R' = C_2H_4OMe]

Reaction of $[Au(SCH_2CO_2H)]$ with triphenylphosphine in ethanol yields $[(Ph_3P)Au(SCH_2CO_2H)]$ which also forms a supramolecular array but has no Au-Au interactions. Instead weak Au-S interactions occur yielding dimers, and in addition carboxylate groups hydrogen bond to nearest neighbours to afford a supramolecular array. Reaction of $[Au(SCMe_2CO_2H)]$ with triphenylphosphine affords $[(Ph_3P)Au(SCMe_2CO_2H)]$. The additional steric bulk provided by the Me groups on the α-carbon of the thiolate prevent any secondary bonding involving Au. Structural studies show only H-bonding between neighbouring carboxylates. Finally the reaction of $[Au(SCH_2CO_2Me)]$ with triphenylphosphine yields $[(Ph_3P)Au(SCH_2CO_2Me)]$, which exists as a simple monomer. There is no steric reason for it not forming a dimer similar to that of $[(Ph_3P)Au(SCH_2CO_2H)]$, illustrating that steric size is only one of the determining factors, and that the subtleties of the interplay between weak intermolecular interactions are still poorly understood in gold chemistry.

1.1.5 HARD-SOFT ACID-BASE PRINCIPLE

Pearson's[19] Hard-Soft Acid-Base principle arose from experimental observations that metals ions are generally either i) small, compact, electropositive and not very polarisable, or ii) larger and much more polarisable. Group i) are classified as "Hard" Lewis acids and include the metals of Group 1 and 2, and the early transition metals, particularly in high oxidation states. The latter group includes the late transition metals, and earlier metals in low oxidation states as in metal carbonyls. It was observed that hard Lewis acids preferentially bind to small, less polarisable, electronegative ligands including F^-, H_2O and NH_3. Soft Lewis acids preferentially bind to larger polarisable ligands including sulphur and phosphorus donor ligands. These Lewis bases were also classified as hard and soft, respectively. There are however, also acids and bases that are defined as "borderline" which can not easily be defined as either hard or soft but occupy a position in the middle of the continuum.

Hardness and softness has been related to polarisability[20], electronegativity[21] and charge densities[20], and various attempts have been made to quantify this property. The assigned values of hardness (η) or softness (σ), where $\eta = 1/\sigma$, are often relative and are dependent on the reference data chosen. To date one of the simplest but most widely used classification originated by Pearson and Parr[22], defines η as simply half the difference between the 1st ionisation energy and the electron affinity of the element, i.e. $\eta = 0.5(I-A)$. Whilst not stated at the time, (I-A) is also the energy gap between the ground state (HOMO) and the lowest excited state (LUMO). This energy gap is small for very polarisable "soft" acids or bases and large for non-polarisable "hard" acids or bases. The values of η have been calculated from experimental data by Pearson[23] for many free Lewis acids (Table 1.3)

and it is clear that Au^+ is significantly softer than the rest of the univalent coinage metal ions, whereas Au^{3+} is harder than either Cu^{2+} or Ag^{2+}. Generally all the coinage metal ions are classified as either "soft" or "borderline", but throughout this Thesis we shall emphasise only their relative hardness.

Acid	η (Ev)
Li^+	35.12
Cu^+	6.28
Cu^{2+}	8.27
Ag^+	6.96
Ag^{2+}	6.70
Au^+	5.60
Au^{3+}	8.40

Table 1.3 Chemical hardness data for some Lewis acids

Many factors other than atomic properties effect the HSAB classification. These include ligand effects. Thus $[ML]^+$ will not usually have the same hardness (η) as $[M]^+$ and it has been noted[20] that the presence of either an anionic ligand, or to a lesser extent a neutral ligand, reduces the electronegativity (χ) and chemical hardness (η) of the metal centre. This will be apparent in the chemistry of Au(I) with oxygen donors as discussed later in this chapter. Similarly the value of η for a Lewis base donor atom will be highly dependent on its substituents; for example water is the "hardest" neutral O-donor ligand (η = 9.4 eV) whereas dimethyl ether is notably softer (η = 8.0 eV).

Pearson defines the HSAB principle in the simple statement: "hard acids prefer to co-ordinate to hard bases, and soft acids prefer to co-ordinate to soft bases", and consequently there is an inherent incompatibility between soft acids and hard metals and between hard acids with soft bases. A nice illustration[24] of the difference in hardness of Au^+ compared with Cu^+ and Ag^+ is illustrated in their reactions with β-diketonates. Both Cu^+ and Ag^+ co-

ordinate to the hard oxygen donor centres of the diketonate, whilst Au^{+} binds to the softer carbon atom, Figure 1.11.

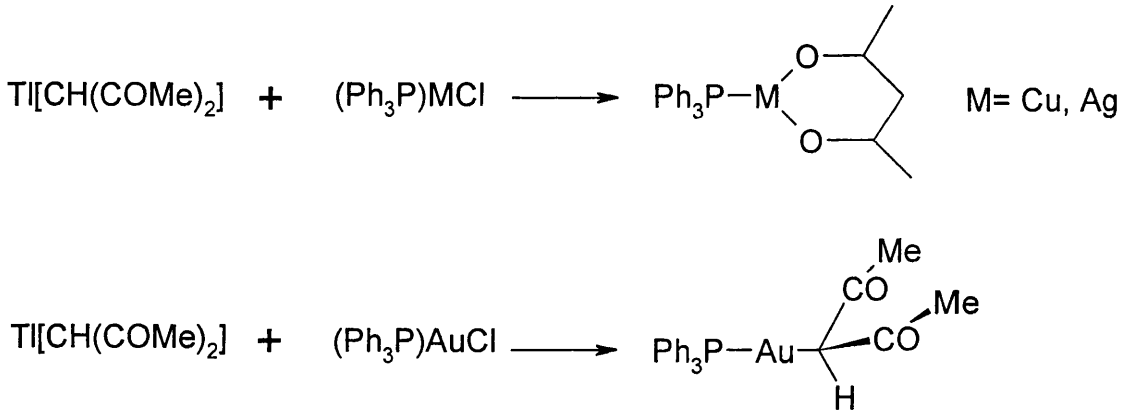

Figure 1.11 Products of reaction of Cu, Ag and Au salts with a β-diketonate

It is important to note that the HSAB principle considers only *relative* stability. It does not rule out soft/hard combinations, such as Au/O complex formation, but merely states that in a competitive environment they are unlikely to form.

SECTION TWO: THE STRUCTURAL CHEMISTRY OF SILVER(I) AND GOLD(I) WITH OXYGEN AND SULPHUR DONORS

1.2.1 SUMMARY

The remainder of this introductory chapter is concentrated on the structural chemistry of Ag(I) and Au(I). The chemical principles that are fundamental to the rationalisation of the properties of these metals and their complexes were introduced in the previous section. Ag(I) and Au(I) are borderline-soft and soft Lewis acids, respectively, according to the Hard-Soft Acid-Base classification and their chemistry reflects this difference. Thus Ag(I) and Au(I) will preferentially bind to sulphur donor ligands in competition with oxygen donors, however in non-competitive environments, Ag(I) and to a lesser extent Au(I) will form complexes with oxygen-donors.

Unsurprisingly the chemistry of these two metals with S-donors is vast and cannot be encapsulated in a short review. In order to focus on the fundamental trends in the structural chemistry of Ag(I) and Au(I), attention will be concentrate on selected examples of two types of Ag(I) and Au(I) complexes:

i) in which the metal centre is co-ordinated to only anionic donor ligands, and phosphine derivatives of these systems.

ii) with neutral macrocyclic oxygen or sulphur donor ligands.

Complexes containing other transition metals, and complexes of ligands containing more than one type of donor atom will not be covered in general.

1.2.2 COMPLEXES OF SILVER(I) CONTAINING OXYGEN-DONOR LIGANDS

The chemistry of Ag(I) with O-donors is extensive, ranging from the simple silver oxide, Ag_2O, to extensive series of complexes containing anionic and neutral donors. This section will concentrate on those Ag(I) compounds in which the metal centre is bound only to O-donors, but for comparative purposes with Au(I), we shall also introduce complexes of Ag(I) that also contain a monodentate tertiary phosphine (PR_3). As described earlier Ag(I) frequently exhibits a linear co-ordination geometry based on dz^2-s hybrid orbitals, but in complexes with hard donors, where the bond exhibits appreciable ionic character, the d^{10} Ag^+ ion has a closed sub-shell of spherical symmetry which allows the metal ion to accommodate a range of co-ordination numbers and geometries, under appropriate conditions as demonstrated in later examples.

1.2.2.1 ANIONIC DONOR LIGANDS

Ag_2O is produced by the action of alkali on any soluble Ag(I) salt, and its structure consists of oxygens in tetrahedral sites co-ordinated to four metal atoms, with each silver having two oxygen near neighbours. On heating to 160 °C Ag_2O forms silver. Another oxide initially characterised as Ag(II)O, is prepared by oxidation of Ag_2O, or other Ag(I) salts, with ozone or sodium thiosulphate. This oxide has since been shown to be $Ag^{I}Ag^{III}O_2$ and is stable to 100 °C. Its structure consists of linear two-co-ordinate Ag(I)(d^{10}) (Ag^{I}-O = 2.18 Å) and Ag(III)(d^8) (Ag^{III}-O = 2.05 Å) in square planar sites. Silver also has some less common oxides, Ag_3O, Ag_2O_3 and $[Ag_6O_8]^+$.

Many simple Ag(I) oxysalts containing O-donors such as nitrate, sulphate, perchlorate, trifluoromethylsulphonate (triflate), and carboxylate are commercially available and stable at room temperature. The "borderline" Lewis acidity of Ag(I) referred to earlier is nicely

illustrated by the structures of the arene adducts of these oxysalts, which exhibit both Ag-O and Ag-C bonds[25a,b,c]. For example in $[Ag(ClO_4)(C_6H_6)]$ the metal is co-ordinated to two benzene rings through two adjacent carbons of each ring (Ag-C = 2.496(6) - 2.634(8) Å), resulting in Bz-Ag-Bz-Ag chain formation. The macromolecular structure is further extended by co-ordination of each Ag(I) to one oxygen of two bridging bidentate perchlorate anions (Ag = 2.680(16) –2.701(16) Å). The metal-arene bond formation results in ring distortion, in which the two C-C bonds of the co-ordinated carbons at 1.35 Å are shorter than those of the other four C-C bonds (1.43 Å). This is thought to result from polarisation of the ring π-system, resulting in increased electron density at the bonds nearest to Ag(I)[25a].

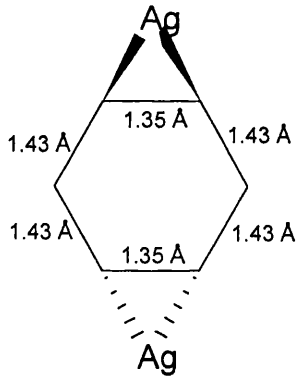

The solid state structure of Ag(I) triflate stabilised by toluene has recently been determined[26] at Bath. Two of five-co-ordinate Ag(I) centres are bridged by one oxygen of two bidentate triflate ligands (Ag-O = 2.421(5) Å), and also to another oxygen of a triflate of an adjacent dimer (Ag-O =2.417(5) Å). The remainder of the co-ordination sphere is completed by a toluene through two Ag – C contacts of 2.457(7) and 2.461(8) Å.

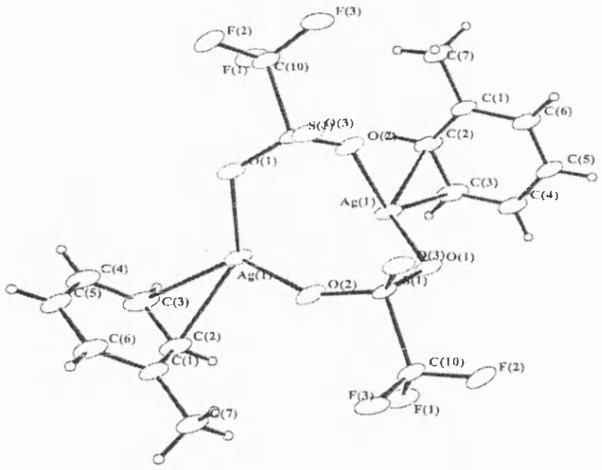

Figure 1.12 Molecular structure of $[(C_6H_5Me)Ag(OTf)]$

The carboxylate derivatives, $[Ag(O_2CR)]_2$, are of particular interest in that they contain bridged Ag dimers containing a central $[AgO\text{-}C\text{-}O]_2$ eight membered ring. These compounds generally are prepared by direct reaction of a silver salt AgX, where X= NO_3, ClO_4, with a carboxylic acid in hot aqueous solution. The structure of a specific carboxylate is dependent on the steric size of the carboxylate ligand, and on the presence or absence of further donors. The co-ordination about the Ag(I) centre varies as illustrated for the structural types A-F, below, and demonstrates the ability of Ag(I) to accommodate a wide range of co-ordination numbers or geometries.

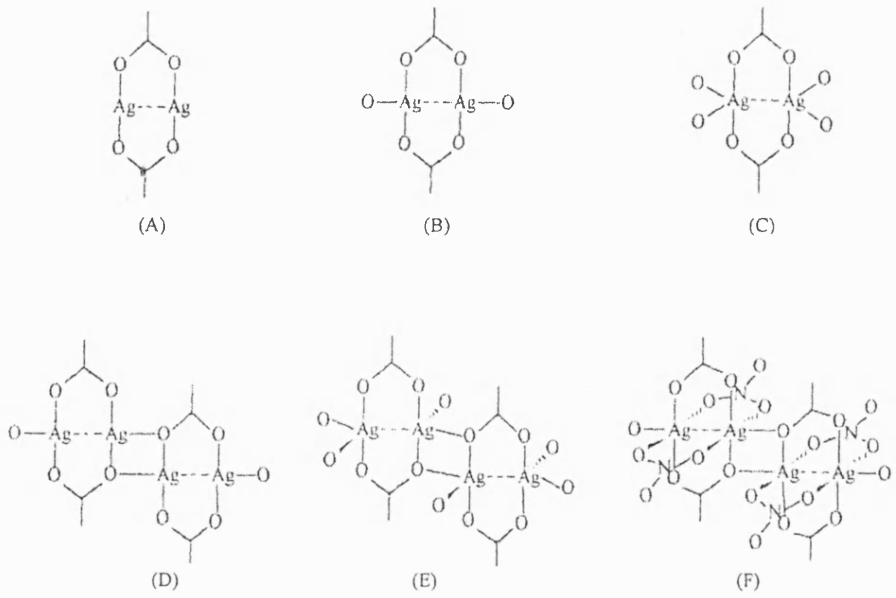

Figure 1.13 Ag(I) carboxylate structural types

For example, $[Ag_2(C_9H_8NO_2)_2(H_2O)_2].2H_2O$ crystallises as the dimer (B) and each Ag(I) co-ordinates terminal waters. The carboxylate Ag(I)-O separations at 2.185(2) and 2.207(3) Å are shorter than the Ag-OH_2 separations (2.518(4) Å) and the Ag...Ag contact of 2.81 Å, is shorter than that in Ag metal (2.89 Å)[8]. Examples of the range of structurally characterised silver(I) carboxylates are shown in Table 1.4. The metal separations, the inter- and intra- molecular Ag-O separations and structural type are also listed.

	Ag...Ag (Å)	Ag-O (Å)		Type
		$Ag\text{-}O_{intra}$	$Ag\text{-}O_{inter}$	
$[Ag_2(O_2CC_6H_4\text{-}p\text{-}OH)_2]$[27]	2.861(1)	2.210(1)	-	A
$[Ag_2(O_2CPh)_2]$[24]	2.921(1)	2.220(2)	-	A
$[Ag_2(O_2CC(CH_3)CHCH_3)_2]$[28]	2.8532(1)	2.490(4)	-	B
$[Ag_2(O_2CC_6H_4\text{-}o\text{-}NHC(O)CH_3)_2(H_2O)_2].2H_2O$[29]	2.813(3)	2.207	-	B
$[Ag_2(O_2CCF_2CF_3)_2]$[30]	2.900(2)	2.606(6)	-	C
$[Ag_2(O_2C(CH_2)_2NH_3)_2(NO_3)_2]$[31]	2.855(4)	2.210(19) 2.198(19)	-	C
$[Ag_2(O_2CCO_2)]$[32]	2.945	2.286	2.551	D
$[Ag_2(O_2CCF_3)_2]$[33]	2.967(3)	2.232(6)	2.249(6)	D
$[Ag_2(O_2CCH_2OPh)_2]$[34]	2.857	2.284	2.431	D
$[Ag_2(O_2CCH_2OC_6F_5)_2]$[35]	2.943(1)	2.203(3)	2.230(2)	D
$[Ag_2(O_2CCH_2OC_6H_5)_2]$[36]	2.866(2)	2.178(9)- 2.286(7)	2.498(4)	D
$[Ag_2(O_2CNMe_2)_2]$[37]	2.837(2)	2.156(9) 2.219(8)	2.600(8)	D
$[Ag_2(3,5\text{-dinitrobenzoate})_2]$[38]	2.835(2)	2.176(5) 2.218(6)	2.655(7)	D
$[Ag_2(O_2CCH_2Cl)_2]$	2.921(3)	2.247(5) 2.306(14)	2.528(4)	E
$[Ag_2(Me_3CH_2CO_2)_2(NO_3)_2]_n$[39]	2.898(1)	2.241(3) 2.334(3)	2.554(3) 2.497(3)	E
$[Ag_2(PyCH_2CO_2)_2(NO_3)_2]_n$ same ref as above	2.814(2)	2.211(6)- 2.466(7)	2.466(7)	E

Table 1.4 Silver(I) carboxylate derivatives

Silver(I) phosphine derivatives $[(R_3P)_nAg]^+$ (n = 1-3) readily form complexes with a range of anionic oxygen donors. These complexes are prepared by metathesis of $[(R_3P)_nAgCl]$ with an alkali metal salt. For example, $[(Me_3P)_nAgCl]$ (n=1,2,3)[40] reacts with sodium trimethylsilanolate to form products of the general formula $[(Me_3P)_nAgOSiMe_3]$, where n = 1, 2 or 3. This type of complexes of general formula $[(R_3P)_nAg(X)]$ (X = O_2CR, NO_3, OTf) can also be formed by reaction of AgX with n equivalents of phosphine (n = 1-3). Examples of structurally characterised monodentate phosphine Ag(I) complexes of oxygen donors include $[(PPh_3)Ag(O_2CC(CH_3)CHCH_3)]$[25], $[(PPh_3)_2Ag(O_2CCH_3)]$[41], and $[(PPh_3)_3Ag_3(OTf)_3]$[42]. The complexes also illustrate the tendency of Ag(I) to form a range of co-ordination numbers varying from 2 to 4. The Ag(I)-O separations in these complexes span the same range as those in the Ag(I) carboxylates discussed above. Interesting examples of the variety in these compounds are the phosphine Ag(I) nitrates, $[(PPh_3)_2AgNO_3].C_6H_6$[43] and $[(PPh_3)_2AgNO_3]_2$[44](Figure 1.14). In both the Ag(I) atom has a distorted tetrahedral geometry, but in the solvated monomer the Ag-O separations are notably longer (2.463(2) and 2.572(2) Å) than in the dimer (2.340(3) and 2.341(3) Å).

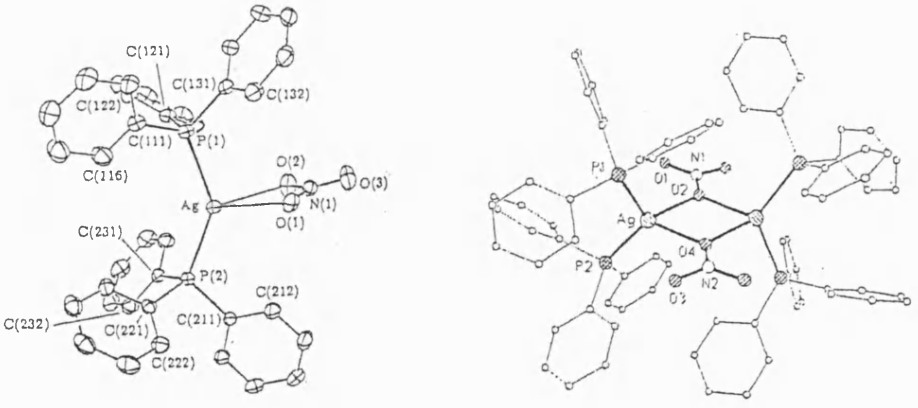

Figure 1.14

The only structurally characterised Ag(I) siloxide is $\{[Ag(PPh_3)]_2(\mu\text{-}OMe_2SiOSiMe_2O)\}_2$ which was formed serendipitously during recrystallisation of [2-(dimethylaminomethyl) phenyl]silver(I) from toluene in the presence of triphenylphosphine and silicone grease[45]. In

the solid state the complex contains six-membered heterosiloxane rings with both three and four co-ordinate Ag(I) atoms. The Ag-O separations are in the range 2.025(12) – 2.376(12) Å.

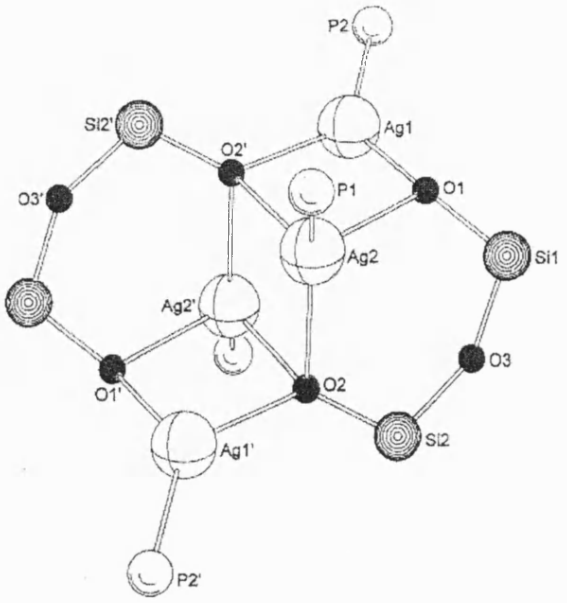

Figure 1.15 The core structure of $\{[Ag(PPh_3)]_2(\mu\text{-}OMe_2SiOSiMe_2O)\}_2$

1.2.2.2 NEUTRAL OXYGEN LIGANDS

Thus far all the examples considered have featured anionic oxygen donors. There are several examples of neutral Ag(I) complexes containing polyether donors, such as $[Ag(\text{hexafluoropentane-dionato})(CH_3O(CH_2CH_2O)_mCH_3)]$[46], where m = 2 (diglyme), 3 (triglyme) or 4 (tetraglyme). They are prepared by reaction of silver(I) oxide with the diketonate ion and the polyether in THF, as shown below in Figure 1.16, for tetraglyme.

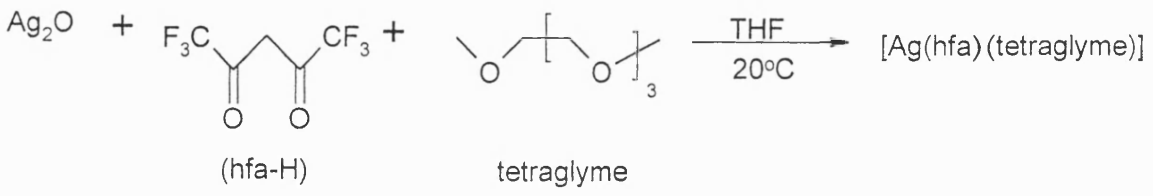

Figure 1.16

An analogous reaction involving diglyme affords a dimer $[Ag(hfa)(diglyme)]_2$, which decomposes in air to give a mixture of products including $[Ag(hfa)(O_2CCF_3)(diglyme)_2]$. The complexes contain seven- and six-co-ordinate Ag(I) respectively. The latter complex contains three different oxygen donors with the shortest bonds to Ag being those from the trifluoroacetate oxygens at 2.266(3) and 2.304(3) Å, (Table 1.5, Figure 1.17).

Compound	C.N	Ag...Ag (Å)	Ag-O_{hfa}(Å)	Ag-O_{glyme}(Å)
$[Ag(hfa)(diglyme)]_2$	7	2.9226(9)	2.528(4)-2.621(4)	2.486(4)-2.657(4)
$[Ag(hfa)(O_2CCF_3)(diglyme)_2]$	6	2.9513(6)	2.468(3)-2.537(3)	2.496(3)-2.545(3)
[Ag(hfa)(tetraglyme)]	6	-	2.416(3)-2.441(3)	2.543(3)-2.742(3)

Table 1. 5 Structural parameters for Ag(I)-glyme derivatives

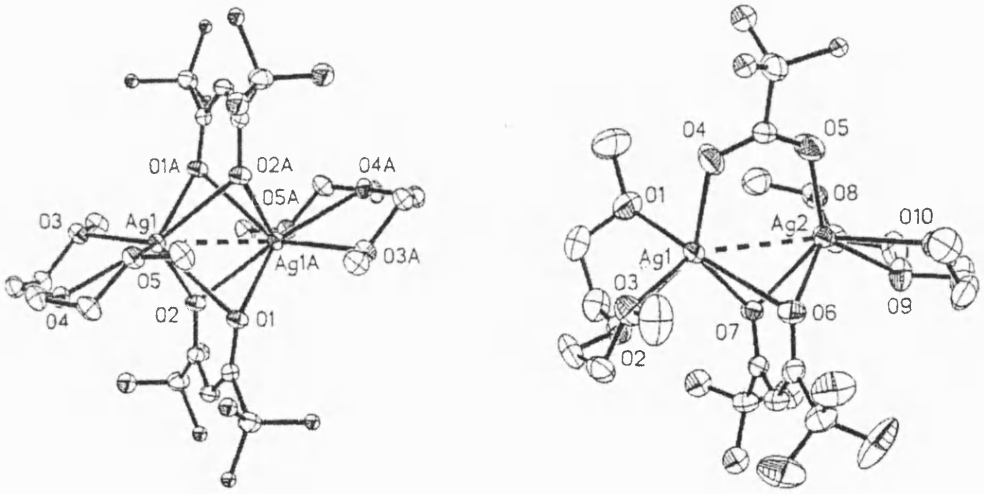

Figure 1. 17 Structures of $[Ag(hfa)(diglyme)]_2$ and $[Ag(hfa)(O_2CCF_3)(diglyme)]$

Naturally occurring polyethers such as the antibiotics emericid[47] and nigiricin[48] (Figure 1.18) which show selectivity to alkali metal cations in biological systems, have been structurally characterised as their silver salts. They show multiple Ag-O_{ether} co-ordination, as do the silver derivatives of grisorixin[49] and lysocellin[50].

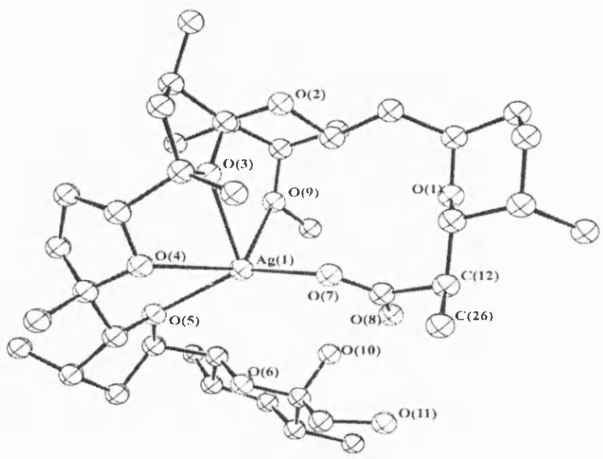

Figure 1.18 Solid state structure of [Ag(nigericin)]+, [nigericin = $C_{40}H_{67}O_{11}$]

Much less structural data is available on Ag(I)-neutral macrocylic O-donors. Although several solution studies of silver(I) complexes of crown-ethers have been published[51a-c], solid state structures of such species have until recently been rare. Indeed the majority of X-ray crystal structures reported of crown-ethers contain other softer donor atoms such as N or S replacing one or more oxygen atoms.

An important part of the driving force for metal-oxygen bond formation involving polydentate macrocycles is their enhanced stability compared to their open chain counterparts that is encompassed in the term the "macrocyclic effect"[52]. For neutral macrocycles, containing n O-donors, the enthalpic contribution to the free energy of formation is expected to be less than that provided by an analogous monodentate anionic O-donor ligands, but entropic contribution is greater.

Until very recently only two structurally characterised examples of simple Ag(I)/crown-ether complexes were known. The complex $\{[(CH_2O)_6Ag_2][Ag][AsF_6]_3\}$[53], (Figure 1.19) was formed by reacting silver hexafluoroarsenate with the oxymethylene trimer $(CH_2O)_3$ at low temperature in liquid SO_2. The resulting 12-crown-6, $(CH_2O)_6$, complexes two metal ions; each metal is complexed to three oxygens [Ag(I)-O = 2.458(5) Å].

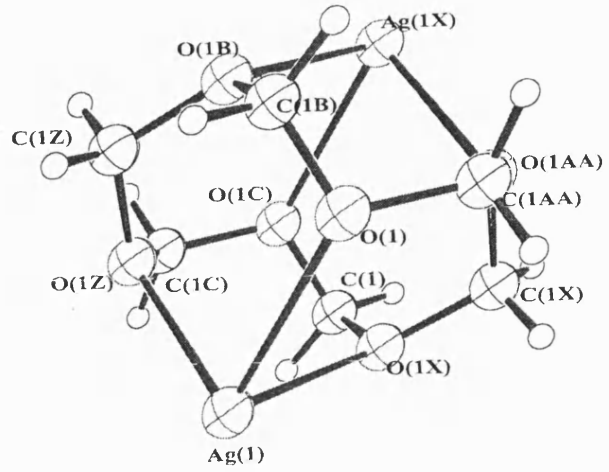

Figure 1.19 **The core structure of $[(CH_2O)_6Ag_2]_2^+$**

In an analogous reaction (Figure 1.20) with ethylene oxide in liquid SO_2, a white solid Ag(I) complex was isolated in low yield and shown to be $\{[Ag(12\text{-crown-}4)_2]^+[AsF_6]^-\}$[54].

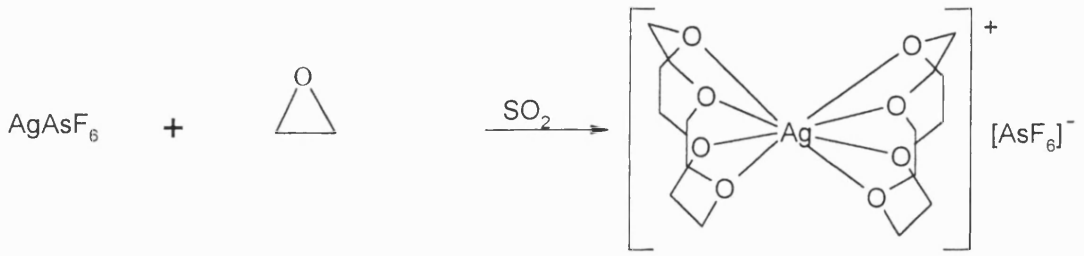

Figure 1.20

Crystals for the solid-state structure determination were grown from liquid SO_2, and the complex was found to adopt a sandwich structure (Figure 1.21) containing eight-co-ordinate Ag(I). The geometry at the metal centre was reported to be essentially cubic but with the two opposing faces rotated by 30°. The Ag-O bond lengths average 2.57Å. The eight individual Ag-O separations from which this average was obtained were not reported.

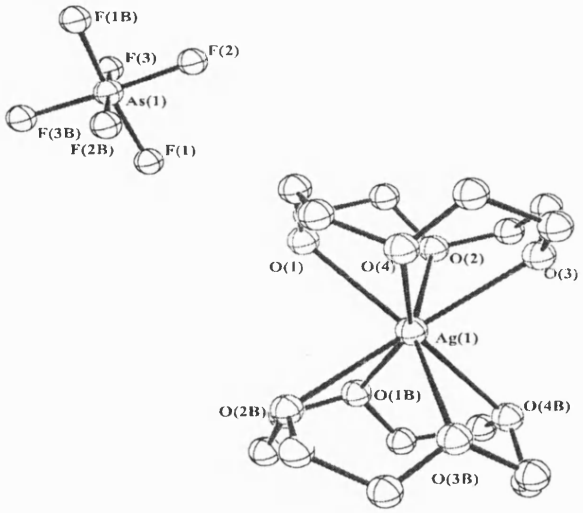

Figure 1.21 Solid state structure of $\{[Ag(12\text{-crown-}4)_2]^+[AsF_6]^-\}$

The structure of $[Ag(dibenzo\text{-}18\text{-}crown\text{-}6)(NO_3)]$[55], in which the metal centre is co-ordinated to six oxygens of the crown (Ag-O = 2.639(8) - 2.871(8) Å) and to one oxygens of the nitrate (Ag-O = 2.439(11) Å) was also reported briefly in 1987. Since that communication, no further examples of crown ether complexes of Ag(I) were reported until August 1998 during the course of this study. The structures of Ag(I) complexes of 15-crown-5 and benzo-15-crown-5 (Figure 1.22) were then reported[56], both of which exhibited only Ag(I)-O interactions.

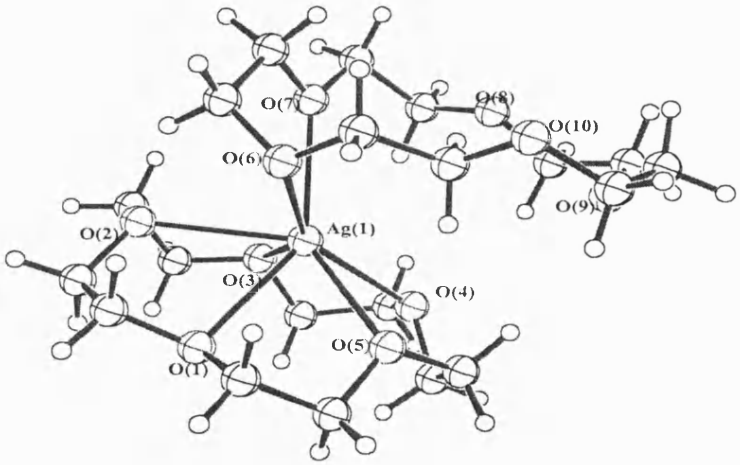

Figure 1. 22 Solid state structure of $\{[Ag(15\text{-crown-}5)_2][SbF_6]\}$

Subsequently the same group reported[57] the structures of $\{[Ag(aza\text{-}15\text{-}crown\text{-}5)_2][SbF_6]\}$ and $\{[Ag(N\text{-}allylaza\text{-}15\text{-}crown\text{-}5)_2][SbF_6]\}$. Both these complexes exhibit one Ag-N and

four Ag-O interactions. Several structurally characterised examples of Ag(I) complexes of crown-ethers containing both O- and S- donor atoms have also been reported. In $\{[Ag_2([15]aneS_2O_3)_3][PF_6]_2\}$ and $\{[Ag_n([15]aneS_2O_3)_n][PF_6]_n\}$ both Ag-S and Ag-O bonds occur[58], as illustrated below (Figure 1.23). The structures of Ag(I) complexes thiacrown-ethers containing a maleonitrile (mn) substitutent[59a,b], $[Ag(mn\text{-}[12]aneS_2O_2)_2][PF_6]$, $[Ag(mn\text{-}[12]aneS_2O_2)_2][ClO_4]$, $[Ag(mn\text{-}[15]aneS_2O_3)_2][PF_6]$, $[Ag(mn\text{-}[15]aneS_2O_3)][ClO_4]$, $[Ag(mn\text{-}[18]aneS_2O_4)][PF_6]$, and $[Ag(mn\text{-}[21]aneS_2O_5)_2][PF_6]$ have also been determined. Each of these maleonitrile-thiacrown-ether complexes exhibits both Ag-S and Ag-O bonds as well as Ag-N bonds involving the mn side chains.

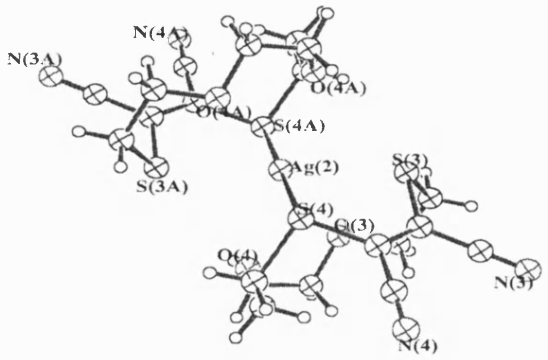

Figure 1. 23 The solid state structures of $[Ag_2([15]aneS_2O_3)_3][PF_6]_2$

A further example of a silver complex exhibiting co-ordination to both hard oxygen atoms and a soft π-bond has also been reported[60]. Complexation of $AgNO_3$ by a (ethylenoxy)oxy-bridged stilbene yielded $[Ag(stilbene)(NO_3)]$, Figure 1.24. The eight co-ordinate metal ion is bonded to a bidentate nitrate (Ag-O = 2.438 and 2.531 Å), and to four oxygens of the macrocycle (Ag-O = 2.511-2.791 Å). The co-ordination sphere is completed by co-ordination to the π-bond of the stilbene (Ag-C = 2.566 and 2.716 Å). Other examples of Ag(I) complexes of crown-ethers containing either N- or S-donor atoms, can be found in the literature[61,62].

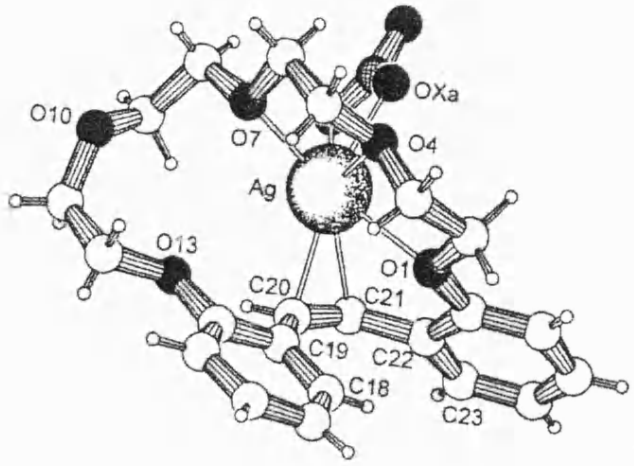

Figure 1. 24 Ag(I) complex of a stilbene derivative

1.2.3 COMPLEXES OF GOLD(I) CONTAINING OXYGEN-DONOR LIGANDS

The chemical softness of gold has a dominant affect on the whole chemistry of the metal. As Au(III) is not as soft as Au(I), it is able to form an oxide Au_2O_3, that decomposes on gentle heating. This is the only characterised binary oxide of gold and its structure is polymeric with the d^8 Au(III) ion achieving square planar co-ordination (Au-O: 1.93-2.07 Å)[8]. Examples of homoleptic Au(III) complexes containing O-donors are also known and include $K^+[Au(NO_3)_4]^-$[63a,b], $[(Me_3SiO)_3Au]_2$ and $Na^+[(Me_3SiO)_4Au]^-$[64]. The structure of $K^+[Au(NO_3)_4]^-$ has been determined and the metal again exhibits square-planar co-ordination with Ag(III)-O separations of 2.00 ± 0.02 Å. There are no comparable Au(I) compounds.

Until very recently the only reported gold(I)-oxygen bonded molecular species contained a phosphine ligand. The $[(R_3P)Au]^+$ moiety must be considered separately from that of Au^+ as has been noted earlier, the co-ordination of a ligand to the metal centre will effect the metal's valence orbitals and consequently its "hardness" of the metal. The $[(R_3P)Au]^+$ fragment can be considered as being isolobal with H^+ or R^+, that is symmetry and approximate energies of the frontier orbitals correspond[65].

Complexes of the type $[(PR_3)AuX]$, where X = O-anion, are generally prepared by metathesis reaction of a metal salt, MX, [where $M = Na^+$, K^+, Tl^+ or Ag^+) with $[(PR_3)AuCl]$. The driving force for this reaction being the elimination of MCl (Figure 1.25). These compounds all decompose at elevated temperatures or on exposure to light.

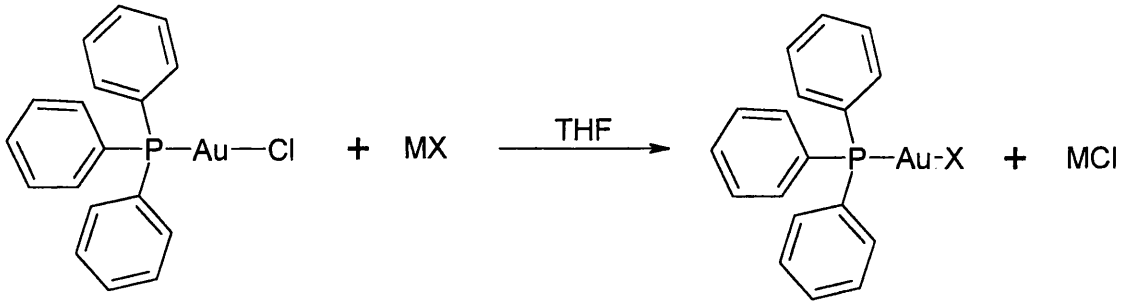

Figure 1.25

The only Au(I) compound containing an Au(I)-O bond reported that does not include a tertiary phosphine ligand is $[(Me_3CNC)Au(ONO_2)]$[66] prepared by metathesis of $[(Me_3CNC)AuCl]$ with silver(I) nitrate. The product of this reaction is only stable at low temperatures (-25 °C) and in an atmosphere of dichloromethane. Of the structurally characterised complexes of this type (Table 1.6) each exhibits linear two-co-ordinate Au(I). The structure of one such complex is illustrated in Figure 1.26.

	Au(I)-O (Å)	Au(I)-P (Å)
$(Me_3CNC)Au(ONO_2)$[66]	2.062(9)	-
$(PMe_3)Au(ONO_2)$[66]	2.090(6)	2.219(2)
$(PPh_3)Au(ONO_2)$[67]	2.199(5)	2.199(5)
$(PMePh_2)Au(OSiMe_3)$[68]	1.986(1)	2.202(1)
$(PPh_3)Au(O_2CCH(CH_3)_2)$[69]	2.047(6)	2.213(2)
$(PPh_3)Au(O_2CCH(OH)CH_3)$[69]	2.038(16)	2.219(4)
$(PPh_3)Au(O_2CCH_3)$[69]	2.033(6)	2.207(3)
$(PPh_3)Au(O_2CCF_3)$[70]	2.107(9)	2.204(5)
$(CF_3CO_2)Au(\mu\text{-dppf})Au(O_2CCF_3)$[71]	2.078(3)	2.219(2)
$(PPh_3)Au(O_2CC_6H_5)$[72]	2.063(6)	2.213(3)
$(PPh_3)Au(O_2CNEt_2)$[34]	2.047(7)	2.212(2)
$(P(o\text{-tol})_3)Au(OSO_2CF_3)$[54]	2.110(3)	2.225(1)
$(PPh_3)Au(O_2CCHNHC(O)C_6H_5)$[73]	2.077(5)	2.212(2)
$(PPh_3)Au(O_2CC(CH_3)NHC(O)C_6H_5)$[72]	2.070(12) 2.069(13)	2.210(5)
$(PPh_3)AuOSO_2OAu(PPh_3)$[74]	2.063	2.216
$(PPh_3)Au(OC_6Cl_5)$[75]	2.047	2.215
$(PPh_3)Au(OC_6H_4\text{-}o\text{-}Br)$[76]	2.025	2.214
$(PPh_3)Au(OC_6H_4\text{-}p\text{-}Me).MeC_6H_4\text{-}p\text{-}OH$[77]	2.033	2.2115(9)
$(PPh_3)Au(OCH_2CF_3)$[78]	-	-
$(PPh_3)Au(OCH(CF_3)_2)$[78]	-	-
$(PCy_3)Au(OCH_2CF_3)$[78]	-	-
$(PCy_3)Au(OCH(CF_3)_2)$[78]	-	-

Table 1. 6 Gold(I)-oxygen bonded compounds

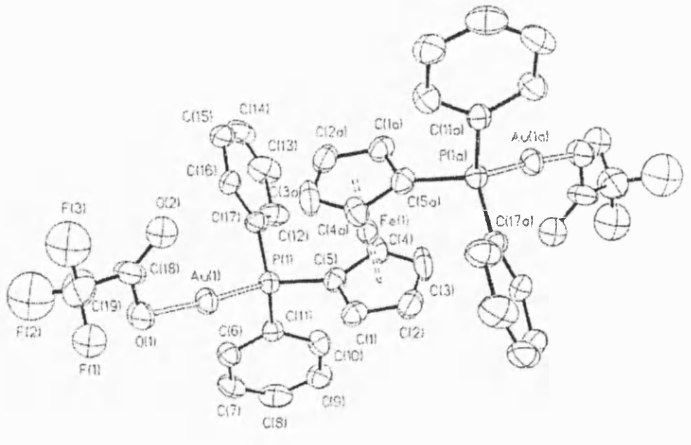

Figure 1. 26 Structure of $[(CF_3CO_2)Au(\mu\text{-dppf})Au(O_2CCF_3)]$

Auriophilicity is very common in Au(I) chemistry, but these weak interactions are limited by the steric bulk of ligands bound to the metal centre. Of the compounds listed in Table 1.6 above only $[(PMe_3)Au(ONO_2)]$ and $[(Me_3CNC)Au(ONO_2)]$ aggregate. In

$[(Me_3CNC)Au(ONO_2)]$ the complex forms a chain with alternating Au...Au interactions of 3.296(1) and 3.324(1) Å, in which adjacent molecules pack head to tail as shown in Figure 1.27 Analogous structures have been reported for $[(Me_3CNC)Au(X)]$ {X= Cl, Br, CN)[79].

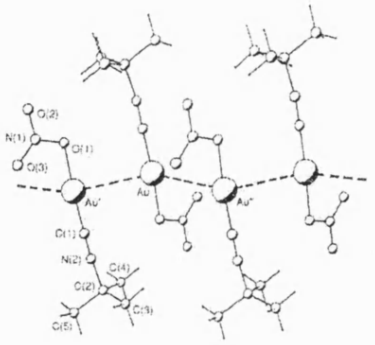

Figure 1. 27 The packing of $[(Me_3CNC)Au(ONO_2)]$

The complex $[(Me_3P)Au(ONO_2)]$ also aggregates by two Au...Au contacts (3.2795(6) and 3.2783(6) Å) but to form trimers rather than dimers. The trimers associate via longer Au...Au contacts of 3.449(1) Å at the limit of Au...Au bonds, to afford a polymeric chain structure[67].

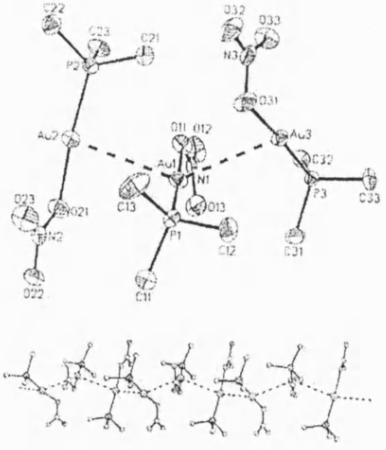

Figure 1. 28 Trimeric structure of $[(Me_3P)Au(ONO_2)]$

Auriophilic interactions enable Au(I) to form some unusual derivatives. Given that $[LAu]^+$ (where L is a neutral ligand such as PPh_3), is isolobal with H^+ and R^+, it might be expected that $(AuL)^+$ could form analogues of H_2O or R_2O. Attempts to synthesise these neutral compounds yielded some rather unexpected results. Attempted preparation of $(LAu)_2O$ was unsuccessful and instead novel hypervalent or hyper-auriated compounds were formed

including $[(LAu)_3O]^+ X^-$ and $[(LAu)_4O]^{2+}[X^-]_2$ [L = PPh_3 and X = BF_4^-, CF_3COO^-, MnO_4^-][80]. These compounds can be readily synthesised, via the reaction of $[(PR_3)AuCl]$ first with $AgBF_4$, and then with alkali, or from $[(R_3P)AuCl]$ and silver oxide in the presence of sodium tetrafluoroborate. These hyper-auriated compounds are stabilised by gold atoms through three Au...Au interactions.

The size of the phosphine ligand affects the geometry of the pyramidal $[(R_3PAu)_3O]^+$ moiety[81,82]. Oxonium salts containing bulky phosphines such as P(*o*-tol)$_3$ and P(^{i}Pr)$_3$, crystallise as monomeric $[(R_3PAu)_3O]^+$ units, each containing three Au...Au interactions. Oxonium salts with L = Ph_3P or $P(NEt_2)_3$ dimerise through two Au...Au intermolecular interactions of 2.9 -3.2 Å between two units with aligned parallel edges forming an Au_4 unit (**1**). Oxonium salts containing L = PMe_3 dimerise through alignment of two crossed edges still allowing four Au...Au contacts (**2**), Figure 1.29.

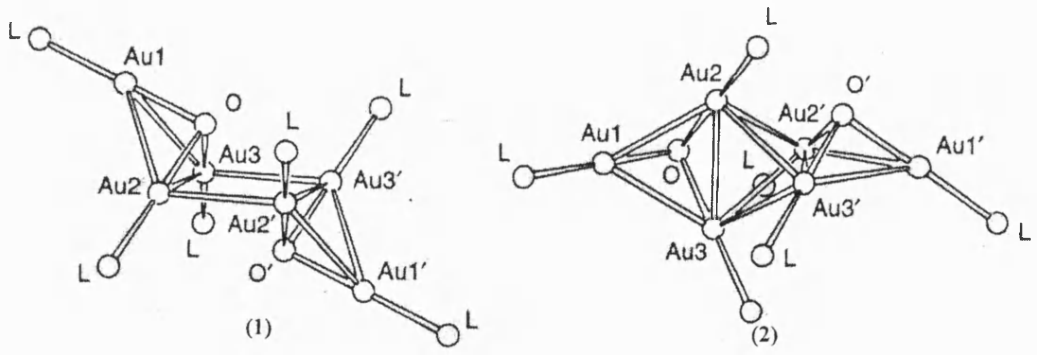

Figure 1.29 Two structures of oxonium dimers

1.2.4 COMPLEXES OF SILVER(I) CONTAINING SULPHUR-DONOR LIGANDS

Examples of the variety of co-ordination numbers and geometries that Ag(I) is capable of attaining were illustrated in the discussion of its chemistry with O-donors. The ability to form such a wide range of stable co-ordination systems is further demonstrated in the

chemistry of Ag(I) with S-donors, particularly the anionic thiolate ligands and neutral thiacrowns.

1.2.4.1 ANIONIC DONOR LIGANDS

The Ag(I) thiolates can generally be classified as homoleptic thiolates, $[Ag(SR)]_n$, bisthiolate cationic complexes $[Ag(SR)_2]^+X^-$, and phosphine Ag(I) thiolate adducts, $[(PR_3)_nAg(SR)]$. Of these only the homoleptic derivatives are considered in this sub-section. Homoleptic thiolates are generally insoluble, which is attributed to polymeric aggregation due to the bridging ability of the ligand and requirement of a co-ordination number higher than 1 for Ag(I). However, a significant number of homoleptic thiolates which are prepared by reaction of thiol (RSH, R = aryl, alkyl) with a silver salt have been structurally characterised.

The structure of $[Ag(SC(SiMe_2Ph)_3)]_3$ represents the simplest class of homoleptic Ag(I) thiolates, it contains a puckered six-membered ring, Ag_3S_3[83] with all three silvers two-co-ordinate (Figure 1.30).

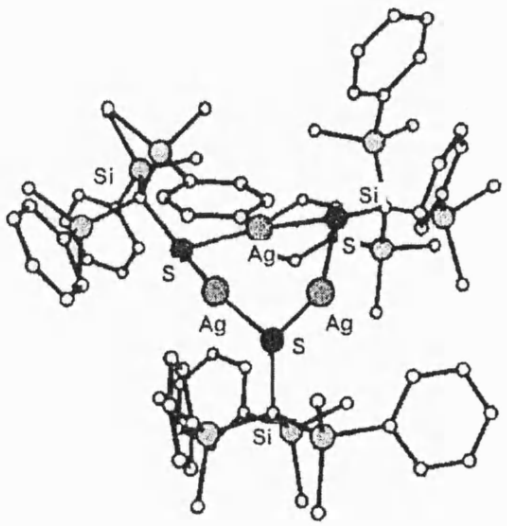

Figure 1. 30 The molecular structure of $[Ag(SC(SiMe_2Ph)_3)]_3$

Silver(I) thiolates containing an Ag_4S_4 core are exemplified by$[Ag(SC(SiMe_3)_3]_4$[83], $[Ag(SSi(O^tBu)_3]_4$[84], and $\{[Ag(SCH(SiMe_3)_2]_4\}_2$[83]. In each Ag_4S_4 core the co-ordination about silver is close to linear, except for the bridging Ag(I) in $\{[Ag(SCH(SiMe_3)_2]_4\}_2$ which has a T-shaped co-ordination geometry.

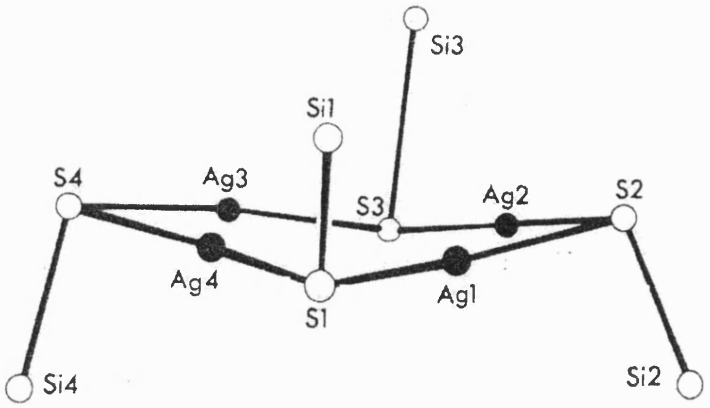

Figure 1. 31 Ag_4S_4 core of $\{[Ag(SC(SiMe_3)_3]_4\}$

Both $[Ag_5(\mu^2\text{-}S(CH_2)_3NHMe_2]_3[\mu^2\text{-}S(CH_2)_3NMe_2]_3][ClO_4]_2$[85] and $[Ag_5(S^tBu)_6]^-$[86] contain a Ag_5S_6 trigonal bipyramidal cage containing linear and trigonal Ag(I) atoms.

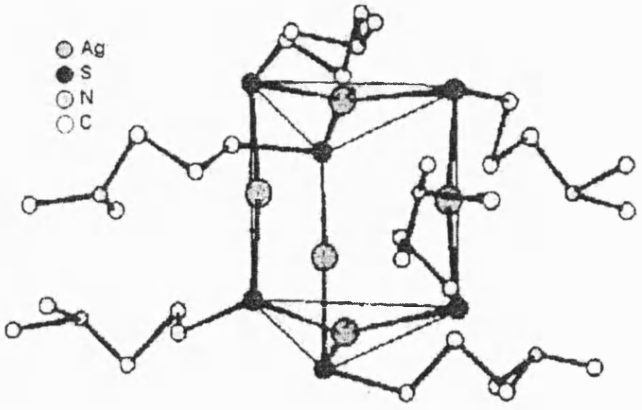

Figure 1. 32 Structure of the $[Ag_5(\mu^2\text{-}S(CH_2)_3NHMe_2]_3[\mu^2\text{-}S(CH_2)_3NMe_2]_3]^{2+}$ ion

The structural core of $[Ag(SC_5H_3N\text{-}3\text{-}SiMe_2Ph)]_6$[87] has been described as a paddle wheel, consisting of a Ag_6S_6 core. Each core sulphur atom is doubly bridging and bound to three

silver atoms (Figure 1.33). In $[Ag_6(SC_6H_4Cl)_6(PPh_3)_5]$[88] there is a central Ag_5S_6 core with three terminal phosphines, and an $Ag(PPh_3)_2$ appendage bonded to two thiolate bridges.

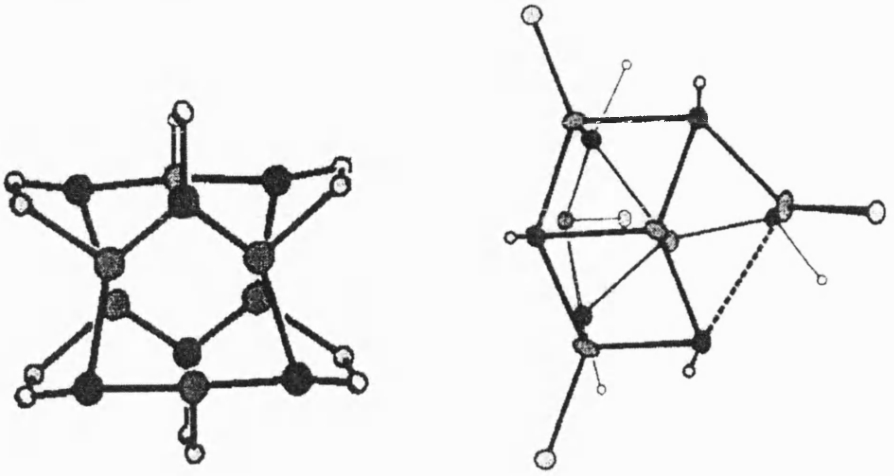

Figure 1. 33 Ag_6 cores of $[Ag(SC_5H_3N\text{-}3\text{-}SiMe_2Ph)]_6$ and $[Ag_6(SC_6H_4Cl)_6(PPh_3)_5]$

There are also complexes containing eight or more Ag(I) centres, such as $[Ag(SCMeEt_2)]_8$[84], and $[Ag(SC_6H_{11})]_{12}$, which form large macrocyclic Ag_8S_8 (Figure 1.34) and $Ag_{12}S_{12}$ cores, respectively. Finally, there are a few examples of structurally characterised polymeric Ag(I) thiolates including $[Ag(SCMeEt_2)]_n$[89], $\{[Ag(SC_6H_2{}^iPr_3]_4CHCl_3\}_n$[90], and $[Ag_4\{SCH_2(SiMe_3)\}_3]_n$[90]. All form one-dimensional polymers.

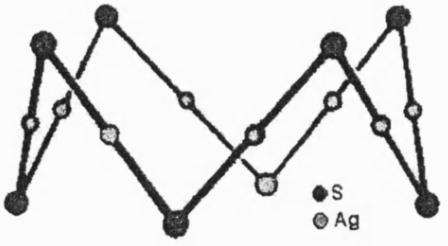

Figure 1. 34 Structures of Ag_8S_8 core and $[Ag(SC_6H_{11})]_{12}$

1.2.4.2 NEUTRAL DONOR LIGANDS

In Section 1.2.2.2, the compatibility of Ag^+ with oxacrown-ethers was considered, and examples given of complexes of Ag(I) with macrocycles containing both O and S donors.

Unsurprisingly Ag(I) forms stable complexes with a number of thiacrown-ethers, often formed by direct reaction of the thiacrown with a silver(I) salt in a polar solvent under reflux[91].

Reaction of $AgClO_4$ with excess [12]aneS_3 yields a compound that was characterised in the solid-state as $[\{Ag_3([12]aneS_3)_3\}\{Ag([12]aneS_3)_2\}][ClO_4]_4$. The individual $\{Ag_3([12]aneS_3)_3\}^{3+}$ and $\{Ag([12]aneS_3)_2\}^{+}$ moieties are illustrated in Figure 1.35[92]. The Ag(I) centre is distorted octahedral in $\{Ag([12]aneS_3)_2\}^{+}$, with metal-sulphur contacts in the range 2.697(5)-2.753(5). In contrast the metal is highly distorted tetrahedral in trimeric $\{Ag_3([12]aneS_3)_3\}^{3+}$ and the Ag-S separations are in a wider range 2.480(2)-2.724(2) Å.

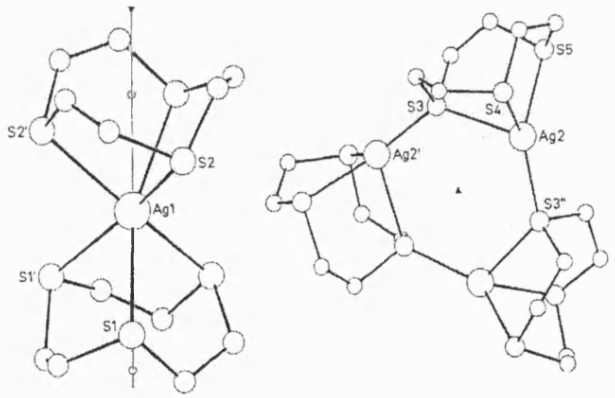

Figure 1. 35 $\{Ag_3([12]aneS_3)_3\}^{3+}$ and $\{Ag([12]aneS_3)_2\}^{+}$

Reaction of $AgNO_3$ with [15]aneS_5 followed by addition of $NaBPh_4$ afforded $[Ag_2([15]aneS_5)_2][BPh_4]_2$[93], (Figure 1.36). One Ag(I) is bound to three sulphurs of one macrocycle (Ag-S = 2.529(4), 2.608(4), 2.907(3) Å) and one of another (Ag-S = 2.537(4) Å) resulting in distorted tetrahedral co-ordination. The second Ag(I) centre is bound to four sulphurs of one thiacrown (Ag-S = 2.558(4), 2.623(5), 2.716(5), 3.131(3) Å) and to one sulphur of the second macrocycle.

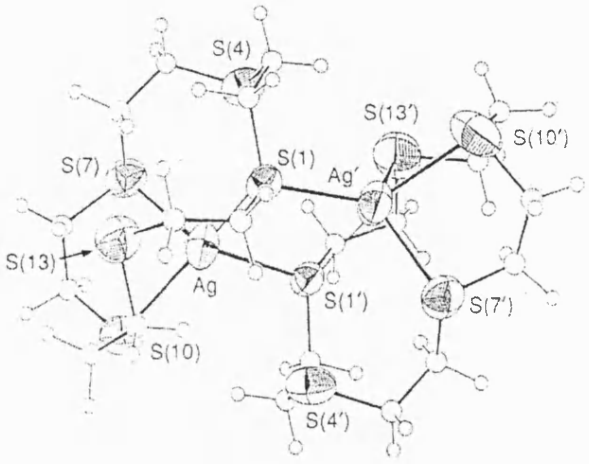

Figure 1. 36 $[Ag_2([15]aneS_5)_2]^{2+}$

Ag(I) also forms complexes with larger thiacrown ligands, such as [18]aneS_6, which is a S-donor equivalent to 18-crown-6. The Ag^+ ion fits inside the cavity of the macrocycle in [Ag([18]aneS_6)]Br, as illustrated in Figure 1.37[94].

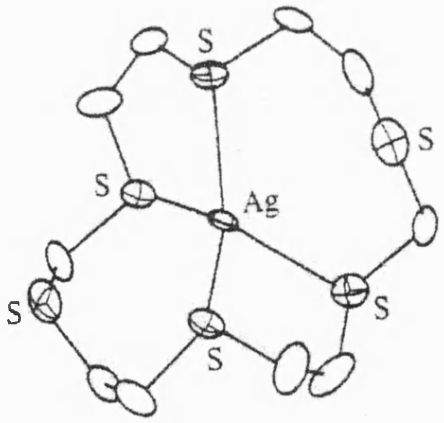

Figure 1. 37 $[Ag([18]aneS_6)]^+$

1.2.5 COMPLEXES OF GOLD(I) CONTAINING SULPHUR-DONOR LIGANDS

The chemistry of "soft" Au(I) with "soft" S-donor ligands is very extensive, not least because of the many industrial and medical applications of these complexes. Much effort has been put into the research of Au(I) thiolates and their phosphine adducts which have notable biomedical uses. For example Myocrysin and Auranofin (Figure 1.38) are effective

anti-rheumatoid arthritis drugs. Gold(I) thiolates are important in "liquid gold" formulations in the ceramics industry and increasingly all areas of gold chemistry are being assessed for catalytic activity. The Au(I) thiolates can be classified into 3 types analogous to those already considered for Ag(I). These are homoleptic thiolates $[Au(SR)]_n$, bisthiolates $[M][Au(SR)_2]$, and phosphine adducts $[(PPh_3)Au(SR)]$.

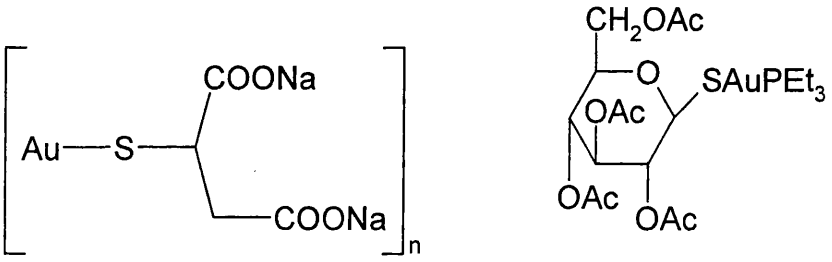

Myocrysin Auranofin

Figure 1. 38

Although Au(III) sulphide, Au_2S_3, is known and provides the only example of a metal that has a higher enthalpy of formation for its sulphide than for its oxide [$\Delta H_f°(Au_2O_3)$ = -13 kJ mol^{-1}, $\Delta H_f°(Au_2S_3)$ = -1116 $kJmol^{-1}$], there are no Au(III) homoleptic thiolates. This is thought to be a result of the highly reducing nature of the $[SR]^-$ group. In fact the earliest preparations of Au(I) thiolates involved reduction of Au(III), usually, "hydrogen" tetrachloroaurate, "$[HAuCl_4]$", with excess thiol. This reaction is effective but potentially expensive if the thiol is not readily available. The preferred high yield preparation involves initial reduction of Au(III) with a sulphide[95], such as methionine[96] or THT[97], and then *in situ* addition of one equivalent of thiol (Figure 1.39).

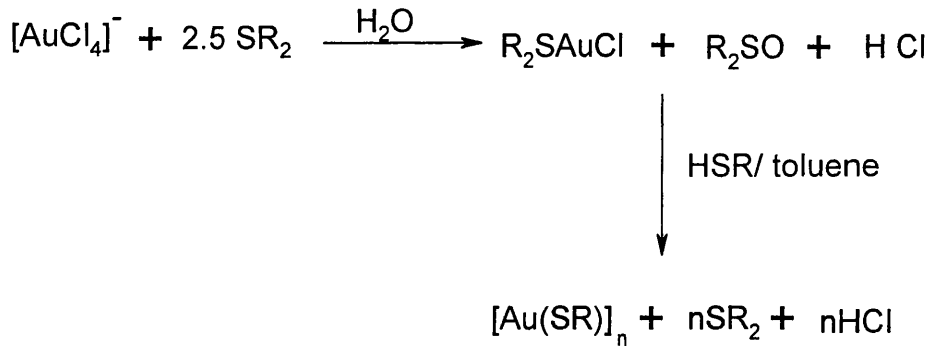

Figure 1.39 General preparation of homoleptic gold(I) thiolates

A large number of $[Au(SR)]_n$ compounds have been prepared by this route but the majority of these compounds are poorly soluble, as noted in an early study by Parish[98] *et al* who isolated $[Au(SR)]_n$ derivatives with R = Et, Pr^i, Bu^n, $(CH_2)_2NH_2$, CH_2CO_2H, Ph, $C_{12}H_{25}$, $C_{18}H_{37}$, C_6H_{11}. However, some substituted aryl thiolates $[Au(C_6H_4\text{-}R')]_n$ (R' = *-p*-Me, *-p*-Et, *-p*-Pr^i, *-p*-Bu^s, *-p*-Bu^t) show limited solubility. A key property of medically active homoleptic Au(I) thiolates is water solubility, and this also generally increases if the thiolate contains carboxylate or hydroxyl groups[99100].

Insolubility is attributed to the homoleptics having polymeric structures composed of two-co-ordinate Au(I) centres. Two co-ordinate halide complexes $[AuX]_n$, where X = halide, have been shown to polymerise via halide bridges, Figure 1.40, which gives credence to this hypothesis.

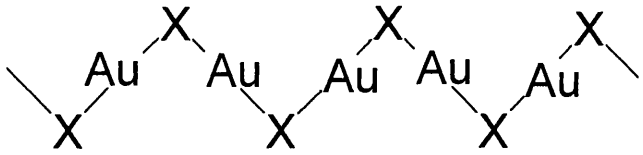

Figure 1.40 Polymeric structure of $[AuX]_n$

As noted above the R group on sulphur plays a significant role in determining the solubility of $[Au(SR)]_n$ complexes. Increased substitution at the α-carbon increases solubility. Thus compounds with a primary α-carbon, e.g. $[Au(SEt)]_n$, have very poor solubility; solubility

increases for those with a secondary α-carbon and compounds with a tertiary α-carbon generally have high organic solubility. In the case of aromatic thiolates an increase in the steric bulk of group in the *para* position tends to increase the solubility of the product in organic media.

Determination of the degree of polymerisation, "n", by structural determination was limited for many years to just three examples considered below. The complex $[Au(SC_6H_4\text{-}2,4,6\text{-}{}^{i}Pr_3)]_6$ was synthesised by reaction of $[Au(CO)Cl]$ with $HSC_6H_4\text{-}2,4,6\text{-}{}^{i}Pr_3$ in ether at -78 °C. This compound can also be prepared at room temperature by the general method illustrated earlier. Its structure is shown in Figure 1.41. The Au_6S_6 core is unlike that found for $[Ag(SR)]_6$ and consists of a 12-membered macrocycle in a chair conformation.

The co-ordination about the metal centre is approximately linear, and there are no significant differences in the Au-S separations in the Au_6S_6 ring. Only two Au...Au contacts at 3.45 Å fall slightly below twice the van der Waals radii of gold (3.50 Å).

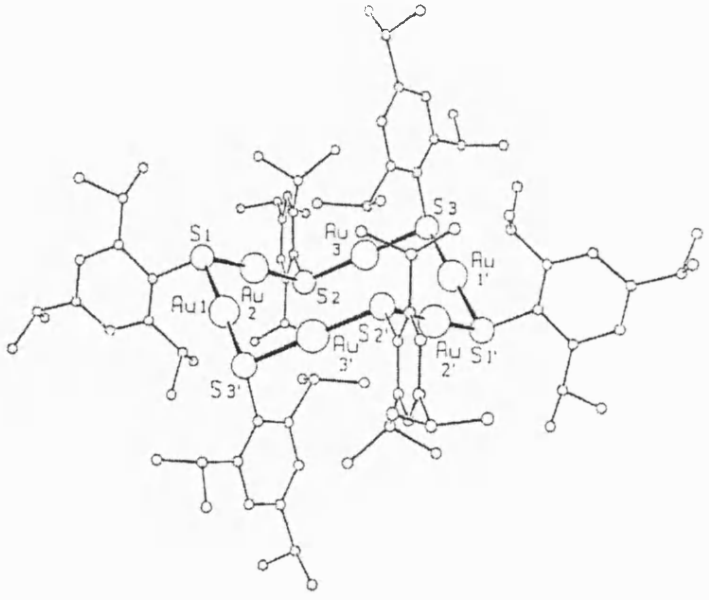

Figure 1.41

Au-S (Å)	Au...Au (Å)	S-Au-S (°)	Au-S-Au (°)
2.285(3)	3.4469(7)	175.4(1)	104.5(1)
2.278(3)	3.6077(7)	176.0(1)	97.6(1)
2.295(3)	3.6379(7)	177.5(1)	105.4(1)
2.285(3)			
2.291(3)			
2.286(3)			

Table 1.7 Selected bond lengths and angles for $[Au(SC_6H_4\text{-}2,4,6\text{-}^iPr_3)]_6$

Both $[Au(SC(SiMe_3)_3)]_4$ and $[Au(SSi(OCMe_3)_3)]_4$ have tetrameric structures containing a square planar Au_4S_4 core (Figure 1.42 and 1.43) analogous to the Ag_4S_4 core of $\{[Ag(SC(SiMe_3)_3]_4\}$ (Figure 1.31). The Au-S contacts are analogous to those of the hexamer, but four Au...Au contacts in each are shorter and within the range accepted for auriophilic interaction (Table 1.8).

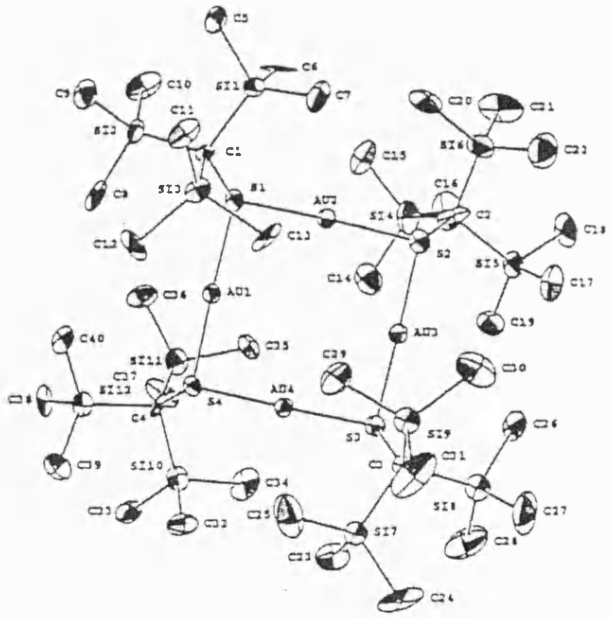

Figure 1.42 The solid state structure of $[Au(SC(SiMe_3)_3)]_4$

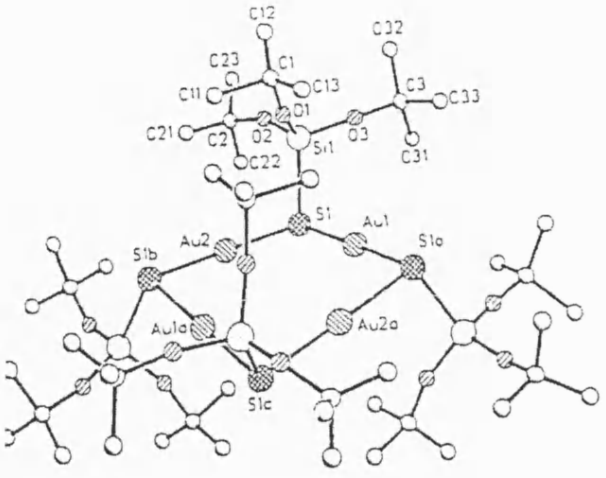

Figure 1.43 Molecular structure $[Au(SSi(OCMe_3)_3)]_4$

	Au-S (Å)	Au...Au (Å)	S-Au-S (°)	Au-S-Au (°)
$[Au(SSi(OCMe_3)_3)]_4$	2.297(5) 2.310(5) 2.309(5) 2.298(5) 2.303(5) 2.315(5) 2.305(5) 2.302(5)	3.30	177.0(2) 177.5(2) 177.1(2) 178.5(2)	92.6(2) 91.4(4) 91.6(2) 91.9(2)
$[Au(SC(SiMe_3)_3)]_4$	2.296(4) 2.284(4)	3.248(1)	178.8(2) 178.3(2)	90.3(2)

Table 1. 8 Selected bond lengths and angles for $[Au(SSi(OCMe_3)_3)]_4$ and $[Au(SC(SiMe_3)_3)]_4$

Bis(thiolato)gold(I) complexes, $[Au(SR)_2]^+[X]^-$, can be synthesised by reaction of tetrahydrathiophene gold chloride with excess thiolate ligand in the presence of an appropriate counter ion (Figure 1.44). The ionic bis-thiolates have significantly better solubility than their homoleptic siblings. Structural analysis of these compounds has shown them to exist as linear two-co-ordinate monomers with no short Au...Au contacts. The Au-S bonds are all typically in the range 2.26-2.29 Å.

$$[Au(THT)Cl] + 2HSR + NH_3 \longrightarrow [NH_4][Au(SR)_2] + HCl + THT$$

$$[NH_4][AuCl_2] + 2HSR \longrightarrow [NH_4][Au(SR)_2] + 2HCl$$

Figure 1.44 Route to $M^+[Au(SR)_2]^-$ complexes

Linear two-co-ordinate derivatives $[(PR_3)Au(SR)]$ which which are generally highly soluble in non-polar solvents are easily prepared by two methods. Firstly reaction of the appropriate homoleptic thiolate with excess phosphine, or alternatively, by reaction of $[(PR_3)AuCl]$ with thiol in the presence of base (Figure 1.45).

$$[Au(SR)]_n + nPPh_3 \longrightarrow [(PPh_3)Au(SR)]$$

$$[(PPh_3)AuCl] + HSR + NH_3 \longrightarrow [(PPh_3)Au(SR)] + NH_4Cl$$

Figure 1. 45

Several of these compounds have been crystallised, and as noted earlier, a key factor that may prevent Au…Au bond formation is the steric bulk of the ligands. Solid-state structures of the series $[(PPh_3)Au(SC_6H_2\text{-}2,4,6\text{-}R_3)]$ [R= H, Et, ^{i}Pr][101] demonstrate this point. Whilst The complex $[(PPh_3)Au(SPh)]$ dimerises through one Au…Au contact of 3.135(3) Å in (Figure 1.46), both $[(PPh_3)Au(SC_6H_2\text{-}2,4,6\text{-}Et_3)]$ and $[(PPh_3)Au(SC_6H_2\text{-}2,4,6\text{-}^iPr_3)]$ are monomeric with all Au…Au separations >> 3.5 Å. In each the P-Au-S arrangements are linear, and the Au-S contacts are all within the narrow range 2.25-2.30 Å.

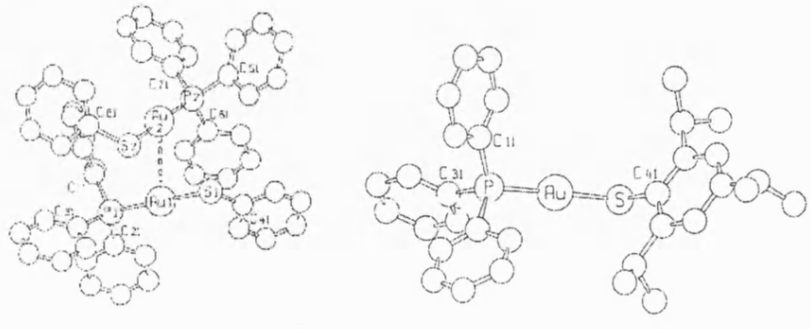

Figure 1. 46 Solid state structures of $[(PPh_3)Au(SPh)]$ and $[(PPh_3)Au(SC_6H_2\text{-}2,4,6\text{-}Et_3)]$

Au(I) also forms hyperaurated complexes with sulphur by reaction of $[PPh_3Au]^+[X]^-$, with a source of S^{2-} (e.g. H_2S) or with the RS^- ion, Figure 1.47. These hypervalent species are stabilised by auriophilic contacts and contain linear two-co-ordinate Au(I) centres, as do their oxygen analogues, Au-S separations are all ≈ 2.30 Å. Typical examples are $\{[(PPh_3)Au]_4S\}\{BF_4\}_2$[102] and $\{[(PPh_3)Au]_4S\}\{OTf\}_2$.[103]

$$[Ph_3PAu]^+OTf^- \xrightarrow{H_2S} [(Ph_3PAu)_nS][OTf]_{n-2} \quad (n = 2,3,4)$$

Figure 1. 47 Route to hypervalent sulphur derivatives

Attempts to prepare Au(I) complexes of thiacrown-ethers, by reaction of $[(THT)_2Au][PF_6]$ with [15]aneS_5, [18]aneS_6, Me_2[18]aneN_2S_4, and [16]aneS_4 yielded 1:1 complexes, in which the preference of the d^{10} Au(I) ion for linear two-co-ordination is exemplified. For example $[Au_2([15]aneS_5)_2][PF_6]_2$, contains two Au(I) atoms co-ordinating to a single sulphur from each thiacrown-ether (Ag-S = 2.30 Å), as illustrated in Figure 1.48. However, in $[Au([18]aneS_6)][PF_6]$, the Au(I) centre is four-co-ordinate through two short Au-S contacts (Au-S = 2.32 Å, S-Au-S = 155.9 °) and two much longer Au-S contacts (2.86 and 2.87 Å), as shown in Figure 1.48.

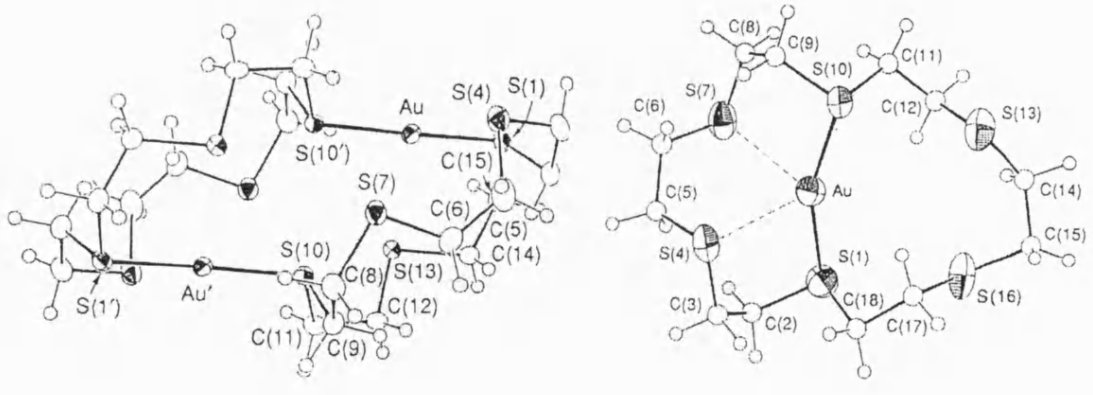

Figure 1. 48 Molecular structure of $[Au([18]aneS_6)][PF_6]$ and $[Au_2([15]aneS_5)_2][PF_6]_2$

1.3 CONCLUSIONS

Secondary metal bonding and the HSAB concept have been shown to play an important role in the chemistry of these two metals. While Au...Au interactions are common and stabilise unusual species such as the hyperaurated complexes, examples of Ag...Ag contacts are found in complexes where bridging ligands support close approach of the metal atoms. Thus for silver this form of secondary bonding is not the significant driving force that it is in gold chemistry.

In comparing the chemistry of Ag(I) and Au(I) with analogous O- and S- donor ligands some general conclusions can be drawn from the literature. The co-ordination chemistry of Ag(I) indicates it to be a true "borderline" metal forming an extensive range of complexes with both O- and S-donors. By contrast Au(I) is softer and forms a considerable range of complexes with "soft" S-donor ligands, but its chemistry with "hard" O-donors is limited to complexes that also contain a soft donor such as phosphine or isocyanide. Even then these complexes are very unstable and readily decompose to a gold film.

Whilst both Ag(I) and Au(I) are d^{10} ions their modes of co-ordination differ considerably. Whilst Au(I) has a strong tendency to form linear, two-co-ordinate complexes which can be explained by formation of *sd*-hybrid orbitals, Ag(I) frequently behaves as the spherical Ag^{+} and accommodates an exceptionally wide range of co-ordination numbers and geometries.

1.4 REFERENCES

[1a)] D. Thompson, *Gold Bulletin*, **31**, 111 (1998); [b)]L. Prati, G. Martra, *Gold Bulletin*, **32**, 96 (1999)

[2a)]C.F. Shaw III, *Chem. Rev.*, **99**, 2589 (1999); [b)] R.V. Parish, *Interdiscip. Sci. Rev.*, **17**, 221 (1992); [c)] C.F. Shaw III, *Gold: Progress in Chemistry, Biochemistry and Technology*, 259, John Wiley & Sons, London (1999)

[3] R.G. Pearson, *J. Am. Chem. Soc.*, **85**, 3533 (1963)

[4] J. Emsley, *The Elements, 3rd Ed.*, Clarendon Press (1998)

[5] F.A. Cotton, G. Wilkinson, *Advanced Inorganic Chemistry 3rd Ed.*, Wiley Interscience, 534 (1972)

[6] D.F. Shriver, P.W. Atkins, C.H. Langford, *Inorganic Chemistry*, OUP, 217 (1989)

[7] S.A. Cotton, *Chemistry of the Precious Metals*, Blackie Academic, 322 (1997)

[8] P. Pyykkö, J.P. Descaux, *Acc. Chem. Res.*, **12**, 226 (1979)

[9] *Handbook of Chemistry and Physics 70th Ed*, F-189, CRC Press (1989)

[10] P. Pyykkö, *Chem. Rev.*, **97**, 597 (1997)

[11] K.P. Hall, D.M.P. Mingos, *Prog. Inorg. Chem.*, **32**, 264 (1984)

[12] P. Pyykkö, Y. Zhao, *Angew. Chem. Int. Ed. Engl.*, **30**, 604 (1991)

[13] M.A. Rawashdeh-Omary, M.A. Omary, H.H. Patterson, *J. Am. Chem. Soc.*, **122**, 10371 (2000)

[14a)] J. Coyle, V. McKee, J. Nelson, *J. Chem. Soc., Chem. Commun.*, 709 (1998); [b)]S.M. Kuang, Z.Z. Zhang, Q.G. Wang, T.C.W. Mak, *J. Chem. Soc., Chem. Comm.*, 581 (1998)

[15a)] S.S. Pathaneni, G.R. Desiraju, *J. Chem. Soc., Dalton Trans.*, 319 (1993); [b)] H. Schmidbaur, W. Graf, G. Müller, *Angew. Chem. Int. Ed. Engl.*, **27**, 417 (1988); [c)] K. Angermaier, E. Zeller, H. Schmidbaur, *J. Organomet. Chem.*, **472**, 371 (1994)

---

[16] D.M.P. Mingos, *J. Chem. Soc., Dalton Trans.*, 561 (1996)

[17] C.E. Briant, B.R.C. Theobald, J.W. White, L.K. Bell, D.M.P. Mingos, *J. Chem. Soc., Chem. Commun.*, 201 (1981)

[18] P.T. Bishop, P.A. Marsh, A.K. Brisdon, B.J. Brisdon, M.F. Mahon, *J. Chem. Soc., Dalton Trans.*, 675 (1998)

[19a)] R.G. Pearson, *Structure and Bonding*, **80,** 1 (1993);[b)] R.G. Pearson, *Chemical Hardness: Applications to Molecules and Solids*, Wiley VCH (1997)

[20] J.L. Gázquez, *Structure and Bonding*, **80,** 28 (1993)

[21] K. Sen, *Structure and Bonding*, **80,** 87 (1993)

[22] R. Parr, R.G. Pearson, *J. Am. Chem. Soc.*, **105**, 1503 (1983)

[23] R.G. Pearson, *Inorg. Chem.*, **27**, 734 (1988)

[24] D. Gibson, B.F.G. Johnson, J. Lewis, *J. Chem. Soc. (A),* 367 (1970)

[25a)] H.G. Smith, R.E. Rundle, *J. Am. Chem. Soc.,* 5075 (1958); [b)] E.A.H. Griffith, E.L. Amma; *J. Am. Chem. Soc.,* 5407 (1974) [c)] T.C.W. Mak, W.C. Ho, N.Z. Huang, *J. Organomet. Chem.*, **251**, 413 (1983)

[26] A.L. Johnson, M.G. Davidson, Unpublished results, University of Bath (2001)

[27] B.T. Usabaliev, E.M. Movsumov, I.R. Amiraslonov, A.I. Akhmedov, A.A. Musaev, K.S. Mamedov, *J. Struct. Chem.*, **22**, 73 (1981)

[28] V. Ogrodnik, Ph.D. Thesis, University Of Bath (1999)

[29] G. Smith, A.N. Reddy, K.A. Byriel, C.H.L. Kennard, *Polyhedron.* **13**, 2425 (1994)

[30] A.E. Blakeslee, J.L. Hoard, *J. Am. Chem. Soc.*, **78**, 3029 (1956)

[31] M.E. Kamwaya, E. Papavinasam, S.G. Teoh, R.K. Rajaram, *Acta Cryst. Sect. C*, **40**, 1318 (1984)

---

[32] D.Y. Naumov, A.V. Virovets, N.V. Podberezskaya, E.V. Boldyreva, *Acta Cryst. Sect. C.*, **51**, 60 (1995)

[33] R.G. Griffin, J.D. Ellet, Jr., M. Mehring, J.G. Bullitt, J.S. Waugh, *J. Chem. Phys.*, **57**, 2147 (1972)

[34] G. Smith, D.S. Sagatys, C.A. Campbell, D.E. Lynch, C.H.L. Kennard, *Aust. J. Chem.*, **43**, 1707 (1990)

[35] T.C.W. Mak, W.H. Yip, C.H.L. Kennard, G. Smith, E.J. O'Reilly, *Aust. J. Chem.*, **41**, 683 (1988)

[36] G. Smith, D.S. Sagatys, C.A. Campbell, D.E. Lynch, C.H.L. Kennard, *Aust. J. Chem.*, **43**, 1707 (1990)

[37] R. Alessio, D.B.D. Amico, F. Calderazzo, U. Englert, A. Guarini, L. Labella, P. Strasser, *Helv. Chim. Acta*, **81**, 219 (1998)

[38] D. Ülkü, M.N. Tahir, E.M. Mozsumov, *Acta Cryst. Sect. C*, **52**, 2678 (1996)

[39] X.M. Chen, T.C.W. Mak, *J. Chem. Soc., Dalton Trans.*, 1219 (1991)

[40] H. Schmidbaur, J. Adlokofer, A. Shiotani, *Chem. Ber.*, **105**, 3389 (1972)

[41a)] R.M. Harker, Ph.D. Thesis, University of Bath (1996); [b)] S.W. Ng, A.H. Othman, *Acta Cryst. Sect. C*, **53**, 1396 (1997)

[42] R. Terroba, M.B. Hursthouse, M. Laguna, A. Mendia, *Polyhedron*, **18**, 807 (1999)

[43] C.S.W. Harker, E.R.T. Tiekink, , *Acta Cryst. Sect. C*, **45**, 1815 (1989)

[44] P.G. Jones, *Acta Cryst. Sect. C*, **49**, 1148 (1993)

[45] D.A. Edwards, R.M. Harker, M.F. Mahon, K.C. Molloy, *J. Chem. Soc., Dalton Trans.*, 3509 (1997)

[46] J.A. Darr, M. Poliakoff, A.J. Blake, W.S., Li, *Inorg. Chem.*, **37**, 5491 (1998)

[47] C. Riche, C. Pascard-Billy, *J. Chem. Soc., Chem. Commun.*, 951 (1975)

M. Koenuma, H. Kinashi, N. Otake, S. Sato, Y. Saito, *Acta Cryst. Sect. B,* **32**, 1267 (1976)

[48] M. Shiro, H. Koyama, *J. Chem. Soc. (B)*, 243 (1970)

[49] M. Alleaume, D. Hickel, *J. Chem. Soc. (B),* 1422 (1970)

[50] M. Koenuma, H. Kinashi, N. Otake, S. Sato, Y. Saito, *Acta Cryst. Sect. B,* **32**, 1267 (1976)

[51a)] A. El Bachiri, A. Hagege, M. Burgard, *J. Membrane Science,* **121,** 159 (1996); [b)] H.J. Buschmann, E. Schillmeyet, *Inorg. Chim. Acta,* **298**, 120 (2000); [c)] H.J. Buschmann, E. Schillmeyet, *J. Electroanal. Chem.,* **474**, 188 (1999)

[52] A.E. Martell, R.D. Hancock, R.J. Motekaitis, *Co-ord. Chem. Rev.,* **133**, 39 (1994)

[53] H.W. Roesky, E. Peymann, J. Schimkowiak, M. Noltemeyer, W. Pinkert, G.M. Sheldrick, *J. Chem. Soc., Chem. Commun.,* 981 (1983)

[54] P. Jones, T. Gries, H. Grutzmacher, H.W. Roesky, J. Schimkowiak, G.M. Sheldrick, *Angew. Chem. Int. Ed. Engl.,* **23**, 376 (1984)

[55] L. Zuacai, S. Meicheng, *Acta Sci. Nat.*, 17 (1987)

[56] P.D. Prince, J.W. Steed, *J. Supra. Chem.,* **10**, 155 (1998)

[57] P.D. Prince, P.J. Cragg, J.W. Steed, *J. Chem. Soc., Chem. Commun.*, 1179 (1999)

[58] A.J. Blake, G. Reid, M. Schroder, *J. Chem. Soc., Chem. Commun.,* 1074 (1992)

[59a)] H.J. Drexler, H. Reinke, H.J. Holdt, *Chem. Ber.* **129**, 807 (1996); [b)] H.J. Drexler, M. Grotjahn, E. Klienpeter, H.J. Holdt, *Inorg. Chim. Acta,* **285**, 305 (1999)

[60] T. Futterer, A. Merz, J. Lex, *Angew. Chem. Int. Ed. Engl.,* **36**, 611 (1997)

[61] K. Hirotsu, I, Miyahara, T. Higuchi, M. Toda, H. Tsukube, K. Matsumoto, *Chem. Let.,* 699 (1992)

[62] W. Liang, S. Liu, R. Lucas, D.O. Miller, *Polyhedron*, **17**, 1323 (1998)

[63a)] C.D. Garner, S.C. Wallwork, *J. Chem. Soc., Chem. Commun.,* 108 (1969); [b)] C.D. Garner, S.C. Wallwork, *J. Chem. Soc. (A),* 3092 (1970);

[64] F. Schindler, H. Schmidbaur, *Angew. Chem. Int. Ed. Engl.*, **6**, 683 (1967)

[65] H. Schmidbaur, *Chem. Soc. Rev.*, 391 (1995)

[66] T. Mathieson, A.G. Langdon, N.B. Milestone, B.K. Nicholson, *J. Chem. Soc., Chem. Commun.*, 371 (1998)

[67] T. Mathieson, A. Schier, H. Schmidbaur, *J. Chem. Soc., Dalton Trans.*, 3881 (2000)

[68] A. Bauer, A. Schier, H. Schmidbaur, *Acta Cryst. Sect. C,* **51**, 2030 (1995)

[69] J.P. Fackler, Jr., M.N.I. Khan, C. King, R.J. Staples, R.E.P. Winpenny, *Organomet.*, **10**, 2178 (1991)

[70] M. Presenberger, A. Schier H. Schmidbaur, *J. Chem. Soc., Dalton Trans.*, 1654 (1999)

[71] P.M.N. Low, Z.Y. Zhang, T.C.W. Mak, T.S.A. Hor, *J. Organomet. Chem.* **539**, 45 (1997)

[72] P.G. Jones, R. Schelbach, *J. Chem. Soc., Chem. Commun.*, 1338 (1988)

[73] P.G. Jones, R. Schelbach, *Inorg. Chem. Acta.*, **182**, 239 (1991)

[74] R. Hehbein, P.G. Jones, K. Meyer-Bäse, E. Scharzmann, G.M. Sheldrick, *Z. Naturforsch, Teil B,* **40**, 1029 (1985)

[75] L.G. Kuz'mina, Y.T. Struchlov, *Koord. Khim.*, **14**, 1262 (1988)

[76] L.G. Kuz'mina, O.Y. Burtsuva, N.V. Dvortsuva, M.A. Porai-Koshita, *Koord. Khim.*, **15,** 773(1989)

[77] L.G. Kuz'mina, Y.T. Struchkov, E.I. Smylova, *Koord. Khim.*, **15**, 368 (1989)

[78] S. Komiya, M. Iwata, T. Sone, A. Fukuoka, *J. Chem. Soc., Chem. Commun.*, 1109 (1992)

[79] T.J. Mathieson, A.G. Langdon, N.B. Milestone, B.K. Nicholson, *J. Chem. Soc., Dalton Trans.*, 201 (1999)

[80] A.N. Nesmeyanov, E.G. Perevalova, Y.T. Struchkov, M.Y. Antipin, K.I. Grandberg, Y.P. Dyadchenko, *J. Organomet. Chem.*, **201**, 343 (1980)

[81] Y. Yang, V. Ramamoorthy, P.R. Sharp, *Inorg. Chem*, **32**, 1946 (1993)

[82] P.G. Jones, *Gold Bull.*, **14**, 102 (1981)

[83] K. Tang, M. Aslam, E. Block, T. Nicholson, J. Zubieta, *Inorg. Chem.*, **26**, 1488 (1987)

[84] W. Wojnowski, M. Wojnowski, K. Peters, E.M. Peters, H.G. von Schnering, *Z. Anorg. Allg., Chem.*, **530**, 79 (1985)

[85] P. Gonzalez-Duarte, J. Sola, j. Vives, X. Solans, *J. Chem. Soc., Chem. Commun.*, 1641 (1987)

[86] I. Dance, *Polyhedron*, **5**, 1037 (1986)

[87] E.Block, D. Macherone, S.N. Shaikh, J. Zubieta, *Polyhedron*, **9**, 1429 (1990)

[88] I.G. Dance, L.J. Fitzpatrick, M.L. Scudder, *Inorg. Chem.*, **23**, 2276 (1984)

[89] I.G.. Dance, l.J. Fitzpatrick, A.D. Rae, M.L. Scudder, *Inorg. Chem.*, **22**, 3785 (1983)

[90] K. Tang, J. Yang, Q. Yang, Y. Tang, *J. Chem. Soc. Dalton Trans.*, 2297 (1989)

[91] A.J. Blake, M. Schröder, *Ad. Inorg. Chem.*, **35**, 1 (1990)

[92] H.J. Küppers, K. Weighardt, Y.H. Tsay, C. Krüger, B. Nuber, J. Weiss, *Angew. Chem. Int. Ed. Engl.*, **26**, 575 (1987)

[93] A.J. Blake, R.O. Gould, G. Reid, M. Schröder, *J. Chem. Soc., Dalton Trans.*, 974 (1990)

[94] P.J. Blower, J.A. Clarkson, S.C. Rawle, J.A.R. Hartman, R.E. Wolf, R. Yagbasan, S.G. Bott, S.R. Cooper, *J. Am. Chem. Soc.*, **28**, 4040 (1989)

[95] A.K. Al-Sa'ady, C.A. Mc Auliffe, R.V. Parish, *Inorganic Syntheses,* Wiley, 191

[96] G. Natile, E. Bordignon, L. Cattalini, *Inorg. Chem.*, **15**, 247 (1976)

[97] R. Uson, A. Laguna, M. Laguna, *Inorganic Syntheses,* Wiley, **26**, 85 (1989)

[98] A.K.H. Al-Sa'ady, K. Moss, C.A. McAuliffe, R.V. Parish, *J. Chem. Soc., Dalton Trans.*, 1609 (1984)

[99] P.A. Marsh, Ph.D. Thesis, University of Bath (1998)

[100] A.A. Isab, P.J. Sadler, *J. Chem. Soc., Dalton Trans,* 1657 (1981)

[101] M. Nakamoto, W. Hiller, H. Schmidbaur, *Chem. Ber.*, **126**, 605 (1993)

[102] H. Schmidbaur, *Chem. Soc. Rev.*, 391 (1995)

[103] F. Canales, M.C. Gimeno, P.G. Jones., A. Laguna, *Angew. Chem. Int. Ed. Engl.*, **33**, 769 (1994)

CHAPTER TWO: CROWN ETHER COMPLEXES OF SILVER(I) SALTS

2.1 INTRODUCTION

This Chapter details the synthesis, characterisation and crystal structures of a range of complexes exhibiting interactions between Ag(I) and the crown-ether ligands 12-crown-4, 15-crown-5, 18-crown-6, benzo-18-crown-6, and dibenzo-18-crown-6. Macrocyclic crown-ethers containing only oxygen donor centres are expected to have a high affinity for metals classified as "hard" Lewis acids. Silver is classified as "borderline soft" by Pearson[1], but its chemistry offers many examples of complexes formed with both anionic O-donor ligands, e.g. $[(PPh_3)Ag(OSO_2CF_3)]$[2], and neutral O-donor ligands, e.g. [Ag(hexafluoropentanedio-nato)$(CH_3O(CH_2CH_2O)_3CH_3)]$[3]. As noted in Chapter One, complexes of Ag(I) with hard donor ligands have ionic character in which the d^{10} Ag^+ ion[4] has no strong preferences for any particular co-ordination number or geometry.

In our studies complex formation involving direct reaction between Ag(I) salts and macrocyclic crown-ethers has been investigated. Structural trends in two series of crown-ether/silver salt complexes have been examined as noted below:

i) By studying the interactions of a single crown-ether, 15-crown-5, with the range of silver salts $AgNO_3$, AgOTf, $AgBF_4$, $AgPF_6$, AgOAc, AgO_2CCF_3 and AgO_2CPh, the effects on complex formation of the silver counter ion, varying from the strongly co-ordinating and bridging acetate to the weakly co-ordinating tetrafluoroborate, have been determined.

ii) By studying the reactions of one silver(I) salt, silver(I) triflate, with the range of crown-ethers 12-crown-4, 15-crown-5, 18-crown-6, benzo-18-crown-6

and dibenzo-18-crown-6, the effects of varying the ring size and rigidity of the crown-ether have been probed.

These two ranges of complexes are summarised below [**C3**, **C7**, **C11**, **C13** & **C15**] and [**C5 – C8**], within the complete series of complexes **C1-C16** which have been synthesised and characterised in this study. The solid-state structures, thermolysis and solution behaviour of several of the complexes will be discussed later in this Chapter. General features of the whole series will also be reviewed.

	$AgBF_4$	$AgPF_6$	AgOTf	$AgNO_3$
12-crown-4	**C1**	**C2**	**C3**	**C4**
15-crown-5	**C5**	**C6**	**C7**	**C8**
18-crown-6	**C9**	**C10**	**C11**	**C12**
benzo-18-crown-6			**C13**	**C14**
dibenzo-18-crown-6			**C15**	**C16**

*** NOTE: The above table does not include all Ag(I) salt/crown-ether combinations investigated.**

Figure 2.1

2.2 SYNTHESIS AND PROPERTIES

Unsubstituted crown-ethers, 12-crown-4, 15-crown-5 and 18-crown-6, all have good solubilities in many common solvents. Monobenzo- and dibenzo-18-crown-6 are more hydrophobic than 18-crown-6, and they are soluble in a more restricted range of solvents. Initially reactions with silver salts were carried out in a range of solvents including methanol, ethanol, DCM and THF. Eventually all reactions were carried out in THF rather than in methanol as favoured by Steed[5] *et al.* Product isolation combined with starting material solubility was found to be most favourable in THF, and yields were in the range 42-87 %. No obvious correlation was found between yields and either the crown-ether or the silver salt used. All of the complexes were isolated as white microcrystalline solids when pure.

The silver(I) materials chosen as starting materials varied from salts of strongly co-ordinating and potentially bridging bidentate anions $[OAc]^-$, $[O_2CCF_3]^-$ and $[O_2CPh]^-$, co-ordinating and potentially bidentate anions $[NO_3]^-$ and $[OTf]^-$, and the poorly co-ordinating anions $[BF_4]^-$ and $[PF_6]^-$. All reactions were carried out with a molar ratio of silver salt to crown-ether of 2:1 as well as with lower mole ratios. The quantities of reactants used and specific experimental details are provided in Chapter 5 of this Thesis.

Reactions of Ag(I) acetate, trifluoroacetate and benzoate with each of the five crown-ethers in either THF or ethanol at room or elevated temperatures yielded only starting materials. Ag(I) benzoate has a low solubility in common solvents, and reactions were carried out using a suspension of the salt, which may have hindered reactivity. However it is more likely that the stable polymeric structure of all these silver(I) carboxylates as discussed in Chapter One, accounts for the lack of reactivity towards crown ethers.

The products of the reactions of $AgNO_3$ and AgOTf with the crown-ethers, 12-crown-4, 15-crown-5 and 18-crown-6 are all soluble in THF and were conveniently precipitated from THF using cyclohexane. Products were finally recrystallised from DCM/hexane at room temperature. They are soluble in DCM, THF, chloroform, ethanol, methanol and water. These complexes are hydrophilic and **C3** and **C4** form stable hydrates.

The products of the reactions of $AgNO_3$ and AgOTf with the crown-ethers benzo-18-crown-6 and dibenzo-18-crown-6 precipitated from THF. These complexes are soluble in warm THF and have some solubility in chlorinated solvents. They were recrystallised from DCM/hexane at room temperature provided this was done quickly and in the absence of moisture.

The products of the reactions of $AgBF_4$ and $AgPF_6$ with the crown-ethers 12-crown-4, 15-crown-5 and 18-crown-6 also precipitated from THF, and were recrystallised from DCM/hexane at room temperature. They are soluble in DCM, chloroform, ethanol, methanol and water. These species are all quite hydrophilic, especially in solution, but they also slowly decompose and turn brown in the solid-state in the presence of moist air and light.

The product of the reaction of 1,1'-dimethylsila-11-crown-4 with $AgBF_4$ precipitated from THF and was found to be analytically pure after washing with cold diethyl ether. The complex was found to be soluble in DCM, chloroform, ethanol, and methanol and was observed to decompose rapidly in solution.

2.3 CHARACTERISATION

Each complex has been characterised by infrared spectroscopy and elemental analysis for carbon, hydrogen, and nitrogen where appropriate. Crystal structure determinations were carried out on **C6**, **C7**, **C8, C11, C13**, and **C15**, and NMR spectra and thermolysis studies were carried out on representative examples of **C3**, **C4**, **C5**, **C6**, **C7**, **C11**, **C13**, and **C15**. The stoichiometry and infrared spectra of the whole series will first be discussed. The remainder of the Chapter will focus on the properties of the two series of Ag(I)/crown-ether complexes.

The hygroscopic nature of these complexes meant that it was difficult to obtain accurate elemental analyses for the anhydrous compounds in all cases, and this is reflected in the analyses obtained for **C3**, **C4**, **C5**, and **C6**, which showed inclusion of water and formation of monohydrates. Infrared data for these complexes showed the presence of co-ordinated water. Slow crystallisation of [Ag(dibenzo-18-crown-6)(OTf)] **C15** from warmed DCM, resulted in the incorporation of a molecule of water and half a molecule of DCM forming [Ag(dibenzo-18-crown-6)(H_2O)][OTf].0.5CH_2Cl_2, **C15a**.

With the exception of **C1**, **C2**, **C3**, **C6** and **C10**, all the complexes possess a 1:1 AgX:crown-ether stoichiometry. Complexes **C1**, **C2** and **C3** (X = BF_4, PF_6 and OTf respectively) each containing 12-crown-4, form 1:2 complexes. These are expected to be analogues of the known hexafluoroarsenate derivative {[Ag(12-crown-4)$_2$]$^+$[AsF_6]$^-$}[6] and although the crystal structures of **C1** and **C2** have not been determined, their infrared spectra are consistent with an analogous ionic formulation. Characteristic ν(C-O)[7] stretches of co-ordinated crown-ether are observed in the range 1300-1000 cm^{-1}, and the IR active ν(B-F)[8] and ν(P-F) [9] stretches of the free anions are reported to be 1070 and 533 cm^{-1} for [BF_4]$^-$ and

865, 835, 559, 530 cm^{-1} for $[PF_6]^-$. IR bands characteristic of tetrahedral $[BF_4]^-$ and octahedral $[PF_6]^-$ are also observed in other complexes containing these anions, {[Ag(15-crown-5)]$^+$[BF_4]$^-$}, **C5**, {[Ag(15-crown-5)]$^+$[PF_6]$^-$}, **C6**, {[Ag(18-crown-6)]$^+$[BF_4]$^-$}, **C9** and {[Ag(18-crown-6)]$^+$[PF_6]$^-$}, **C10**.

The triflate and nitrate anions are more strongly co-ordinating than $[BF_4]^-$ or $[PF_6]^-$ and are able to complex by more than one mode of co-ordination, as illustrated below (Figure 2.2). It is sometimes possible to differentiate between unidentate and bidentate co-ordination from vibrational data as generally the separation of the two highest frequency IR active bands is larger for bidentate co-ordination. Unfortunately the stretches ν(NO) for $[NO_3]^-$[10] at 1370, 828, 695 cm^{-1}, ν(C-F)[11] for ionic $[SO_3CF_3]^-$ at 1120-1350 and 680-780 cm^{-1} and ν(S-O)[8] for $[SO_3CF_3]^-$ at 1165-1213 cm^{-1} overlap with the strong absorptions for the ether modes at ν(CO) 1300-1000 cm^{-1}, so limiting the diagnostic usefulness of this form of spectroscopy.

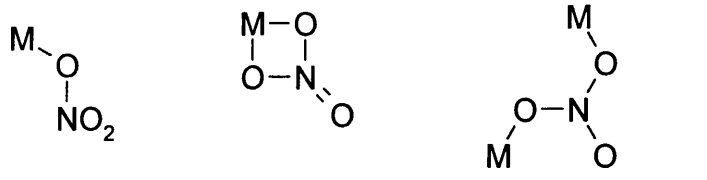

"Unidentate" "Bidentate" "Bridging bidentate"

Figure 2.2

It is very interesting to note that silver nitrate forms a 1:1 complex with 12-crown-4, whereas silver triflate forms a 1:2 complex under similar conditions. The only complexes other than those containing 12-crown-4 that do not form 1:1 complexes are **C6** and **C10**. **C6** analyses as [Ag(15-crown-5)$_2$(H_2O)]$^+$[PF_6]$^-$; the structure of this compound was determined and will be discussed further later in this Chapter. Elemental analysis of **C10**

reveals its stoichiometry to be {[Ag(18-crown-6)][PF_6].0.518-crown-6}. Its structure was not determined but it is possible that the second crown-ether is shared between two [Ag(18-crown-6)][PF_6] units and is hydrogen bonded to the counter ion. For example in [Ag(15-crown-5)$_2$]$^+$[SbF_6]$^{-5}$ the counter ion is involved in a complex array of C-H...F interactions.

2.3.1 ^{1}H- AND ^{13}C- NMR SPECTROSCOPY

The solution behaviour of the representative examples from the two series of Ag(I)-crown-ether complexes **C3**, **C5**, **C6**, **C7**, **C8**, **C11**, **C13** and **C15**, was investigated by NMR in order to gain additional information on their solution state. Both **C13** and **C15** which contain aromatic substituted crown ethers are much less soluble in chlorinated solvents, and this prevented collection of meaningful ^{1}H and ^{13}C NMR data for **C15** and ^{13}C NMR data for **C13** in the same solvent used for data collection for the other complexes.

Compound	^{1}H NMR ($CDCl_3$)/ ppm	^{13}C NMR ($CDCl_3$)/ ppm
C3	3.73, s, 16H, **CH_2**	65.8, s, 8C, **CH_2**
12-crown-4	3.70, s, 16H, **CH_2**	70.2, s, 8C, **CH_2**
C5	3.78, s, 20H, **CH_2**	69.3, s, 10C, **CH_2**
C6	3.72, s, 20H, **CH_2**	69.7, s, 10C, **CH_2**
C7	3.78, s, 20H, **CH_2**	69.5, s, 10C, **CH_2**
C8	3.73, s, 20H, **CH_2**	69.6, s, 10C, **CH_2**
15-crown-5	3.69, s, 20H, **CH_2**	70.3, s, 10C, **CH_2**
C11	3.72, s, 24H, **CH_2**	69.7, s, 12C, **CH_2**
18-crown-6	3.69, s, 24H, **CH_2**	70.4, s, 12C, **CH_2**
C13	3.66-4.12 (20H, m, 10 x **CH_2**)	
	6.77-6.89 (4H, m, 4 x **CH**)	
benzo-18-crown-6	4.11, 3.85, 3.71, 3.66, 3.63	
	(20H, m, 10 x **CH_2**)	
	6.8-7.0, m, (4H, m, 4x **CH**),	

Table 2.1 NMR data

As it is apparent from Table 2.1, both the ^{1}H- and ^{13}C-NMR spectra of each complex in $CDCl_3$ are closely analogous to the spectra of the free crown ether in the same solvent. This indicates that all these complexes probably dissociate in solution. Addition of either another equivalent of 15-crown-5 or of AgOTf, to a $CDCl_3$ solution of **C7,** produced no additional resonances or changes in chemical shifts from those observed in the ^{1}H or ^{13}C-NMR of **C7** in the same solvent.

2.3.2 THERMAL GRAVIMETRIC ANALYSIS

The thermal stability of, **C3**, **C5**, **C6**, **C7**, **C8**, **C11**, **C13** and **C15** were investigated by solid-state Thermal Gravimetric Analysis, TGA. Thermolysis was carried out on finely powdered samples under an atmosphere of nitrogen at a flow rate of 20 cm^3min^{-1}, and the same rate of heating (20 °C min^{-1}). The thermal analyses of complexes **C3**, **C7** and **C11** were also carried out in air in order to observe any differences caused by the presence of oxygen. Weight loss (% w/w) against temperature (°C) is shown for **C3** in air (Figure 2.3). Relevant data for **C3** and all other complexes are tabulated in Table 2.2.

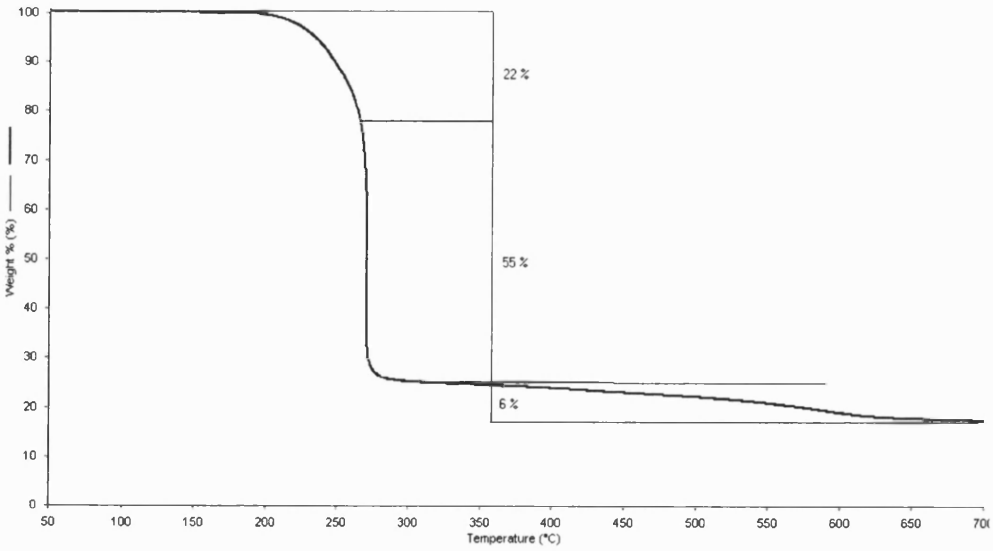

Figure 2.3 TGA data for [Ag(12-crown-4)$_2$][OTf], C3

Very little weight loss occurs for **C3**, or for any of the other anhydrous complexes, below 200 °C. Thereafter thermal decomposition is fast. The initial weight loss of *ca* 22 % for **C3** between 200 and 250 °C corresponds fairly closely to the RMM of the $[CF_3SO_3]^-$ possibly indicating silver oxide or fluoride formation on decomposition of the anion as expulsion of crown commences. At 265 °C, a 55 % weight loss occurs very rapidly corresponding to the loss of the crown ether ligand. The mass of the residue is 24 % of the initial mass, and it is likely to be a silver salt which slowly decomposes between 270 and 625 °C (Figure 2.3) to silver (found 19.0 %, calculated 18.7 %). Microanalyses of **C3**, **C5**, **C6** and **C15** showed them to be hydrated and this is apparent from their thermolysis in which an initial weight loss of 2-4 % occurs just above 100 °C.

		N_2 (20 cm^3min^{-1})				Air (20 cm^3min^{-1})			
	W_{Ag} (%)	T_{10} (°C)	T_{50} (°C)	T_{dec} (°C)	W_{dec} (%)	T_{10} (°C)	T_{50} (°C)	T_{dec} (°C)	W_{dec} (%)
C3	17.6	225	255	490	18	245	270	680	17
C5	24.7	310	330	720	21				
C6	15.4	275	310	360	15				
C7	22.4	240	250	480	22	250	255	430	23
C8	27.4	280	295	420	27				
C11	20.5	260	265	495	21	255	260	435	19
C13	18.8	300	315	720	21				
C15	17.3	300	305	710	20				

Table 2.2 [W_{Ag}= % Ag mass of complex, T_{10} = temperature after 10% wgt loss, T_{50} = temperature after 50% wgt loss, T_{dec} = Temperature after total decomposition, W_{dec} = mass of solid left after complete decomposition]

Thereafter all eight complexes appear to decompose in a similar way to **C3**. The thermolysis of complexes **C3**, **C7** and **C11** in air showed no notable differences from

studies in nitrogen below 300 °C. The only significant differences occur at high temperature where **C3** continues to decompose up to 680 °C in air compared to T_{dec} of 480 °C in N_2.

2.3.3 SOLID-STATE STRUCTURAL STUDIES

Solid-state structure determinations have been carried out on one series of complexes formed between 15-crown-5 and the three silver salts AgX, where X= $[NO_3]^-$, $[PF_6]^-$ and $[OTf]^-$, and on a second series of complexes formed between silver triflate and the crown-ethers 15-crown-5, benzo-18-crown-6 and dibenzo-18crown-6. These studies revealed the structural characteristics of a representative cross-section of Ag(I)-oxacrown ether complexes, so permitting trends to be discerned.

2.3.3.1 STRUCTURAL COMPARISON OF 15-CROWN-5 DERIVATIVES OF THREE SILVER SALTS

By varying the counter ion in Ag(I) complexes of 15-crown-5, we intended to observe the effects of anion type on solid-state structure. X-ray crystallographic studies on each of the products resulting from the direct reaction of 15-crown-5 with $AgPF_6$, AgOTf, and $AgNO_3$. Complex **C5**, formed by reaction between 15-crown-5 and $AgBF_4$, was also prepared and crystallised, but it decomposed over a few days.

Molecular Structure of[Ag(15-crown-5)(H_2O)][15-crown-5][PF_6], C6

The salt $AgPF_6$ reacted in THF with 15-crown-5 in a 1:1 ratio to afford a white powdery product, and on cooling the remaining reaction solution to 5 °C, X-ray quality crystals precipitated. Both powder and crystals incorporated water and analysed as {[Ag(15-crown-5)(H_2O)]$^+$[15-crown-5][PF_6]$^-$}, **C6**, (Figure 2.4). These crystals were found to be air and moisture sensitive, and X-ray data were collected at low temperature. Selected bond angles

and distances are summarised in Tables 2.3 and 2.4, respectively. Further structural data are provided in Appendix 1.

The central Ag(1) atom in **C6** is six co-ordinate but the geometry cannot be described as either octahedral or trigonal prismatic. Ag(1) sits above the centre of one crown to which it is co-ordinated through five Ag-O interactions of between 2.515(4) and 2.693(4) Å (Table 2.3). It also binds to one water molecule through a much shorter Ag-O interaction of 2.327(4) Å. The co-ordinated water molecule is hydrogen-bonded to a second 15-crown-5, through two O-H...O bonds of 2.07Å (H(11A)-O(7) & H(11B)-O(10)). No abnormally short contacts were observed between adjacent molecules. Similar H-bonding between a metal-ligated water molecule and a "free" crown-ether has been observed in a number of metal crown-ether complexes including {[Li(benzo-15-crown-5)(H_2O)]$_2$[Cu_4I_6].2(benzo-15-crown-5)}[12], {[$VOCl_2(OH)_2$].18-crown-6.2H_2O}[13], {$Eu(NO_3)_3(OH_2)_3$].18-crown-6}[14], and {[$UO_2Cl_2(OH_2)_2$(12-crown-4)].12-crown-4}.[15] As noted earlier in this Chapter infrared spectra of this complex indicates the presence of ionic $[PF_6]^-$, in keeping with the solid state structure.

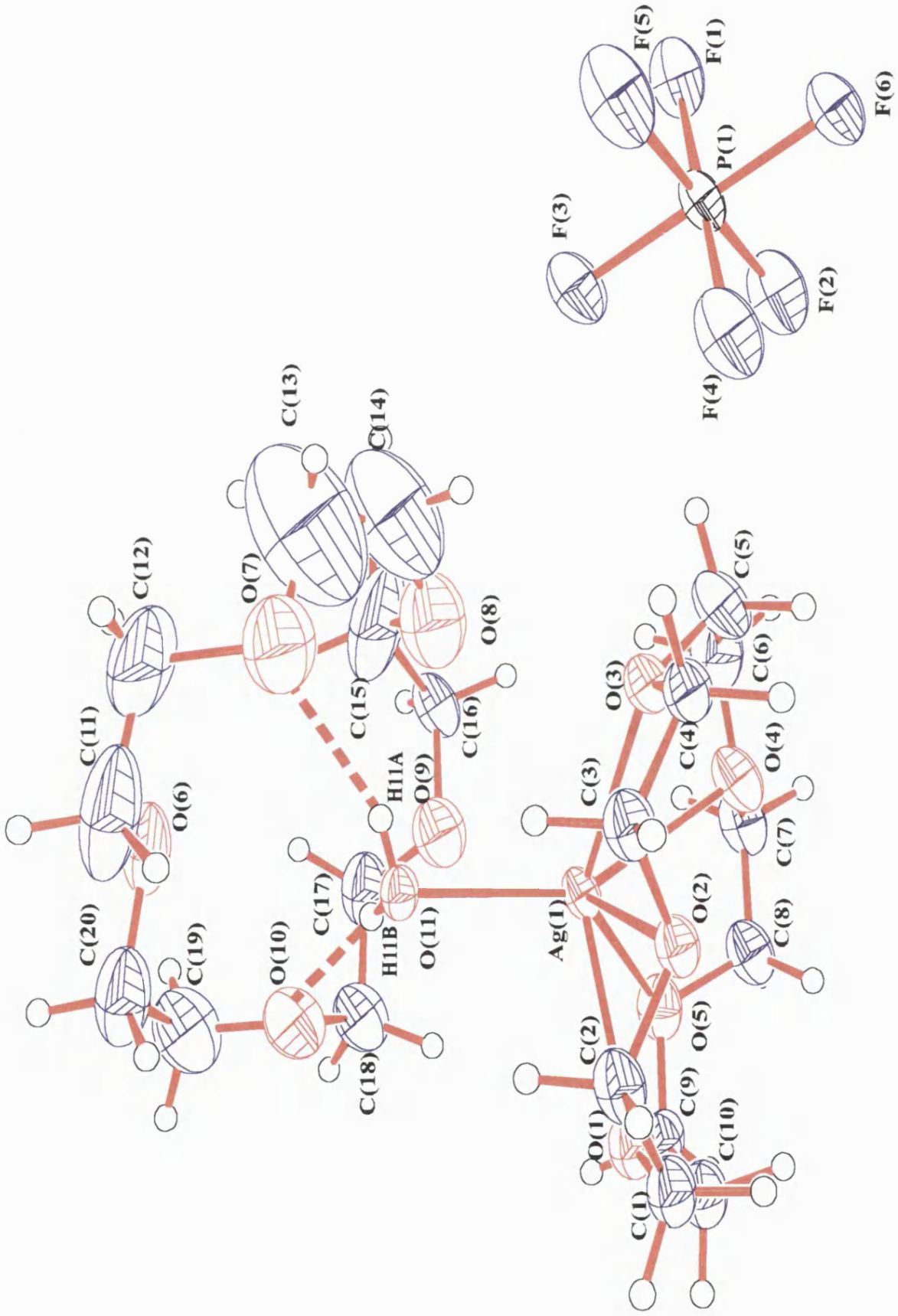

Figure 2. 4 The molecular structure of C6

Bond	Length (Å)
Ag(1)-O(1)	2.614(4)
Ag(1)-O(2)	2.693(4)
Ag(1)-O(3)	2.564(4)
Ag(1)-O(4)	2.495(4)
Ag(1)-O(5)	2.515(4)
Ag(1)-O(11)	2.327(4)

Table 2.3 Selected bond lengths for C6

Atoms	Angle (°)	Atoms	Angle (°)
O(11)-Ag(1)-O(4)	150.4(2)	O(4)-Ag(1)-O(1)	112.11(14)
O(11)-Ag(1)-O(5)	135.0(2)	O(5)-Ag(1)-O(1)	66.12(13)
O(4)-Ag(1)-O(5)	68.23(14)	O(3)-Ag(1)-O(1)	126.09(13)
O(11)-Ag(1)-O(3)	90.8(2)	O(11)-Ag(1)-O(2)	85.63(13)
O(4)-Ag(1)-O(3)	66.08(14)	O(4)-Ag(1)-O(2)	98.98(13)
O(5)-Ag(1)-O(3)	133.61(14)	O(5)-Ag(1)-O(2)	117.36(12)
O(11)-Ag(1)-O(1)	96.19(14)	O(3)-Ag(1)-O(2)	63.62(12)

Table 2.4 Selected bond angles for C6

Molecular Structure of [Ag(15-crown-5)(OTf)], C7

X-ray diffraction quality crystals of [Ag(15-crown-5)(OTf)], **C7**, were also grown from a dichloromethane solution stored at 5 °C for one week. These crystals were found to be air and moisture stable, and for this complex data were collected at room temperature. The molecular structure of **C7** is shown in Figure 2.5. Selected bond angles and distances are summarised in Tables 2.5 and 2.6, respectively. Further structural data are provided in Appendix 1.

Complex **C7** has a monoclinic unit cell, with half a molecule per asymmetric unit. The complex has a mirror plane defined by the atoms Ag(1), O(1), O(5), S(1) and F(1). The metal centre is bonded to five oxygens of the crown-ether and two oxygens from the bidentate triflate. The geometry about the silver cannot be described as any of the standard seven-co-ordinate geometries (pentagonal bipyramid or capped octahedral or capped trigonal prismatic). The silver atom is raised above the plane created by the five coplanar oxygens of the crown by 1.38 Å. The Ag-O_{ether} separations are in the range 2.479(3) - 2.554(3) Å compared to the notably longer Ag(I)...$O_{triflate}$ separation of 2.655(3) Å.

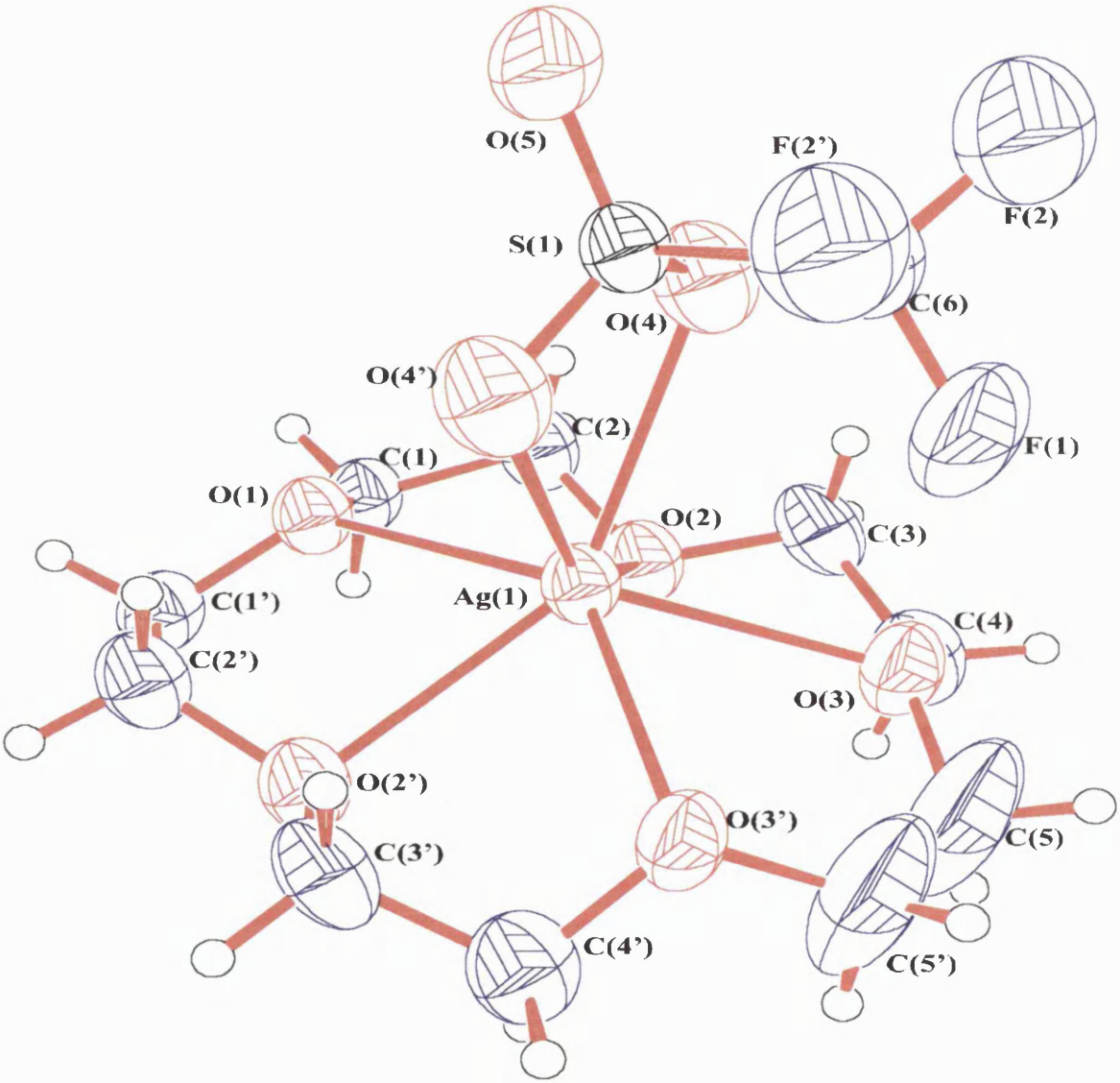

Figure 2.5 Molecular structure of C7

Bond	Length (Å)
Ag(1)-O(1)	2.512(3)
Ag(1)-O(2)	2.554(3)
Ag(1)-O(2')	2.554(3)
Ag(1)-O(3)	2.479(3)
Ag(1)-O(3')	2.479(3)
Ag(1)-O(4)	2.655(3)
Ag(1)-O(4')	2.655(3)

Table 2.5 Selected bond lengths for C7

Atoms	Angle (°)	Atoms	Angle (°)
O(3)'-Ag(1)-O(3)	68.83(13)	O(1)-Ag(1)-O(4)'	98.95(10)
O(3)-Ag(1)-O(2)	67.85(9)	O(2)'-Ag(1)-O(4)'	94.96(9)
O(1)-Ag(1)-O(2)	66.92(7)	O(2)-Ag(1)-O(4)'	144.05(10)
O(2)-Ag(1)-O(2)'	107.85(12)	O(3)-Ag(1)-O(4)'	122.17(10)
O(4)'-Ag(1)-O(4)	53.15(14)	O(3)-Ag(1)-O(4)	91.53(10)
O(4)-S(1)-O(4)'	112.6(3)	O(5)-S(1)-O(4)	116.0(2)
S(1)-O(4)-Ag(1)	96.9(2)	O(5)-S(1)-O(4)'	116.0(2)

Table 2.6 Selected bond angles for C7

Molecular Structure of {[Ag(15-crown-5)]$^+$[NO$_3$]$^-$}, C8

Suitable crystals of {[Ag(15-crown-5)]$^+$[NO_3]$^-$}, **C8**, for X-ray studies were grown as for **C7**. Data on these air and moisture sensitive crystals were collected at room temperature. The molecular structure of **C8** is shown in Figure 2.6 and selected bond lengths and angles are summarised in Tables 2.7 and 2.8, respectively with further structural data located in Appendix 1.

The solid-state structure of **C8** shows the central Ag(1) atom to be 7-co-ordinate, though the geometry around the metal has low symmetry as in **C7**. As in the previous complex Ag(1) is bonded to all five oxygens of the crown-ether, with the Ag-O separations in the range 2.519(6) - 2.635(6) Å, and it is unsymmetrically bound to the bidentate nitrate group, with Ag-O separations of 2.420(6) and 2.566(7) Å.

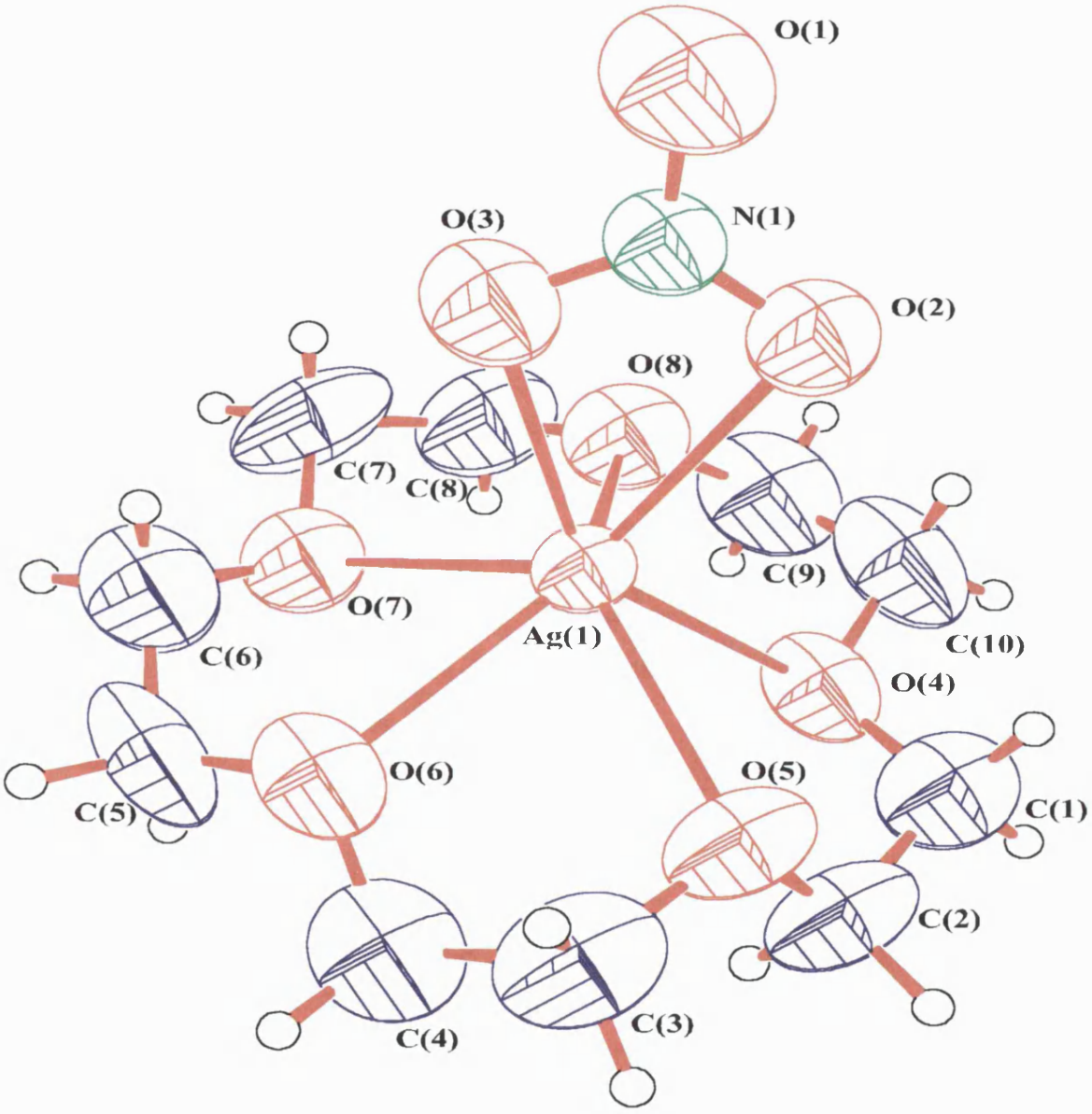

Figure 2. 6 Molecular structure of C8

Bond	Length (Å)
Ag(1)-O(1)	2.420(6)
Ag(1)-O(2)	2.566(7)
Ag(1)-O(4)	2.635(6)
Ag(1)-O(5)	2.466(6)
Ag(1)-O(6)	2.519(6)
Ag(1)-O(7)	2.534(7)
Ag(1)-O(8)	2.573(6)

Table 2. 7 Selected bond lengths for C8

Atoms	Angle (°)	Atoms	Angle (°)
O(1)-Ag(1)-O(5)	103.4(2)	O(5)-Ag(1)-O(2)	136.3(2)
O(1)-Ag(1)-O(6)	125.9(3)	O(6)-Ag(1)-O(2)	98.7(2)
O(5)-Ag(1)-O(6)	68.8(3)	O(7)-Ag(1)-O(2)	99.9(2)
O(1)-Ag(1)-O(7)	144.4(2)	O(1)-Ag(1)-O(8)	95.8(3)
O(5)-Ag(1)-O(7)	112.1(2)	O(5)-Ag(1)-O(8)	127.8(2)
O(6)-Ag(1)-O(7)	67.9(2)	O(6)-Ag(1)-O(8)	132.3(3)
O(1)-Ag(1)-O(2)	49.0(2)	O(7)-Ag(1)-O(8)	64.5(3)
		O(2)-Ag(1)-O(8)	92.2(2)

Table 2. 8 Selected bond angles for C8

The single example of a Ag(I) complex of 15-crown-5 together with the three examples of Ag(I) complexes of the 15-crown-5 derivatives, benzo-15-crown-5, aza-15-crown-5 and *N*-allylaza-15-crown-5 reported by J. Steed's group[5ab], make interesting comparisons with the structures of **C6**, **C7**, and **C8** reported herein. $\{[Ag(15\text{-crown-}5)_2]^+[SbF_6]^-\}$[17a] and $\{[Ag(benzo\text{-}15\text{-crown-}5)_2]^+[SbF_6]^-\}$, which were formed by direct reaction of $AgSbF_6$ with the oxacrown-ether in methanol in quantitative yields, adopt sandwich structures, (Figure 2.7), and in this respect are analogous to that of $[Ag(12\text{-crown-}4)_2][AsF_6]$[5].

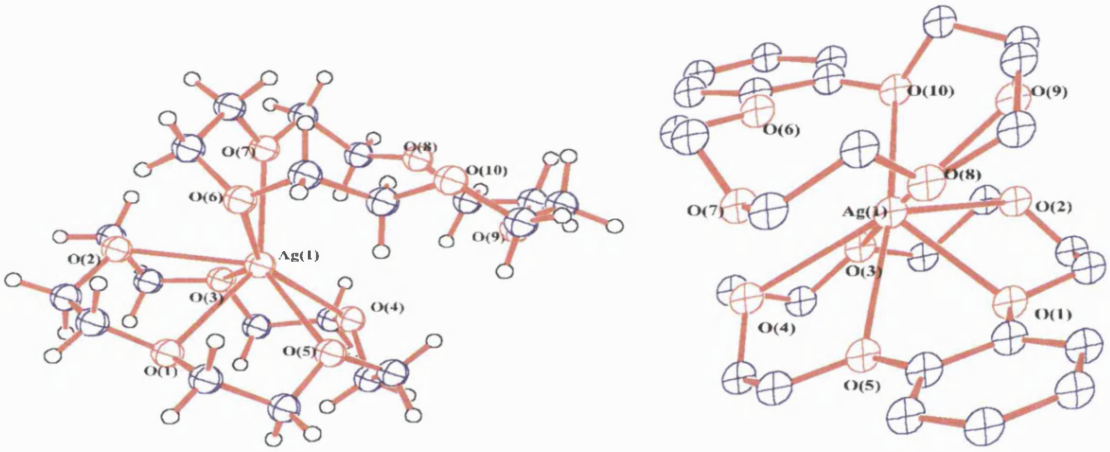

Figure 2. 7 $\{[Ag(15\text{-crown-}5)_2]^+$ and $\{[Ag(benzo\text{-}15\text{-crown-}5)_2]^+$

The central Ag(I) atom in both 15-crown-5 and benzo-15-crown-5 complexes were shown to be seven-co-ordinate, binding to all five oxygen atoms of one crown-ether, and to two O-atoms of the other. The co-ordination is noted to be "highly unsymmetrical", and the Ag-O separations in $\{[Ag(15\text{-crown-}5)_2]^+[SbF_6]^-\}$ are in the range 2.537(2)-2.633(2) Å, whilst those for $\{[Ag(benzo\text{-}15\text{-crown-}5)_2]^+[SbF_6]^-\}$ they are 2.597(7)-2.751(7) Å. The two oxygens donated by the second crown ether replace the co-ordination sites filled by a molecule of water in **C6** and by the anion in **C7** and **C8**.

The ranges of Ag-O_{ether} separations for **C6**, **C7** and **C8** are 2.495(4)-2.693(4) Å, 2.479(3)-2.554(3) Å and 2.466(6)-2.635(6) Å, respectively. Thus each of the three complexes **C6**, **C7** and **C8** exhibit Ag-O contacts that are shorter than any found in {[Ag(15-crown-5)$_2$]$^+$[SbF_6]$^-$}. In addition complex **C7** has five extremely short Ag-O_{ether} bonds.
An uncertanty in discussing "bond" lengths is the distinction between an Ag-O bonding interaction and a non-bonding Ag...O separation, since some O_{ether} centres will be held close to a metal centre by conformational constraints but may not interact with it at all. In the case of the two [SbF_6]$^-$ complexes[17ab] the non-bonding Ag-O_{ether} separations are reported to be >3.0 Å. As described earlier in this Chapter we consider an Ag-O bonding separation to be less than the combined van der Waals radii of the two elements which is 3.10 Å.[16] Interestingly in {[Ag(15-crown-5)$_2$]$^+$[SbF_6]$^-$} two of the three uncoordinated O_{ether} are directed away from, rather than towards, the metal centre and form intermolecular C-H...O interactions of 2.51 Å. The conformation of the ring in {[Ag(benzo-15-crown-5)$_2$]$^+$[SbF_6]$^-$} and in **C6**, **C7** and **C8** prevent this possibility, and no intermolecular interactions were observed.

Steed's group[17ab] extended their studies of non-complementary host-guest studies to complexes formed between Ag(I) and aza-15-crown-5. Direct reactions of aza-15-crown-5 and *N*-allylaza-15-crown-5 with $AgSbF_6$ in methanol yielded 2:1 and 1:1 complexes respectively. In {[Ag(aza-15-crown-5)][SbF_6]}, the metal centre is six-co-ordinate, binding to one N and four O-donors of one crown, and to just the N atom of the other. Again the co-ordination geometry around the metal is of low symmetry. The preference of the metal for N-donors is demonstrated by the shortness of the two Ag-N contacts at 2.304(2) and 2.2759(19) Å. The Ag-O separations are notably longer in both azacrown complexes (2.6807(16)-2.7199(16) Å), compared with those found in the oxacrown complexes

synthesised in our study, and those reported in the literature[17b]. Two oxygens of the second azacrown form intermolecular C-H...O hydrogen bonds of 2.58 and 2.62 Å.

The metal centre in {[Ag(*N*-allylaza-15-crown-5)][SbF_6]} is seven-co-ordinate being bound to the four oxygens of the azacrown (Ag-O in the range 2.400(2)-2.773(3)) and to the azacrown nitrogen (Ag-N = 2.515(4) Å). However the metal is also bound intermolecularly to the two carbons of the allyl unit of an adjacent complex (Ag-C of 2.363(4) and 2.393(4), resulting in the formation of a co-ordination polymer.

The aim of this first part of the study on crown-ethers was to investigate the effect of varying the counter ion on Ag(I) complexes of 15-crown-5. In each of the three 15-crown-5 complexes **C6**, **C7** and **C8** the Ag(I) is co-ordinated to all five oxygens of the crown. The Ag-O separations are significantly shorter than their combined van der Waals radii (3.10 Å) and comparable to those found in other 15-crown-5 complexes, though longer than those in silver oxides (2.05 - 2.29 Å)[17]. We have observed that co-ordination of the anions $[NO_3]^-$ and $[OTf]^-$ is preferred to the co-ordination of a second crown-ether as occurs in $[Ag(15\text{-crown-}5)_2]^+[SbF_6]^-$. In complex **C6** the counter-ion does not co-ordinate, but a molecule of water incorporated during recrystallisation preferentially binds to the metal and H-bonds to a second crown-ether which is not bonded to the metal.

As discussed earlier in this Chapter, the co-ordination behaviour exhibited in these complexes by Ag(I) is analogous in some respects to that of an alkali metal. The spherical silver cation has no strong preferences for particular co-ordination geometries, so explaining the structural diversity provided by our studies as well as those of others.

In each of the complexes reported by Steed, the $[SbF_6]^-$ anion plays a significant role in crystal packing through a large number of C-H...F interactions. Neither **C6**, **C7** or **C8** display any significant counter-ion interactions of this type nor do **C6**, **C7** or **C8** have any other notable intermolecular interactions in their solid-state structures.

2.3.3.2 STRUCTURAL COMPARISON OF CROWN-ETHER DERIVATIVES OF SILVER TRIFLATE

By complexing a single silver(I) salt, silver(I) triflate, with a range of crown-ethers, 12-crown-4, 15-crown-5, 18-crown-6, benzo-18-crown-6 and dibenzo-18-crown-6, we intended to observe the effects of varying the ring size and rigidity of the crown-ether on the stoichiometry of the products and their solid-state structures. X-ray structure studies have now been determined on each of the products resulting from the direct reaction of 15-crown-5, 18-crown-6, benzo-18-crown-6 and dibenzo-18-crown-6 with AgOTf.

The complex **C3**, formed by reaction between 12-crown-4 and AgOTf, was also prepared and crystallised from both DCM and cyclohexanone but attempts at determining its structure failed due to crystal twinning. The solid-state structure of [Ag(15-crown-5)(OTf)], **C7**, which was discussed in the previous section of this Chapter, will be included in the comparison with the other complexes in this series.

Molecular Structure of [Ag(18-crown-6)(OTf)], C11

X-ray diffraction quality crystals of [Ag(18-crown-6)(OTf)], **C11**, were grown by slow evaporation of a dichloromethane solution held at 5 °C over 2 months. These crystals were found to be air and moisture sensitive and data were collected at 26.5 K. The molecular structure of **C11** is shown in Figure 2.8, and selected bond lengths and angles are summarised in Tables 2.9 and 2.10, respectively. Further structural data are provided in Appendix 1.

Complex **C11** has an orthorhombic unit cell, with four molecules unit cell. The seven-co-ordinate silver like previous examples, is of low symmetry. The metal centre is bonded to all six oxygens of the 18-crown-6 and one oxygen of the unidentate triflate completes the

ordination sphere. The Ag-O_{ether} separations are in the range 2.602(3) - 2.771(3) Å and the Ag-$O_{triflate}$ interaction is much shorter at 2.355(3) Å. No long range intermolecular interactions are observed.

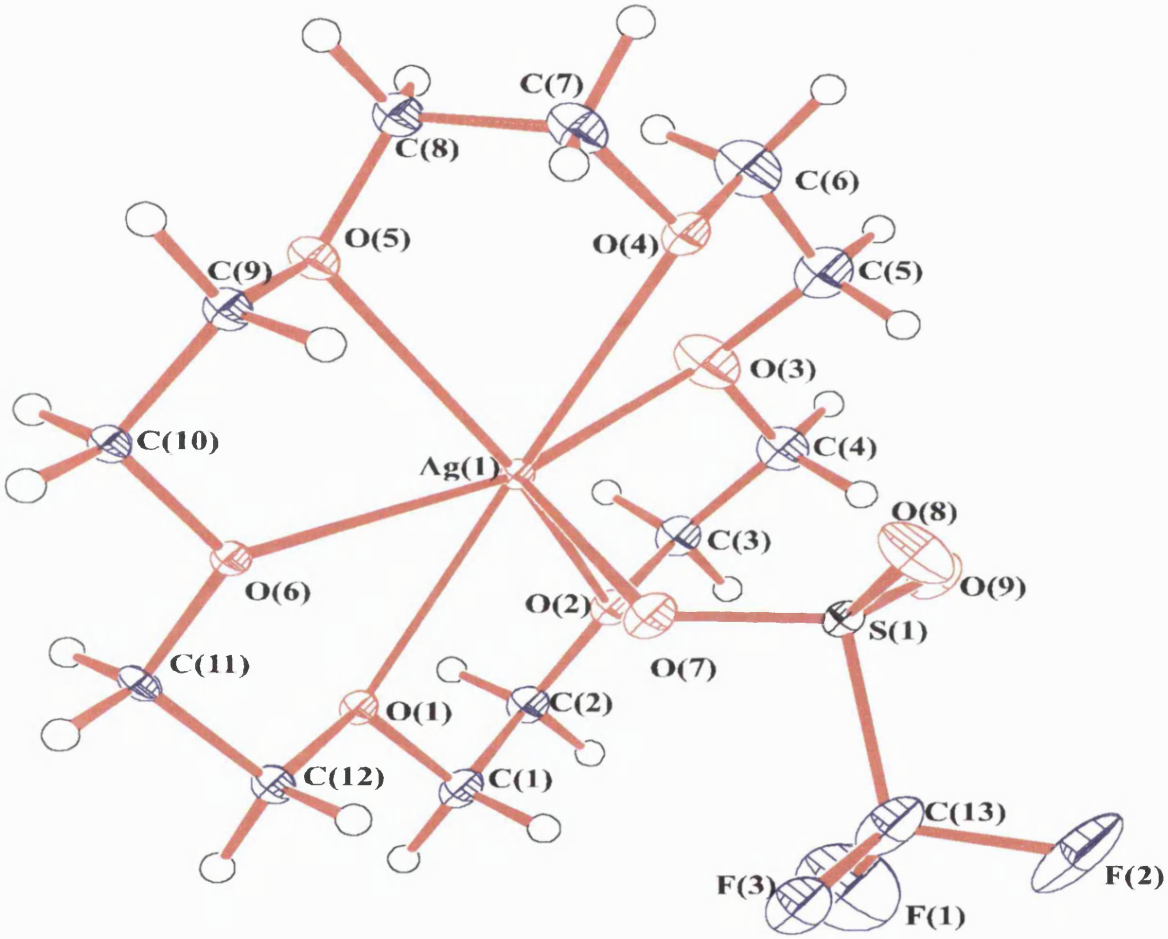

Figure 2.8 Molecular structure of C11

Bond	Length (Å)
Ag(1)-O(1)	2.771(3)
Ag(1)-O(2)	2.619(3)
Ag(1)-O(3)	2.602(3)
Ag(1)-O(4)	2.736(3)
Ag(1)-O(5)	2.733(3)
Ag(1)-O(6)	2.680(3)
Ag(1)-O(7)	2.355(3)

Table 2.9 Selected bond lengths for C11

Atoms	Angle (°)	Atoms	Angle (°)
O(7)-Ag(1)-O(3)	114.95(12)	O(7)-Ag(1)-O(2)	98.78(10)
O(3)-Ag(1)-O(2)	63.37(10)	O(7)-Ag(1)-O(6)	79.64(9)
O(3)-Ag(1)-O(6)	164.87(10)	O(2)-Ag(1)-O(6)	120.51(9)
O(7)-Ag(1)-O(5)	108.50(11)	O(3)-Ag(1)-O(5)	107.66(10)
O(2)-Ag(1)-O(5)	152.24(9)	O(6)-Ag(1)-O(5)	61.62(8)
O(7)-Ag(1)-O(4)	87.16(10)	O(3)-Ag(1)-O(4)	64.13(11)
O(2)-Ag(1)-O(4)	124.33(9)	O(6)-Ag(1)-O(4)	115.03(9)
O(5)-Ag(1)-O(4)	63.58(9)	O(7)-Ag(1)-O(1)	86.87(9)
O(3)-Ag(1)-O(1)	122.21(10)	O(2)-Ag(1)-O(1)	60.64(8)
O(6)-Ag(1)-O(1)	59.89(8)	O(5)-Ag(1)-O(1)	114.82(8)
O(4)-Ag(1)-O(1)	172.83(9)		

Table 2.10 Selected bond angles for C11

Molecular Structure of [Ag(benzo-18-crown-6)(OTf)], C13

[Ag(benzo-18-crown-6)(OTf)], **C13,** was dissolved in warmed chloroform and then slowly cooled to ice-bath temperatures, so yielding X-ray diffraction quality crystals which were found to be air and moisture stable. Data on this complex were collected at 170 K. The molecular structure of **C13**, is shown in Figure 2.9. Selected bond lengths and angles are summarised in Tables 2.11 and 2.12, respectively. Further structure data are given in Appendix 1.

Complex **C13** has a monoclinic unit cell, with 4 molecules unit cell. The central Ag(1) is nine-co-ordinate. Ag(1) is co-ordinated to all six oxygens of benzo-18-crown-6 ($Ag\text{-}O_{ether}$ in the range 2.668(3) - 2.991(3) Å), and to an oxygen atom of the unidentate triflate ligand (Ag-O = 2.4189(17)). The co-ordination sphere is completed by the two carbon atoms of the arene ring of an adjacent complex, (Ag-C = 2.618(2) and 2.822(2) Å). The resulting dimerisation of the two complexes through two short Ag(1)...C(7) contacts has a noticeable affect on the C-C bond lengths of the arene. The ring exhibits alternating long and short separations suggesting a degree of triene character in the ring rather than complete delocalisation.

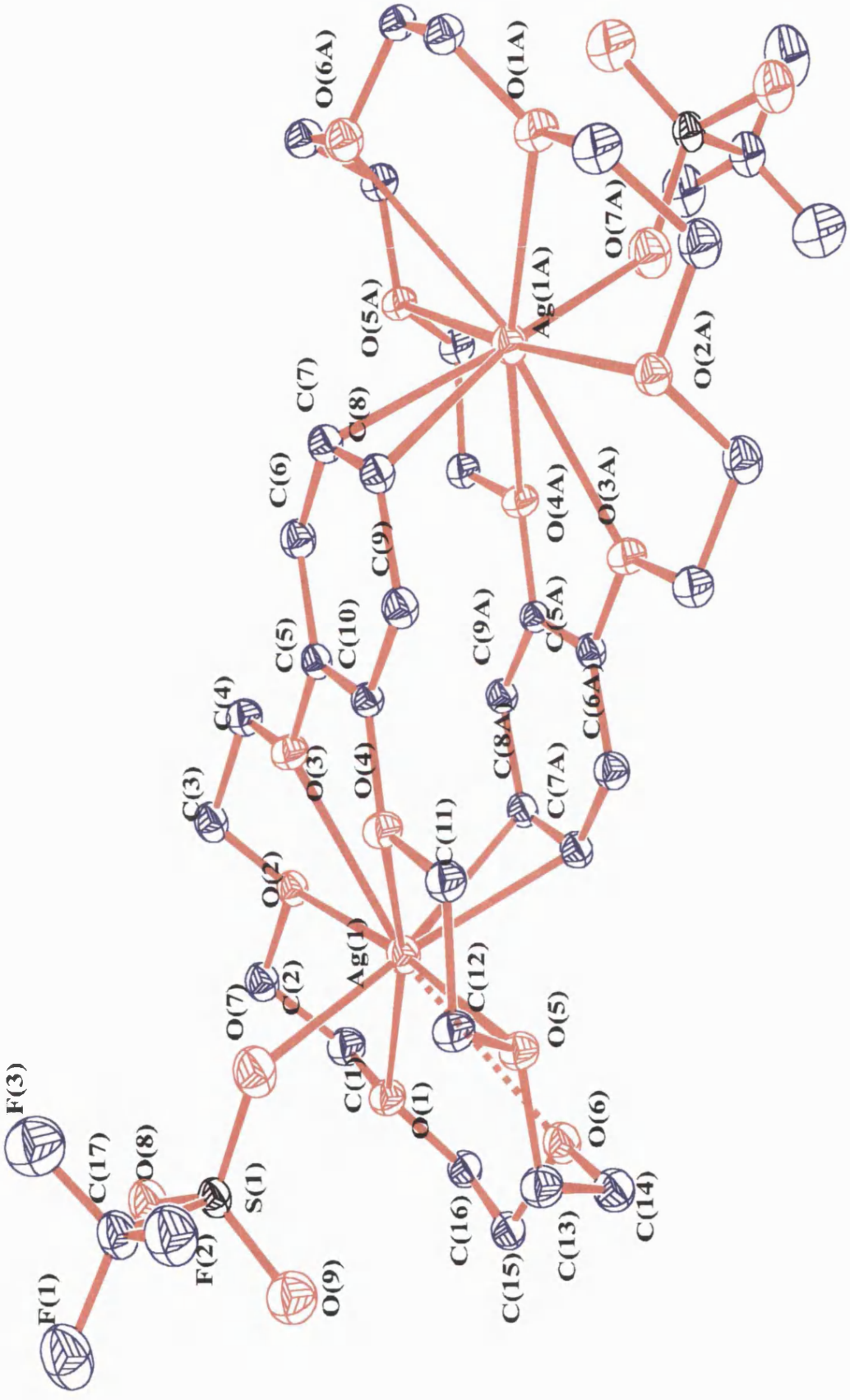

Figure 2. 9 Dimeric structure of C13 (Hydrogens removed for clarity)

Bond	Length (Å)	Bond	Length (Å)
Ag(1) - O(1)	2.668(3)	Ag(1) - C(7)	2.618(2)
Ag(1) - O(2)	2.669(3)	Ag(1) - C(8)	2.822(2)
Ag(1) - O(3)	2.720(3)	C(10) - C(9)	1.386(3)
Ag(1) - O(4)	2.744(3)	C(9) - C(8)	1.405(3)
Ag(1) - O(5)	2.735(3)	C(8) - C(7)	1.382(3)
Ag(1) - O(6)	2.991(3)	C(7) - C(6)	1.404(3)
Ag(1) - O(7)	2.419(2)	C(6) - C(5)	1.379(2)
		C(5) - C(10)	1.409(2)

Table 2.11 Selected bond lengths for C13

Atoms	Angle (°)	Atoms	Angle (°)
O(7)-Ag(1)-O(1)	83.57	O(1)-Ag(1)-O(2)	63.77
O(7)-Ag(1)-O(2)	88.96	O(2)-Ag(1)-O(3)	62.76
O(7)-Ag(1)-O(3)	87.79	O(3)-Ag(1)-O(4)	56.02
O(7)-Ag(1)-O(4)	81.46	O(4)-Ag(1)-O(5)	62.01
O(7)-Ag(1)-O(5)	85.29	O(5)-Ag(1)-O(6)	59.88
O(7)-Ag(1)-O(6)	102.64	O(6)-Ag(1)-O(1)	60.18
O(1)-Ag(1)-O(4)	164.82	O(7)-Ag(1)-C(7)	166.39
O(2)-Ag(1)-O(5)	174.14	O(7)-Ag(1)-C(8)	184.32
O(3)-Ag(1)-O(6)	168.86	C(7)-Ag(1)-C(8)	29.12

Table 2.12 Selected bond angles of C13

Molecular Structure of [Ag(dibenzo-18-crown-6)(OTf)], C15

[Ag(dibenzo-18-crown-6)(OTf)], **C15,** was dissolved in warmed dichloromethane and then allowed to cool at room temperature to afford X-ray diffraction quality crystals. During recrystallisation one equivalent of water and 0.5 equivalent of dichloromethane were incorporated into the crystal, despite attempts to keep the solution anhydrous. The crystals of $[Ag(dibenzo\text{-}18\text{-}crown\text{-}6)(H_2O)]^+[OTf]^-.0.5CH_2Cl_2$ were found to be air and moisture stable, and data were collected at 150 K. The dimeric structure of **C15**, is shown in Figure 2.10 and selected bond lengths and angles are given in Tables 2.13 and 2.14.

Complex **C15** has a monoclinic unit cell, with 8 molecules per asymmetric unit. The central Ag(1) is nine-co-ordinate. Ag(1) is co-ordinated to all six oxygens of dibenzo-18-crown-6 ($Ag\text{-}O_{ether}$= 2.5658(17)-2.9745(3) Å) and to an oxygen of the incorporated water molecule (Ag-O = 2.3291(19) Å). The co-ordination sphere is completed by atoms C(3) and C(4) of one aromatic ring of an adjacent complex, Ag(1)-C = 2.437(2) and 2.684(2) Å, respectively. The resulting dimerisation of the two complexes through four short Ag(1)...C contacts has a noticeable effect on the C-C bond lengths of the arene, and as with **C13** the ring exhibits triene-like alternating long and short C-C separations.

The co-ordinated water hydrogen bonds to the non-co-ordinated triflate (O(10)-H(1A)...O(7)-S(1) = 1.858 Å). The incorporated solvent molecule DCM hydrogen bonds to two adjacent triflate ions building a macromolecular structure.

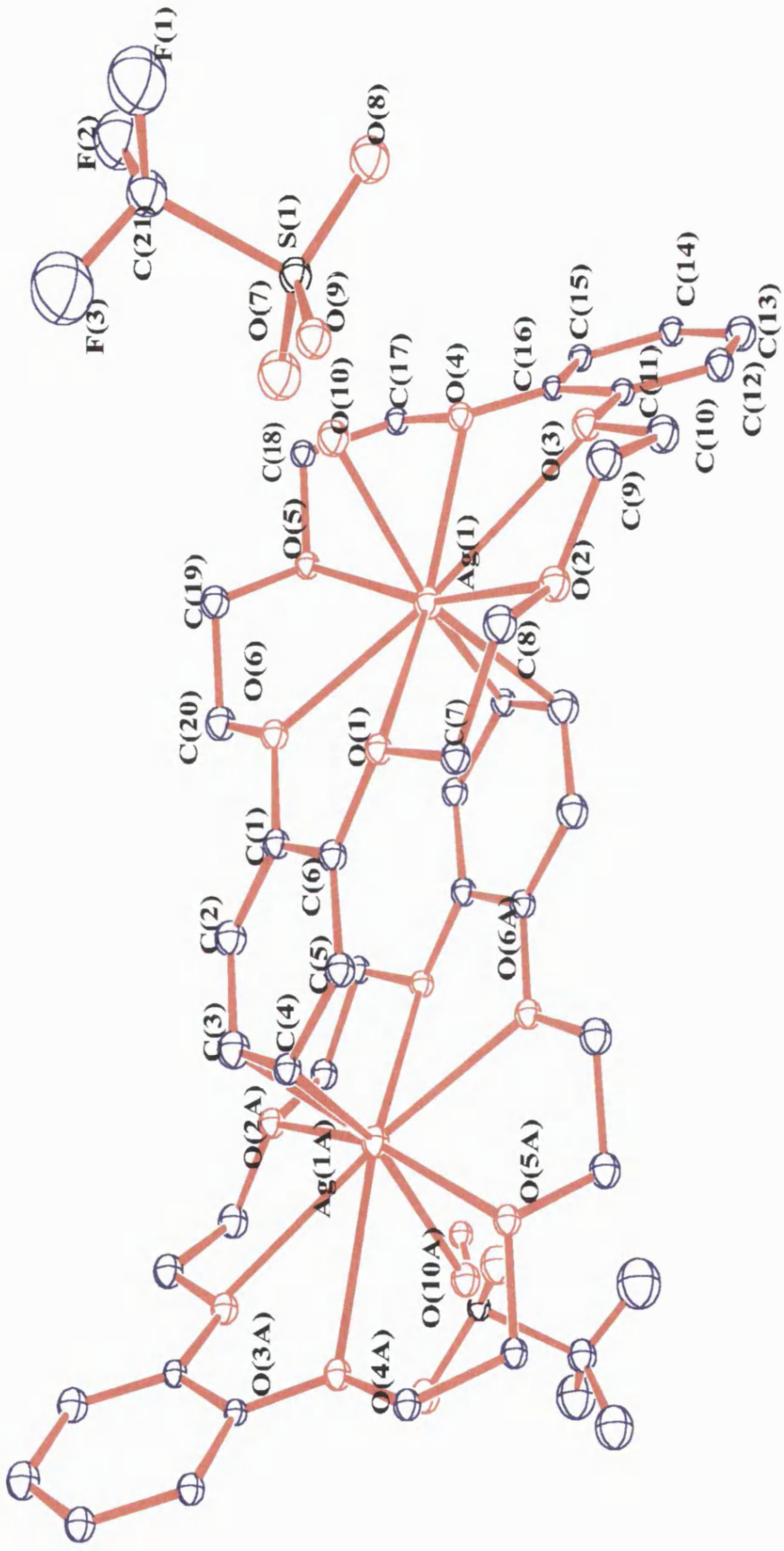

Figure 2. 10 Dimeric structure of C15

Bond	Length (Å)	Bond	Length (Å)
Ag(1)-O(1)	2.694(2)	Ag(1)-C(3)	2.437(2)
Ag(1)-O(2)	2.696(2)	Ag(1)-C(4)	2.684(2)
Ag(1)-O(3)	2.888(2)	C(1)-C(2)	1.379(3)
Ag(1)-O(4)	2.975(2)	C(2)-C(3)	1.408(4)
Ag(1)-O(5)	2.750(2)	C(3)-C(4)	1.385(4)
Ag(1)-O(6)	2.5658(17)	C(4)-C(5)	1.400(4)
Ag(1)-O(10)	2.3291(19)	C(5)-C(6)	1.382(3)
		C(1)-C(6)	1.413(3)

Table 2.13 Selected bond lengths of C15

Atoms	Angle (°)	Atoms	Angle (°)
O(10)-Ag(1)-O(1)	94.80(7)	O(1)-Ag(1)-O(2)	62.88(7)
O(10)-Ag(1)-O(2)	89.59(7)	O(2)-Ag(1)-O(3)	61.17(6)
O(10)-Ag(1)-O(3)	80.56(7)	O(3)-Ag(1)-O(4)	52.03(7)
O(10)-Ag(1)-O(4)	72.68(6)	O(4)-Ag(1)-O(5)	56.67(6)
O(10)-Ag(1)-O(5)	77.13(6)	O(5)-Ag(1)-O(6)	65.18(6)
O(10)-Ag(1)-O(6)	92.11(7)	O(6)-Ag(1)-O(1)	58.59(6)
O(1)-Ag(1)-O(4)	167.05(6)	O(10)-Ag(1)-C(3)	159.23(8)
O(2)-Ag(1)-O(5)	165.64(7)	O(10)-Ag(1)-C(4)	145.56(7)
O(3)-Ag(1)-O(6)	172.36(6)	C(3)-Ag(1)-C(4)	30.97(8)

Table 2.14 Selected bond angles of C15

Of the four triflate complexes that were studied by X-ray crystallography, [Ag(15-crown-5)(OTf)], **C7**, [Ag(18-crown-6)(OTf)], **C11**, [Ag(benzo-18-crown-6)(OTf)], **C13**, and $[Ag(dibenzo\text{-}18\text{-}crown\text{-}6)(H_2O)]^+[OTf]^-.0.5CH_2Cl_2$, **C15**, it is noticeable that varying the size and rigidity of the crown-ether has a significant effect on the structure of the product. The Ag(I) co-ordination number varies from seven for **C7** and **C11**, to nine for **C13** and **C15**, but the symmetry of the primary co-ordination sphere in these four complexes cannot be defined by any of the standard geometries for their respective co-ordination numbers.

In **C7** the triflate anion is bidentate, but in **C11** and **C13** it is unidentate. In **C15** it not co-ordinated to Ag at all. The $Ag\text{-}O_{triflate}$ separation is shorter for co-ordination in unidentate **C11** and **C13**, (2.355(3) and 2.4189(17) Å, respectively), than for bidentate co-ordination in **C7** (2.655(3) Å). This compares with a separation of 2.236(12) – 2.546(12) Å in of a bridging triflate in $[PPh_3AgOTf]$[18] and 2.421(2) Å in of unidentate triflate in $[(C_6H_5Me)AgOTf]$[19]. In **C15** the triflate is replaced with a co-ordinated water, Ag-O = 2.3291(19) Å, with a bond length which is comparable to the co-ordinated water in **C5** (2.327(4) Å).

The dimerisation of **C13** and **C15** through four Ag-C contacts has a significant effect on the co-ordinated aromatic rings of both complexes, each displaying alternating long and short C-C bonds (Table 2.15). Whilst metal co-ordination disrupts the aromaticity of the rings, the planarity and interring angles are not affected, Table 2.16. Aryl co-ordination to Ag^+ occurs in many complexes including $[(C_6D_6)_3Ag(BF_4)]$[20], and $[(C_6H_6)Ag(ClO_4)]$[21], in which the average Ag-C separation is slightly longer than in **C13** and **C15** at 2.54 Å.

Similar behaviour has recently been reported in $[Ag(L)]_2[OTf]_2$ {L = 7-oxo-2,5,11-trithia-8-azatetradecane-[12]-*ortho*benzenophane), which dimerise through two Ag-C contacts of 2.677(14) and 2.85(2) Å, as illustrated below[22].

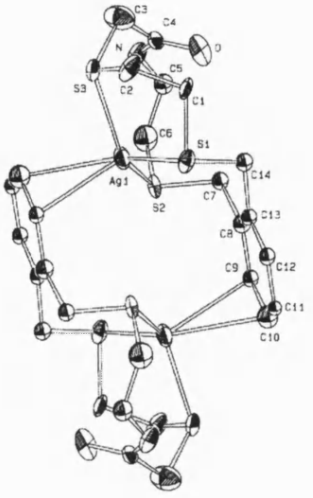

Figure 2. 11

Compound **C13**	Bond length (Å)	Compound **C15**	Bond length (Å)
C(10) - C(9)	1.386(3)	C(1)-C(2)	1.379(3)
C(9) - C(8)	1.405(3)	C(2)-C(3)	1.408(4)
C(8) - C(7)	1.382(3)	C(3)-C(4)	1.385(4)
C(7) - C(6)	1.404(3)	C(4)-C(5)	1.400(4)
C(6) - C(5)	1.379(2)	C(5)-C(6)	1.382(3)
C(5) - C(10)	1.409(2)	C(1)-C(6)	1.413(3)

Table 2.15 Aromatic bond lengths in C13 and C15

Compound **C13**	Bond angle (°)	Compound **C15**	Bond angle (°)
C(5)-C(6)-C(7)	120.07	C(1)-C(6)-C(5)	119.89
C(6)-C(7)-C(8)	120.05	C(6)-C(5)-C(4)	119.65
C(7)-C(8)-C(9)	120.39	C(5)-C(4)-C(3)	120.58
C(8)-C(9)-C(10)	119.22	C(4)-C(3)-C(2)	119.65
C(9)-C(10)-C(5)	120.44	C(3)-C(2)-C(1)	119.42
C(10)-C(5)-C(6)	119.81	C(2)-C(1)-C(6)	120.47

Table 2.16 Aromatic bond angles in C13 and C15

2.4 CONCLUSIONS

In this investigation the ability of crown-ethers to bind to silver(I) and form complexes has been shown to be comparable in structural terms to that of the alkali metals. The size of Ag^+ is close to that of K^+ (Table 2.17), which has been shown[23] to fit within the cavity of 18-crown-6 but not in 15-crown-5. The solid-state structures obtained in this study demonstrate the same to be true for Ag^+.

Crown –Ether	Cavity Diameter (Å)	M^+	Ionic Radius (Å)
12-crown-4	1.20-1.50	Ag^+	1.15
15-crown-5	1.70-2.20	Au^+	1.37
18-crown-6	2.60-3.20	K^+	1.38

Table 2.17

From the structural plots of **C6, C7, C8, C11, C13** and **C15** it can be shown that Ag^+ resides above the plane of the O-atoms in 15-crown-5 in **C6, C7**, and **C8**, but almost inside the cavity of the 18-crown-6 based ethers in **C11, C13** and **C15**. The better fit of the metal ion, as well as the additional Ag-O contact in the larger crown, will enhance the macrocyclic effect and stabilise the Ag^+ ion, resulting in weaker co-ordination to the counter-ion.

	C6	C7	C8	C11	C13	C15
Greatest deviation of O atoms from idealised plane (Å)	0.481(3)	0.778(3)	0.492(5)	0.748(2)	0.467(1)	0.097(2)
Distance of Ag from plane (Å)	1.102(2)	1.379(2)	1.038(3)	0.280(1)	0.075(1)	0.254(1)

Table 2. 18

Calculations on the planarity of the oxygens of the crown-ether were carried out using Shelx-L, in order both to assess the deviations of each oxygens from the idealised plane, and also to determine the distance of the metal from this plane. The results of these calculations are shown in Table 2.18. The metal is more than 1 Å above the oxygen plane in complexes

of 15-crown-5 (**C6**, **C7** and **C8**), compared to less than 0.3 Å above the planes of the O-atoms in complexes of the 18-crown-6 derivatives.

2.5 REFERENCES

[1] R.G. Pearson, *J. Am. Chem. Soc.*, **85**, 3533 (1963)

[2] R.G. Griffin, J.D. Ellett Jr., M. Mehring, J.G. Bullitt, J.S. Waugh, *J. Chem. Phys.*, **57**, 2147 (1972)

[3] J.A. Darr, M. Poliakoff, A.J. Blake, W.S., Li, *Inorg. Chem.*, **37**, 5491 (1998)

[4] J.S. Bradshaw, R.M. Izatt, A.V. Bordunov, C.Y. Zhu, J.K. Hathaway, *Comp. Supramol. Chem.*, **1**, 68, Pergammon, London (1996)

[5a)] P.D. Prince, J.W. Steed, *J. Supramol. Chem.*, **10**, 155 (1998); [b)] P.D. Prince, P.J. Cragg, J.W. Steed, *J. Chem. Soc., Chem. Commun.*, 1179 (1999)

[6] P. Jones, T. Gries, H. Grutzmacher, H.W. Roesky, J. Schimkowiak, G.M. Sheldrick, *Angew. Chem. Int. Ed. Engl.*, **23**, 376 (1984)

[7] R.M. Silverstein, G.C. Bassler, T.C. Morrill, *Spectrometric Identification of Organic Compounds, 5th Ed.*, John Wiley & Sons, Inc. Ch. 2 (1991)

[8] K. Nakamoto, *Infrared and Raman Spectra of Inorganic and Co-ordination Compounds (4th Ed)*, John Wiley and Sons, USA (1986)

[9] J. Emsley, D.Hall, *The Chemistry of Phosphorus,* Harper & Row (1976)

[10] I. Nakagawa, J.L. Walter, *J. Chem. Phys.*, **51**, 1389 (1969)

[11] N.B. Coltrup, L.H. Daly, S.E. Wiberley, *Introduction to Infrared and Raman Spectroscopy*, Academic Press, London, 314 (1964)

[12] A. Nurtaeva, W.M. Holt, *Acta. Cryst. Sect C,* **55**, 1453 (1999)

[13] V.S. Sergienko, V.K.Borzunov, *Koord. Khim.*, **17**, 1072 (1991)

[14] R.D. Rogers, A.N. Rollins, *J. Chem. Crystallogr.*, **24** , 321 (1994)

[15] R.D. Rogers, M.M. Benning, R.D. Etzenhouser, A.N. Rollins, *J. Chem. Soc., Chem. Commun.*, 1586 (1989)

---

[16] *Handbook of Chemistry and Physics 70th Ed*, F-189, CRC Press (1989)

[17] W. Beesk, P.G. Jones, H. Rumpel, E. Schwarzmann, G.M. Sheldrick, *J. Chem. Soc., Chem. Commun.*, 664 (1981)

[18] R. Terroba, M.B. Hursthouse, M. Laguna, A. Media, *Polyhedron*, **18**, 807 (1999)

[19] A.L. Johnson, M.G. Davidson, Unpublished results, University of Bath (2001)

[20] A.S. Batsanov, S.P. Crabtree, J.A.K. Howard, C.W. Lehmann, M. Kilner, *J. Organomet. Chem.*, **550**, 59 (1998)

[21] H.G. Smith, R.E. Rundle, *J. Am. Chem. Soc.*, 5075 (1958)

[22] H.O. Davies, J.R. Dilworth, D.V. Griffiths, J.R. Miller, Y. Zheng, *Polyhedron,* **18**, 459 (1999)

[23] F. Vögtle, *Supramolecular Chemistry,* John Wiley and Sons, Chichester, 38 (1993)

CHAPTER THREE: HOMOLEPTIC GOLD(I) THIOLATES AND THEIR TRIPHENYLPHOSPHINE DERIVATIVES

3.1 INTRODUCTION

In Chapter One it was noted that the chemistry of Au(I) is dominated by its preference to bind to soft donor atoms, particularly S- and P-donor ligands, and for its formation of secondary metal-metal interactions under sterically favourable conditions. Of particular interest in this research programme has been the chemistry of the homoleptic Au(I) thiolates, $[Au(SR)]_n$, in view of the medical applications of both the homoleptic gold(I) thiolates such as myocrysin (Figure 3.1), and their phosphine derivatives $[(PR_3)Au(SR')]$ such as auranofin[1a,b,c].

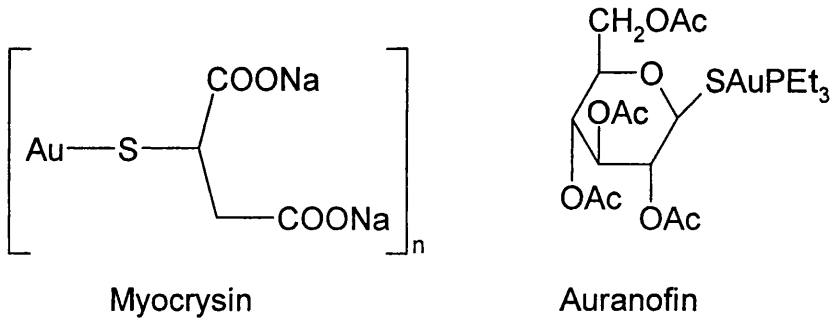

Figure 3.1

Many examples of homoleptic gold(I) thiolates $[Au(SR)]_n$ and phosphine gold(I) thiolates $[(R'_3P)Au(SR)]$ had been reported[2ab] before and during this study, but the extent of aggregation of most homoleptic compounds had not been determined, with the exception of the three examples, $[Au(SC_6H_4\text{-}2,4,6\text{-}^iPr_3)]_6$[3], $[Au\{SC(SiMe_3)_3\}]_4$[4] and $[Au\{SSi(O\text{-}t\text{-}CMe_3)_3\}]_4$[5], discussed in Chapter One. The poor solubility of many these complexes has prevented either crystal growth for X-ray structure or molecular weight determinations.

It has been shown previously[6] that trends in solubility can be established from patent literature, and that for a limited number of examples the solubility in organic solvents of the homoleptic aryl thiolates varies with the substitution pattern on the aryl ring.

In this study a range of homoleptic aryl thiolates have been synthesised and characterised in order to observe the effects on solubility and association of substituent type and substitution pattern in the ring. Complexes with aryl thiolate ligands containing the electron donating group OMe, the electron withdrawing group CF_3, and a secondary arene ring have been investigated. The intention was to compare their structures, where possible, with those of the readily soluble thiolates **G1** and **G2**, whose structures were determined in the early stages of this study. Triphenylphosphine derivatives of this series of homeleptics have also been synthesised resulting in the two ranges of compounds summarised in Table 3.1.

R	$[Au(SR)]_n$	$[(Ph_3P)Au(SR)]$
C_6H_4-*p*-CMe_3	**G1**	**P1**
C_6H_4-*o*-CMe_3	**G2**	**P2**
C_6H_5	**G3**	**P3**
C_6H_4-*o*-CF_3	**G4**	**P4**
C_6H_4-*m*-CF_3	**G5**	**P5**
C_6H_4-*p*-CF_3	**G6**	**P6**
C_6H_4-*o*-OMe	**G7**	**P7**
C_6H_4-*m*-OMe	**G8**	**P8**
C_6H_4-*p*-OMe	**G9**	**P9**
$C_{11}H_7$	**G10**	**P10**

Table 3.1 Summary of compounds prepared

In Section **3.4** a brief report on a preliminary study of the reactions of Au(III) with dipyridyldisulphide is also discussed.

3.2 HOMOLEPTIC GOLD(I) THIOLATES, $[Au(SR)]_n$

3.2.1 SYNTHESIS AND PROPERTIES

The preparative routes to homoleptic thiolates are well established and the methods used in this study are modified from those reported in the literature[7]. The quantities of the reactants used and specific experimental details are provided in Chapter 5 of this Thesis. In all cases methionine ($HO_2CCH(NH_2)CH_2CH_2CH_2SCH_3$) in ethanol was added to aqueous hydrogen tetrachloroaurate in order to reduce Au(III) to Au(I), and all reported data refer to products obtained via this route. Preparations of **G4** and **G7** were also carried out using tetrahydrathiophene, THT, as the reductant. Initial preparations of the homoleptic thiolates were carried out as outlined in Figure 3.2. Thiol dissolved in toluene was added in equimolar amounts to a stirred aqueous ethanol solution of the intermediate $[(HO_2CCH(NH_2)CH_2\,CH_2CH_2(CH_3)S)AuCl]$ *in situ.*

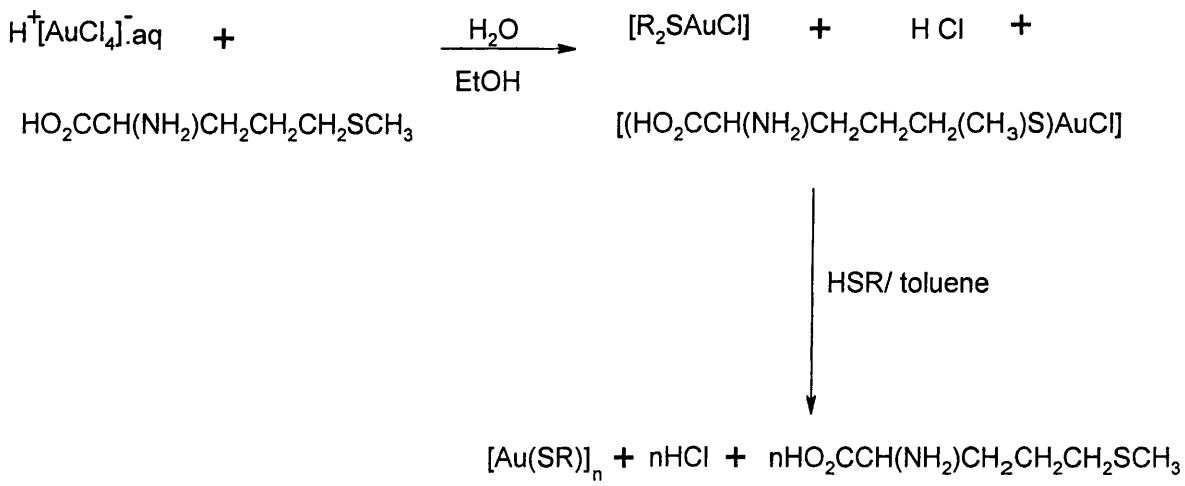

Figure 3.2

In order to isolate the homoleptics **G1** and **G2** the toluene phase containing the product was separated from the aqueous ethanol phase, and the product was precipitated by slow addition of methanol. The resultant yellow powders are both easily soluble in aromatic and chlorinated solvents. The other eight complexes **G3 - G10** precipitated directly as white

solids from the stirred reaction mixture. As they all proved insoluble in toluene and ethanol, the preparative method was then modified so that neat thiol was added dropwise to a solution of the Au(I) intermediate in aqueous ethanol. All products are stable to air and light and yields were in the range 63 - 98 %. Although **G1** and **G2** have very good solubility in a range of organic solvents, complexes **G3 – G10** are insoluble in all common solvents.

Initial attempts to prepare **G4** as above, resulted in the precipitation of a white solid which decomposed rapidly in the presence of water to form Au^0. Elemental analysis and infrared data, indicated that the Au(I) intermediate [$(HO_2CCH(NH_2)CH_2CH_2CH_2(CH_3)S)AuCl$], **R1**, had been precipitated. This complex had not been isolated previously and further study revealed that its preparation is better achieved in the absence of thiol. Data for **R1**, and also for [(THT)AuCl], **R2**, are given in Chapter Five.

3.2.2 CHARACTERISATION

The characterisation of each of the homoleptic Au(I) thiolates, $[Au(SR)]_n$, **G1-10**, by infrared spectroscopy and elemental analysis for carbon and hydrogen are described below. Subsequent sections introduce the crystal structure determinations, NMR, FAB Mass spectra and Raman Spectra of the soluble complexes **G1** and **G2**. Finally the results of thermogravimetric analysis (TGA) of **G1 – G10** are discussed.

Absorptions characteristic of each thiolate ligand were observed in the infrared spectrum of each complex, as detailed in the Experimental section of this Thesis. The data were of limited use as spectral bands were broad due to the polymeric nature of many of these complexes, and so spectra were primarily used to analyse for impurities. None of the spectra showed signals due to free thiol [ν(S-H) stretch at 2500 cm^{-1}], nor was there any evidence of any solvent incorporation in the initial powdered products. Solvent incorporation was observed in crystals of both **G1** and **G2** after deposition from concentrated solutions of toluene, xylene or ethoxybenzene (phenetole). The broad and weak ν(Au-S) stretch can be observed[2b] in the far infrared region 310-340 cm^{-1}, but this region was not investigated in this study.

3.2.2.1 SOLID-STATE STRUCTURAL STUDIES

Solid-state structure determinations were carried out on crystals of the homoleptic gold(I) thiolates $[\{Au(SC_6H_4\text{-}p\text{-}CMe_3)\}_n]$, **G1**, and $[\{Au(SC_6H_4\text{-}o\text{-}CMe_3)\}_n]$, **G2**, in order to compare their degree of aggregation and structures with those of the other known homoleptics, $[Au(SR)]_n$, {R = C_6H_4-2,4,6-$^iPr_3$, n = 6; R = $C(SiMe_3)_3$, n = 4; and R = $Si(O\text{-}t\text{-}CMe_3)_3$, n = 4}[3,4,5].

X-ray quality crystals of $[\{Au(SC_6H_4\text{-}p\text{-}CMe_3)\}_n]$, **G1** were grown from toluene, however the crystals incorporated solvent and desolvated in the X-ray beam. Suitable crystals were then obtained from warmed ethoxybenzene. These too incorporated solvent, and analysed as $[\{Au(SC_6H_4\text{-}p\text{-}CMe_3)\}_{10}].0.8C_8H_{10}O$, **G1a**. However, they were found to be air and moisture stable and did not decompose in the X-ray beam. X-ray data was collected at room temperature. Selected bond distances and angles are summarised in Tables 3.2 and 3.3, respectively. The structure of the gold core and the full structure are illustrated in Figures 3.3 and 3.4, respectively. Further structural data are provided in Appendix 2.

The structure of **G1a** consists of a $Au_{10}S_{10}$ core, made up of two interpenetrating pentagons defined by five S atoms and five Au atoms arranged in an alternating pattern about the periphery, as illustrated in Figure 3.3. It provides a novel example of an inorganic [2]catenane. An Au atom from the opposite ring occupies the centre of each Au_5S_5 ring. The co-ordination about each gold centre is almost linear (S-Au-S = 172.60 – 178.01 °), and each ring is a regular planar pentagon. The $Au_{10}S_{10}$ core is strengthened by a total of nine close Au....Au contacts (2.97 – 3.12 Å). All involve either Au(1) or Au(6) atoms, with much longer Au....Au separations (average = 3.59 Å) occurring around the periphery of each pentagon. The angle between the two planes (defined by the five peripheral gold atoms of each ring) is 83°.

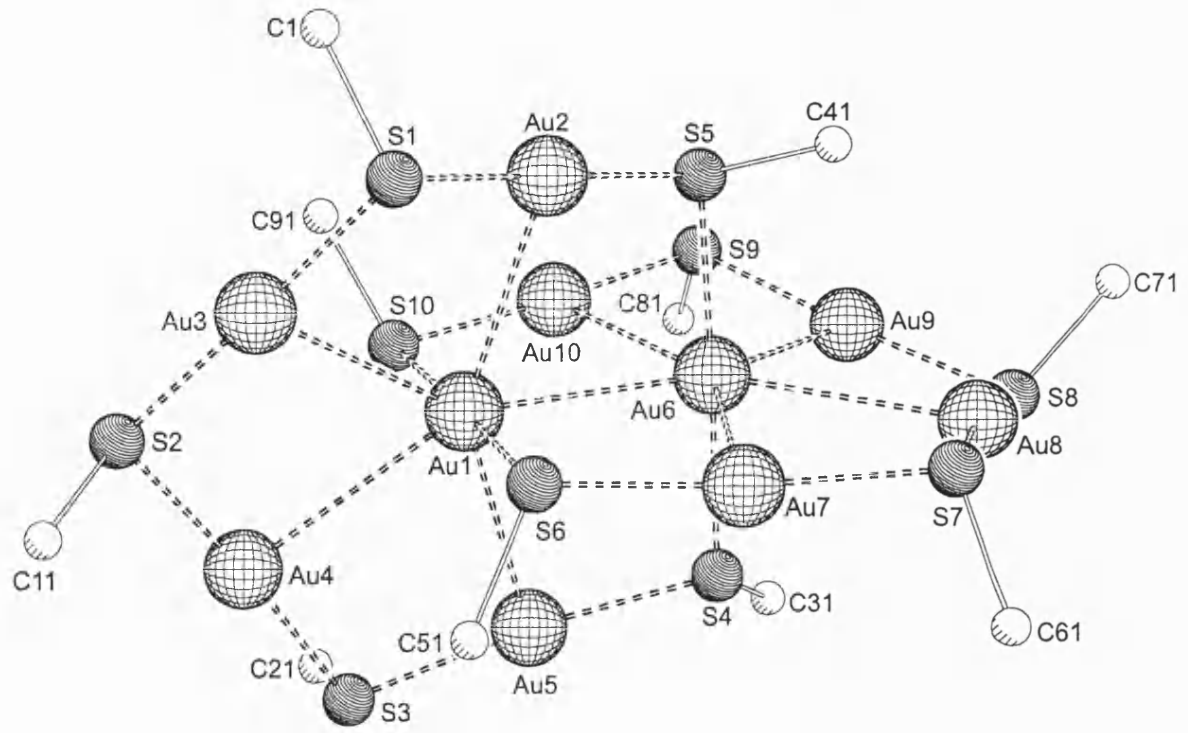

Figure 3. 3 $Au_{10}S_{10}C_{10}$ core of G1a

All four Au(1)/Au(6)-S bond lengths are 2.343(3) Å, whilst the remaining sixteen Au-S separations are shorter and lie within the narrow range 2.289(4) – 2.313(4) Å. It appears that in **G1a** the Au-S bonds involving the central atoms are slightly lengthened, presumably because of the effect of the multiple Au….Au interactions involving Au(1) and Au(6). The structure of this unique core can be readily rationalised by consideration of the structural parameters found in many other thiolates. The normal linear co-ordination about Au atoms combined with Au-S separations of 2.30 Å and an angular Au-S-Au arrangement averaging 105° defines a planar pentagon of side 4.6 Å. These geometric constraints maximise the number of stabilising Au....Au contacts possible for an in-plane Au located at the centre of the ring, and impose a value of 3.0 Å for each Au....Au "spoke" in the pentagonal cartwheel. The organic groups attached to each sulphur do not have any favoured orientation about the edge of each ring, but all Au-S-C angles are within the range 101.9 – 108.1°. The ethoxybenzene does not interact with the catenane.

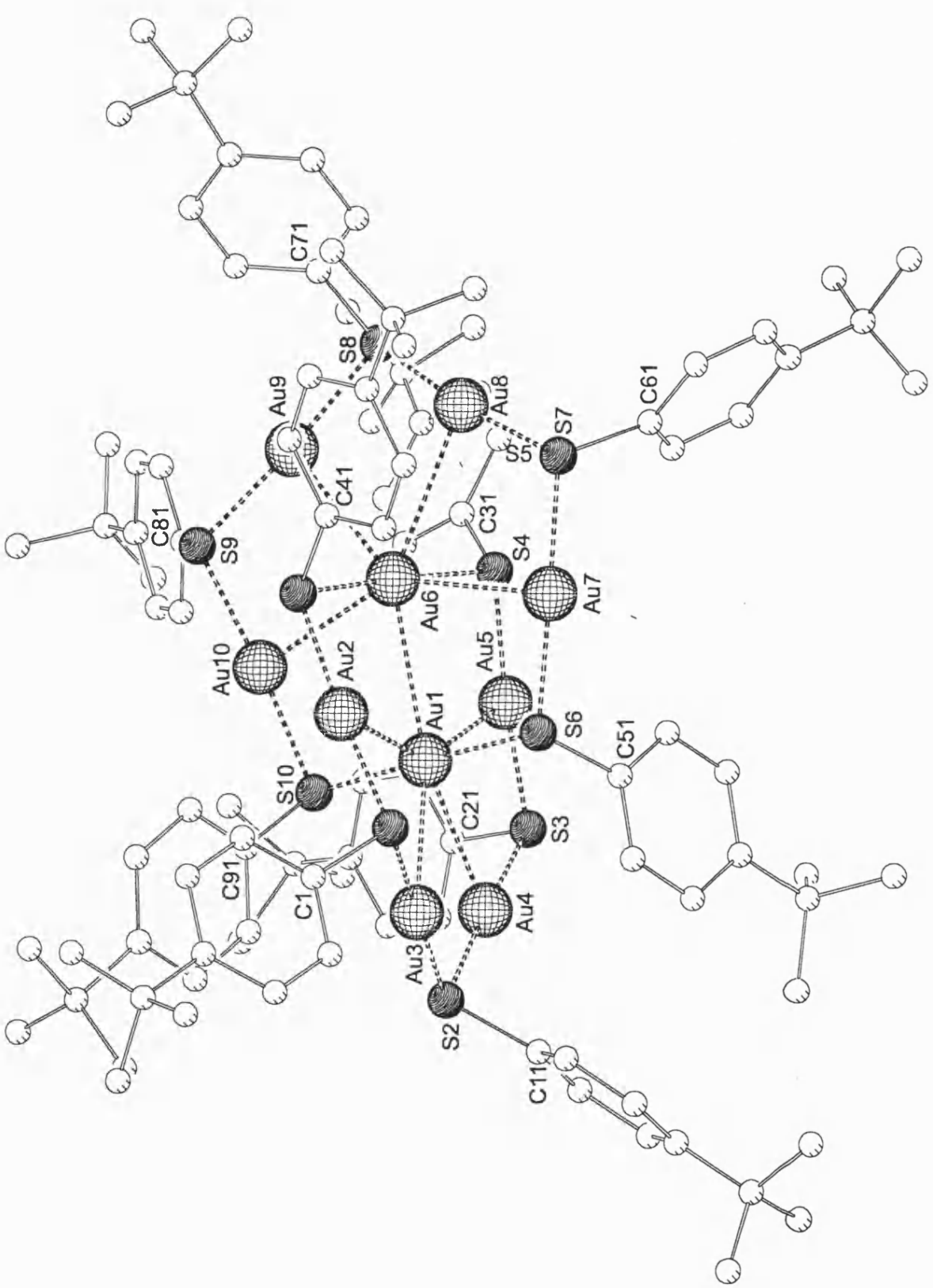

Figure 3. 4 Full Structure of G1a

Bond	Length (Å)	Bond	Length (Å)
Au(1)-S(10)	2.342(4)	Au(8)-S(7)	2.313(4)
Au(1)-S(6)	2.343(3)	Au(9)-S(9)	2.289(4)
Au(2)-S(1)	2.294(4)	Au(9)-S(8)	2.299(4)
Au(2)-S(5)	2.313(4)	Au(10)-S(10)	2.294(4)
Au(3)-S(2)	2.296(4)	Au(10)-S(9)	2.297(4)
Au(3)-S(1)	2.302(4)	Au(1)-Au(2)	2.9735(9)
Au(4)-S(3)	2.301(4)	Au(1)-Au(5)	2.9840(10)
Au(4)-S(2)	2.304(4)	Au(1)-Au(3)	3.0338(11)
Au(5)-S(3)	2.294(4)	Au(1)-Au(6)	3.0462(11)
Au(5)-S(4)	2.303(4)	Au(1)-Au(4)	3.1182(11)
Au(6)-S(5)	2.343(4)	Au(6)-Au(10)	3.0452(10)
Au(6)-S(4)	2.343(4)	Au(6)-Au(9)	3.0501(12)
Au(7)-S(6)	2.299(4)	Au(6)-Au(7)	3.0996(12)
Au(7)-S(7)	2.306(4)	Au(6)-Au(8)	3.1234(11)
Au(8)-S(8)	2.299(4)		

Table 3. 2 Selected bond lengths for G1a

Atoms	Angle (°)	Atoms	Angle (°)
S(10)-Au(1)-S(6)	178.01(13)	Au(2)-S(1)-Au(3)	102.74(14)
S(1)-Au(2)-S(5)	175.89(13)	Au(3)-S(2)-Au(4)	101.10(14)
S(2)-Au(3)-S(1)	177.46(14)	Au(5)-S(3)-Au(4)	100.2(2)
S(3)-Au(4)-S(2)	175.19(14)	Au(5)-S(4)-Au(6)	103.36(14)
S(3)-Au(5)-S(4)	173.67(13)	Au(2)-S(5)-Au(6)	99.5(2)
S(5)-Au(6)-S(4)	175.46(13)	Au(7)-S(6)-Au(1)	107.26(14)
S(6)-Au(7)-S(7)	172.52(12)	Au(7)-S(7)-Au(8)	100.58(14)
S(8)-Au(8)-S(7)	172.60(20)	Au(9)-S(8)-Au(8)	102.0(2)
S(9)-Au(9)-S(8)	175.20(20)	Au(9)-S(9)-Au(10)	103.7(2)
S(10)-Au(10)-S(9)	175.35(14)	Au(10)-S(10)-Au(1)	101.17(14)

Table 3. 3 Selected bond angles for G1a

X-ray quality crystals of [{Au(SC_6H_4-*o*-CMe_3)}$_n$] were grown from ethoxybenzene. These crystals were air and moisture stable, and were characterised as [{Au(SC_6H_4-*o*-CMe_3)}$_{12}$].2[C_6H_5OEt], **G2a**. X-ray data were collected on **G2a** at room temperature. Selected bond angles and distances are summarised in Tables 3.4 and 3.5, respectively. The structure of **G2a,** with the solvent removed for clarity, is illustrated in Figure 3.5. Further structural data are provided in Appendix 2.

The central core of **G2** can also be described as a [2]catenane, but neither of the two interpenetrating hexagons, each defined by a total of 12 alternating S and Au atoms, is planar. The near linear S-Au-S arrangement with Au-S separations in the range 2.287(6) - 2.325(5) (average 2.30 Å) persists in both hexagonal units, but Au....Au contacts between the central gold atoms in each ring, Au(1) and Au(7), and those on the periphery vary widely (3.19 - 3.69 Å), and as such are in the same range as Au....Au contacts between gold atoms around the periphery. Buckling in the second ring permits just two relatively short transannular Au...Au contacts [Au(2)....Au(8), 3.16; Au(6)...Au(8) 3.21 Å]. All Au....Au contacts less than twice the Bondi[8] van der Waal's radius of gold are listed in Table 3.4.

The interpenetrating rings in **G2a** are distorted from planarity, resulting in a total of twelve Au...Au contacts in the range 3.16– 3.30 Å, six of which do not involve a central atom. The interplanar angle between two best planes defined by the peripheral gold atoms of each ring is 79°. The ligands alternate above and below the planes of each ring, but show no preference for any orientation, the Au-S-C angles all fall within the range, 98.7 – 115.8 °.

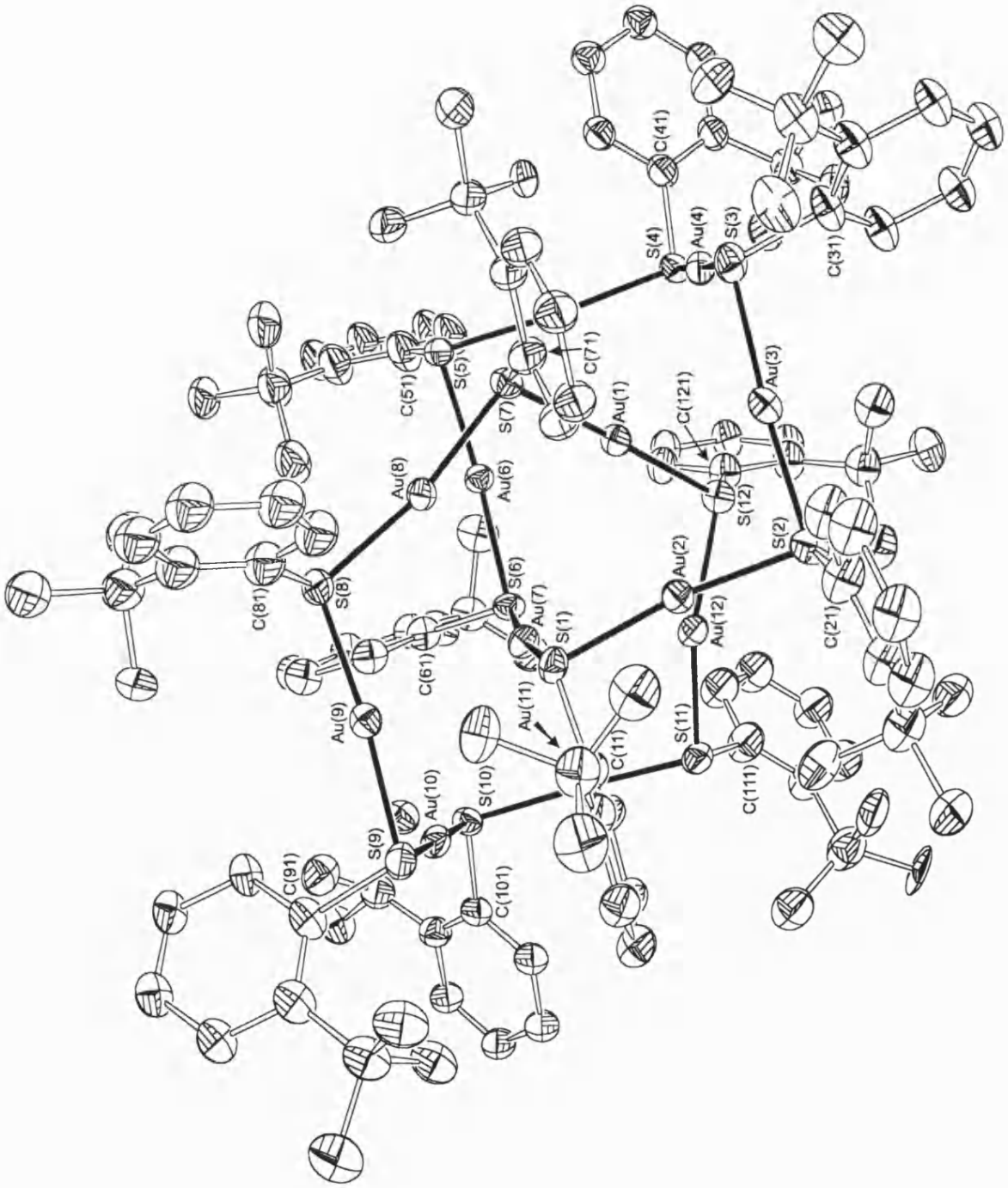

Figure 3.5 Full structure of G2a

Bond	Length (Å)	Bond	Length (Å)
Au(1)-S(12)	2.300(5)	Au(11)-S(11)	2.287(6)
Au(1)-S(7)	2.325(5)	Au(11)-S(10)	2.289(6)
Au(2)-S(2)	2.301(6)	Au(12)-S(11)	2.300(6)
Au(2)-S(1)	2.318(5)	Au(12)-S(12)	2.316(6)
Au(3)-S(3)	2.287(6)	Au(1)-Au(6)	3.191(2)
Au(3)-S(2)	2.315(6)	Au(1)-Au(4)	3.1993(14)
Au(4)-S(3)	2.300(7)	Au(1)-Au(3)	3.256(2)
Au(4)-S(4)	2.312(7)	Au(1)-Au(5)	3.277(2)
Au(5)-S(5)	2.310(6)	Au(1)-Au(2)	3.3172(14)
Au(5)-S(4)	2.310(5)	Au(2)-Au(12)	3.1649(14)
Au(6)-S(5)	2.307(5)	Au(2)-Au(3)	3.299(2)
Au(6)-S(6)	2.310(5)	Au(3)-Au(4)	3.376(2)
Au(7)-S(6)	2.307(6)	Au(4)-Au(5)	3.282(2)
Au(7)-S(1)	2.321(6)	Au(5)-Au(6)	3.2064(14)
Au(8)-S(7)	2.297(5)	Au(6)-Au(8)	3.2058(14)
Au(8)-S(8)	2.309(5)	Au(7)-Au(12)	3.2068(14)
Au(9)-S(8)	2.308(6)	Au(7)-Au(8)	3.2282(14)
Au(9)-S(9)	2.324(6)	Au(7)-Au(9)	3.3348(14)
Au(10)-S(9)	2.298(7)	Au(9)-Au(10)	3.325(2)
Au(10)-S(10)	2.301(6)	Au(10)-Au(11)	3.1878(14)

Table 3. 4 Selected bond lengths for G2a

Atoms	Angle (°)	Atoms	Angle (°)
S(12)-Au(1)-S(7)	178.1(2)	Au(2)-S(1)-Au(7)	93.9(2)
S(2)-Au(2)-S(1)	166.4(2)	Au(2)-S(2)-Au(3)	91.2(2)
S(3)-Au(3)-S(2)	175.4(2)	Au(3)-S(3)-Au(4)	94.8(2)
S(3)-Au(4)-S(4)	177.9(2)	Au(5)-S(4)-Au(4)	90.5(2)
S(5)-Au(5)-S(4)	176.3(2)	Au(6)-S(5)-Au(5)	88.0(2)
S(5)-Au(6)-S(6)	168.9(2)	Au(7)-S(6)-Au(6)	95.2(2)
S(6)-Au(7)-S(1)	171.0(2)	Au(8)-S(7)-Au(1)	104.1(2)
S(7)-Au(8)-S(8)	168.4(2)	Au(9)-S(8)-Au(8)	108.1(2)
S(8)-Au(9)-S(9)	172.6(2)	Au(10)-S(9)-Au(9)	92.0(2)
S(9)-Au(10)-S(10)	178.2(2)	Au(11)-S(10)-Au(10)	88.0(2)
S(11)-Au(11)-S(10)	176.9(2)	Au(11)-S(11)-Au(12)	105.4(2)
S(11)-Au(12)-S(12)	162.8(2)	Au(1)-S(12)-Au(12)	105.2(2)

Table 3. 5 Selected bond angles for G2a

It is evident from packing considerations that the bulky *t*-butyl substituent in the ortho position of the arene ring prevents the formation of a structural analogue of **G1a**. There are no secondary Au....S interactions of significance in either **G1a** or **G2a**. It is clear that these two examples of inorganic [2]catenanes are a rare and interesting structural type. There has been only one other report of a [2]catenane species involving gold[9], (Figure 3.6). Reaction of $[Au(NH_3)_2]^+[BF_4]^-$ with ^{t}BuCCH in acetonitrile results in the formation of $[Au(^t BuCCH)]_{12}$ in high yield. The system self-assembles into two interlocking rings containing multiple short inter- and intra-ring Au...Au contacts in the range 3.2 – 3.5 Å, though the communication does not detail how regular these contacts are and which metal centres they involve. The angle between the two rings is 64.5 °.

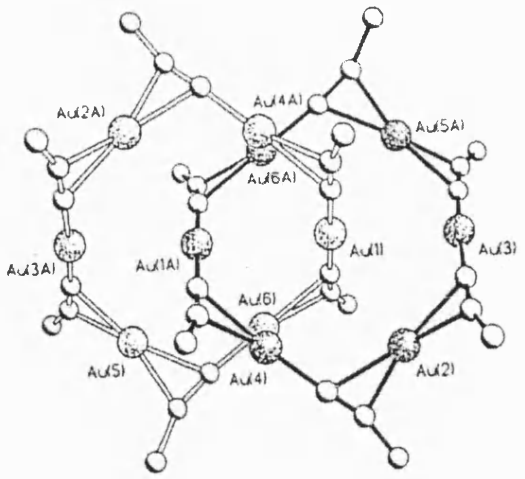

Figure 3. 6 The structure of [Au(^{t}BuCCH)]$_{12}$

The structures of **G1a** and **G2a**, together with the previously reported structures of [Au(SC_6H_4-2,4,6-$^i Pr_3$)]$_6$, [Au{$SC(SiMe_3)_3$}]$_4$ and [Au{SSi(O-t-$CMe_3)_3$}]$_4$, offer some insight into the range of oligomeric structures formed by homoleptic gold(I) thiolates. One of the most significant differences between the structures adopted by **G1a** and **G2a** compared with the three previously reported is the extent of Au…Au bonding. [Au(SC_6H_4-2,4,6-$^i Pr_3$)]$_6$ (Fig 3.7) forms a six-membered ring containing six Au…Au separations in the range 3.44 – 3.63 Å. Only two of these contacts are shorter than the 3.50 Å considered as the upper limit of Au…Au interaction. Further aggregation is presumable prevent by the steric bulk of the ligand.

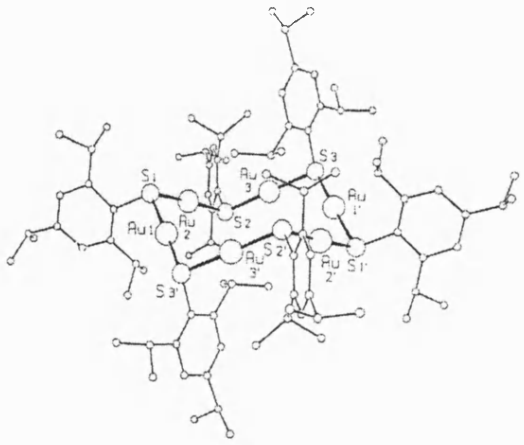

Figure 3. 7 Structure of [Au(SC_6H_4-2,4,6-$^i Pr_3$)]$_6$

The two tetramers $[Au\{SC(SiMe_3)_3\}]_4$ and $[Au\{SSi(OCMe_3)_3\}]_4$ (Figure 3.8) each contain four Au...Au contacts in the range 3.19-3.35 Å, and it seems likely that the bulk of the ligands prevents larger ring or catenane formation.

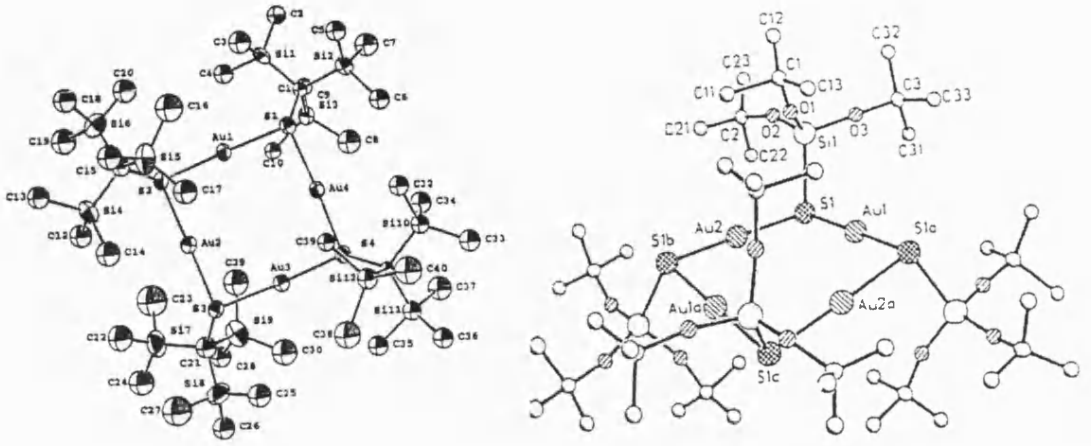

Figure 3. 8 Structures of $[Au\{SC(SiMe_3)_3\}]_4$ and $[Au\{SSi(O\text{-}t\text{-}CMe_3)_3\}]_4$.

	Au...Au (Å)	Au-S (Å)	S-Au-S (°)
$[\{Au(SC_6H_4\text{-}p\text{-}CMe_3)\}_{10}]$ .0.8$[C_6H_5OEt]$, **G1a**	2.97 – 3.12	2.294 – 2.342	172.5 – 177.5
$[\{Au(SC_6H_4\text{-}o\text{-}CMe_3)\}_{12}]$ .2$[C_6H_5OEt]$, **G2a**	3.16– 3.30	2.287 – 2.325	162.8 – 178.2
$[Au(SC_6H_4\text{-}2,4,6\text{-}^iPr_3)]_6$	3.44 – 3.63	2.275 – 2.295	175.4 – 177.5
$[Au\{SC(SiMe_3)_3\}]_4$	3.30	2.297 – 2.310	177.0 – 178.5
$[Au\{SSi(OCMe_3)_3\}]_4$	3.24	2.284 – 2.296	178.8 - 178.3

Table 3. 6 Selected bond lengths and angles for $[Au(SR)]_n$

It seems likely that the insoluble homoleptics isolated both in this study and previously[2b] adopt highly condensed or polymeric structures stabilised by Au...Au contacts. One important factor that influences the degree of aggregation is the bulk of the thiolate ligand, but it is interesting to note that slight variations in the substitution pattern of aryl ligands results in complexes with very different solubilities, and presumably structures (**G1** and **G2** compared with **G3–G10**).

3.2.2.2 ^{1}H NMR SPECTROSCOPY

The weakness of a single aurophilic interaction generally results in its complete disruption on dissolution, but occasionally an equilibrium is observed between gold-gold bonded and non bonded species. Such is the case with $[Au_2(SC_6H_4\text{-}p\text{-}Me)_2(\mu\text{-dppm})]$, where dppm = $Ph_2PCH_2PPh_2$, for which Bruce *et al*[10] showed that a temperature dependent equilibrium occurred in CD_2Cl_2 between conformations with and without an intramolecular Au...Au interactions. A multiplicity of Au...Au interactions, as occurs in **G1**, is expected to stabilise the core structure to higher temperatures.

^{1}H- and ^{13}C-NMR spectra of $[Au(SC_6H_4\text{-}p\text{-}CMe_3)]_{10}$, G1

The room temperature proton NMR spectrum of **G1** was recorded in deuterated DCM, the NMR data are summarised in the Experimental Chapter. The spectra contains three sets of signals in both the methyl and aromatic regions in the ratio 2:2:1. The methyl region is the clearest in which the three singlets are clearly separated, at 1.18, 1.30 and 1.33 ppm. The $Au_{10}S_{10}$ core (Figure 3.9) consists of two interpenetrating Au_5S_5 pentagons stabilised by nine Au...Au interactions, and provided this core remains intact on dissolution at room temperature, the signals can be assigned to the three sets of R groups comprising those on S(4), S(5), S(6), S(10) all of which are bound to Au(1) or Au(6), those on S(1), S(3), S(7), S(9), and finally those on S(2) and S(8). This interpretation is only valid if the spatial orientation of the R groups is not fixed, and within sets the various alkyl and aromatic protons become equivalent on the NMR time scale.

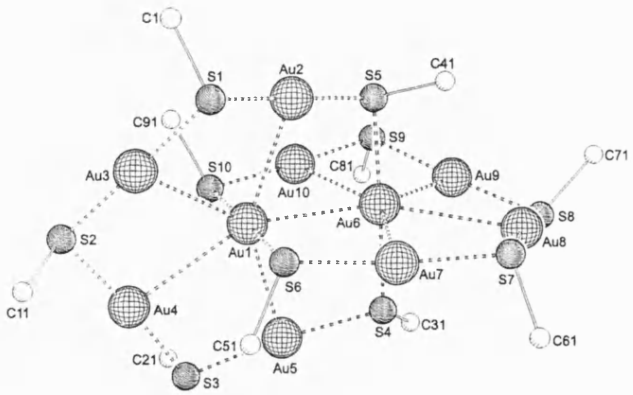

Figure 3. 9 [$Au_{10}S_{10}$] core of G1a

At lower temperatures line broadening of all peaks is followed by band splitting of some signals. Thus at – 85 °C the signal at 1.18 ppm splits into two broad bands centred at 1.08 and 1.19 ppm, as ligand motion is restricted. Similar line broadening and splitting occurs in the aromatic region but overlapping signals prevent delineation of the total number and relative intensities of all bands in the low temperature spectrum. We have confirmed Parish's previous findings[2b] that at elevated temperatures single sets of methyl and aromatic resonances are observed. This may reflect a concerted dynamic motion of the core, or its fragmentation. If the latter, then the core must reform on cooling as the original pattern is re-established with no evidence of any other species. It is interesting to note that when Parish *et al*[2b] first isolated these complexes, a pentagonal structure [$Au_5(SR)_5$] was postulated for **G1**, based on NMR observations.

^{13}C-NMR data for **G1** was collected in deuterated chloroform at room temperature only. These data are summarised in Chapter Five. Smaller chemical shift changes result in overlapping bands, thus only two signals were observed in the aliphatic region for the methyl carbons (31.2(7) and 31.3(6) ppm) together with a further two bands for the quarternary carbons (34.4(4) and 34.4(8) ppm) and eleven signals in the aromatic region. Nevertheless these data are compatible with the proton data.

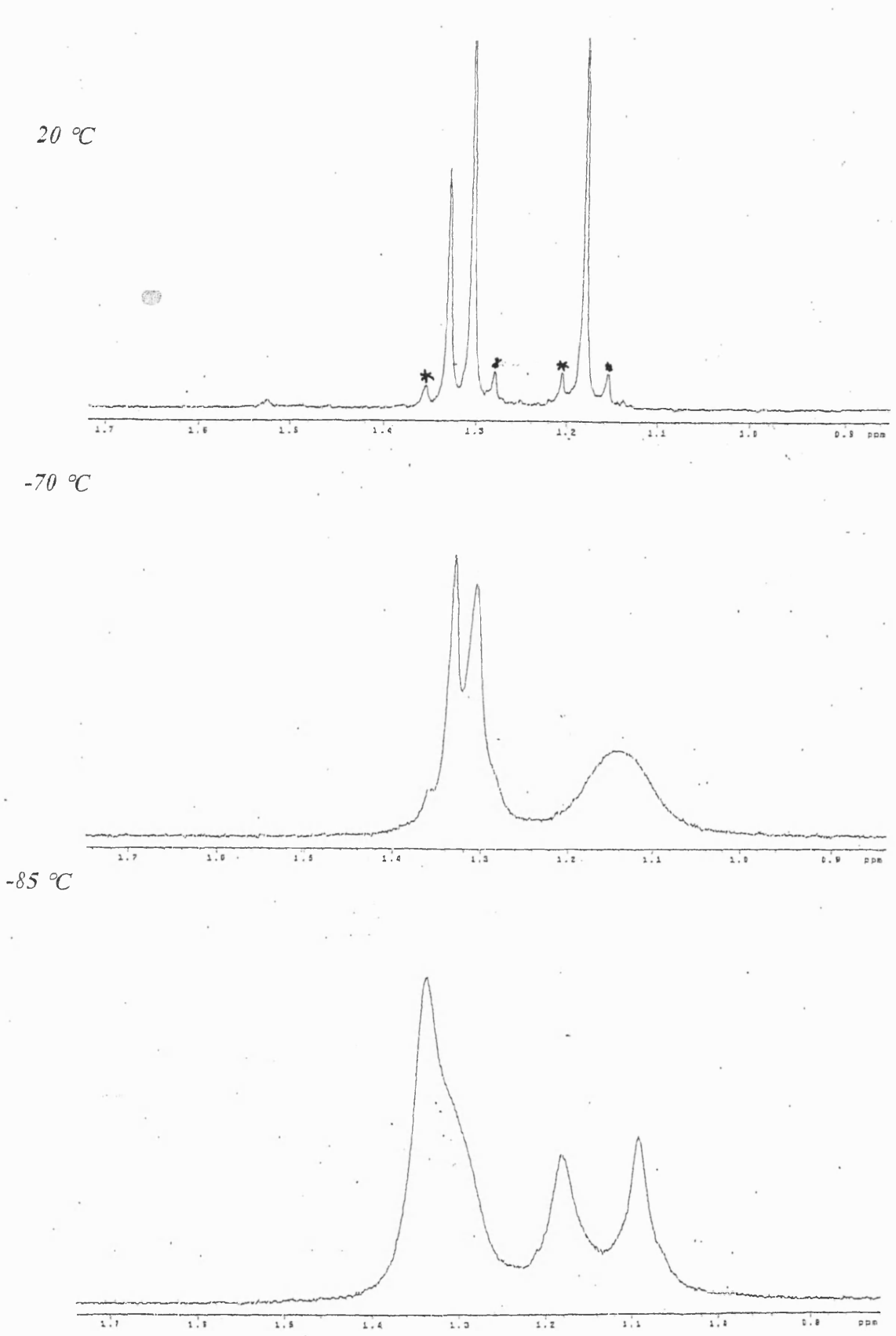

Figure 3. 10 Variable Temperature ^{1}H-NMR for G1 (aliphatic region) {* Spinning side bands}

^{1}H- and ^{13}C-NMR spectra of [Au(SC_6H_4-o-CMe_3)]$_{12}$, G2

The ^{1}H-NMR spectrum of **G2** was recorded in deuterated DCM and is summarised in Chapter Five. The spectrum is more complex than that of **G1**, and it is both temperature and solvent dependent, with evidence of more than one species being present in solution both at ambient temperatures and low temperatures. In the methyl region three bands in an intensity ratio of 1:1:1, are centred at 1.08, 1.53 and 2.10 ppm. The aromatic region is very complex and assignment of the total number of peaks and their intensities was not possible. Assuming the [$Au_{12}S_{12}$] (Figure 3.11) core which is stabilised by 12 Au…Au interactions, remains intact in the major species in solution, the R groups can be assigned to three sets comprising those on S(1), S(6), S(12), S(7), those on S(2), S(5), S(8), S(11) and those on S(3), S(4), S(9), S(10). The minor species gives rises to four weak resonances in the aliphatic region at 1.19, 1.27, 1.78 and 1.89 ppm. The intensity of these signals compared to the major species, and also the chemical shift of these four resonances are solvent and temperature dependent, as evident from Figure 3.12.

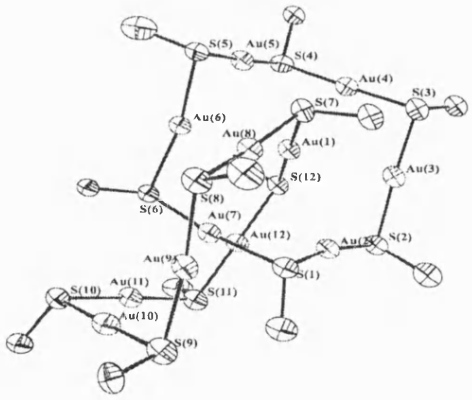

Figure 3. 11 $Au_{12}S_{12}$ core

Room temperature ^{13}C-NMR studies were carried out in deuterated chloroform, and three methyl peaks and three quarternary carbon signals were observed at 30.5, 30.7 and 32.0 ppm, and 36.4, 36.6 and 37.7 ppm respectively. This corresponds well with ^{1}H-NMR data. The aromatic region revealed sixteen of the eighteen resonances expected, excluding any consideration of the minor isomer.

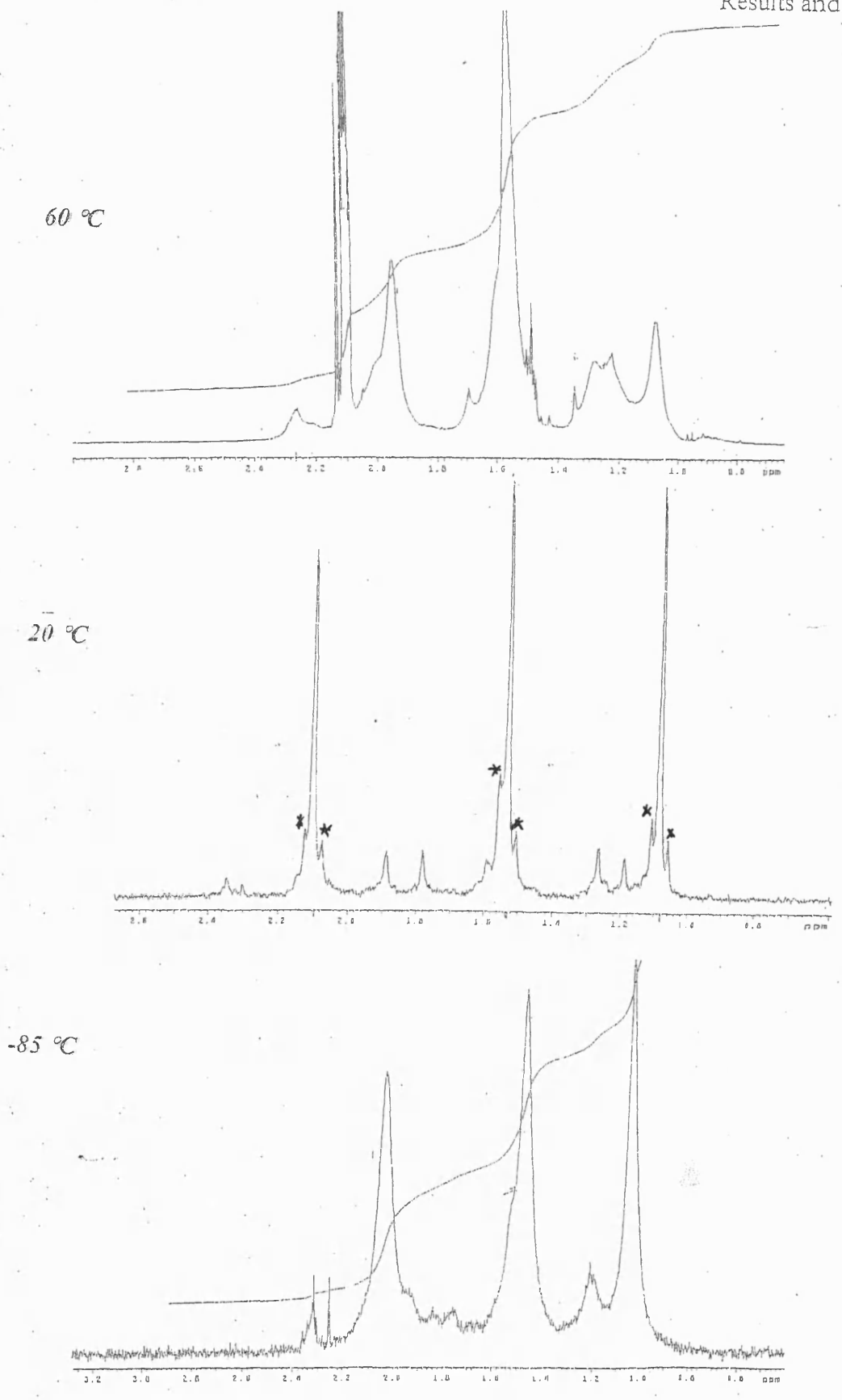

Figure 3. 12 Variable temperature ^{1}H-NMR spectrum of G2 (aliphatic region) {* Spinning side bands}

3.2.2.3 MASS SPECTROMETRY

The FAB (Fast Atom Bombardment) mass spectra of **G1a** and **G2** have been recorded at Bath to 3000 Daltons and for **G1a** to 4000 Daltons using the EPSRC Mass Spectrometry facility at Swansea, in each case using *para*-nitrobenzylalcohol. Gold is 100 % abundant as ^{197}Au and consequently exhibits no isotope pattern. Sulphur has three significant isotopes, ^{32}S (95 %), ^{33}S(0.76 %) and ^{34}S (4.22 %), whilst carbon has two, ^{12}C (98.9 %) and ^{13}C (1.1 %), as does hydrogen has two ^{1}H (99.99 %) and ^{2}H (0.01 %). Both **G1a** and **G2** contain in excess of one hundred carbons resulting in complicated isotope patterns for larger fragments due in particular to the isotopes of carbon and sulphur.

The most obvious decompositions pathways for both compounds would be expected to involve the loss of the following fragments individually or in some cases together:

i) All or part of the R group, C_6H_4-CMe_3 (RMM = 133.27)

ii) Thiolate ligand -SC_6H_4-CMe_3 (RMM = 165.33)

iii) Loss of sulphur (RMM = 32.06)

iv) Loss of gold (RAM = 196.97)

These clusters of the general type $Au_xS_yR_z$ are to be expected. Analysis of the results of this study was complicated by the near equivalence of the fragment S + SR (RMM = 197.33) and Au (RAM = 196.97). Consequently a mass loss of 197 could be due to loss of either. For higher mass fragments the mass of 3 S_2R units (591.99) is very similar to the mass of 3Au (590.91) and addition or subtraction of one proton will make the two fragments virtually indistinguishable. This anomaly meant that interpretation of the spectra of either **G1a** and **G2** is of limited value as alternative assignments could be made for several major fragments. For this reason a higher range Mass Spectral study using the EPSRC service was not carried out on **G2**.

G1a: The high mass study did not show the presence of $[Au(SC_6H_4\text{-}p\text{-}CMe_3)]_{10}$, **G1** at 3621, the most intense peak at 3716 corresponded to $Au_{10}S_3(SR)_{10}$. Fragments with masses greater than 3716 were also apparent, and some of these have been tentatively assigned to higher clusters formed by addition of Au, S or SR to Au_{10} species. All fragments of lower mass that could be assigned fit the general formulation $Au_xS_yR_z$, as summarised in Table 3.7.

G2: Since a high mass study was not undertaken for G2 the molecular ion was not observed. The highest mass fragment at 2731 is assigned as $Au_8(SR)_9$. Other assignments fit the general formula $Au_xS_yR_z$, which suggests that the bonded R group does not easily fragment by loss of CMe_3.

Fragments of G1a	*m/z*	*Fragments of G2*	*m/z*
$Au_{11}S_2(SR)_{11}$	3882	$Au_8(SR)_7$	2731
	3833	$Au_8S_2(SR)_6$	2631
	3800	$Au_9(SR)_5$	2599
	3768	$Au_9S(SR)_4$	2568
$Au_{10}S_3(SR)_{11}$	3716		2513
$Au_{10}S_3(SR)_{10}$	3551		2493
	3411		2469
	3366	$Au_8(SR)_5$	2403
	3303		2294
	3247		2263
$Au_9R_2(SR)_9$	3196		2232
	2990	$Au_6(SR)_6$	2175
	2972		2135
	2912		2101
	2845		2071
	2777	$Au_6(SR)_5$	2007
?	2640	$Au_6S_4(SR)_4$	1967
$Au_6R_1(SR)_6$	2142		1870
$Au_5S(SR)_6$	2008		1837
$Au_5S_2(SR)_4$	1708		1806
$Au_5(SR)_4$	1645	$Au_5S_3(SR)_4$	1743
		$Au_5S_2(SR)_4$	1705
		$Au_5S(SR)_4$	1678
		$Au_5S(SR)_3$	1508
		$Au_5(SR)_3$	1476
		?	1311
		$Au_3(SR)_5$	1253

Table 3. 7 Major fragments for G1a and G2, R = $C_6H_4CMe_3$

3.2.2.4 RAMAN SPECTROSCOPY

Powdered samples of the crystals of **G1a** and **G2a** were analysed by Raman spectroscopy courtesy of the Chemistry Department at UMIST. The spectrum of $[Au(SC_6H_4\text{-}p\text{-}CMe_3)]_{10}.0.8[C_6H_5OEt]$, **G1a,** is strong, (Figure 3.13), but samples of $[Au(SC_6H_4\text{-}o\text{-}CMe_3)]_{12}.2[C_6H_5Et]$, **G2a,** immediately degraded in the monochromatic laser beam and no spectrum was obtained. The region above 400 cm^{-1} is expected to be dominated by ligand absorptions and as noted in Table 3.8 strong aromatic ring mode was observed, as expected[11], at 1591 cm^{-1} and ring twisting at 588 and 453 cm^{-1}. The ν(CS) stretch at 1078 cm^{-1} is comparable to that reported[12] at 1000 cm^{-1}. The ν(AuS) stretch is comparable to the band reported[13] for $[Au(SCN)_2]^-$ at 306 cm^{-1}. It has been suggested[12] that ν(AuAu) vibrations occur in the range 64-162 cm^{-1}. The band at 156 cm^{-1} may be assigned to this vibration. Strong ν(C-H) stretches are also observed above 2900 cm^{-1}

Assignment	Observed (cm^{-1})
ν(Aryl)	1591s
ν(CS)	1078s
ν(aryl)	739m
ν(aryl)	588m
ν(aryl)	453w
ν(AuS)	310w
ν(AuAu)	156w

Table 3.8 Selected Raman data

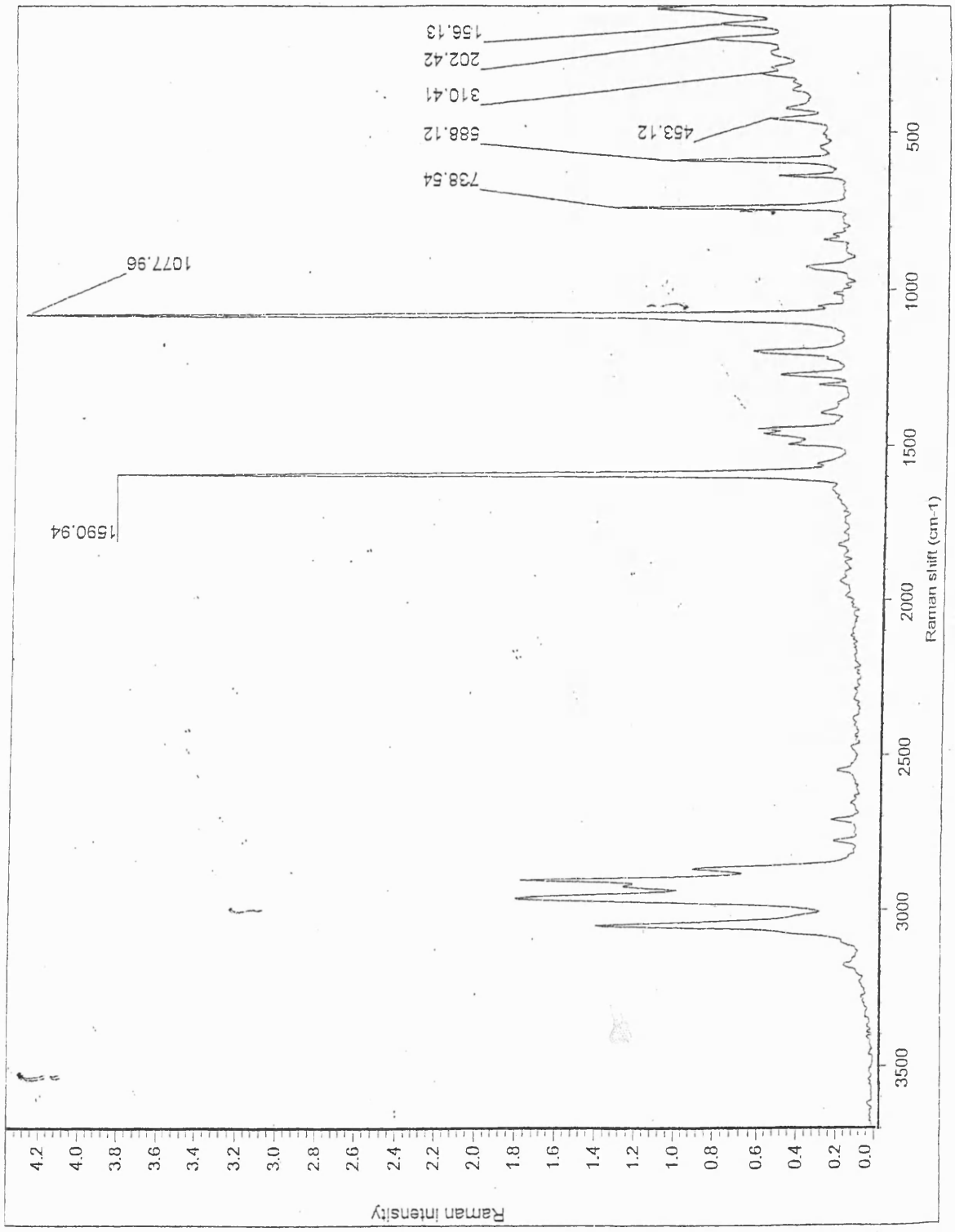

Figure 3.13 Raman spectra of G1a

3.2.2.5 THERMAL GRAVIMETRIC ANALYSIS

The use of gold(I) thiolates as precursors for gold films is well established and industrially important. However, thermolysis data have not been reported previously for the complexes **G1a-G10** in the literature and consequently the thermal gravimetric analysis (TGA) of this series was included in this study.

Thermolysis was carried out on powdered samples of **G1a–G10** under an inert atmosphere of nitrogen at a flow rate of 20 cm^3min^{-1}, and a heating rate of 20 °C min^{-1}. Relevant data are tabulated in Table 3.9. The thermal analyses of complexes **G3- G9** were also carried out in air in order to observe any differences caused by the presence of oxygen (Table 3.10). All compounds other than **G1a** and **G6** were observed to decompose in a two stage process The decomposition of **G1a** and **G6** involves an additional weight loss of less than 5 % w/w at relatively low temperatures. The plots of data for **G1a** illustrating the three stage decomposition is shown for **G1a** in Figure 3.14.

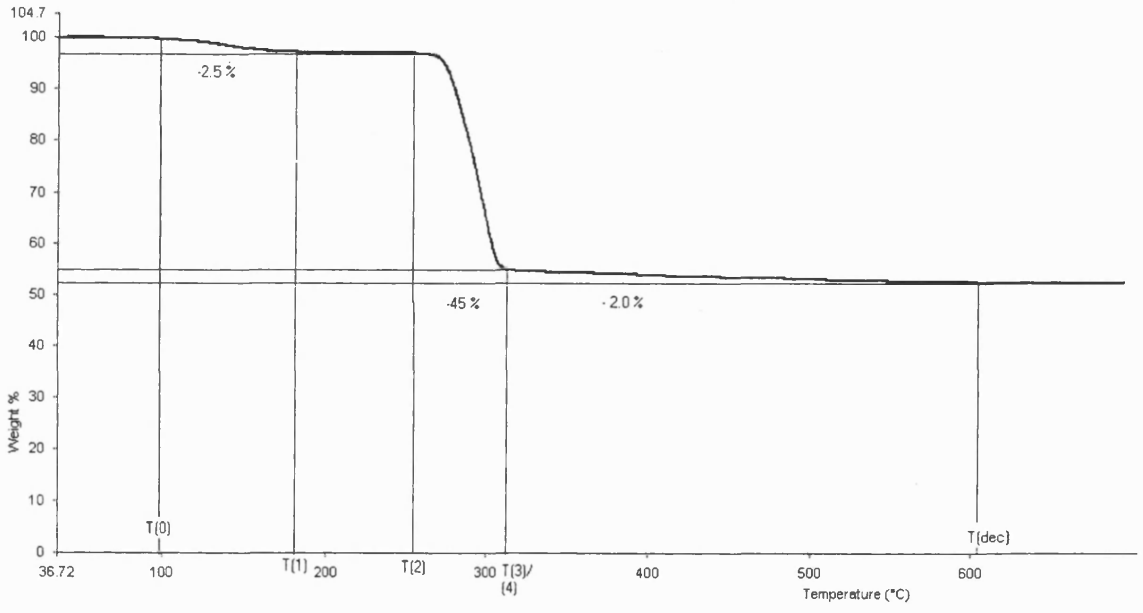

Figure 3. 14 TGA of G1a under nitrogen

Weight losses for the three stages can generally be explained as:

Stage (i) Loss of any incorporated solvent.

Stage (ii) Loss of ligand R group, and partial loss of sulphur, leaving Au_2S,

$$[AuSR]_n \rightarrow nAu_2S + nR_2S$$

Stage (iii) Formation of metallic gold

$$nAu_2S \rightarrow 2nAu + S_n$$

$\{[Au(SC_6H_4\text{-}p\text{-}CMe_3)].0.8C_8H_{10}O\}$, **G1a** contains 0.8 of ethoxybenzene and the initial mass loss of 2.5 % which occurs between 100 (T_0) and 170 (T_1) °C corresponding closely to the mass of ethoxybenzene (calculated as 2.6 %) in the sample. **G2-G10** were all characterised as solvent free, and apart from **G6** they are stable until the stage (ii) decomposition which occurs within the range 210-380 °C, and correspond to a loss of R_2S. Stage (iii) decompositions account for a loss of 0.5 – 3.0 % by mass over a wider range of 250 to 650 °C. In all cases the mass of the remaining golden coloured residue corresponds within experimental error to that expected for gold.

Thermolysis of $[AuSC_6H_4\text{-}p\text{-}CF_3]$, **G6**, in both air and N_2 was atypical in that it showed a mass loss of 5 % between 150 and 250 °C. Neither elemental analysis not infrared spectroscopy showed incorporation of solvent or thiol, and it seems likely that another impurity in the test sample, or an error in measurement, may be the source of the anomaly. Time restrictions prevented the preparation of a new sample for further investigation.

	W_{Au} (%)	T_0 (°C)	T_1 (°C)	$-W_1$ (%)	T_2 (°C)	T_3 (°C)	-W (%)	T_4 (°C)	T_{dec} (°C)	-W (%)	W_{dec} (%)
G1a	52.9	100	170	2.5	270	310	43.0	310	605	2.0	52.5
G2	54.4	-	-	-	250	320	44.5	320	650	3.0	53.5
G3	64.4	-	-	-	210	270	38.5	270	450	0.5	61.0
G4	52.6	-	-	-	220	265	44.0	270	420	1.0	52.5
G5	52.6	-	-	-	215	260	43.0	260	580	1.5	52.5
G6	52.6	140	230	4.5	250	320	45.5	320	700	1.0	49.0
G7	58.6	-	-	-	245	315	42.5	310	420	1.0	57.5
G8	58.6	-	-	-	200	350	40.0	350	580	1.0	58.0
G9	58.6	-	-	-	250	340	38.5	350	570	1.0	58.5
G10	55.3	-	-	-	260	380	43.5	380	560	2.0	54.5

Table 3. 9 [W_{Au}= % mass of Au in compound, T_0 = temperature at which decomposition begins, T_1,T_2,...= temperature at which gradient of TGA plot occur , T_{dec} = Temperature after total decomposition, W_{dec} = mass of solid left after complete decomposition]

Studies of the thermolysis of several of these complexes in air showed only small differences in behaviour from thermolysis under an inert environment, and the percentage mass losses for each stage for each compound do not significantly differ. There are slight differences in the temperatures at which decomposition starts. For example, compound **G5** begins to decrease in mass at 215 °C in nitrogen, but 270 °C in air.

	W_{Au} (%)	T_1 (°C)	T_2 (°C)	-W (%)	T_3 (°C)	T_{dec} (°C)	-W (%)	W_{dec} (%)
G3	64.4	200	270	37.0	270	455	1.0	62.0
G4	52.6	240	270	45.5	270	500	2.0	53.0
G5	52.6	270	320	47.5	-	-	-	52.5
G6	52.6	240	305	45.0	305	400	0.5	51.0
G7	58.6	250	320	40.0	320	455	1.0	59.0
G8	58.6	220	320	40.0	320	495	1.5	58.5
G9	58.6	215	320	40.0	320	490	1.5	58.5

Table 3. 10 TGA data for complexes G3-G9 under air. [W_{Au}= % mass of Au in compound, T_0 = temperature at which decomposition begins, T_1,T_2,...= temperature at which gradient of TGA plot occur , T_{dec} = Temperature after total decomposition, W_{dec} = mass of solid left after complete decomposition]

3.3 TRIPHENYLPHOSPHINE GOLD(I) THIOLATES, [(PPh$_3$)Au(SR)]

3.3.1 SYNTHESIS AND PROPERTIES

The complexes **P1-P10** where each prepared by addition of each of the homoleptic thiolates **G1-G10** to excess phosphine dissolved in toluene. However, due to the insolubility of **G3-G10**, the preparation of **P3-P10**, differed slightly from that of **P1** and **P2**. **G1** and **G2** both have good solubility in non-polar solvents, and they were reacted directly with excess triphenylphosphine in toluene to yield **P1** and **P2**, respectively. The products were precipitated from solution with acetonitrile. They were further purified by recrystallisation from toluene by slow addition of acetonitrile.

However, the insoluble reactants **G3-G10** were each added as a finely divided powder to a stirred toluene solution of excess triphenylphosphine. After 24 hours at room temperature all of the solid had reacted producing a colourless solution which was filtered and treated with diethyl ether to afford the product. Purification was achieved by recrystallisation from hot toluene. All complexes were dried in a vacuum oven at 70 °C and then stored in air. Quantities of reactants and specific experimental details are provided in Chapter Five of this Thesis.

It is interesting to note that a recent report[14] indicates that many complexes of the type [(R$_3$P)Au(SR')] including [(Ph$_3$P)Au(SPh)][15], **P7**, and [(Et$_3$P)Au(SPh)][16] are unstable. This has not been substantiated in this study. **P3, P7, P8, P9** and **P10** have very high solubilities and are difficult to isolate from solution. Oils were obtained in many attempts, but once isolated as solids, **P7** and **P8** showed no sensitivity to moisture or light. Other complexes in the series, **P1-P6** and **P10** were completely stable. The observed elemental analysis of **P10** deviated significantly from the expected composition, suggesting the presence of either

solvent or impurity. Repeated attempts to isolate [(Ph_3P)Au(SC_6H_4-*p*-OMe)], **P9**, were unsuccessful.

3.3.2 CHARACTERISATION

Each compound **P1-P8** and **P10** was characterised by infrared spectroscopy, elemental analysis for carbon and hydrogen, NMR and TGA. The crystal structures of **P1** and **P4** have been determined by X-ray crystallography. Elemental analyses for all nine compounds are in good agreement with the formula [(Ph_3P)Au(SR)]. Infrared spectra shows characteristic absorptions for phosphine and thiolate ligands. Data for all these compounds is detailed in Chapter Five of this Thesis. ^1H NMR solution studies were carried out on all nine complexes and are reported in the Experimental section.

3.3.2.1 SOLID-STATE STRUCTURAL STUDIES

The many reported structural studies of phosphine gold(I) thiolates have been described in Chapter One. All [(PR_3)Au(SR)] reported[17a-c] adopt a linear two-co-ordinate geometry about the metal centre. In this study the structures of two such complexes [(Ph_3P)Au(SC_6H_4-*p*-CMe_3)], **P1**, and [(Ph_3P)Au(SC_6H_4-*o*-CF_3)], **P4**, were determined in order to compare the Au-S separations with those in **G1a**, **G2a**, as well as with analogues in the literature.

Slow evaporation of a toluene solution of the complex [(Ph_3P)Au(SC_6H_4-*p*-CMe_3)], **P1** resulted in the formation of air and moisture stable X-ray quality crystals. Data were collected at room temperature. Selected bond angles and distances are summarised in Tables 3.11 and 3.12, respectively. Further structural data are provided in Appendix 2. The co-ordination geometry about the metal is very close to linear, with Au bound to the sulphur atom of the thiolate (Au-S = 2.287(2) Å), and the phosphorus centre of the phosphine (Au-P = 2.2575(13) Å). There are no additional weak inter- or intra- molecular contacts as occur in the homoleptic thiolates. The molecular structure of **P1** is illustrated in Fig 3.12.

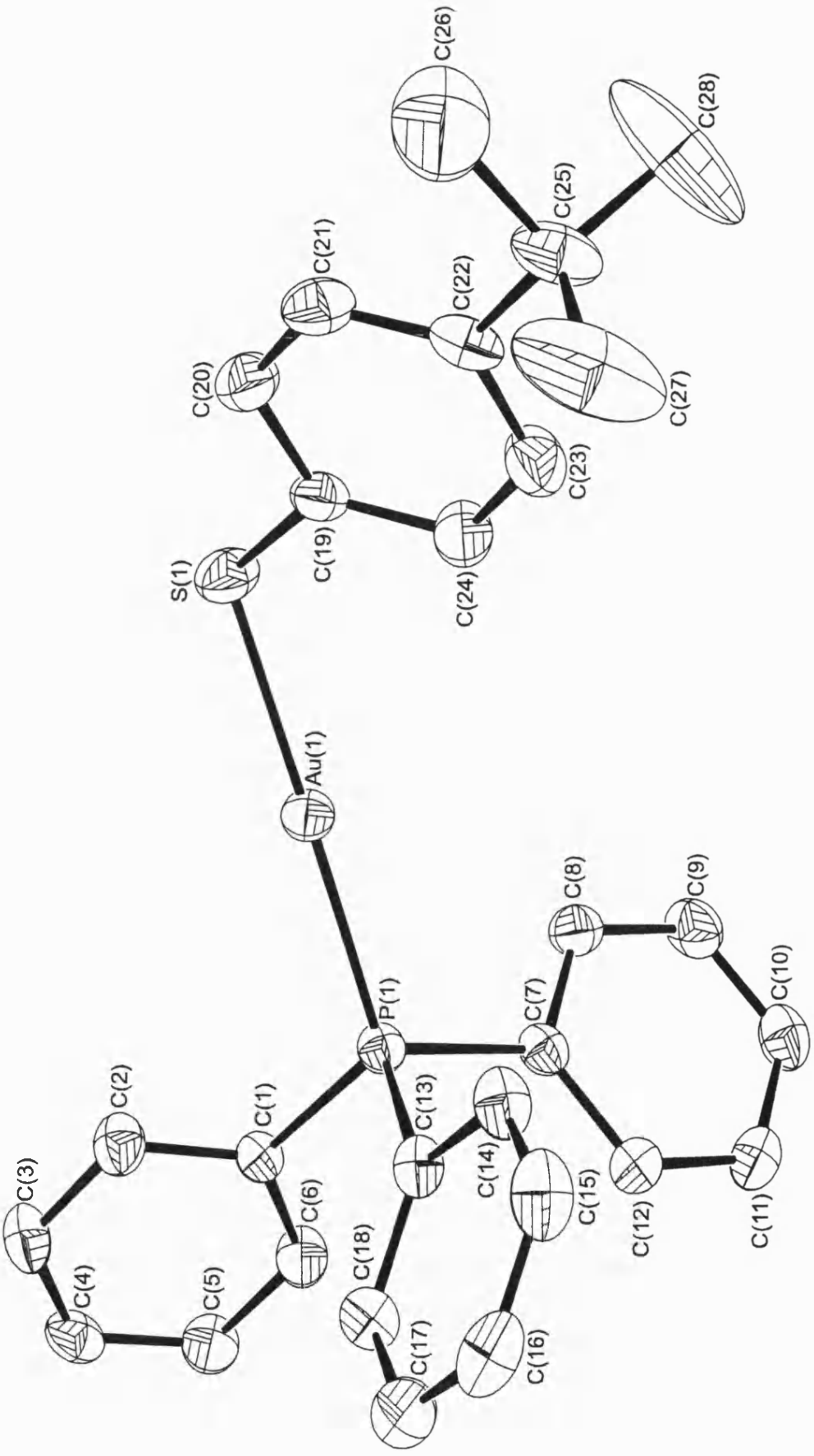

Figure 3.15 Molecular structure of P1

Bond	Length (Å)	Bond	Length (Å)
Au(1)-P(1)	2.2575(13)	C(11)-C(12)	1.380(7)
Au(1)-S(1)	2.287(2)	C(13)-C(14)	1.385(7)
P(1)-C(1)	1.809(5)	C(13)-C(18)	1.388(7)
P(1)-C(13)	1.820(5)	C(14)-C(15)	1.372(9)
P(1)-C(7)	1.820(5)	C(15)-C(16)	1.389(10)
S(1)-C(19)	1.764(6)	C(16)-C(17)	1.376(9)
C(1)-C(2)	1.382(7)	C(17)-C(18)	1.374(8)
C(1)-C(6)	1.388(7)	C(19)-C(24)	1.389(8)
C(2)-C(3)	1.390(8)	C(19)-C(20)	1.389(8)
C(3)-C(4)	1.371(8)	C(20)-C(21)	1.387(8)
C(4)-C(5)	1.370(8)	C(21)-C(22)	1.376(9)
C(5)-C(6)	1.380(8)	C(22)-C(23)	1.387(9)
C(7)-C(12)	1.386(7)	C(22)-C(25)	1.541(8)
C(7)-C(8)	1.393(7)	C(23)-C(24)	1.374(8)
C(7)-C(8)	1.393(7)	C(25)-C(28)	1.422(11)
C(8)-C(9)	1.380(8)	C(25)-C(27)	1.445(11)
C(9)-C(10)	1.365(8)	C(25)-C(26)	1.606(12)
C(10)-C(11)	1.385(8)		

Table 3.11 Bond lengths for P1

Atoms	Angle (°)	Atoms	Angle (°)
P(1)-Au(1)-S(1)	177.79(4)	C(14)-C(13)-C(18)	119.1(5)
C(1)-P(1)-C(13)	104.4(2)	C(14)-C(13)-P(1)	118.4(4)
C(1)-P(1)-C(7)	107.3(2)	C(18)-C(13)-P(1)	122.5(4)
C(13)-P(1)-C(7)	103.3(2)	C(15)-C(14)-C(13)	120.5(6)
C(1)-P(1)-Au(1)	114.6(2)	C(14)-C(15)-C(16)	120.0(6)
C(13)-P(1)-Au(1)	113.4(2)	C(17)-C(16)-C(15)	119.7(6)
C(7)-P(1)-Au(1)	112.9(2)	C(18)-C(17)-C(16)	120.3(6)
C(19)-S(1)-Au(1)	106.2(2)	C(17)-C(18)-C(13)	120.3(5)
C(2)-C(1)-C(6)	119.0(4)	C(24)-C(19)-C(20)	117.1(5)
C(2)-C(1)-P(1)	118.0(4)	C(24)-C(19)-S(1)	124.7(4)
C(6)-C(1)-P(1)	122.8(4)	C(20)-C(19)-S(1)	118.2(4)
C(1)-C(2)-C(3)	119.8(5)	C(21)-C(20)-C(19)	120.8(5)
C(4)-C(3)-C(2)	120.3(5)	C(22)-C(21)-C(20)	122.6(5)
C(3)-C(4)-C(5)	120.2(5)	C(21)-C(22)-C(23)	115.8(5)
C(4)-C(5)-C(6)	120.0(5)	C(21)-C(22)-C(25)	123.1(6)
C(1)-C(6)-C(5)	120.6(5)	C(23)-C(22)-C(25)	121.1(6)
C(12)-C(7)-C(8)	118.8(5)	C(24)-C(23)-C(22)	122.9(6)
C(12)-C(7)-P(1)	122.4(4)	C(23)-C(24)-C(19)	120.9(6)
C(8)-C(7)-P(1)	118.7(4)	C(28)-C(25)-C(27)	121.4(10)
C(9)-C(8)-C(7)	119.9(5)	C(28)-C(25)-C(22)	110.2(6)
C(10)-C(9)-C(8)	121.3(5)	C(27)-C(25)-C(22)	110.4(6)
C(9)-C(10)-C(11)	119.1(5)	C(28)-C(25)-C(26)	105.3(9)
C(12)-C(11)-C(10)	120.5(5)	C(27)-C(25)-C(26)	98.0(9)
C(11)-C(12)-C(7)	120.5(5)	C(22)-C(25)-C(26)	110.4(7)

Table 3.12 Selected bond angles for P1

X-ray quality crystals of [(Ph_3P)Au(SC_6H_4-*o*-CF_3)], **P4**, were grown by slowly cooling a concentrated toluene solution to -5 °C. These crystals were also found to be air and moisture stable, and data were collected at 170 K. Selected bond angles and distances are summarised in Tables 3.13 and 3.14, respectively. Further structural data are provided in

Appendix 2. The molecular structure of **P4** is illustrated in Figure 3.13. The central Au(I) atom bonded to the S-donor of the thiolate ligand (Au-S = 2.3006(8) Å) and to the P-donor of the phosphine (Au-P = 2.2606(8) Å). The P-Au-S angle is 173.2 ° is slightly less than that in the *para* substituted **P1** (177.8 °).

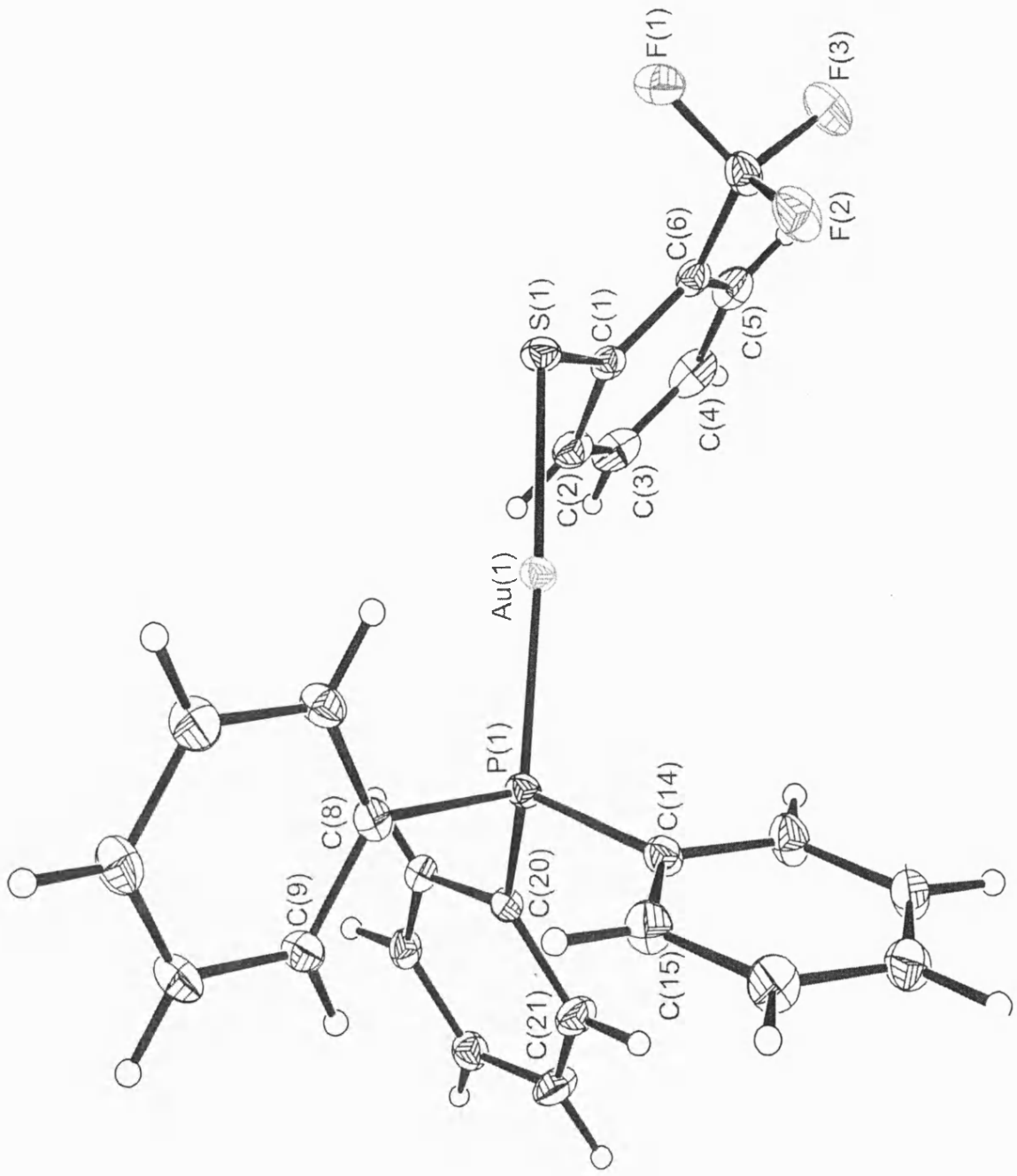

Figure 3.16 Molecular structure of P4

Bond	Length (Å)	Bond	Length (Å)
Au(1)-P(1)	2.2607(8)	C(8)-C(13)	1.393(4)
Au(1)-S(1)	2.3006(8)	C(9)-C(10)	1.384(5)
S(1)-C(1)	1.776(3)	C(10)-C(11)	1.381(5)
P(1)-C(20)	1.814(3)	C(11)-C(12)	1.387(5)
P(1)-C(14)	1.819(3)	C(12)-C(13)	1.382(5)
P(1)-C(8)	1.820(3)	C(14)-C(15)	1.390(4)
F(1)-C(7)	1.346(4)	C(14)-C(19)	1.398(4)
F(2)-C(7)	1.345(4)	C(15)-C(16)	1.395(5)
F(3)-C(7)	1.342(4)	C(16)-C(17)	1.376(5)
C(1)-C(2)	1.394(4)	C(17)-C(18)	1.383(5)
C(1)-C(6)	1.416(4)	C(18)-C(19)	1.390(5)
C(2)-C(3)	1.391(6)	C(20)-C(21)	1.388(4)
C(3)-C(4)	1.377(7)	C(20)-C(25)	1.394(4)
C(4)-C(5)	1.379(6)	C(21)-C(22)	1.394(5)
C(5)-C(6)	1.387(5)	C(22)-C(23)	1.387(5)
C(6)-C(7)	1.498(5)	C(23)-C(24)	1.380(5)
C(8)-C(9)	1.392(4)	C(24)-C(25)	1.390(4)

Table 3.13 Selected bond lengths for P4

Atoms	Angle (°)	Atoms	Angle (°)
P(1)-Au(1)-S(1)	173.18(3)	C(9)-C(8)-P(1)	121.8(2)
C(1)-S(1)-Au(1)	105.5(1)	C(13)-C(8)-P(1)	118.6(2)
C(20)-P(1)-C(14)	106.7(1)	C(10)-C(9)-C(8)	119.8(3)
C(20)-P(1)-C(8)	115.9(1)	C(11)-C(10)-C(9)	120.6(3)
C(14)-P(1)-C(8)	105.1(1)	C(10)-C(11)-C(12)	119.7(3)
C(20)-P(1)-Au(1)	114.0(1)	C(13)-C(12)-C(11)	120.2(3)
C(14)-P(1)-Au(1)	115.1(1)	C(12)-C(13)-C(8)	120.1(3)
C(8)-P(1)-Au(1)	110.2(1)	C(15)-C(14)-C(19)	119.5(3)
C(2)-C(1)-C(6)	117.7(3)	C(15)-C(14)-P(1)	121.6(2)
C(2)-C(1)-S(1)	120.5(3)	C(19)-C(14)-P(1)	118.9(2)
C(6)-C(1)-S(1)	121.8(2)	C(14)-C(15)-C(16)	119.8(3)
C(3)-C(2)-C(1)	120.9(4)	C(17)-C(16)-C(15)	120.2(3)
C(4)-C(3)-C(2)	120.8(4)	C(16)-C(17)-C(18)	120.5(3)
C(3)-C(4)-C(5)	119.2(3)	C(17)-C(18)-C(19)	119.7(3)
C(4)-C(5)-C(6)	121.1(4)	C(18)-C(19)-C(14)	120.2(3)
C(5)-C(6)-C(1)	120.3(3)	C(21)-C(20)-C(25)	119.3(3)
C(5)-C(6)-C(7)	118.4(3)	C(21)-C(20)-P(1)	123.5(2)
C(1)-C(6)-C(7)	121.3(3)	C(25)-C(20)-P(1)	117.2(2)
F(3)-C(7)-F(2)	105.7(3)	C(20)-C(21)-C(22)	119.8(3)
F(3)-C(7)-F(1)	105.6(3)	C(23)-C(22)-C(21)	120.6(3)
F(2)-C(7)-F(1)	106.3(3)	C(24)-C(23)-C(22)	119.8(3)
F(3)-C(7)-C(6)	112.4(3)	C(23)-C(24)-C(25)	119.9(3)
F(2)-C(7)-C(6)	113.6(3)	C(24)-C(25)-C(20)	120.6(3)
F(1)-C(7)-C(6)	112.6(3)	C(9)-C(8)-C(13)	119.6(3)

Table 3.14 Selected bond angles for P4

The Au-S and Au-P separations for **P1** and **P4** are very similar to those of other compounds of this type reported, as illustrated in Table 3.15. It appears that the arene substitution pattern in the thiolate ligand has no significant effect on either Au-S/P separations. The P-Au-S angles deviates from linearity by 7 ° in **P4**, which may be due to the presence of a

sterically bulky *ortho* -CF_3 substituent, however this could also be due to electronic factors. Note that in the dimer $[(PPh_3)Au(SPh)]_2$[13] one of the P-Au-S angles is 175.9 °which cannot be explained by steric arguments.

	Au-S (Å)	Au-P (Å)	Au-S-C (°)	P-Au-S (°)
$[(PPh_3)Au(SC_6H_4$-*p*-$CMe_3)]$ **P1**	2.287(2)	2.2575(13)	106.2(2)	177.79(4)
$[(PPh_3)Au(SC_6H_4$-*o*-$CF_3)]$ **P4**	2.3006(8)	2.2607(8)	105.5(1)	173.18(3)
$[(PPh_3)Au(SPh)]_2$ **P3**[13]	2.318(3), 2.316(3)	2.269(3), 2.278(3)	108.6(4)	179.0(1), 175.9(1)
$[(PPh_3)Au(SC_6H_4$-*o*-OMe)]**P7**	2.296(2), 2.324(2)	2.266(2), 2.283(2)	105.0(2)	175.2(1), 176.2(1)
$[(PPh_3)Au(SC_6H_4$-*p*-$NMe_2)]$[16c]	2.298(2)	2.259(1)	104.1(2)	176.53(4)
$[(PPh_3)Au(SC_6H_4$-*p*-$NMe_3)][PF_6]$[16c]	2.293(3)	2.259(3)	103.6(2)	175.52(5)

Table 3.15 Bond length and angles for $[(PPh_3)Au(SC_6H_4$-R)]

Whereas $[(PPh_3)Au(SPh)]_2$[13] has been shown to dimerise through Au...Au contacts of 3.13 Å, neither **P1** nor **P4** exhibit any auriophilic interactions, though the reasons for this are not entirely clear. It has been suggested[18] that a significant factor that influences the presence or absence of Au...Au interactions is the steric bulk of the thiolate and the phosphine ligands. The orientation of the thiolate ligands varies very little in the representative examples in Table 3.15, as demonstrated by the Au-S-C angle. Substitution of the aryl ring prevents dimer formation, and consequently the nature and position of the substituent in the ring appears to have little effect.

3.3.2.2 THERMAL GRAVIMETRIC ANALYSIS

Thermolysis was carried out on powdered samples of **P1 – P8** and **P10** under an atmosphere of nitrogen at a flow rate of 20 cm^3min^{-1}, and a heating rate of 20 °C min^{-1}. Relevant data are tabulated in Table 3.16. Thermal analyses of complexes **P3, P4**, **P7** and **P8** were also carried out in air for comparative purposes (Table 3.17). An example of data for **P6** under N_2, is shown in Figure 3.17.

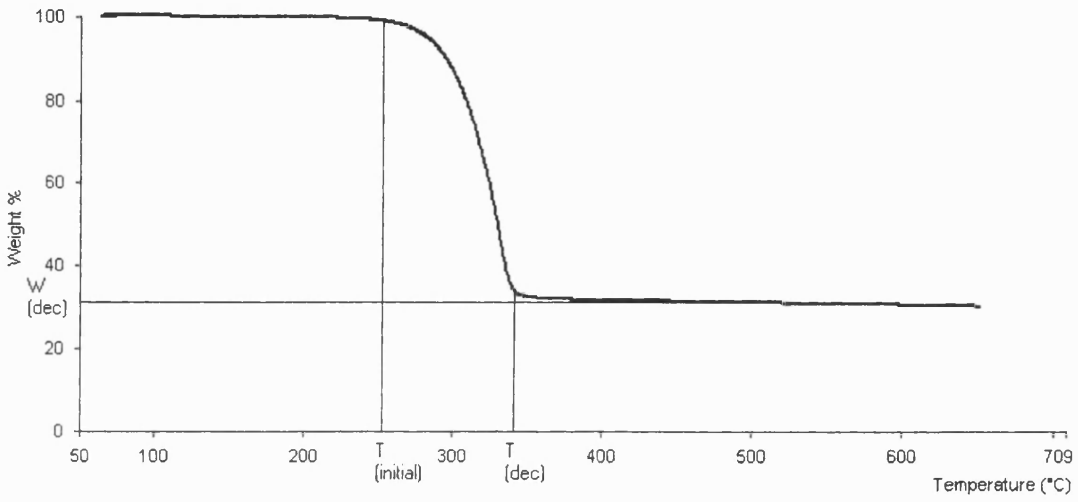

Figure 3.17 TGA of P6 under N_2

The decomposition of $[(Ph_3P)Au(SC_6H_4\text{-}p\text{-}CF_3)]_n$, **P6,** is representative of almost all of this series. Mass losses for **P1-P9** and **P10**, can be accounted for generally by three stages.

Stage (i) Loss of any incorporated solvent.

Stage (ii) Loss of phosphine and sulphide, resulting in Au_2S, formation

$$[AuSR]_n \rightarrow nAu_2S + nR_2S + PPh_3$$

Stage (iii) Formation of metallic gold

$$nAu_2S \rightarrow 2nAu + S_n$$

In each case the final mass of the residue corresponds closely to the gold content of the initial complex. As only **P7** and **P8** contain solvent which is lost at between 100 and 160 °C, TGA data in Tables 3.16 and 3.17 refers only to stage (ii) and (iii) processes only.

	W_{Au} (%)	T_0 (°C)	T_1 (°C)	$-W_1$ (%)	T_2 (°C)	T_{dec} (°C)	-W (%)	W_{dec} (%)
P1	31.5	250	350	68.0	350	520	1.5	30.5
P2	31.5	230	270	65.5	270	650	3.5	31.0
P3	34.7	200	350	68.0	350	470	1.0	31.0
P4	31.0	270	360	66.5	360	620	3.0	30.5
P5	31.0	290	380	69.0	-	-	-	31.0
P6	31.0	250	340	66.5	340	520	1.5	32.0
P7	32.9	180	370	64.0	370	640	4.5	31.5
P8	32.9	225	320	63.5	320	600	5.0	31.5
P10	31.9	220	365	64.5	365	500	5.0	29.5

Table 3.16 TGA for P1-8 and P10 in nitrogen. [W_{Au}= % mass of Au in compound, T_0 = temperature at which decomposition begins, T_1,T_2,...= temperature at which gradient of TGA plot occur , T_{dec} = Temperature after total decomposition, W_{dec} = mass of solid left after complete decomposition]

The presence of oxygen has no significant effect on the thermolytic behaviour of any of the four complexes investigated under both atmospheres.

	W_{Au} (%)	T_0 (°C)	T_1 (°C)	-W (%)	T_2 (°C)	T_{dec} (°C)	-W (%)	W_{dec} (%)
P1	31.5	240	350	69.0	350	600	1.0	30.0
P4	31.0	305	390	65.5	390	540	4.0	30.5
P7	32.9	250	335	66.0	335	580	3.0	31.0
P8	32.9	270	340	67.5	340	505	1.5	31.0

Table 3. 17 TGA for P1, P4, P7 and P8 in air. [W_{Au}= % mass of Au in compound, T_0 = temperature at which decomposition begins, T_1,T_2,...= temperature at which gradient of TGA plot occur , T_{dec} = Temperature after total decomposition, W_{dec} = mass of solid left after complete decomposition]

3.4 GOLD-2,2'-DITHIOPYRIDINE REACTIONS

2,2'-dithiopyridine, $(PyS)_2$, is a disulphide and so unlike RSH acts as an oxidising agent, consequently in the presence of Au(III) it was expected to act as a ligand and not as a reducing agent. A brief study was undertaken in order to determine whether Au(III) thiolates could be prepared using this ligand.

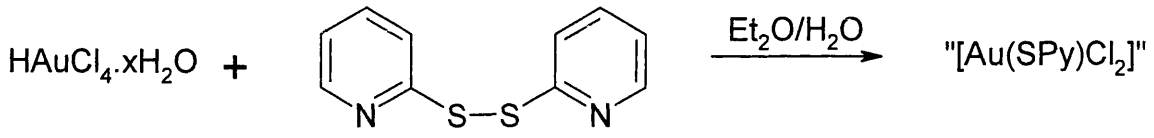

Figure 3.18

Reaction of an aqueous solution hydrogen tetrachloroaurate with excess dipyridine disulphide in ether resulted in the precipitation of an orange solid that had very low solubility but was very sparingly soluble in alcohol. Infrared data and elemental analysis indicated that the product had the empirical formula $[Au(SPy)Cl_2]$, **G11**, for which various formulations based on square planar Au(III) including those below are possible.

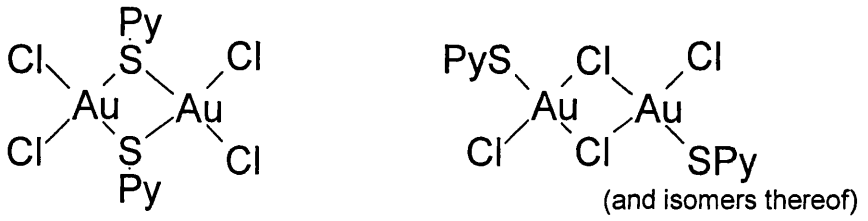

Figure 3. 19

This product was then reacted with triphenylphosphine in toluene in order to cleave any thiolate or chloride bridges and produce a soluble adduct. The reaction produced an immediate precipitation of a red solid, which on filtration and washing very rapidly lost its colour. Once again the product was insoluble in common solvents, and in view of the intractable nature of the products, the investigation was not pursued further.

3.5 CONCLUSIONS

Reduction of $HAuCl_4$ with methionine in aqueous media results in the formation of an unstable Au(I) sulphide intermediate which reacts readily *in situ* with appropriate aryl thiol to form complexes **G1 – G10** in high yield. An aim of this study was to examine the effect on the solubility and solid state structure of homoleptic gold(I) aryl thiolates by substitution with electron donating OMe groups, electron withdrawing CF_3 groups, and with a second aryl ring, in order to compare them with **G1** and **G2**. With the exception of compounds **G1** and **G2** these compounds are insoluble in all common solvents and structural determination of complexes **G3 – G10** was not possible.

The [2]catenane structures of both **G1a** and **G2a** form in such a way as to maximise Au...Au interactions whilst retaining the standard linear two-co-ordinate geometry about Au(I). Variable temperature NMR studies indicate that the $[Au_nS_n]$ core is stable in solution. Due to the problems of similar masses of two possible fragments the mass spectrometric analysis of **G1a** and **G2** was of limited use.

Compounds **G1-G8** and **G10** readily react with triphenylphosphine to form monomeric compounds **P1-P8** and **P10** of the form $[(Ph_3P)Au(SR)]$ and these compounds exhibit good solubility in organic solvents. $[Au(SC_6H_4\text{-}m\text{-}OMe]$, **G9** reacts with PPh_3 to presumably form $[(Ph_3P)Au(SC_6H_4\text{-}m\text{-}OMe)]$, **P9**, but due to high solubility was hard to isolate. The solid state structures of **P1** and **P4** are typical of the substituted triphenylphosphine Au(I) aryl thiolates, neither containing Au...Au contacts.

3.6 REFERENCES

[1a]C.F. Shaw III, *Chem. Rev.*, **99**, 2589 (1999); [b] R.V. Parish, *Interdiscip. Sci. Rev.*, **17**, 221 (1992); [c] C.F. Shaw III, *Gold: Progress in Chemistry, Biochemistry and Technology,* 259, John Wiley & Sons, London (1999)

[2a] J.P. Fackler Jr., W.E. van Zyl, B.A. Prihoda, *Gold: Progress in Chemistry, Biochemistry and Technology,* 259, John Wiley & Sons, London (1999); [b] A.K.H. Al-Sa'ady, K. Moss, C.A. McAuliffe, R.V. Parish, *J. Chem. Soc., Dalton Trans.,* 1609 (1984)

[3] I. Schroter, J. Strähle, *Chem. Ber.*, **124**, 2161 (1991) [b]Y.Y. Tong, A.J.L. Pombeiro, D.L. Hughes, R.L. Richards, *Trans. Met. Chem.*, **20**, 372 (1995)

[4] P.J. Bonasia, D.E. Gindleberger, J. Arnold, *Inorg. Chem.*, **32**, 5126 (1993)

[5] W. Wojnowski, B. Becker, J. Sassmannhausen, E.M. Peters, K. Peters, H.G. Von Schnering, *Z. Anorg. Allg. Chem.* **620,** 1417 (1994)

[6] P.A. Marsh, Ph.D. Thesis, University of Bath (1998) and Patent references therein

[7] A.K.H. Al-Sa'ady, K. Moss, C.A. McAuliffe, R.V. Parish, *J. Chem. Soc., Dalton Trans.*, 1609 (1984)

[8] A.J. Bondi, *J. Phys. Chem.*, **64**, 441 (1964)

[9] D.M.P. Mingos, J. Yau, S. Menzer, D.J. Williams, *Angew. Chem. Int. Ed. Engl.*, **34**, 1894 (1995)

[10] R. Narayanaswamy, M.A. Young, E. Parkhurst, M. Ouelette, M.E. Kerr, D.M. Ho, R.C. Elder, A.E. Bruce, M.R.M. Bruce, *Inorg. Chem.*, **32**, 2506 (1993)

[11] K. Nakamoto, *Infrared and Raman Spectra of Inorganic and Co-ordination Compounds, 4th Ed*, John Wiley and Sons (1988)

[12] N.B. Colthup, L.H. Daly, S.E. Wiberley, *Introduction to Infrared and Raman Spectroscopy,* Academic Press (1964)

[13] G.A. Bowmaker, *Gold: Progress in Chemistry, Biochemistry and Technology,* 841, John Wiley & Sons, London (1999)

[14] M. Nakamoto, W. Hiller, H. Schmidbaur, *Chem. Ber.*, **126**, 605 (1993)

[15] G.E. Coates, C. Kowala, J.M. Swan, *Aust. Chem.,* **19**, 539 (1966)

[16] C. Kowala, J.M. Swan, *Aust. Chem.,* **16**, 547 (1966)

[17a)] J.P. Fackler, R.J. Staples, A. Elduque, T.Grant, *Acta Cryst. Sect. C,* **50,** 520 (1994); [b)] M.M. Muir, S.I. Cuadrado, J.A. Muir, *Acta Cryst. Sect, C*, **50**, 1420 (1989); [c)] L.S. Ahmed, W. Clegg, D.A. Davies, J.R. Dilworth, M.R.J. Elsegood, D.V. Griffiths, L. Horsburgh, J.R. Miller, N. Wheatley, *Polyhedron*, **18**, 593 (1999)

[18] K. Angermaier, E. Zeller, H. Schmidbaur, *J. Organomet. Chem.,* **472**, 371 (1994)

CHAPTER FOUR: CHEMISTRY OF GOLD WITH OXYGEN DONOR LIGANDS

4.1 INTRODUCTION

The HSAB concept indicates that reactions of soft metals, such as gold, with hard oxygen donors are unfavourable in competitive environments containing softer donors. In non-competitive environments the formation of Au-O bonds is not ruled out, but these bonds are expected to be labile and in the presence of a soft donor the bond will be easily cleaved. From a strategic point of view relatively weak bonds between donor and acceptor could be of benefit for some industrial purposes, and of interest in aqueous gold formulations and gold ceramic interactions. Thus a gold containing aqueous formulation that has stability at room temperature but decomposes cleanly at relatively low temperature to deposit a uniform gold film could mean significant cost savings industrially. In addition, the decomposition products of complexes of oxygen donor ligands are less environmentally harmful compared with sulphur, nitrogen or phosphorus donor ligands.

In Chapter One the limited range of gold(I) complexes containing oxygen donor ligands was demonstrated, and this chemistry is limited by the thermodynamic and kinetic stability of the Au(I)-O linkage. The known compounds can be classified as either of the type $[(PR_3)Au(OR)]$ or $\{[(PR_3)Au]_nO\}^{m+}\{X^-\}_m$, [n = 3 or 4, m = 1 or 2]. Both types contain linear, two-co-ordination about Au(I), with Au co-ordinated to an O-donor and a "soft" donor ligand (PR_3 or CNR).

Pearson's calculated values of hardness[1], η, based on experimental data, suggest that whilst Ag^+ (η = 6.96 eV) is harder than Au^+ (η = 5.60 eV), it is softer than Au^{3+} (η = 8.40 eV). Thus Au(III) might simplistically be expected to have a more extensive chemistry with oxygen donors than either Au(I) or Ag(I). In fact the number of reported examples of Au(III) containing oxygen donors is rather limited and there are significantly less reported

than those of Au(I). However, Au(III) offers the only well characterised example of a binary gold oxide, Au_2O_3, and Au(III) anionic complexes such as $K^+[Au(NO_3)_4]^-$[2a,b]. This complex was first prepared by reaction of dinitrogen pentoxide with anhydrous potassium tetrabromoaurate(III), contains four monodentate nitrate ligands in a square planar arrangement around Au. The Au-O contacts all fall within the range 2.00 ± 0.02 Å, whereas the Au(I)-O contacts reported for complexes of the type $[(PR_3)Au(OR)]$ are on average slightly longer (range 1.99 – 2.11 Å)[3a-g].

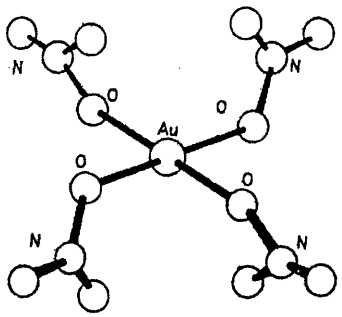

Figure 4.1 Structure of $K^+[Au(NO_3)_4]^-$

Gold(III) bromide also reacts with sodium trimethylsilanoate to yield an unstable dimer, $[Au_2(OSiMe_3)_6]$[4], which on treatment with excess sodium trimethylsilanoate affords unstable sodium tetrakis(trimethylsiloxy)aurate(III), Figure 4.2. NMR and IR were used to elucidate the identities of these products.

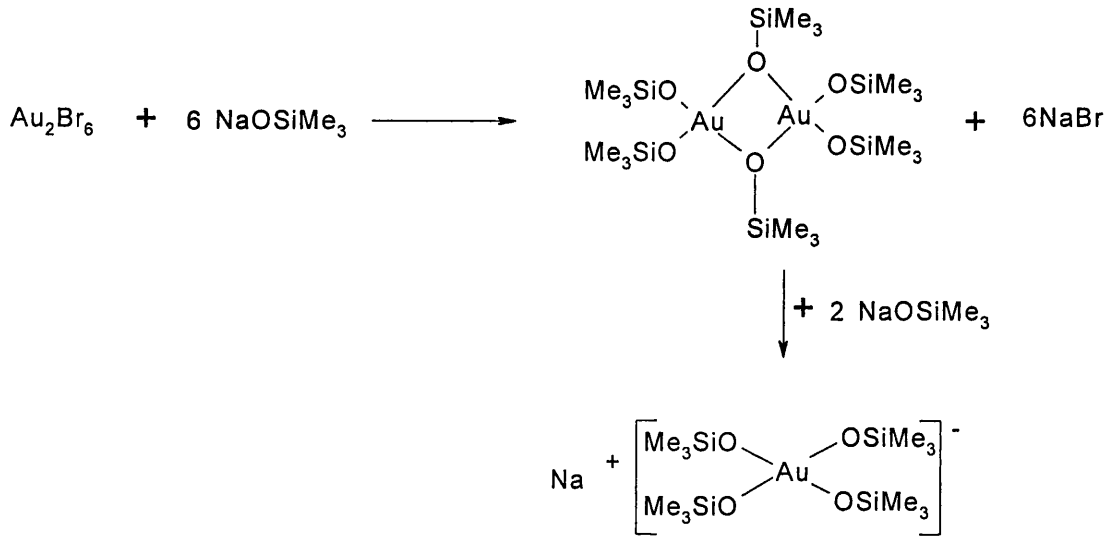

Figure 4.2

The only other Au(III) siloxide reported, Figure 4.3, is formed by reaction of dimethylgold(III)bromide with sodium trimethylsilanolate yielding $[Me_2AuOSiMe_3]_2$, which sublimes at 40°C and decomposes at 135°C.

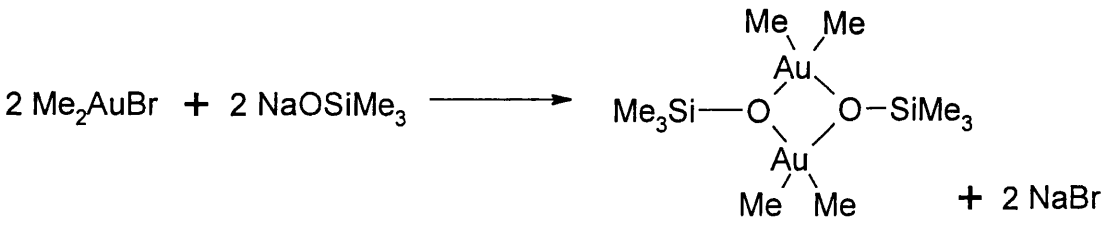

Figure 4. 3

The very brief investigations outlined in this chapter fall into three areas:

1. Studies of the reactions of Au(I) and Au(III) with neutral, macrocyclic oxygen donors, specifically crown-ethers.
2. Studies of the reactions of Au(I) complexes with anionic oxygen donor ligands, specifically alkali metal alkoxides, phenoxides and siloxides.
3. Studies of the reactions of Au(I) and Au(III) with the silsesquixoane, $[Cy_7Si_7O_9(OH)_3]$.

4.2 ATTEMPTED PREPARATION OF CROWN-ETHER COMPLEXES OF GOLD

As discussed in Chapter 2, metal centres co-ordinated to macrocylic polydentate n-donor atom ligands, such as crown-ethers, are additionally stabilised by the "macrocyclic effect" with respect to n-monodentate ligands. No stable examples of gold complexes containing neutral oxygen donor ligands have been reported. In an attempt to synthesise the first example of a crown-ether complex of gold, the reactions of a number of crown-ethers with Au(I) and Au(III) derivatives have been studied.

In Chapter Two it was noted that Ag(I) will readily react with crown-ethers to afford complexes with a variety of co-ordination numbers and geometries and that Ag^+ fits completely into the cavity of an approximately planar donor set of six O-atoms in 18-crown-6. Since the ionic radius of Ag^+ is less than that of Au^+, but greater than that of Au^{3+}, Au(I) is likely to be compatible with larger macrocycles and Au(III) with smaller macrocycles. Smaller crown-ethers might be capable of forming "sandwich" derivatives with any reasonable sized metal ions.

M	Radii/Å (Pauling)[5]
Ag^+	1.13
Au^+	1.37
Au^{3+}	0.91

Table 4. 1 Ionic radii of metal ions

The only commercially available source of Au(III) containing O-donor ligands is $K^+[Au(NO_3)_4]^-$. It has very limited solubility in organic solvents but attempts were made to displace the nitrate ligands by reaction with the crown-ethers 12-crown-4, 15-crown-5 and 18-crown-6. Reactions were carried out in THF at (-78 °C) under similar conditions to those used for preparing Ag(I) crown derivatives, but no reaction was observed. Attempts were repeated at room temperature, but again only starting materials were isolated. Finally

the solutions were gently refluxed, resulting in the deposition of a gold film. Further attempts were abandoned.

For reactions involving Au(I), an acetone solution of 12-crown-4, 15-crown-5 or 18-crown-6 was stirred for 48 hours with one equivalent of [(THT)AuCl], **R2**. No reaction was observed and only starting materials were isolated. The reaction was repeated at reflux for 6 hours. Again no reaction was observed, other than the deposition of gold from THT starting materials.

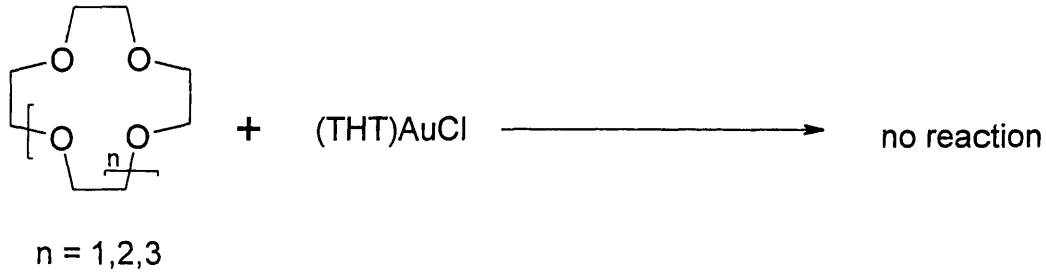

Figure 4. 4

It seems that the macrocyclic effect provided by the crown-ethers is unable to overcome the affinity of Au(III) for anionic O-donors at ambient temperatures. The reverse is true for Ag(I) which is softer than Au(III), indicating that "hard" or "soft" considerations are only one factor in determining the direction of a reaction. As $K^+[Au(NO_3)_4]^-$ is unstable to heat, the decomposition which occurred on heating may or may not involve an intermediate crown-ether complex. It was also found that the crowns were unable to displace THT from [(THT)AuCl], **R2**.

4.3 GOLD(I) COMPLEXES OF ANIONIC OXYGEN DONORS

4.3.1 ATTEMPTED PREPARATIONS OF HOMOLEPTIC GOLD(I) COMPLEXES, $[Au(OR)]_n$ (R = Ph or $SiMe_3$)

The most commonly used method for the preparation of homoleptic gold(I) thiolates involves reduction of Au(III) with a sulphide, followed by *in situ* addition of a thiolate or thiol in an organic solvent into which any soluble product is extracted. As there are no reports of comparable reactions carried out using alcohols or metal alkoxides, a brief attempt was made to prepare a homoleptic phenoxide and siloxide by this procedure. A solution of $HAuCl_4$ was reduced with methionine in ethanol/water, and the resulting Au(I) solution was transferred by cannula into a Schlenk tube containing a suspension of NaOR (R = Ph or $SiMe_3$) in toluene, and the solution was stirred under nitrogen at -78 °C. In both reactions a gold film was deposited within 15 minutes. Attempts to prepare homoleptic Au(I) complexes of O-donors by this route were abandoned.

4.3.2 PREPARATIONS OF TRIPHENYLPHOSPHINE GOLD(I) ALKOXIDES AND PHENOXIDES $[(PPh_3)Au(OR)]$ (R = Me, Et, ^{t}Bu, Ph, C_6H_4-p-CMe_3 and C_6H_4-o-CMe_3)]

A reasonable number of complexes of the type $[(PPh_3)Au(OX)]$ and $[(PPh_3)Au(OR)]$ have been reported, where OX represents siloxide, carboxylate, nitrate and triflate, and OR represent alkoxides and phenoxides, see Chapter Two. These are generally formed by metathesis of $[(PPh_3)AuCl]$, **R1**, with a metal salt, M^+OR^- [M = Ag, Na, K, or Tl]. The preparation and solid-state structures have been reported for two aryloxides, $[(PPh_3)Au(OC_6H_4\text{-}o\text{-}Br)]$[6] and $[(PPh_3)Au(OC_6Cl_5)]$[7]. There are no reported structures of simple straight chain alkoxides, although four compounds whose preparation has been reported are fluorine substituted alkoxides[8] of the type $[(PR_3)Au(OR')]$, {R=Cy and Ph, R' = CH_2CF_3 and $CH(CF_3)_2$}.

Initial attempts to prepare simple triphenylphosphine Au(I) alkoxides, [(PPh_3)Au(OR)], where R = Me, Et and Bu^t by the established method, yielded in each case an orange/yellow coloured THF solution at –78 °C. Attempts to isolate the product by removal of solvent or by addition of hexane resulted in decomposition to a purple solid within an hour. More success was achieved in reactions involving phenoxides. Initially the preparation of the known [(PPh_3)AuOPh][9].0.5H_2O, **A1**, was carried out by reacting sodium phenate with [(PPh_3)AuCl], **R1**, in THF, at – 78 °C. The identity of **A1** was confirmed by IR, elemental analysis and NMR, but attempts to grow crystals for a structure determination were unsuccessful. Attempts were then made to prepare O-analogues of **P1** and **P2**.

Sodium salts of HOC_6H_4-*p*-CMe_3 and HOC_6H_4-*o*-CMe_3 were prepared by direct reaction with NaH in THF. Once gas evolution had ceased the resulting solution was transferred to a Schlenk flask containing a THF solution of [(PPh_3)AuCl], **R1**. The solution quickly turned orange, and salt precipitated. The solid was removed by filtration and volatiles removed *in vacuo* to leave a light orange solid. This was redissolved in DCM and reprecipitated by addition of hexane. Analysis suggested the product to be [(PPh_3)Au(OH)], **A2**, and not [(PPh_3)Au(OC_6H_4-*p*-CMe_3)] as expected. This compound appears to be stable in the solid-state at room temperature under nitrogen for weeks, but slowly decomposes in solution to deposit a gold film. To date, attempts to grow crystals of this unusual product have been unsuccessful.

4.4 ATTEMPTED REACTIONS OF GOLD WITH A SILASESQUIOXANE

A short study of the reaction of the silasesquioxanes $[(Cy)_7Si_7O_9(OH)_3]$, **R5**, and $[Cy_7Si_7O_{12}P]$, **R6**, with gold was carried out. The cubic triol, $[(Cy)_7Si_7O_9(OH)_3]$, **R5** has a vacant Si site in one corner and is considered the best current model for the surface of silica[10ab]. Silasesquioxanes have considerable potential as model compounds for the surfaces of ceramics, and they are also potential precursors to ceramic dyes[11]. There are extensive reports of **R5** complexing with metals[12a-d], but to date there are no reports of the reaction of gold derivatives with **R5**. The synthesis of **R5** involves a long hydrolytic condensation reaction in which cyclohexyltrichlorosilane is dissolved in an acetone/water solution and left for four months[13], (Figure 4.5).

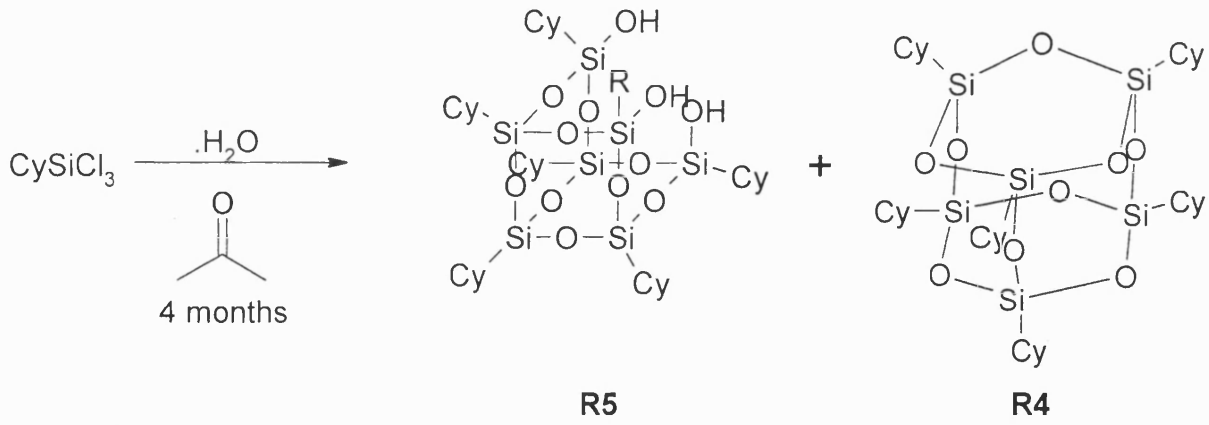

Figure 4. 5

Both **R4** and **R5** were prepared in good yield, as described in the experimental section of this Thesis. Equimolar quantities of **R5** and $HAuCl_4$ were dissolved in THF, and three equivalents of 1,4-diazabicyclo[5,4,0]-undecan-7-ene, and a small amount of acetonitrile (0.5 cm^3) was added (Figure 4.6). After 2 hours a red oil had formed but after the solvent was decanted off, the oil decomposed to a gold film before it could be investigated further.

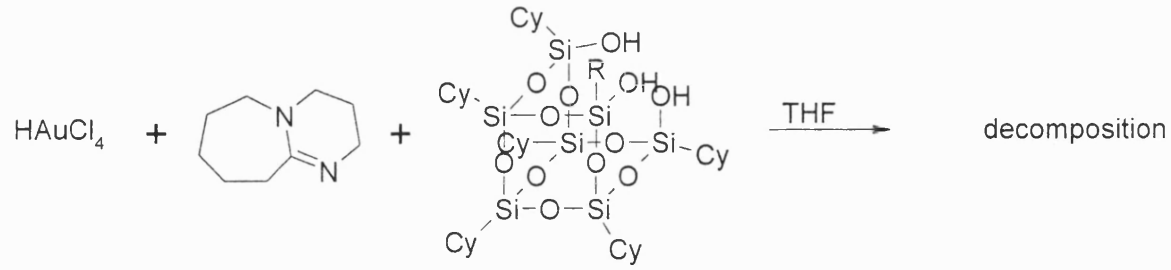

R5

Figure 4. 6

Reaction of **R5** with PCl_3 in the presence of organic base (i.e. NEt_3) forms the phosphite $[Cy_7Si_7O_{12}P]$[14], **R6**, as illustrated below (Figure 4.7). The Tolman cone angle for the phosphite has been calculated to be 167 °, which is notably larger than that of triphenylphosphine (145 °), but not as large as tri-*tert*-butylphosphine (182 °). The large steric size of the phosphite is expected to have a significant effect on the chemistry of the ligand.

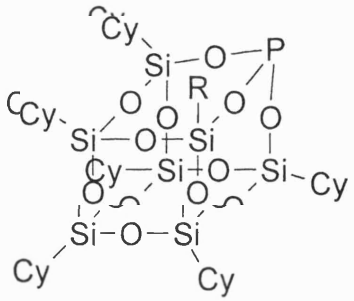

R6

Figure 4. 7

Given the bulky nature of the ligand, an attempt was made to co-ordinate the phosphite to Au(I) by reaction of a supension of [(THT)AuCl], **R2,** with a THF solution of **R6**. However, no reaction was observed. It was found that excess **R6** in THF did not react with an aqueous solution of "$HAuCl_4$", unlike PPh_3, indicating that it is a considerably weaker base.

4.5 CONCLUSIONS

Attempts to prepare Au(I) and Au(III)-crown-ether complexes were unsuccessful which contrasts with the ease with which Ag(I) forms this class of complex. These studies have confirmed the major differences between the chemistry of gold(I) and silver(I). Whereas the d^{10} Ag(I) ion will readily accommodate different geometries and co-ordination numbers in the presence of hard donor ligands, Au(I) appears to prefer linear two-co-ordination irrespective of donor type. In addition, the only reported Au(I) complexes of O-donors contain a soft donor ligand trans to oxygen, and this study has not added to the known examples, other than by the preparation of $[(PPh_3)Au(OH)]$, **A2**. This compound has reasonable stability, which might be attributed to H-bonding and/or auriophilic interactions.

4.6 REFERENCES

[1] R.G. Pearson, *Inorg. Chem.*, **27**, 734 (1988)

[2a)] C.D. Garner, S.C. Wallwork, *J. Chem. Soc., Chem. Commun.*, 108 (1969); [b)] C.D. Garner, S.C. Wallwork, *J. Chem. Soc. (A)*, 3092 (1970);

[3a)] T. Mathieson, A. Schier, H. Schmidbaur, *J. Chem. Soc., Dalton Trans.*, 3881 (2000); [b)] A. Bauer, A. Schier, H. Schmidbaur, *Acta Cryst. Sect. C*, **51**, 2030 (1995); [c)] J.P. Fackler, Jr., M.N.I. Khan, C. King, R.J. Staples, R.E.P. Winpenny, *Organomet.*, **10**, 2178 (1991); [d)] M. Presenberger, A. Schier H. Schmidbaur, *J. Chem. Soc., Dalton Trans.*, 1654 (1999);

[e)]P.M.N. Low, Z.Y. Zhang, T.C.W. Mak, T.S.A. Hor, *J. Organomet. Chem.* **539**, 45 (1997);

[f)]P.G. Jones, R. Schelbach, *J. Chem. Soc., Chem. Commun.*, 1338 (1988); [g)] P.G. Jones, R. Schelbach, *Inorg. Chem. Acta.*, **182**, 239 (1991)

[4] F. Schindler, H. Schmidbaur, *Angew. Chem. Int. Ed. Engl.*, **6**, 683 (1967)

[5] J. Emsley, *The Elements, 3rd Ed.*, Clarendon Press (1998)

[6] L.G. Kuz'mina, O.Y. Burtsuva, N.V. Dvortsuva, M.A. Porai-Koshita, *Koord. Khim.*, **15,** 773 (1989)

[7] L.G. Kuz'mina, Y.T. Struchlov, *Koord. Khim.*, **14**, 1262 (1988)

[8] S. Komiya, M. Iwata, T. Sone, A. Fukuoka, *J. Chem. Soc., Chem. Commun.*, 1109 (1992)

[9] E.G. Perevalova, E.I. Smyslova, K.I. Granberg, Y.T. Struchlov, L.G. Kuz'mina, D.N. Kravtsov, *Koord. Khim.*, **15**, 504 (1989)

[10a)] F.J. Feher, D.A. Newman, J.F. Walzer, *J. Am. Chem. Soc.*, **111**, 1741 (1989); [b)] F.J. Feher, D.A. Newman, *J. Am. Chem. Soc.*, **112**, 1931 (1990)

[11] R.H. Baney, M. Itoh, A. Sakakibara, T. Suzuki, *Chem. Rev.*, **95**, 1409 (1995)

[12a)] K. Wada, M. Nakashita, A. Yamamoto, T. Mitusudo, *J. Chem. Soc., Chem. Commun.*, 133 (1998); [b)] F.J. Feher, D. Soulivong, F. Nguyen, J.W. Ziller, *Angew. Chem. Int. Ed. Engl.*, **37**, 2663 (1998); [c)] H.C.L. Abbenhuis, A.D. Burrows, H. Kooijman, M. Lutz, M.T.

Palmer, R.A. van Santen, A.L. Spek, *J. Chem. Soc., Chem. Commun.*, 2627 (1998); [d] F.J. Feher, T.A. Budzichowski, *Polyhedron,* **14**, 3239 (1995)

[13] C.C. Rainford, Ph.D. Thesis, University of Bath (1997)

[14] F.J. Feher, T.A. Budzichowski, *Organomet.*, **10**, 812 (1991)

CHAPTER FIVE: EXPERIMENTAL

5.1 INTRODUCTION

The great majority of the synthetic work reported in this thesis was carried out at the University of Bath. However the author spent a short industrial placement of two weeks at the Johnson Matthey Technology Centre in Reading, during which time compounds **C5 - C9** were synthesised. A very limited amount of NMR characterisation was also carried out at Johnson Matthey.

5.2 SYNTHETIC TECHNIQUES

5.2.1 SAFETY

University health and safety guidelines[1] were adhered to while carrying out laboratory work. Standard safety clothing (nitrile gloves, laboratory coat and eye protection) was worn at all times whilst in the laboratory. Overnight and hazardous reactions were carried out in the special operations unit in the Department. Due to their stench thiols and organic sulphides were treated with extra care. University safety guidelines involved online notification[2] of the Departmental Safety Committee of their use, and all reactions were carried out in the special operations unit. Residues containing thiol or organic sulphides reactions were destroyed using thick household bleach prior to disposal.

5.2.2 GENERAL REACTION PROCEDURES

Reactions were carried out routinely under an inert atmosphere of dry nitrogen gas. Preparations involving silver or gold were normally studied in the absence of light to minimise decomposition. Products were routinely dried in a vacuum oven.

5.2.3 REAGENTS

All reagents used were obtained from commercial suppliers. Solids were routinely dried in a vacuum oven, liquid crown ethers were dried over molecular sieves (number 3A), other solutions and liquid reagents were used as delivered. An aqueous solution of hydrogen tetrachloroaurate (41.61 %wt Au) was provided by the CASE project sponsors Johnson Matthey Plc.

5.2.4 SOLVENTS

THF, toluene and diethyl ether were dried by distillation over sodium wire[3] and DCM was dried over calcium hydride. All other solvents were dried over molecular sieves (number 3A). NMR solvents were purchased from Aldrich and used as supplied, or if necessary, following desiccation over 3A molecular sieves.

5.2.5 ANALYTICAL TECHNIQUES

Infrared analyses were carried out using a Nicolet 510P or Perkin Elmer 1600 FT-IR spectrometer on solid samples mulled with nujol between sodium chloride discs. Fluid samples were suspended between NaCl discs. Raman analysis of **G1** was carried out by Dr A.K. Brisdon, Department of Chemistry, UMIST on a Nicolet Nexis Spectrometer equipped with a Raman attachment.

Elemental analysis for carbon, hydrogen and nitrogen were carried out by Mr Alan Carver in the Department microanalysis facility using a CARLO-ERBA 1106 analyser. Elemental analysis for phosphorus was carried out at the Department of Pure and Applied Chemistry, University of Strathclyde.

Routine ^{1}H- and ^{13}C-NMR spectra were recorded on JEOL 270 and EX400 instruments. Variable temperature ^{1}H-NMR studies were carried out on a JEOL EX400 instruments. Unless otherwise stipulated NMR studies at ambient temperature were carried out in deuterated chloroform using tetramethylsilane as a reference. Variable temperature studies on **G1** and **G2** employed DCM as a solvent at low temperature and toluene at high temperature.

Single crystal X-ray crystallography was carried out by Dr Mary Mahon and the author, on a CAD4 X-ray difractometer for compounds **G1**, **G2, P1, C6**, **C7** and **C8**. Structures of **P4, C11**, **C13** and **C15** were determined using an Enraf Nonius KAPPA CCD difractometer. Structures were solved using Shelx[4], XPMA[5] Ortex and Oscail[6] software.

Thermal decomposition studies were carried out on a Perkin Elmer thermogravimetric analyzer TGA7. Mass spectrometric examination of **G1** was carried out under FAB conditions to 4,000 Daltons at 7kV at the EPSRC national MS Service Centre, Chemistry Department, University of Wales, Swansea. Mass spectrometric examination of **G2** was carried out by C. Cryer at the University of Bath, Mass Spectrometry Unit using a Micromass Autospec M, double focusing, magnetic sector instrument under FAB conditions to 3,000 Daltons at 8kV.

5.3 PREPARATIONS OF CROWN ETHER CONTAINING SILVER(I) COMPLEXES

5.3.1 GENERAL PROCEDURE

A series of crown ether containing silver(I) complexes **C1-C17** were prepared in the absence of light and under an N_2 atmosphere using the general preparative procedure outlined below:

The finely divided silver salt was added to a stirred solution of crown ether in dry THF (15 cm^3), and the clear solution initially formed was stirred at room temperature for 24 hours. Reactions involving 12-crown-4, 15-crown-5, and 1,1'-dimethylsila-11-crown-4 were carried out in a ratio of two equivalents of crown to one of the silver salt. 18-Crown-6 was reacted with equimolar amounts of silver salts. Benzo-18-crown-6 and dibenzo-18-crown-6 were reacted in a slight molar excess due to their poor solubility.

The products of the reactions of silver salts containing the non-co-ordinating counter ions, $[BF_4]^-$ and $[PF_6]^-$, precipitated from the stirred solution. These were then isolated by filtration and washed with cold THF. Each product was recrystallised from DCM/hexane and dried under vacuum. Crystals for X-ray structure determinations were grown by slow evaporation of a concentrated DCM solution.

The products of the reactions of the silver salts with the more strongly co-ordinating counter ions, $[OTF]^-$ and $[NO_3]^-$, remained in solution. In these cases the solvent was evaporated to half volume and cyclohexane added to initiate precipitation of the product. The solid was then isolated by filtration, and washed with cold THF and then cyclohexane. Each product was recrystallised from DCM/hexane. Crystals of **C6**, **C7**, **C8, C11**, and **C15** suitable for crystallographic studies were grown by slow evaporation of a concentrated DCM solution and crystal of **C13** where grown from a concentrated chloroform solution.

This same procedure was used in order to study the reactions of silver acetate, trifluoroacetate and benzoate. Each reaction yielded only starting materials. The same preparations were also attempted using ethanol and acetone in place of THF, but only starting materials were isolated. Reactions in each solvent were also carried out at elevated temperatures but again with negative results.

All non-crystalline products were dried in a vacuum oven at room temperature.

5.3.2 CHARACTERISATION

The quantities of reactants used in each preparation are listed below together with experimental yields, elemental analyses and selected IR data for each compound. ^{1}H-NMR and ^{13}C-NMR data are listed for a representative example of each type of crown ether complex, and for the complete range of 15-crown-5 compounds.

[Ag(12-crown-4)$_2$][BF$_4$], C1

$AgBF_4$ (0.24 g, 1.2 mmol) and 12-crown-4 (0.40 cm^3, 2.4 mmol)

Light brown solid (0.23 g, 42 %)

Analysis: Found (calculated for $C_{16}H_{32}O_8BF_4Ag$): C, 35.1 (35.1); H, 5.90 (5.92) %

IR: ν(COC) 1095s, 1058s, 1018s, ν(BF) 912m, 843m cm^{-1}

[Ag(12-crown-4)$_2$][PF$_6$], C2

$AgPF_6$ (0.31 g, 1.2 mmol) and 12-crown-4 (0.40 cm^3, 2.4 mmol)

Light grey powder (0.47 g, 63 %)

Analysis: Found (calculated for $C_{16}H_{32}O_8PF_6Ag$): C, 31.6 (31.8); H, 5.31 (5.33) %

IR: ν(COC) 1303m, 1290m, 1251m, 1134s, 1092s, 1020s, ν(PF) 915s, 877m, 837s cm^{-1}

[Ag(12-crown-4)$_2$][OTf].H$_2$O, C3

AgOTF (0.30 g, 1.2 mmol) and 12-crown-4 (0.40 cm^3, 2.4 mmol)

White powder (0.61 g, 87 %)

Analysis: Found (calculated for $C_{17}H_{32}O_{11}SF_3Ag$): C, 33.1 (33.4); H, 5.29 (5.25) %

IR: ν(OH) 3400w, 1654m, ν(COC) 1273s, 1221w, 1147s, 1133s, 1090s, 1028s, 1018s cm^{-1}

^{1}H-NMR (400 MHz, $CDCl_3$): δ 3.73 ppm (s, 16H, C**H**$_2$)

^{13}C-NMR (400 MHz, $CDCl_3$): δ 65.8 ppm (s, 8C, **C**H$_2$)

[Ag(12-crown-4)][NO_3], C4

$AgNO_3$ (0.20 g, 1.2 mmol) and 12-crown-4 (0.40 cm^3, 2.4 mmol)

White powder (0.39 g, 63 %)

Analysis: Found (calculated for $C_8H_{16}O_7NAg$): C, 27.7 (27.8); H, 4.71 (4.65); N, 4.0 (4.1)%

IR: ν(COC or NO) 1314s, 1296s, 1243s, 1100s, 1045s cm^{-1}

[Ag(15-crown-5)][BF_4].1H_2O, C5

$AgBF_4$ (0.47 g, 2.4 mmol) and 15-crown-5 (0.96 cm^3, 4.8 mmol)

White powder (0.48 g, 78 %)

Analysis: Found (calculated for $C_{10}H_{22}O_6BF_4Ag$): C, 27.9 (27.7); H, 5.15 (5.12) %

IR: ν(OH) 3642m, 3556m; ν(HOH) 1619m; ν(COC) 1356s, 1292s, 1250s, 1130s, 1099s;

ν(BF) 912s, 876s, 840S cm^{-1}

^{1}H-NMR: (400 MHz, $CDCl_3$) δ 3.78 (20H, s, 10 x C**H**$_2$) ppm

^{13}C-NMR (400 MHz, $CDCl_3$): δ 69.3 (10C, s, 10 x **C**H_2) ppm

[Ag(15-crown-5)(H_2O)(15-crown-5)][PF_6], C6

$AgPF_6$ (0.61 g, 2.4 mmol) and 15-crown-5 (0.96 cm^3, 4.8 mmol)

White powder (0.45 g, 54 %)

Analysis: Found (calculated for $C_{20}H_{42}O_{11}PF_6Ag$): C, 33.9 (33.8); H, 5.95 (5.91); P, 4.34 (4.36)

%

IR: ν(OH) 3409m; ν(HOH) 1667m; ν(COC) 1296m, 1250m, 1099s, 1038m; ν(PF) 941m cm^{-1}

^{1}H-NMR (400 MHz, $CDCl_3$): δ 3.72 ppm (s, 20H, C**H**$_2$)

^{13}C-NMR (400 MHz, $CDCl_3$): δ 69.7 ppm (s, 10C, **C**H_2)

[Ag(15-crown-5)][OTf], C7

AgOTF (0.60 g, 2.4 mmol) and 15-crown-5 (0.96 cm^3, 4.8 mmol)

White powder (0.30 g, 74 %)

Analysis: Found (calculated for $C_{11}H_{20}O_8SF_3Ag$): C, 27.9 (27.8); H, 4.27 (4.21) %

IR: ν(COC) 1352m, 1298s, 1258s, 1228s, 1156s, 1089s, 1023s; ν(CF) 946s, 850w, 828m; cm^{-1}

^{1}H-NMR: (270 MHz, $CDCl_3$) δ 3.78 ppm (20H, s, 10 x C**H**$_2$).

^{13}C-NMR: (270 MHz, $CDCl_3$) δ 69.5 ppm (10C, s, 10 x **C**H$_2$)

[Ag(15-crown-5)][NO_3], C8

$AgNO_3$ (0.40 g, 2.4 mmol) and 15-crown-5 (0.96 cm^3, 4.8 mmol)

White powder (0.59 g, 81 %)

Analysis: Found (calculated for $C_{10}H_{20}O_8NAg$): C, 30.7 (30.6); H, 5.19 (5.18);

N, 3.50 (3.59) %

IR: ν(COC or NO) 1402s, 1354s, 1298s, 1253m, 1239s, 1111s, 1093s, 1048s, 1032s, 940s,

853s cm^{-1}

^{1}H-NMR (270 MHz, $CDCl_3$) δ 3.73 (20H, s, 10 x C**H**$_2$) ppm

^{13}C-NMR (270 MHz, $CDCl_3$) δ 69.6 (10C, s, 10 x **C**H$_2$) ppm

[Ag(18-crown-6)][BF_4], C9

$AgBF_4$ (0.47 g, 2.4 mmol) and 18-crown-6 (0.63 g, 2.4 mmol)

White powder (0.42 g, 59 %)

Analysis: Found (calculated for $C_{12}H_{24}O_6BF_4Ag$): C, 31.5 (30.6); H, 5.18 (5.13) %

IR: ν(COC) 1354w, 1290w, 1257s, 1105br, 1049br, ν(BF) 949m, 927m, 841m cm^{-1}

[Ag(18-crown-6)][PF_6].0.5(18-crown-6), C10

$AgPF_6$ (0.60 g, 2.4 mmol) and 18-crown-6 (0.63 g, 2.4 mmol)

White powder (0.71 g, 76 %)

Analysis: Found (calculated for $C_{18}H_{36}O_9PF_6Ag$): C, 33.3 (33.3); H, 5.51 (5.58) %

IR: ν(COC) 1301w, 1251w, 1107br, 1096m, ν(PF) 947w, 843s cm^{-1}

[Ag(18-crown-6)][OTf], C11

AgOTf (0.20 g, 0.8 mmol) and 18-crown-6 (0.21 g, 0.80 mmol)

White powder (0.31 g, 75 %)

Analysis: Found (calculated for $C_{13}H_{24}O_9SF_3Ag$): C 30.3 (30.2); H 4.66 (4.65) %

IR: ν(COC) 1307s, 1183s, 1120s, 1089s, 1024m, 994s cm^{-1}

^{1}H-NMR (400 MHz, $CDCl_3$): δ 3.72 ppm (s, 24H, C**H**$_2$)

^{13}C-NMR (400 MHz, $CDCl_3$): δ 69.7 ppm (s, 12C, **C**H_2)

[Ag(18-crown-6)(NO_3)], C12

$AgNO_3$ (0.20 g, 0.8 mmol) and 18-crown-6 (0.21 g, 0.80 mmol)

White powder (0.35 g, 59 %)

Analysis: Found (calculated for $C_{12}H_{24}O_9NAg$): C, 32.8 (33.2); H, 5.41 (5.57);

N, 2.93 (3.20) %

IR: ν(COC or NO) 1353s, 1278m, 1251s, 1104s, 1035w, 961m, 950s cm^{-1}

[Ag(benzo-18-crown-6)][OTf], C13

AgOTf (0.40 g, 1.5 mmol) and benzo-18-crown-6 (0.60 g, 1.8 mmol)

White powder (0.40 g, 47 %)

Analysis: Found (calculated for $C_{17}H_{24}SO_9F_3Ag$): C 35.9 (35.9); H 4.34 (4.25) %

IR: ν(aromatic C-C) 1594m, 1506s, 1489s, ν(COC) 1330m, 1256m, 1230s, 1130s, 1029m, ν(CF) 994m, 932m cm^{-1}

^{1}H-NMR: (270 MHz,$CDCl_3$) δ 3.66 - 4.12 (20 H, m, 10 x C**H**$_2$), 6.77-6.89 ppm (4H, m, 4 x C**H**) ppm

[Ag(benzo-18-crown-6)][NO_3], C14

$AgNO_3$ (0.26 g, 1.5 mmol) and benzo-18-crown-6 (0.60 g, 1.8 mmol)

White powder (0.51 g, 62 %)

Analysis: Found (calculated for $C_{16}H_{24}NO_9Ag$): C 29.3 (29.5); H 3.72 (3.71); N 4.20 (4.30) %

IR: ν(aromatic C-C) 1588s, 1507m, ν(COC or NO) 1342s, 1305s, 1259s, 1222s, 1132m, 1056m, 955m, 932w cm^{-1}

[Ag(dibenzo-18-crown-6)][OTf], C15

AgOTf (0.40 g, 1.5 mmol) and dibenzo-18-crown-6 (0.65 g, 1.8 mmol)

White powder (0.82 g, 78 %)

Analysis: Found (calculated for $C_{21}H_{24}O_9F_3SAg$): C 40.9 (40.3); H 4.00 (3.92) %

IR: ν(aromatic C-C) 1586w, ν(COC) 1305(m), 1182(m), 1119(s), 1088(s), 1069(s), 1026(m), 994(w), 741(s), 721(s), 694(s) cm^{-1}

[Ag(dibenzo-18-crown-6)(H_2O)][OTf].0.5CH_2Cl_2, C15a

A sample of **C15** dissolved in warmed CH_2Cl_2 and allowed to cool gently at room temperature yielding crystals, which where shown to incorporate one equivalent of water and half an equivalent of DCM.

Analysis: Found (calculated for $C_{21.5}H_{27}O_{10}F_3SClAg$): C 38.2 (38.1); H 4.02 (4.02) %

IR: ν(OH) 3592m, 3429m, ν(HOH) 1731s, ν(aromatic C-C) 1621s, 1591s, 1504s, ν(COC) 1363w, 1286s, 1254s, 1220s, 1156m, 1123s, 1067s, 1030s, ν(CF) 959m, 946s, 764s cm^{-1}

[Ag(dibenzo-18-crown-6)][NO_3], C16

$AgNO_3$ (0.26 g, 1.5 mmol) and dibenzo-18-crown-6 (0.65 g, 1.8 mmol)

Insoluble white powder (0.51 g, 56 %)

Analysis: Found (calculated for $C_{20}H_{24}NO_9Ag$): C 44.7 (45.3); H 4.97 (4.56); N 2.68 (2.64) %

IR: ν(aromatic C-C) 1593m, 1504s, 1425s, ν(COC or NO) 1327m, 1299s, 1255s, 1219s, 1128s, 1057s, 954s, 780s cm^{-1}

[Ag(1,1'-dimethylsila-11-crown-4)][BF_4], C17

$AgBF_4$ (0.23 g, 1.2 mmol) and 1,1'-dimethylsila-11-crown-4 (0.48 cm^3, 2.4 mmol)

Light brown powder (0.33 g, 82 %)

Analysis: Found (calculated for $C_8H_{18}SiO_4BF_4Ag$): C, 23.2 (23.8); H, 4.21 (4.47) %

IR: ν(COC) 1346w, 1298w, 1271w, 1246w, 1122s, 1076s, 1030s, ν(BF) 983s, 942s, 885s cm^{-1}

5.4 HOMOLEPTIC GOLD(I) THIOLATES AND THEIR TRIPHENYLPHOSPHINE DERIVATIVES

5.4.1 STARTING MATERIALS

Preparation of [$(HO_2CCH(NH_2)CH_2CH_2CH_2SCH_3)AuCl$], R1

R1 was prepared by isolating the intermediate in reduction of Au(III) using methionine[7].

$HAuCl_4.3H_2O$ (1.0 g, 2.5 mmol) in water (10 cm^3) was added to $HO_2CCH(NH_2)CH_2CH_2CH_2SCH_3$, (methionine) (0.75 g, 5.0 mmol) in ethanol (10 cm^3) and the solution stirred for 20 minutes. The clear colourless solution that formed was added dropwise to toluene (30 cm^3) resulting in the precipitation of a white powder. The solid was isolated by filtration and dried under vacuum. The solid was found to be water soluble but decomposes rapidly in solution to Au^0.

White solid (0.67 g, 88%)

Analysis: Found (calculated for $C_6H_{12}NO_2SClAu$): C, 16.9 (18.6); H, 3.88 (3.06); N, 4.02 (3.55) %

IR: ν(OH) and ν(NH) 3332s, 3280m, (br), ν(C-O) 1740s, ν(HOH) 1586w; 1521w, ν(S-C) 1112m cm^{-1}

Preparation of [(THT)AuCl][8], R2

Tetrahydrothiophene (2.4 cm^3, 27.0 mmol) was added dropwise to a solution of $HAuCl_4.3H_2O$ (6.0 g, 15 mmol) in water (5 cm^3) and the solution stirred for 20 minutes. The white precipitate was removed by filtration at the end of the reaction, washed with cold ethanol and then dried under vacuum. The product is only slightly soluble in acetone and was stored under N_2.

Light brown powder (3.19 g, 78 %)

Analysis: Found (calculated for C_4H_8SClAu): C, 15.2 (15.0); H, 2.52 (2.50) %

IR: ν(S-C) 1113m cm^{-1}

5.4.2 HOMOLEPTIC GOLD(I) THIOLATES

Preparation of $[Au(SC_6H_4\text{-}p\text{-}CMe_3)]_{10}$, G1[9]

$HAuCl_4.3H_2O$ (1.00 g, 2.5 mmol) in water (10 cm^3) was added, dropwise, to a stirred solution of methionine (0.75 g, 5.0 mmol) in ethanol (10 cm^3). Stirring was continued until the solution became colourless, indicating reduction of Au(III) to Au(I). HSC_6H_4-*p*-CMe_3, (0.40 cm^3, 2.4 mmol) dissolved in toluene (10 cm^3), was then added to the Au(I) solution and stirred for one hour forming a yellow solution. The two layers were allowed to separate, and the aqueous layer discarded. The toluene solution was dried over anhydrous sodium carbonate, and then filtered to leave a clear yellow solution. The required product was precipitated as a yellow powder on dropwise addition of methanol (40 cm^3). The product was collected by filtration, washed well with methanol and dried *in vacuo.*

Yellow powder, 89 % yield (reported yield 98 %)[9]

Analysis: Found (calculated for $C_{10}H_{13}SAu$): C, 33.8 (33.1); H, 3.60 (3.60) %;

IR: ν(aryl CH) 1267m, ν(S-C) 1116m, 1011m cm^{-1}

^{1}H-NMR at 20 °C: (400 MHz, CD_2Cl_2) δ 1.18 (36H, s, 4 x $C(\mathbf{CH_3})_3$), 1.30 (36H, s, 4 x $C(\mathbf{CH_3})_3$), 1.33 (18H, s, 2 x $C(\mathbf{CH_3})_3$), 6.93 (8H, m, 8 x *m*-**CH**), 7.32 (8H, m, 8 x *m*-**CH**), 7.36 (4H, m, 4 x *m*-**CH**), 7.55 (4H, m, 4 x *o*-**CH**), 7.63 (8H, m, 8 x *o*-**CH**), 7.68 (8H, m, 8 x *o*-**CH**) ppm

^{13}C-NMR at 20 °C: (400 MHz, $CDCl_3$) δ 31.2(7) ($C(\mathbf{CH_3})_3$), 31.3(6) ($C(\mathbf{CH_3})_3$), 34.4(4) ($\mathbf{C}(CH_3)_3$), 34.4(8) ($\mathbf{C}(CH_3)_3$), 125.5, 125.6, 125.6, 125.8, 130.4, 130.9, 131.2, 132.3, 132.4, 133.6, 149.9, 150.1 ($\mathbf{C}_{aryl}$) ppm

Samples of the product were recrystallised from concentrated solutions of each of the solvents ethoxybenzene (phenetole), toluene, and xylene. Yellow crystals suitable for X-ray structural analysis were obtained from each, but incorporated solvent. Crystals grown from

ethoxybenzene were finally selected for data collection. Their formula was $[Au(SC_6H_4\text{-}p\text{-}CMe_3)]_{10}.0.8C_6H_5OC_2H_5$, **G1a.**

Preparation of $[Au(SC_6H_4\text{-}o\text{-}CMe_3)]_{12}$, G2

G2 was prepared as for **G1** using $HAuCl_4.3H_2O$ (1.00 g, 2.5 mmol), methionine (0.75 g, 5.0 mmol) and $HSC_6H_4\text{-}o\text{-}CMe_3$ (0.40 cm^3, 2.4 mmol)

Light yellow powder (1.05 g, 84 %)

Analysis: Found (calculated for $C_{10}H_{13}AuS$): C, 32.9 (33.1); H, 3.49 (3.60) %

IR: ν(aryl C-C) 1473m, ν(S-C) 1120m cm^{-1}

^{1}H-NMR at 20 °C: (400 MHz, CD_2Cl_2) δ 1.08 (36H, s, 4 x $C(CH_3)_3$), *1.19*, 1.27**, 1.53 (36H, s, 4 x $C(CH_3)_3$), *1.78*, 1.89**, 2.10 (36H, s, 4 x $C(CH_3)_3$), *2.32**, 6.97, 7.10, 7.27, 7.48, 8.16, 8.25, 9.44 (156 x H_{aryl}) ppm (* minor species; intensities mot measured)

^{13}C-NMR at 20 °C: (400 MHz, $CDCl_3$) δ 30.5(1) ($C(CH_3)_3$), 30.6(7) ($C(CH_3)_3$), 31.9(9) ($C(CH_3)_3$), 36.3(9) ($C(CH_3)_3$), 36.6(2) ($C(CH_3)_3$), 37.6(6) ($C(CH_3)_3$), 124.6, 125.0, 125.8, 126.7, 126.9, 127.2, 128.0, 130.8, 133.0, 133.5, 140.2, 140.4, 141.5, 149.8, 149.9, 151.0 (C_{aryl}) ppm

Light yellow crystals were obtained from a concentrated ethoxybenzene (phenetole) solution of **G2,** their formula was shown by X-ray Crystallographic structure determination to be $[Au(SC_6H_4\text{-}o\text{-}CMe_3)]_{12}.2.0C_6H_5OC_2H_5$, **G2a.**

Preparation of $[Au(SPh)]_n$, G3

$HAuCl_4.3H_2O$ (1.0 g, 2.5 mmol) in (5 cm^3) was added (dropwise) to a solution of methionine (0.75 g, 5.0 mmol) dissolved in ethanol (5 cm^3). After stirring for 20 minutes a colourless solution was formed. Thiophenol (0.4 cm^3, 3.5 mmol) was added dropwise and the mixture

was stirred for a further hour, during which time a white precipitate formed. The solid was isolated by filtration, washed with toluene and then ethanol and dried under vacuum. The product was found to be insoluble in all common solvents.

Light yellow solid (0.74 g, 86%)

Analysis: Found (calculated for C_6H_5SAu): C, 24.9 (23.5); H, 1.86 (1.63) %

IR: ν(aryl C-H) 1253w, ν(S-C) 1127m cm^{-1}

Preparations of $[Au(SC_6H_4\text{-}CF_3)]_n$ [G4 = ortho, G5 = meta and G6 = para]

$HAuCl_4.3H_2O$ (1.0 g, 2.5 mmol) in water (5 cm^3) was added dropwise to a solution of methionine (0.75 g, 5.0 mmol) in ethanol (5 cm^3), and the resulting colourless solution stirred for 20 minutes. Trifluoromethyl thiophenol (0.4 cm^3, 3.0 mmol) was added dropwise to the clear solution and stirring was continued for a further hour. The resulting white solid was isolated by filtration, washed with toluene and then ethanol, and dried under vacuum at 60 °C. Compounds **G4-6** were each found to be insoluble in all common solvents.

G4: **$[Au(SC_6H_4\text{-}o\text{-}CF_3)]_n$**

White solid (0.47 g, 63 %)

Analysis: Found (calculated for $C_7H_4SF_3Au$): C, 22.8 (22.6); H, 1.21 (1.07) %

IR: ν(aryl C-C) 1589w, 1569w; ν(aryl C-H) 1260m; ν(C-F) 1175s, 1113s; ν(S-C) 1094s cm^{-1}

G5: **$[Au(SC_6H_4\text{-}m\text{-}CF_3)]_n$**

White powder (0.56 g, 75 %)

Analysis: Found (calculated for $C_7H_4SF_3Au$): C, 23.1 (22.6); H, 1.17 (1.07) %

IR: ν(aryl C-C) 1570s; ν(aryl C-H) 1296s, 1236s;ν(C-F) 1165s, 1124s; ν(S-C) 1099s cm^{-1}

G6: **[Au(SC_6H_4-*p*-CF_3)]$_n$**

White powder (0.56 g, 75 %)

Analysis: Found (calculated for $C_7H_4SF_3Au$): C, 23.1 (22.6); H, 1.15 (1.07) %

IR: ν(aryl C-C) 1653s, 1601s; ν(aryl C-H) 1326, ν(C-F) 1164s, 1124s; ν(S-C) 1102s cm^{-1}

Preparations of [Au(SC_6H_4-OMe)]$_n$ [G7 = ortho, G8 = meta and G9 = para]

$HAuCl_4.3H_2O$ (1.0 g, 2.5 mmol) in water (5 cm^3) was added dropwise to a solution of methionine (0.75 g, 5.0 mmol) in ethanol (5 cm^3), and the solution stirred for 20 minutes. Methoxy thiophenol (0.4 cm^3, excess) was added dropwise to the resulting colourless solution and the reaction mixture stirred for a further hour. The white precipitate which was formed was isolated by filtration, washed with toluene and then ethanol and dried under vacuum. Compounds **G7-9** were each found to be insoluble in all common solvents.

G7: **[Au(SC_6H_4-*o*-OMe)]$_n$**

White powder (0.66 g, 82 %)

Analysis: Found (calculated for C_7H_7SOAu): C, 25.0 (25.0); H, 2.16 (2.08) %

IR: ν(aryl C-C) 1570m, ν(aryl C-C) and ν(C-O_{aryl}) 1298m, 1270m, 1241s, 1156s, ν(S-C) 1062s, ν(C-O_{Me}) 1024s cm^{-1}

G8: **[Au(SC_6H_4-*m*-OMe)]$_n$**

White powder (0.57 g, 70 %)

Analysis: (calculated for C_7H_7SOAu): C, 25.4 (25.0); H, 2.17 (2.08) %

IR: ν(aryl C-C) 1586m; ν(aryl C-H) and ν(C-O_{aryl}) 1280s, 1241m, 1178s; ν(S-C) 1067m; ν(C-O_{Me}) 1039s, 990m cm^{-1}

G9: **[Au(SC_6H_4-*p*-OMe)]$_n$**

White powder (0.56 g, 69 %)

Analysis: (calculated for C_7H_7SOAu): C, 24.9 (25.0); H, 2.09 (2.08) %

IR: ν(aryl C-C) 1587m, ν(aryl C-H) and ν(C-O_{aryl}) 1282s, 1238s, 1168s; ν(S-C) 1100s, ν(C-O_{Me}) 1025s cm^{-1}

Preparations of [Au($SC_{10}H_7$)]$_n$, G10

$HAuCl_4.3H_2O$ (0.50 g, 1.25 mmol) in water (5 cm^3) was added dropwise to a solution of methionine (0.34 g, 2.4 mmol) in ethanol (5 cm^3) and the solution stirred for 20 minutes. At the end of this period napthalenethiol (0.17 g, 1.0 mmol) was added dropwise to the colourless solution. After further stirring for 1 hour, a white precipitate formed. The product was isolated by filtration, washed with toluene and then ethanol and dried under vacuum. It was found to be insoluble in common solvents.

White solid (0.39 g, 98 %)

Analysis: Found (calculated for $C_{10}H_7SAu$): C, 33.3 (33.7); H, 2.06 (1.98) %

IR: ν(aryl C-C) 1581w; ν(S-C) 1127w cm^{-1}

5.4.3 TRIPHENYLPHOSPHINE GOLD(I) THIOLATES

General procedure for the preparation of [(PPh$_3$)Au(SR)] from soluble [Au(SR)]$_n$ clusters.

Excess triphenylphosphine (2.2 mmol) was stirred for 2 hours with a solution of [Au(SR)]$_n$ (1.8 mmol) in toluene (10 cm^3) at room temperature. Treatment of the colourless solution with acetonitrile afforded the required product that was purified by recrystallisation from toluene/acetonitrile. The quantities of each reactant used in each preparation are listed below together with experimental yields, elemental analysis, ^{1}H-NMR and ^{13}C-NMR data and selected IR data. All non crystalline products were dried in a vacuum oven at 60 °C.

[(PPh$_3$)Au(SC$_6$H$_4$-*p*-^{t}Bu)], P1

[Au(SC$_6$H$_4$-*p*-^{t}Bu)]$_n$, **G1**, (0.30 g, 1.8 mmol) and triphenylphosphine (0.60 g, 2.2 mmol).

White powder (0.52 g, 86 %)

Analysis: Found (calculated for $C_{28}H_{28}SPAu$): C, 54.0 (53.9); H, 4.49 (4.49) %

IR: ν(aryl C-C) 1586s, ν(P-C) 1434s, ν(aryl C-H) 1264m, ν(S-C) 1099s cm^{-1}

^{1}H-NMR (270 MHz, $CDCl_3$): δ 1.28 (9H, s, 3 x C**H**$_3$), 7.18 (4 H, m, SC$_6$**H**$_4$), 7.45-7.55 (15H, m, 1 x P(C$_6$H$_5$)$_3$) ppm

^{13}C-NMR (270 MHz, $CDCl_3$): δ 31.32 (3C, s, 3**C**H$_3$), 34.18 (1C, s, 1**C**(CH$_3$)$_3$), 133.79-137.21 (18C, m, 1 x P(**C**$_6$H$_5$)$_3$) ppm

[(PPh$_3$)Au(S-C$_6$H$_4$-*o*-^{t}Bu)], P2

[Au(S-C$_6$H$_4$-*o*-^{t}Bu)]$_n$, **G2**, (0.30 g, 1.8 mmol) and triphenylphosphine (0.6 g, 2.2 mmol).

White powder (0.55 g, 91 %)

Analysis: Found (calculated for $C_{28}H_{28}SPAu$): C, 54.0 (53.9); H, 4.54 (4.49) %

IR: ν(-*p*-CMe_3) 1732s, ν(aryl C-C) 1586m; ν(P-C) 1434s, ν(aryl C-H) 1288m, 1264s; ν(S-C) 1098s cm^{-1}

General procedure for the preparation of [(PPh$_3$)Au(SR)] from insoluble [Au(SR)]$_n$ clusters.

Powdered $[Au(SR)]_n$ **G3 - G10** (0.60 mmol) was added to a toluene solution (10 cm^3) of excess triphenylphosphine (1.0 mmol) and the reaction mixture stirred at room temperature for 24 hours. Unreacted thiolate was removed by filtration if necessary and the filtrate reduced to half volume under vacuum. Diethyl ether (20 cm^3) was added to deposit the product, which was collected and recrystallised from hot toluene. The quantities of each reactant used in each preparation are listed below together with experimental yields, elemental analyses and selected IR data. ^{1}H-NMR and ^{13}C-NMR data are listed for representative examples. All non-crystalline products were dried in a vacuum oven at 60 °C.

Preparations of [Au(SPh)(PPh$_3$)], P3

$[Au(SC_6H_5)]_n$ (0.20 g, 0.60 mmol), **G3**, was reacted with triphenylphosphine (0.26 g, 1.0 mmol).

Light yellow powder (0.21 g, 61 %)

Analysis: Found (calculated for $C_{24}H_{20}SPAu$): C, 51.1 (50.7); H, 3.60 (3.55) %

IR ν(aryl C-C) 1576s, ν(P-C) 1435s, ν(aryl C-H) 1238m, ν(S-C) 1098s cm^{-1}

^{1}H-NMR (270 MHz, $CDCl_3$): δ 6.89 (1H, m, *p-H* SPh), 6.69 (2H, m, *m-H* SPh), 7.32-7.48 (15H, m, 1 x $P(C_6H_5)_3$), 8.03 (2H, m, *o-H* SPh) ppm

[(PPh$_3$)Au(SC$_6$H$_4$-*o*-CF$_3$)] P4

$[Au(SC_6H_4\text{-}o\text{-}CF_3)]_n$, **G4**, (0.22 g, 0.60 mmol), was reacted with triphenylphosphine (0.26 g, 1.0 mmol).

White crystals (0.17 g, 48 %)

Analysis: Found (calculated for $C_{25}H_{19}PSF_3Au$): C, 47.0 (47.2); H, 3.06 (3.01) %

IR:ν(aryl C-C) 1590m, ν(P-C) 1436m, ν(aryl C-H) 1259s; ν(C-F) 1176m, 1113m, ν(S-C) 1093s cm^{-1}

^{1}H-NMR (270 MHz, $CDCl_3$): δ 7.03 (1H, t, *J*(HH) 8.0 Hz, p-*H* (SC_6H_4-*o*-CF_3)), 7.17 (2H, t, *J*(HH) 8.0 Hz, *m-H* (SC_6H_4-*o*-CF_3)), 7.44-7.56 (15H, m, 1 x $P(C_6H_5)_3$), 7.98 (1 H, d, *J*(HH) 8.0 Hz, *o-H* (SC_6H_4-*o*-CF_3)) ppm

[(PPh_3)Au(SC_6H_4-*m*-CF_3)] P5

[Au(SC_6H_4-*m*-CF_3)]$_n$, **G5**, (0.22 g, 0.60 mmol), was reacted with triphenylphosphine (0.26 g, 1.0 mmol).

White powder (0.24 g, 63 %)

Analysis: Found (calculated for $C_{25}H_{19}PSF_3Au$): C, 47.3 (47.2); H, 3.00 (3.01) %

IR: ν(aryl C-C) 1576w, ν(P-C) 1420s, ν(aryl C-H) 1298m, ν(C-F) 1165m, 1124m; ν(S-C) 1099s cm^{-1}

^{1}H-NMR (270 MHz, $CDCl_3$): δ 7.15-7.25 (2H, m, p-H and *m*-H (SC_6H_4-*m*-CF_3)), 7.43-7.57 (15H, m, 1 x $P(C_6H_5)_3$), 7.69 (1H, d, *J*(HH) 7.2 Hz, *o*-H, (SC_6H_4-*m*-CF_3)), 7.94 (1H, s, *o-H* (SC_6H_4-*m*-CF_3)) ppm

[(PPh_3)Au(SC_6H_4-*p*-CF_3)] P6

[Au(SC_6H_4-*p*-CF_3)]$_n$, **G6**, (0.22 g, 0.60 mmol), was reacted with triphenylphosphine (0.26 g, 1.0 mmol).

White powder (0.34 g, 89 %)

Analysis: Found (calculated for $C_{25}H_{19}PSF_3Au$): C, 47.2 (47.2); H, 2.91 (3.01) %

IR: ν(aryl C-C) 1540m, ν(P-C) 1426s, ν(C-F) 1126s, 1119s; ν(S-C) 1061; cm^{-1}

^{1}H-NMR (270 MHz, $CDCl_3$): δ 7.30 (2H, d, *J*(HH) 8.0 Hz, *m*-H (SC_6H_4-*p*-CF_3)), 7.45-7.57 (15H, m, 1 x $P(C_6H_5)_3$), 7.67 (2H, d, *J*(HH) 8.0 Hz, *o*-H (SC_6H_4-*p*-CF_3)) ppm

[(PPh_3)Au(SC_6H_4-*o*-OMe)], P7

[Au(SC_6H_4-*o*-OMe)]$_n$, **G7**, (0.22 g, 0.60 mmol), was reacted with triphenylphosphine (0.26g, 1.0 mmol).

Colourless crystals (0.20 g, 55 %)

Analysis: Found (calculated for $C_{25}H_{22}SPOAu$): C, 52.2 (50.3); H, 4.00 (3.71) %

IR: ν(aryl CC) 1570m; ν(P-C) 1435m; ν(C-O) 1236s; ν(S-C) 1099m; ν(O-C_{Me}) 1024m cm^{-1}

^{1}H-NMR (270 MHz, $CDCl_3$): δ 3.80 (3H, s, OC**H$_3$**)), 6.78 (3H, m, *m*-H and *p*-H (SC_6H_4-*o*-OMe)), 7.48-7.58 (15H, m, 1 x $P(C_6H_5)_3$), 7.74 (1H, m, *o*-H (SC_6H_4-*o*-OMe)) ppm

[(PPh_3)Au(SC_6H_4-*m*-OMe)], P8

[Au(SC_6H_4-*m*-OMe)]$_n$, **G8**, (0.22 g, 0.60 mmol), was reacted with triphenylphosphine (0.26 g, 1.0 mmol).

Colourless crystals (0.22 g, 60 %)

Analysis: Found (calculated for $C_{25}H_{22}SPOAu$): C, 51.4 (50.3); H, 3.85 (3.71) %

IR: ν(aryl CC) 1576s; ν(P-C) 1435s, ν(O-C_{aryl}) 1238s, ν(S-C) 1098s; ν(O-C_{Me}) 1065m, 1038m cm^{-1}

^{1}H-NMR (270 MHz, $CDCl_3$): δ 3.70 (3H, s, OC**H$_3$**)), 6.55 (1H, m, *p*-H (SC_6H_4-*m*-OMe)), 7.00 (1H, m, *m*-H (SC_6H_4-*m*-OMe)), 7.18 (1H, d, *J*(HH) 1.6 Hz, *o*-H (SC_6H_4-*m*-OMe)), 7.21 (1H, s, *o*-H (SC_6H_4-*m*-OMe)) 7.44-7.57 (15H, m, 1 x $P(C_6H_5)_3$), 7.74 (1H, m, *o*-H (SC_6H_4-*o*-OMe)) ppm

Attempted preparation of [(PPh_3)Au(SC_6H_4-*p*-OMe)], "P9"

$[Au(SC_6H\text{-}p\text{-}OMe)]_n$, **G9**, (0.22 g, 0.60 mmol), was reacted with triphenylphosphine (0.26 g, 1.0 mmol). Attempts to isolate **"P9"** from solution were unsuccessful.

[(PPh_3)Au(Snaph)], P10

$[Au(Snaph)]_n$, **G10**, (0.21 g, 0.60 mmol), was reacted with triphenylphosphine (0.26 g, 1.0 mmol).

White powder (0.29 g, 79 %)

Analysis: Found (calculated for $C_{25}H_{22}SPAu$): C, 58.1 (54.4); H, 3.64 (3.59) %

IR: ν(aryl C-C) 1435m, ν(aryl C-H) 1268m, ν(S-C) 1099m, 1069m; ν(napthyl C-H) 813s, 746m cm^{-1}

^{1}H-NMR (270 MHz, $CDCl_3$): δ 7.28 (1H, s, Snaph), 7.29 (1H, t, Snaph), 7.35 (1H, t, S naph), 7.43-7.70 (15H, m, 1 x $P(C_6H_5)_3$), 7.78 (2H, m, Snaph), 7.98 (1H, d, *J*(HH) 7.9 Hz, *o*-H Snaph), 8.08 (1H, d, *J*(HH) 7.9 Hz, *o*-H Snaph) ppm

5.4.4 GOLD-2,2'-DITHIODIPYRIDINE REACTIONS

Reaction of 2,2'-dithiopyridine [(pyS)$_2$] with hydrogen tetrachloroaurate(III), G11

2,2'-dithiopyridine (Aldrithiol-2) (0.53 g, 2.4 mmol) dissolved in diethyl ether (10 cm^3) was added to a solution of $HAuCl_4.3H_2O$ (0.50 g, 1.25 mmol) in water (10 cm^3). The reaction mixture was stirred in the absence of light. A bright yellow solid precipitated immediately which isolated by filtration from the colourless solution. The solid was washed with alcohol, warm ether, and then dried under vacuum at 60 °C. It was found to be insoluble in all common solvents.

Yellow-green powder (0.31 g, 68 %)

Analysis: Found (calculated for $\{AuCl_2SNC_5H_5\}$): C, 15.8 (15.9); H, 1.35 (1.09); N, 3.61 (3.70) %

IR: ν(aryl C-H) 1277s, ν(aryl C-H) 1157m, ν(C-S) 1048m cm^{-1}

Attempted reaction of G11 with triphenylphosphine, "P11"

G11 (0.20 g) was added as a suspension to PPh_3 (0.26 g, 1.0 mmol) dissolved in toluene (10 cm^3) and the mixture stirred for 2 hours. The bright red solid insoluble solid formed, which was isolated by filtration and washed with ethanol and ether.

Red solid (0.28 g) Analysis Found: C, 32.1; H, 2.66; N, 5.40 %

IR: ν(P-C) 3053w; ν(aryl CC) 1567m; ν(P-C) 1434m; ν(P-C) 1263s; ν(S-C) 1137m cm^{-1}

5.5 CHEMISTRY OF GOLD WITH OXYGEN DONOR LIGANDS

5.5.1 SUMMARY

In this section the reactions and techniques attempted in order to synthesise complexes containing Au(I)-O bonds as discussed in Chapter Four are outlined.

5.5.2 STARTING MATERIALS

Preparation of $[(Ph_3P)AuCl]$[10], R3

A solution of $HAuCl_4.3H_2O$ (1.0 g, 2.5 mmol) in water (5 cm^3) was added dropwise to a cooled (-15 to -20 °C) suspension of finely divided triphenylphosphine (1.3 g, 5.0 mmol) in ethanol (20 cm^3). The reaction mixture was held below O°C and stirred for 60 minutes, during which time the mixture turned from yellow to colourless and a colourless solid precipitated. The product was removed via filtration and recrystallised from boiling ethanol.

Colourless needles (1.18 g, 82 %)

Analysis: Found (calculated for $C_{18}H_{15}ClAu$): C, 43.8 (43.7); H, 3.04 (3.03) %

IR: ν(P-C) 1438s, ν(P-C) 1101 cm^{-1}

^{1}H-NMR (270 MHz, $CDCl_3$): δ 7.49 (m, 15H, 3 x C_6H_5) ppm

Preparation of $[(Cy)_6Si_6O_9]$, R4, and $[(Cy)_7Si_7O_9(OH)_3]$, R5[11]

A solution of trichlorocyclohexylsilane (25 g, 0.11 mol) in acetone (500 cm^3) and water (125 cm^3) was left to stand for 4 months. The solution was shaken regularly and the stopper removed to release any build-up of pressure. After 4 months the majority of the solvent was decanted off and kept. The white residue was collected by filtration and washed with ice-cold acetone. The washings and reaction solution were combined and returned to the reaction vessel for further digestion and product formation. The white residue was dried overnight at 45°C, to yield 4.56 g of crude products.

Isolation of $[(Cy)_6Si_6O_9]$, R4

The crude solid above was stirred at room temperature in 5 times its weight of pyridine (~30 cm^3) for 1 hour. The white crystalline solid remaining was filtered off and the pyridine solution put aside. The white solid was washed with a small amount of pyridine and dried *in vacuo* overnight at 30^0C.

White powder (0.95 g, 1.2 %)

Analysis: Found (calculated for $C_{36}H_{30}O_6Si_6$): C, 52.9 (53.2); H, 8.15 (8.21) %

IR: ν(Si-C) 1277s, 1195s; ν(Si-O) 1107s, 1087s, 1049m, 1022s, 997s, 895s, 852s cm^{-1}

Isolation of $[(Cy)_7Si_7O_9(OH)_3]$, R5

The pyridine solution from the separation of **R4** was poured into 5 times its volume of ice-cold aqueous HCl WITH CARE! (such that 1 cm^3 conc. HCl/1 cm^3 pyridine). Solid clusters of product were pulverised and then the precipitate collected. The crude product was then stirred in excess water to remove any pyridine, aqueous HCl or pyridinium hydrochloride. The solid product was collected and washed with copious quantities of water before being dried overnight at ~50^0C. Crude **R5** was then dissolved in hot diethyl ether (30 cm^3/g of solid) and residual material filtered off. The ether filtrate was concentrated to 25% of its original volume and cooled to afford the pure product as a white microcrystalline solid.

White powder (2.89 g, 23.2 %)

Analysis: Found (calculated for $C_{42}H_{80}O_{12}Si_7$): C, 51.9 (51.8); H, 8.19 (8.47) %

IR: ν(Si-C) 1269s, 1196s; ν(Si-O) 1114s, 1037s, 1028s, 999s, 895s, 848s cm^{-1}

Preparation of $[(Cy)_7Si_7O_{12}P]^{12}$, R6

To a vigorously stirred solution of **R6** (0.40 g, 0.42 mmol) and triethylamine (0.26 cm^3, 1.26 mmol) in dry toluene (25 cm^3) was added one equivalent of trichlorophosphine (0.045 cm^3,

0.42 mmol). The solution was then stirred at room temperature for 1 hour. The resulting reaction mixture was filtered to remove Et_3NHCl and the solvent removed from the filtrate. The solid produced was then extracted with hexane, and the solvent removed from the filtrate under vacuum. The white powder so produced was recrystallised by the slow diffusion of acetonitrile into a toluene solution of the product. The recrystallised material was collected and dried overnight at 40-50°C.

White solid (0.25 g, 62 %)

Analysis: Found (calculated for $C_{42}H_{77}O_{12}Si_7P$): C, 49.8 (50.4); H, 7.89 (7.75) %

IR: ν(Si-C) 1271s; ν(Si-O) and ν(P-O) 1271s (br), 1199s (br), 1116s, 1026s, 893s, 848s cm^{-1}

5.5.3 ATTEMPTED PREPARATIONS OF CROWN-ETHER COMPLEXES OF GOLD

Attempted reaction of "hydrogen tetranitroaurate" with the crown-ethers, 12-crown-4, 15-crown-5 and 18-crown-6

Crown-ether (0.55 mmol) in THF (5 cm^3) was added to a suspension of "$HAu(NO_3)_4$" (0.20 g, 0.45 mmol) in cold dry THF (10 cm^3), and the mixture stirred at 0 °C for 48 hours in the absence of light and air. In each case no reaction occurred, and only starting materials were isolated. The reaction was also attempted in acetone but again no reaction occured. When the reaction was carried at elevated temperature decomposition to a gold film occurred.

Attempted reaction of [(THT)Au(Cl)] with crown-ethers, (12-crown-4, 15-crown-5 and 18-crown-6)

(THT)AuCl, **R2**, (0.19 g, 0.60 mmol) was added to a stirred solution of crown-ether (0.60 mmol) in dry acetone (10 cm^3) and the solution stirred for 48 hours. No reaction was observed the suspension of THTAuCl was removed by filtration, the solvent was removed by vacuum to

yield only crown ether. Heating these solutions to their boiling point resulted in the depositing of a gold film on the reaction vessel.

5.5.4 GOLD(I) COMPLEXES OF ANIONIC OXYGEN DONORS

5.5.4.1 ATTEMPTED PREPARATION OF HOMOLEPTIC GOLD(I) COMPLEXES, $[Au(OR)]_n$, (R = Ph or $SiMe_3$)

$HAuCl_4.3H_2O$ (0.25 g, 0.63 mmol) in water (10 cm^3) was added, dropwise, to a stirred solution of methionine (0.19 g, 1.3 mmol) in ethanol (10 cm^3). Stirring was continued until the solution became colourless, indicating reduction of Au(III) to Au(I). The resulting solution was canullared in to a Schlenk tube containing a toluene (10 cm^3) suspension of finely divided sodium phenolate or trimethylsilonalate (0.9 mmol). After 15 minutes a gold film was deposited on the reaction vessel. The reaction was abandoned.

5.5.4.2 PREPARATION OF TRIPHENYLPHOSPHINE GOLD(I) ALKOXIDES AND PHENOXIDES

Attempted preparation of triphenylphosphine Au(I) alkoxides, $[(PPh_3)Au(OR)]$, {R= Me, Et, and CMe_3}

$(PPh_3)AuCl$, **R1**, in dry THF (10 cm^3) was added to a solution of a sodium alkoxide in THF in a dry Schlenk tube, and the reaction mixture stirred at -78 °C. After 1 hour the precipitate was filtered off. The remaining solution decomposed to quickly produce a purple solid on attempts to remove solvent at 5 °C. Further attempts to isolate these products failed.

Studies of triphenylphosphine Au(I) phenoxides, [(PPh$_3$)Au(OR)], {R= Ph, C$_6$H$_4$-p-CMe$_3$, and C$_6$H$_4$-p-CMe$_3$}

[Au(PPh$_3$)(OC$_6$H$_5$)].0.5H$_2$O, A1

[(PPh$_3$)AuCl] (0.40 g, 0.84 mmol) was reacted with sodium phenoxide (0.14 g, 0.84 mmol) using the preparative method outlined for the alkoxides above. The resulting orange solution was filtered to remove the NaCl precipitate and solvent was removed *in vacuo* to yield a light orange solid. The product was then precipitated from DCM by slow evaporation.

Light orange solid (0.34 g, 74 %)

Analysis: Found (calculated for $C_{24}H_{22}O_2PAu$): C, 51.3 (51.2); H, 3.76 (3.74) %

IR: ν(OH) 3055m, ν(HOH) 1591m, ν(aryl CC) 1435, ν(C-O) 1250, 1165 cm^{-1}

^{1}H-NMR (270 MHz, $CDCl_3$): δ 7.5 (m, 15H, 3 x P(C$_6$**H**$_5$)$_3$), 7.14 (t, 2H, m-C**H**), 7.03 (d, 2H, o-C**H**), 6.70 (t, 1H, p-C**H**) ppm

Attempted preparation of triphenylphosphine Au(I) phenoxides, [(PPh$_3$)Au(OR)] {R = C$_6$H$_4$-ρ-CMe$_3$, C$_6$H$_4$-o-CMe$_3$}

Sodium hydride (1.0 g) was stirred in THF (15 cm^3), in a clean and flame dried Schlenk tube, for 5 minutes to remove the mineral oil coating. The solution was left to settle before removing the oil/solvent solution by pipette. This process was repeated twice more to ensure clean NaH. THF (10 cm^3) was added to the reaction vessel under an atmosphere of dry nitrogen and the mixture stirred. The appropriate alcohol (3.0 mmol) in THF (10 cm^3) was added drop-wise to the stirred solution (CARE - H_2 evolved). The mixture was stirred for a further 60 minutes and the solution transferred to a second Schlenk tube containing [(PPh$_3$)AuCl], **R3**, (1.0 g, 2.0 mmol) in THF. Details of the specific preparations are as follows.

Attempted preparation of [Au(PPh$_3$)(OC$_6$H$_4$-p-CMe$_3$)]

[Au(PPh$_3$)(OH)], A2

Reaction of excess Na(OC$_6$H$_4$-*p*-CMe$_3$) (3.0 mmol), prepared as above, with [(PPh$_3$)AuCl], **R1**, (1.0 g, 2.0 mmol) resulted in the formation of an orange solution, which was filtered to removed NaCl, and solvent removed *in vacuo*. The result light orange solid was extracted into DCM and the solution filtered again, to remove a small amount of undissolved solid, an orange solid was precipitated from solution by addition of hexane.

Orange solid (0.37 g, 39 %)

Analysis: Found (calculated for $C_{18}H_{15}OPAu$): C, 45.2 (45.4), H, 3.30 (3.39) %

IR: ν(OH) 3335s cm^{-1}

^{1}H-NMR (270 MHz, $CDCl_3$): δ 7.49 (m, 15H, P(C_6H_5)$_3$) ppm

Attempted preparation of [Au(PPh$_3$)(OC$_6$H$_4$-o-CMe$_3$)]

Reaction of excess Na(OC$_6$H$_4$-*o*-CMe$_3$) (3.0 mmol) with [(PPh$_3$)AuCl], **R1**, (1.0 g, 2.0 mmol) resulted in the formation of an yellow solution, which was filtered to removed NaCl, and solvent removed *in vacuo* to afford a light yellow oil. The oil was dissolved in DCM and hexane added slowly to encourage precipitation. A purple precipitate slowly formed from the orange solution. Repeated attempts to isolate the light yellow product were unsuccessful.

5.5.5 ATTEMPTED REACTION OF GOLD WITH A SILSESQUIOXANE

Attempted reaction of $HAuCl_4$ with $[(Cy)_7Si_7O_9(OH)_3]$, R5

Powdered **R5** (0.30 g, 0.39 mmol) was added to $HAuCl_4$ (0.18 g, 0.39 mmol) and 1,4-diazabicyclo[5,4,0]undec-7-ene (0.24 cm^3, 1.56 mmol) in THF (30 cm^3) and MeCN (1.0 cm^3) and the solution stirred for two hours. After this time a red oil had formed which was decanted off, the oil decomposed to a gold film before it could be characterised.

Attempted reaction of [(THT)AuCl], R2 with $[(Cy)_7Si_7O_{12}P]$, R6

Finely powdered [(THT)AuCl], **R2**, was added to a solution of $[(Cy)_7Si_7O_{12}P]$, **R6**, in THF and the mixture was stirred for 48 hours. No reaction was observed and only starting materials were isolated.

Attempted preparation of $[(Cy)_7Si_7O_{12}P]AuCl$

A solution of $[(Cy)_7Si_7O_{12}P]$, **R6**, in propan-2-ol (10 cm^3) was added to $HAuCl_4$ (0.5 g, 1.25 mmol) in water (10 cm^3), and the solution stirred for twenty four hours. No colour change was observed, and slow removal of solvent by evaporation resulted in precipitation of **R6**.

5.6 REFERENCES

[1 a)] *Safety Manual*, University of Bath (1997); [b)] *Health and Safety Policy*, Safety Office, University of Bath (1996)

[2] http://www.bath.ac.uk/departments/chem/safety.bho/thiol.htm

[3] R.J. Errington, *Advanced Practical Inorganic and Metalorganic Chemistry,* Chapman and Hall, London (1997)

[4a)] G.M. Sheldrick, *Acta Cryst. Sect. A*, **46**, 467 (1990); [b)] G.M. Sheldrick, SHELXL, a computer program for crystal structure refinement, University of Göttingen (1993)

[5] L. Zsolnai, G. Huttner, XPMA, a computer program for graphical manipulation of crystal structures, University of Heidelberg, Germany (1994)

[6] P. McArdle, Oscail, software for small molecule structure determination integrating SHELX and ORTEX, *J. Appl. Cryst.*, **28**, 65 (1995)

[7] G. Natile, E. Bordignon, L. Cattalini, *Inorg. Chem.,* **15**, 247 (1976)

[8] R. Uson, A. Laguna, M. Laguna, *Inorganic Syntheses,* Wiley, **26**, 85 (1989)

[9] A.K.H. Al-Sa'ady, K. Moss, C.A. McAuliffe, R.V. Parish, *J. Chem. Soc., Dalton Trans.,* 1609 (1984)

[10] C. Kowala, J.M. Swan, *Aust. J. Chem.,* **19**, 547 (1966)

[11a)] F.J. Feher, D.A. Newman, J.F. Walzer, *J. Am. Chem. Soc.,* **111**, 1741 (1989); [b)] F.J. Feher, T.A. Budzichowski, K.R. Ziller, J.W. Ziller, *J. Am. Chem. Soc.,* **114**, 3859 (1992)

[12] F.J. Feher, T.A. Budzichowski, *J. Am. Chem. Soc.*, **10**, 812 (1991)

CHAPTER SIX: CONCLUSIONS AND FUTURE WORK

6.1 INTRODUCTION

The major aims of the project as laid out in the abstract were to investigate the chemistry of silver and gold with oxygen and sulphur donor ligands. Three different specific areas have been studied during the course of this investigation, and generally the experimental results have supported the theoretical concepts that were introduced in Chapter One. The chemistry of "soft" gold with "hard" oxygen donors has proved to be synthetically challenging, whereas, "borderline" silver readily reacts with neutral macrocyclic oxygen donors at room temperature to form stable complexes, several of which have been characterised crystallographically. Gold reacts readily with "soft" sulphur donors to form stable complexes, and the importance of weak Au...Au interactions in stabilising unusual Au_nS_n cores has been demonstrated in X-ray crystallographic studies. The structural comparison between multi-co-ordinate Ag(I) complexes and alkali metal ions has been made, and attention drawn to the importance of linear two-co-ordination in Au(I) chemistry.

6.2 CROWN-ETHER COMPLEXES OF SILVER(I) SALTS

In Chapter Two, the compounds **C1 - C17** significantly extend the known range of crown-ether complexes of Ag(I). These complexes were produced in high yield, and the solubilities of unsubstituted oxa-crown-ethers (**C1 – C12**) in organic solvents is very high. The stability of the complexes is counter-ion dependent, with complexes of $AgBF_4$ and $AgPF_6$ decomposing over a few days, whilst complexes of AgOTf and $AgNO_3$ were indefinitely stable in the solid-state. A range of these compounds were shown by thermal gravimetric analysis to decompose cleanly to silver metal.

Solid-state structural analyses of two series of these complexes resulted in further information about the co-ordination behaviour of Ag(I). It is apparent from the structures of

the complexes of 15-crown-5 with the three silver salts [AgX, X = PF_6, OTf, NO_3] that whilst the cavity size of 15-crown-5 is not adequate to contain the Ag^+ ion, the crown-ether is capable of complexing the metal ion effectively. In all three complexes [Ag(15-crown-5)(OH_2)(15-crown-5)][PF_6], **C6**, [Ag(15-crown-5)(OTf)], **C7**, and [Ag(15-crown-5)(NO_3)], **C8**, Ag(I) is complexed to an additional oxygen donor. In **C7** and **C8** the co-ordination sphere is completed by the bidentate counterion, but in **C6** a molecule of water is bound to the metal centre as well as hydrogen bonded to a second molecule crown-ether. The co-ordination numbers of silver in **C6, C7** and **C8** are six, seven and seven, respectively, and the co-ordination geometry about the metal cannot be defined by a traditional classification.

The products from the reactions of 18-crown-6, benzo-18-crown-6 and dibenzo-18-crown-6 with silver triflate were [Ag(18-crown-6)(OTf)], **C11**, [Ag(benzo-18-crown-6)(OTf)], **C13**, and [Ag(dibenzo-18-crown-6)(OTf)], **C15**, respectively. Slow recrystallisation of **C15** again resulted in inclusion of water and DCM. The silver co-ordination numbers in complexes **C11, C13** and **C15** are seven, nine and nine, respectively. Both complexes containing benzocrown dimerise through four Ag-C_{aryl} contacts involving the arene ring.

During this study the focus has been on the synthesis and characterisation of novel compounds. A more "industrially" focused investigation might now follow, with the aims of assessing the potential of these systems as precursors to silver films, perhaps by Chemical Vapour Deposition, CVD.

6.3 HOMOLEPTIC GOLD(I) THIOLATES AND THEIR TRIPHENYLPHOSPHINE DERIVATIVES

The aims of the investigation undertaken in Chapter Three were to observe the effects of substitution in the arene ring of homoleptic gold(I) thiolates $[Au(SC_6H_4\text{-}R)]_n$ {R = H, CMe_3, CF_3, OMe} on the solubility and structures of the compounds. Of the complexes prepared only $[Au(SC_6H_4\text{-}p\text{-}CMe_3)]_n$, **G1** and $[Au(SC_6H_4\text{-}o\text{-}CMe_3)]_n$, **G2** were soluble. Subsequent X-ray Crystallographic studies of these complexes revealed n to be 10 and 12 respectively. These are two of only five structurally characterised homoleptic gold(I) thiolates, **G1** and **G2**, and are rare examples of inorganic [2]catenanes. Reaction of **G1-10** with triphenylphosphine resulted in the formation of monomeric derivatives of the type $[(PPh_3)Au(SR)]$, **P1 – P10**, two of which were also structurally characterised.

A preliminary study of the reactions of 2,2'-dithiodipyridine, PyS_2, with gold(III) suggests that the product of the reaction with the empirical formula $[(PyS)AuCl_2]$, **G11**, is a gold(III) thiolate derivative, but it was not possible to fully characterise this product or its reaction product with triphenylphosphine.

In future studies it would be interesting to prepare $HSC_6H_4\text{-}m\text{-}CMe_3$ and use it to synthesise $[Au(SC_6H_4\text{-}m\text{-}CMe_3)]_n$ so that its structure could be determined. The completed series of homoleptic gold(I) thiolates would provide good candidates for theoretical studies into Au...Au bonding interactions.

6.4 CHEMISTRY OF GOLD WITH OXYGEN DONOR LIGANDS

In Chapter Four the limits of the reactivity of Au(I) and Au(III) toward O-donors was clearly demonstrated. Whilst silver(I) will readily bind to crown-ethers where the macrocycle easily displaces weakly co-ordinating groups, the same does not occur for either Au(I) or Au(III). Initial attempts to form either homoleptic gold(I) alkoxide or a siloxide were, not surprisingly, unsuccessful, with all current and past reports of gold(I)/oxygen chemistry indicating that only phosphine supported complexes have any stability. The attempted preparation of $[(PPh_3)Au(OR)]$ {R = alkyl or aryl} caused some synthetic problems. The stability of the alkoxides in solution was low and decomposition occurred before any products could be isolated and characterised, whereas $[(PPh_3)Au(OPh)].0.5H_2O$, **A1**, was easily synthesised, isolated but not characterised crystallographically. Attempts to prepare new aryloxides were unsuccessful, and instead resulted in isolation of $[(PPh_3)Au(OH)]$, **A2** . This is the first example of an Au(I) hydroxide, but further study is needed to confirm this finding with particular emphasis on determining its solid-state structure.

A preliminary study of the reactions of gold derivatives with the silsesquioxane $[Cy_7Si_7O_9(OH)_3]$, **R5**, and $[Cy_7Si_7O_{12}P]$, **R6**, gave negative results, however given the importance of gold film formation on ceramic surfaces, further investigations of the reactions between this metal and molecular models for silica, would be well advised.

APPENDIX 1: X-RAY CRYSTALLOGRAPHIC DATA ON COMPOUNDS C6, C7, C8, C11, C13, AND C15

Summary:

This Appendix contains X-ray crystallographic data on the complexes discussed in Chapter 2. Included are notes on compounds **C6**, **C7**, and **C8**. Crystal and structure refinement data, bond lengths and angles are included for all 6 compounds. Atomic co-ordinates (including hydrogen co-ordinates), isotropic displacement parameters and tables of anisotropic temperature factors for each compound are available as supplementary information on request from the Department of Chemistry.

For identification purposes each compound has been assigned two labels, e.g. **C6** is also **99BJB1.** The former is the systematic label used throughout this thesis to identify $[Ag(15\text{-crown-}5)(H_2O)(15\text{-crown-}5)]^+[PF_6]^-$, whereas the latter was used by the departmental crystallography unit to identify the year, supervisor and structure.

All data given in the subsequent tables are followed by the calculated standard deviations, σ, based on the assumption that the data collected will follow the "normal distribution model". For example in **C6** the Ag(1)-O(11) separation is 2.327(4) Å; the standard deviation, σ, is noted for the last decimal place, i.e. 0.004 Å. Using the normal distribution approximation the "true" value could be within the range of the average separation ± 3σ.

CONTENTS

X-RAY CRYSTALLOGRAPHIC DATA ON:

$[Ag(15\text{-crown-}5)(H_2O)(15\text{-crown-}5)]^+[PF_6]^-$	**C6**
$[Ag(15\text{-crown-}5)(OTf)]$	**C7**
$[Ag(15\text{-crown-}5)(NO_3)]$	**C8**
$[Ag(18\text{-crown-}6)(OTf)]$	**C11**
[Ag(benzo-18-crown-6)(OTf)]	**C13**
$[Ag(\text{dibenzo-}18\text{-crown-}6)(H_2O)]^+[OTf]^-.DCM$	**C15**

X-RAY CRYSTALLOGRAPHIC DATA ON [Ag(15-crown-5)(H_2O)(15-crown-5)]$^+$[PF_6]$^-$, C6, (99BJB1/L.T.)

A crystal of approximate dimensions 0.25 x 0.25 x 0.25 mm was used for data collection.

Crystal data: $C_{20}H_{42}AgF_6O_{11}P$, M = 711.38, Monoclinic, a = 14.183(2), b = 12.624(2), c = 16.506(3) Å , α = 90, β = 105.71(1), γ = 90°, U = 2844.9(8) Å^3, space group $P2_1/n$, Z = 4, D_c = 1.661 gcm^{-3}, μ(Mo-K_α) = 0.857 mm^{-1}, F(000) = 1464. Crystallographic measurements were made at 170(2) K on a CAD4 automatic four-circle diffractometer in the range 2.06<θ<25.01°. Data (5369 reflections) were corrected for Lorentz, polarisation and 11.5% decay of the crystal in the X-ray beam. Data were not corrected for absorption.

The asymmetric unit in this crystal structure consisted of one silver atom to which one water molecule is bound, two crown ether moieties and one hexafluorophosphate anion. The silver-water fragment is sandwiched between the crown ethers and held in place via interactions between the crown oxygens in one of the ethers with the metal and hydrogen bonding between the ligated water hydrogens and two oxygen atoms of the second crown. [O11-O7 2.819(7), O11-O10 2.760(6) Å; O11-H11A-O7 160(8), O11-H11B-O10 166(8)°]

In the final least squares cycles all atoms were allowed to vibrate anisotropically. Hydrogen atoms were included at calculated positions where relevant except on the water molecule where the hydrogen atoms were easily located and refined. There is evidence of some disorder in one of the crown moieties (thermal displacement parameters large). This was not modelled, as the data presented are in fact the third set collected for this compound. It was found that by collecting the data faster at low temperature, the thermal displacement parameters for the atoms in this crown were considerably reduced, and as a consequence seemed to be related to the crystal decay, for which a correction was applied.

The solution of the structure (SHELX86)[1] and refinement (SHELX93)[2] converged to a conventional [i.e. based on 4108 F^2 data with Fo>4σ (Fo)] $R1$ = 0.0534 and $wR2$ = 0.1375. Goodness of fit = 1.043. The max. and min. residual densities were 1.430 and -0.746 eÅ^{-3} respectively. The asymmetric unit (shown in Fig A), along with the labelling scheme used was produced using ORTEX.[3] Crystal data and structure refinement for C6, bond distances and angles are given in Tables A and B.

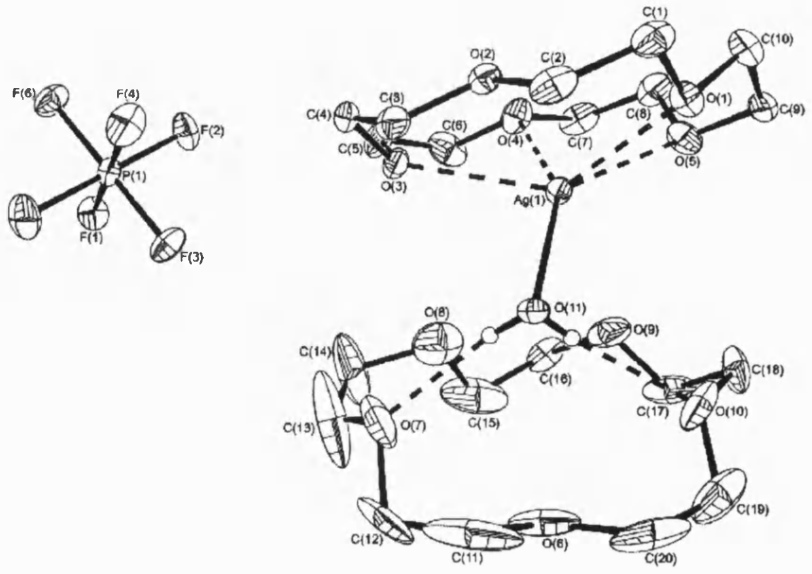

Figure A: The molecular structure of C6

Identification code	**C6** (99bjb1/M.Wiseman / l.t.)
Empirical formula	$C_{20}H_{42}AgF_6O_{11}P$
Formula weight	711.38
Temperature	170(2)°K
Wavelength	0.71069 Å
Crystal system	Monoclinic
Space group	$P2_1/n$
Unit cell dimensions	a = 14.183(2)Å α = 90° b = 12.624(2)Å β = 105.710(10)°
	c = 16.506(3)Å δ = 90°
Volume	2844.9(8) $Å^3$
Z	4
Density (calculated)	1.661 Mg/m^3
Absorption coefficient	0.857 mm^{-1}
F(000)	1464
Crystal size	0.25 x 0.25 x 0.25 mm
Theta range for data collection	2.06 to 25.01°.
Index ranges	0<=h<=16; 0<=k<=14; -19<=l<=18
Reflections collected	5369
Independent reflections	4997 [R(int) = 0.0170]
Refinement method	Full-matrix least-squares on F^2
Data / restraints / parameters	4992 / 0 / 361
Goodness-of-fit on F^2	1.043
Final R indices [I>2σ(I)]	R1 = 0.0534 wR2 = 0.1375
R indices (all data)	R1 = 0.0648 wR2 = 0.1444
Largest diff. peak and hole	1.430 and -0.746 $eÅ^{-3}$
Weighting scheme	calc $w=1/[\sigma^2(Fo^2)+(0.0732P)^2+11.0018P]$ where $P=(Fo^2+2Fc^2)/3$
Extinction coefficient	0.0004(3)

Table A: Crystal data and structure refinement for C6

Ag(1)-O(11)	2.327(4)	O(5)-C(9)	1.425(7)
Ag(1)-O(4)	2.495(4)	O(6)-C(11)	1.321(13)
Ag(1)-O(5)	2.515(4)	O(6)-C(20)	1.528(11)
Ag(1)-O(3)	2.564(4)	O(7)-C(13)	1.28(2)
Ag(1)-O(1)	2.614(4)	O(7)-C(12)	1.510(13)
Ag(1)-O(2)	2.693(4)	O(8)-C(15)	1.285(14)
F(1)-P(1)	1.591(3)	O(8)-C(14)	1.511(13)
F(2)-P(1)	1.589(4)	O(9)-C(17)	1.347(9)
F(3)-P(1)	1.588(3)	O(9)-C(16)	1.509(9)
F(4)-P(1)	1.588(4)	O(10)-C(19)	1.329(11)
F(5)-P(1)	1.596(4)	O(10)-C(18)	1.539(9)
F(6)-P(1)	1.589(3)	C(1)-C(2)	1.478(9)
O(1)-C(10)	1.413(7)	C(3)-C(4)	1.490(9)
O(1)-C(1)	1.436(7)	C(5)-C(6)	1.459(11)
O(2)-C(3)	1.422(7)	C(7)-C(8)	1.469(10)
O(2)-C(2)	1.427(7)	C(9)-C(10)	1.475(9)
O(3)-C(4)	1.400(7)	C(11)-C(12)	1.49(2)
O(3)-C(5)	1.439(8)	C(13)-C(14)	1.26(2)
O(4)-C(6)	1.385(8)	C(15)-C(16)	1.52(2)
O(4)-C(7)	1.414(7)	C(17)-C(18)	1.536(11)
O(5)-C(8)	1.399(8)	C(19)-C(20)	1.475(14)
O(11)-Ag(1)-O(4)	150.4(2)	C(2)-O(2)-Ag(1)	101.5(3)
O(11)-Ag(1)-O(5)	135.0(2)	C(4)-O(3)-C(5)	112.8(5)
O(4)-Ag(1)-O(5)	68.23(14)	C(4)-O(3)-Ag(1)	118.3(3)
O(11)-Ag(1)-O(3)	90.8(2)	C(5)-O(3)-Ag(1)	113.3(3)
O(4)-Ag(1)-O(3)	66.08(14)	C(6)-O(4)-C(7)	117.0(6)
O(5)-Ag(1)-O(3)	133.61(14)	C(6)-O(4)-Ag(1)	105.6(4)
O(11)-Ag(1)-O(1)	96.19(14)	C(7)-O(4)-Ag(1)	108.9(3)
O(4)-Ag(1)-O(1)	112.11(14)	C(8)-O(5)-C(9)	115.8(5)

O(5)-Ag(1)-O(1)	66.12(13)	C(8)-O(5)-Ag(1)	111.3(4)
O(3)-Ag(1)-O(1)	126.09(13)	C(9)-O(5)-Ag(1)	113.4(3)
O(11)-Ag(1)-O(2)	85.63(13)	C(11)-O(6)-C(20)	110.9(9)
O(4)-Ag(1)-O(2)	98.98(13)	C(13)-O(7)-C(12)	109.9(13)
O(5)-Ag(1)-O(2)	117.36(12)	C(15)-O(8)-C(14)	112.1(11)
O(3)-Ag(1)-O(2)	63.62(12)	C(17)-O(9)-C(16)	109.0(6)
O(1)-Ag(1)-O(2)	63.75(12)	C(19)-O(10)-C(18)	115.0(7)
F(3)-P(1)-F(4)	89.9(2)	O(1)-C(1)-C(2)	108.6(5)
F(3)-P(1)-F(2)	89.9(2)	O(2)-C(2)-C(1)	107.8(5)
F(4)-P(1)-F(2)	90.4(2)	O(2)-C(3)-C(4)	108.2(5)
F(3)-P(1)-F(6)	179.7(2)	O(3)-C(4)-C(3)	108.4(5)
F(4)-P(1)-F(6)	90.0(2)	O(3)-C(5)-C(6)	111.0(5)
F(2)-P(1)-F(6)	90.0(2)	O(4)-C(6)-C(5)	112.4(6)
F(3)-P(1)-F(1)	90.4(2)	O(4)-C(7)-C(8)	108.9(5)
F(4)-P(1)-F(1)	179.4(2)	O(5)-C(8)-C(7)	111.1(5)
F(2)-P(1)-F(1)	90.2(2)	O(5)-C(9)-C(10)	114.5(5)
F(6)-P(1)-F(1)	89.8(2)	O(1)-C(10)-C(9)	107.5(5)
F(3)-P(1)-F(5)	90.2(2)	O(6)-C(11)-C(12)	103.3(9)
F(4)-P(1)-F(5)	90.3(2)	C(11)-C(12)-O(7)	109.5(6)
F(2)-P(1)-F(5)	179.3(2)	C(14)-C(13)-O(7)	118.8(14)
F(6)-P(1)-F(5)	90.0(2)	C(13)-C(14)-O(8)	123.0(11)
F(1)-P(1)-F(5)	89.1(2)	O(8)-C(15)-C(16)	103.5(8)
C(10)-O(1)-C(1)	111.5(5)	O(9)-C(16)-C(15)	113.2(6)
C(10)-O(1)-Ag(1)	113.7(3)	O(9)-C(17)-C(18)	105.1(6)
C(1)-O(1)-Ag(1)	115.9(3)	C(17)-C(18)-O(10)	108.8(5)
C(3)-O(2)-C(2)	113.0(5)	O(10)-C(19)-C(20)	108.0(7)
C(3)-O(2)-Ag(1)	101.1(3)	C(19)-C(20)-O(6)	109.9(5)

Table B: Bond lengths [Å] and angles [°] for C6

X-RAY CRYSTALLOGRAPHIC DATA ON [Ag(15-crown-5)(OTf)], C7, (99BJB5/M.WISEMAN/R.T.)

A crystal of approximate dimensions 0.25 x 0.2 x 0.2 mm was used for data collection.

Crystal data: $C_{11}H_{20}AgF_3O_8S$, M = 238.60, Monoclinic , a = 7.899(1), b = 12.133(1), c = 9.300(1) Å, α = 106.45(1)°, U = 854.8(2) Å^3, space group $P21/m$, Z = 4, D_c = 1.854 gcm^{-3}, μ(Mo-K_α) = 1.368 mm^{-1}, $F(000)$ = 480. Crystallographic measurements were made at 293(2)° K on a CAD4 automatic four-circle diffractometer in the range $2.28<\theta<24.97°$. Data (1774 reflections) were corrected for Lorentz and polarization and but not for absorption.

The asymmetric unit in this structure consists of one half of crown–bound silver cation and one half of an anion. The remainder of the molecule is generated via a mirror plane intrinsic in the space group symmetry, on which atoms Ag1, O1, O5, S1, C6 and F1 are located with half site–occupancy.

In the final least squares cycles all atoms were allowed to vibrate anisotropically. Hydrogen atoms were included at calculated positions where relevant.

The solution of the structure (SHELX86)[1] and refinement (SHELX93)[2] converged to a conventional [i.e. based on 1435 F^2 data with $Fo>4\sigma(Fo)$] $R1$ = 0.0336 and $wR2$ = 0.0884. Goodness of fit = 1.020. The max. and min. residual densities were 0.985 and -0.558 eÅ^{-3} respectively. The asymmetric unit (shown in Fig B), along with the labelling scheme used was produced using ORTEX.[3] Crystal data and structure refinement for **C7**, bond distances and angles are given in Tables C and D.

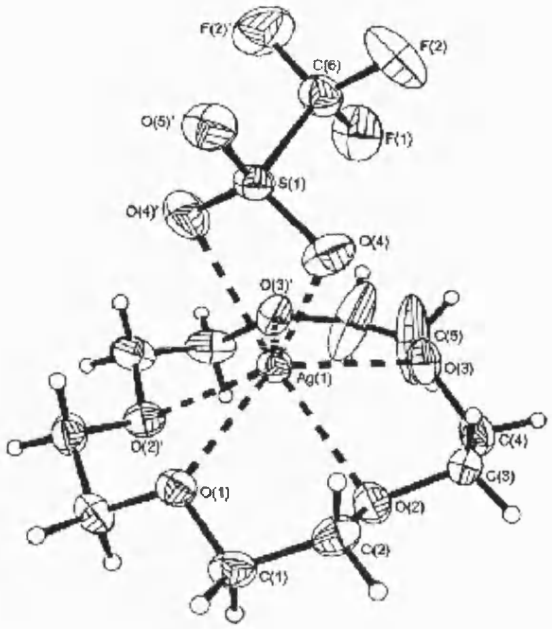

Figure B: Molecular structure of C7

Identification code	**C7** (99bjb5/M.Wiseman/R.T.)
Empirical formula	$C_{11} H_{20} Ag F_3 O_8 S$
Formula weight	238.60
Temperature	293(2) K
Wavelength	0.71069 Å
Crystal system	Monoclinic
Space group	$P2_1/m$
Unit cell dimensions	a = 7.899(1)Å α = 90°
	b = 12.133(1)Å β = 106.45(1)°
	c = 9.300(1)Å γ = 90°
Volume	854.8(2) $Å^3$
Z	2
Density (calculated)	1.854 Mg/m^3
Absorption coefficient	1.368 mm^{-1}
F(000)	480
Crystal size	0.25 x 0.2 x 0.2 mm
Theta range for data collection	2.28 to 24.97 °.
Index ranges	0<=h<=9; 0<=k<=14; -11<=l<=10
Reflections collected	1774
Independent reflections	1585 [R(int) = 0.0159]
Refinement method	Full-matrix least-squares on F^2
Data / restraints / parameters	1581 / 0 / 119
Goodness-of-fit on F^2	1.020
Final R indices [$I>2\sigma(I)$]	R1 = 0.0336 wR2 = 0.0884
R indices (all data)	R1 = 0.0377 wR2 = 0.0926
Largest diff. peak and hole	0.985 and -0.558 $eÅ^{-3}$
Weighting scheme	calc $w=1/[\sigma^2(Fo^2)+(0.0597P)^2+0.7460P]$ where $P=(Fo^2+2Fc^2)/3$
Extinction coefficient	0.0215(23)

Table C: Crystal data and structure refinement for C7

Ag(1)-O(3)#1	2.479(3)	F(2)-C(6)	1.323(5)
Ag(1)-O(3)	2.479(3)	O(1)-C(1)	1.431(4)
Ag(1)-O(1)	2.512(3)	O(1)-C(1)#1	1.431(4)
Ag(1)-O(2)	2.554(3)	O(2)-C(3)	1.421(5)
Ag(1)-O(2)#1	2.554(3)	O(2)-C(2)	1.423(5)
Ag(1)-O(4)#1	2.655(3)	O(3)-C(5)	1.418(6)
Ag(1)-O(4)	2.655(3)	O(3)-C(4)	1.421(6)
S(1)-O(5)	1.421(4)	C(1)-C(2)	1.487(6)
S(1)-O(4)	1.428(3)	C(3)-C(4)	1.480(7)
S(1)-O(4)#1	1.428(3)	C(5)-C(5)#1	1.181(13)
S(1)-C(6)	1.808(6)	C(6)-F(2)#1	1.323(5)
F(1)-C(6)	1.322(7)		
O(3)#1-Ag(1)-O(3)	68.83(13)	O(2)#1-Ag(1)-O(4)#1	94.96(9)
O(3)#1-Ag(1)-O(1)	134.22(9)	O(3)#1-Ag(1)-O(4)	122.17(10)
O(3)-Ag(1)-O(1)	134.22(9)	O(3)-Ag(1)-O(4)	91.53(10)
O(3)#1-Ag(1)-O(2)	122.45(9)	O(1)-Ag(1)-O(4)	98.95(10)
O(3)-Ag(1)-O(2)	67.85(9)	O(2)-Ag(1)-O(4)	94.96(9)
O(1)-Ag(1)-O(2)	66.92(7)	O(2)#1-Ag(1)-O(4)	144.05(9)
O(3)#1-Ag(1)-O(2)#1	67.85(9)	O(4)#1-Ag(1)-O(4)	53.15(14)
O(3)-Ag(1)-O(2)#1	122.45(9)	O(5)-S(1)-O(4)	116.0(2)
O(1)-Ag(1)-O(2)#1	66.92(7)	O(5)-S(1)-O(4)#1	116.0(2)
O(2)-Ag(1)-O(2)#1	107.85(12)	O(3)-Ag(1)-O(4)#1	122.17(10)
O(3)#1-Ag(1)-O(4)#1	91.53(10)	O(1)-Ag(1)-O(4)#1	98.95(10)
O(2)-Ag(1)-O(4)#1	144.05(10)	O(4)-S(1)-O(4)#1	112.6(3)
O(5)-S(1)-C(6)	103.5(3)	C(2)-O(2)-Ag(1)	102.3(2)
O(4)-S(1)-C(6)	103.2(2)	C(5)-O(3)-C(4)	116.7(5)
O(4)#1-S(1)-C(6)	103.2(2)	C(5)-O(3)-Ag(1)	110.5(3)
C(1)-O(1)-C(1)#1	113.3(4)	C(4)-O(3)-Ag(1)	113.3(2)
C(1)-O(1)-Ag(1)	113.8(2)	S(1)-O(4)-Ag(1)	96.9(2)
C(1)#1-O(1)-Ag(1)	113.8(2)	O(1)-C(1)-C(2)	108.8(3)
C(3)-O(2)-C(2)	114.4(3)	O(2)-C(2)-C(1)	106.9(3)
C(3)-O(2)-Ag(1)	102.8(2)	O(2)-C(3)-C(4)	107.1(4)
C(5)#1-C(5)-O(3)	124.8(3)	O(3)-C(4)-C(3)	108.0(3)
F(1)-C(6)-F(2)	105.7(4)	F(1)-C(6)-S(1)	112.5(4)
F(1)-C(6)-F(2)#1	105.7(4)	F(2)-C(6)-S(1)	111.3(3)
F(2)-C(6)-F(2)#1	110.2(6)	F(2)#1-C(6)-S(1)	111.3(3)

Table D: Bond lengths [Å] and angles [°] for C7

Symmetry transformations used to generate equivalent atoms: x,-y+1/2, z

X-RAY CRYSTALLOGRAPHIC DATA ON [Ag(15-crown-5)(NO_3)], C8, (99BJB2/M.WISEMAN)

A crystal of approximate dimensions 0.3 x 0.3 x 0.3 mm was used for data collection.

Crystal data: $C_{10}H_{20}AgNO_8$, M = 390.14, Orthorhombic , a = 9.1560(10), b = 9.9090(10), c = 16.670(2) Å , α = 90, β = 90, γ = 90°, U = 1512.4(3) Å^3, space group $P2_12_12_1$, Z = 4, D_c = 1.713 gcm^{-3}, μ(Mo-K_α) = 1.367 mm^{-1}, F(000) = 792. Crystallographic measurements were made at 293(2)° K on a CAD4 automatic four-circle diffractometer in the range 2.39<θ<24.96°. Data (1591 reflections) were corrected for Lorentz and polarization but not for absorption.

In the final least squares cycles all atoms were allowed to vibrate anisotropically. Hydrogen atoms were included at calculated positions where relevant.

The solution of the structure (SHELX86)[1] and refinement (SHELX93)[2] converged to a conventional [i.e. based on 1370 F^2 data with $Fo>4\sigma(Fo)$] $R1$ = 0.0320 and $wR2$ = 0.0886. Goodness of fit = 1.074. The max. and min. residual densities were 0.605 and -0.411 eÅ^{-3} respectively. The asymmetric unit (shown in Fig. C), along with the labelling scheme used was produced using ORTEX.[3] Crystal data and structure refinement for C6, bond distances and angles are given in Tables E and F.

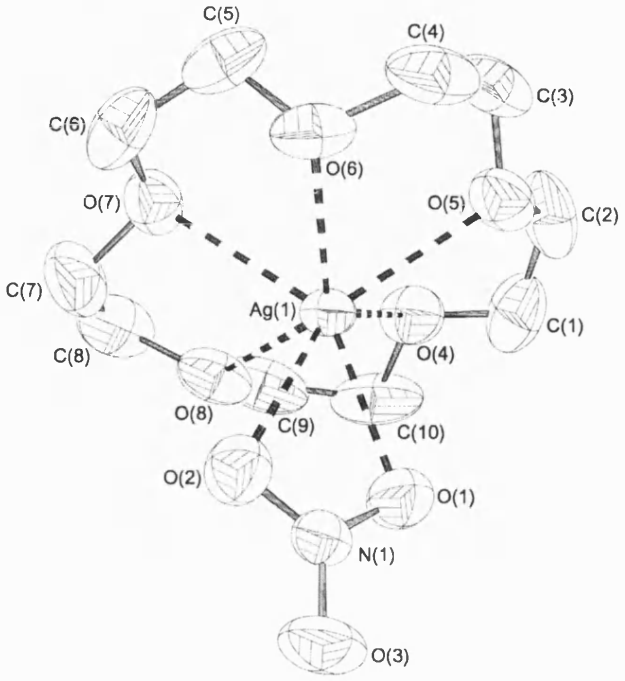

Figure C: Molecular structure of C8

Identification code	**C8** (99bjb2/M.Wiseman)
Empirical formula	$C_{10}H_{20}AgNO_8$
Formula weight	390.14
Temperature	293(2)K
Wavelength	0.71069 Å
Crystal system	Orthorhombic
Space group	$P2_12_12_1$
Unit cell dimensions	a = 9.156(1)Å
	b = 9.909(1)Å
	c = 16.670(2)Å
Volume	1512.4(3) Å^3
Z	4
Density (calculated)	1.713 Mg/m^3
Absorption coefficient	1.367 mm^{-1}
F(000)	792
Crystal size	0.3 x 0.3 x 0.3 mm
Theta range for data collection	2.39 to 24.96 °.
Index ranges	0<=h<=10; 0<=k<=11; 0<=l<=19
Reflections collected	1591
Independent reflections	1537 [R(int) = 0.0116]
Refinement method	Full-matrix least-squares on F^2
Data / restraints / parameters	1533 / 0 / 183
Goodness-of-fit on F^2	1.074
Final R indices [I>2σ(I)]	R1 = 0.0320 wR2 = 0.0886
R indices (all data)	R1 = 0.0372 wR2 = 0.0915
Absolute structure parameter	0.01(10)
Largest diff. peak and hole	0.605 and –0.411 eÅ^{-3}
Weighting scheme	calc w=1/[σ□^{2}(Fo^2)+(0.0607P)^2+0.3791P] where P=(Fo^2+2Fc^2)/3

Extinction coefficient	0.0143(14)

Table E: Crystal data and structure refinement for C8

Ag(1)-O(1)	2.420(6)	O(5)-C(2)	1.44(2)
Ag(1)-O(5)	2.466(6)	O(6)-C(5)	1.377(13)
Ag(1)-O(6)	2.519(6)	O(6)-C(4)	1.438(13)
Ag(1)-O(7)	2.534(7)	C(1)-C(2)	1.47(2)
Ag(1)-O(2)	2.566(7)	C(3)-C(4)	1.49(2)
Ag(1)-O(8)	2.573(6)	C(5)-C(6)	1.44(2)
N(1)-O(2)	1.213(9)	O(8)-C(9)	1.348(14)
N(1)-O(1)	1.214(9)	O(8)-C(8)	1.44(2)
N(1)-O(3)	1.219(8)	O(7)-C(7)	1.386(13)
O(4)-C(10)	1.365(13)	O(7)-C(6)	1.438(13)
O(4)-C(1)	1.37(2)	C(10)-C(9)	1.55(2)
O(5)-C(3)	1.420(14)	C(7)-C(8)	1.42(2)
O(1)-Ag(1)-O(5)	103.4(2)	C(3)-O(5)-C(2)	114.5(9)
O(1)-Ag(1)-O(6)	125.9(3)	C(3)-O(5)-Ag(1)	114.1(7)
O(5)-Ag(1)-O(6)	68.8(3)	C(2)-O(5)-Ag(1)	114.5(7)
O(1)-Ag(1)-O(7)	144.4(2)	C(5)-O(6)-C(4)	113.9(9)
O(5)-Ag(1)-O(7)	112.1(2)	C(5)-O(6)-Ag(1)	111.7(6)
O(6)-Ag(1)-O(7)	67.9(2)	C(4)-O(6)-Ag(1)	110.1(6)
O(1)-Ag(1)-O(2)	49.0(2)	O(4)-C(1)-C(2)	111.0(10)
O(5)-Ag(1)-O(2)	136.3(2)	O(5)-C(2)-C(1)	109.9(9)
O(6)-Ag(1)-O(2)	98.7(2)	O(5)-C(3)-C(4)	108.2(8)
O(7)-Ag(1)-O(2)	99.9(2)	O(6)-C(4)-C(3)	113.3(8)
O(1)-Ag(1)-O(8)	95.8(3)	O(6)-C(5)-C(6)	109.8(10)
O(5)-Ag(1)-O(8)	127.8(2)	C(9)-O(8)-C(8)	113.0(10)
O(6)-Ag(1)-O(8)	132.3(3)	C(9)-O(8)-Ag(1)	118.1(8)
O(7)-Ag(1)-O(8)	64.5(3)	C(8)-O(8)-Ag(1)	112.9(7)
O(2)-Ag(1)-O(8)	92.2(2)	C(7)-O(7)-C(6)	115.4(11)
O(2)-N(1)-O(1)	117.3(7)	C(7)-O(7)-Ag(1)	104.7(7)
O(2)-N(1)-O(3)	122.3(8)	C(6)-O(7)-Ag(1)	106.2(7)
O(1)-N(1)-O(3)	120.4(9)	O(4)-C(10)-C(9)	105.5(9)
N(1)-O(1)-Ag(1)	100.5(5)	O(7)-C(7)-C(8)	108.1(12)
N(1)-O(2)-Ag(1)	93.2(5)	O(8)-C(9)-C(10)	109.4(11)
C(10)-O(4)-C(1)	116.0(11)	C(5)-C(6)-O(7)	110.3(8)
C(7)-C(8)-O(8)	110.6(10)		

Table F: Bond lengths [Å] and angles [°] for C8

X-RAY CRYSTALLOGRAPHIC DATA ON [Ag(18-crown-6)(OTf)], C11, (K01BJB2/M.WISEMAN)

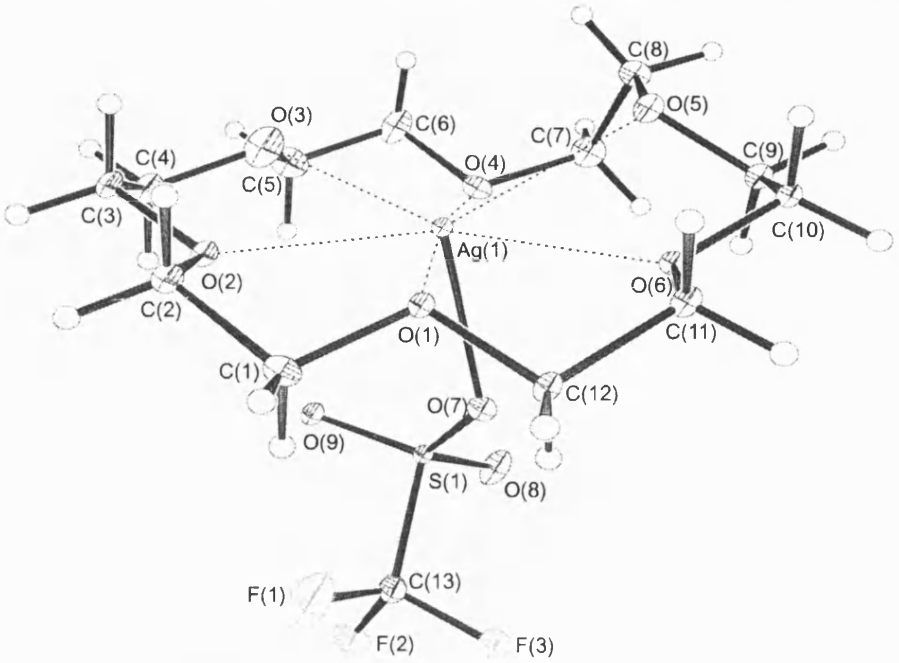

Figure D: Molecular structure of C8

Identification code	**C11** (k01bjb2)
Empirical formula	C13 H24 Ag F3 O9 S
Formula weight	521.25
Temperature	27(2) K
Wavelength	0.71070 Å
Crystal system	Orthorhombic
Space group	$P2_12_12_1$
Unit cell dimensions	a = 8.0270(2)Å α = 90°
	b = 14.4150(3)Å β = 90°
	c = 16.6630(5)Å δ = 90°
Volume	1928.06(9) $Å^3$
Z	4
Density (calculated)	1.796 Mg/m^3
Absorption coefficient	1.225 mm^{-1}
F(000)	1056
Crystal size	0.25 x 0.25 x 0.30 mm
Theta range for data collection	1.87 to 27.48°.
Index ranges	-9<=h<=10; -18<=k<=11; -21<=l<=13
Reflections collected	10144
Independent reflections	4400 [R(int) = 0.0370]
Reflections observed (>2σ)	4134
Refinement method	Full-matrix least-squares on F^2
Data / restraints / parameters	4400 / 0 / 247
Goodness-of-fit on F^2	0.969
Final R indices [I>2σ(I)]	R_1 = 0.0332 wR_2 = 0.0788
R indices (all data)	R_1 = 0.0370 wR_2 = 0.0812
Absolute structure parameter	0.00(3)
Largest diff. peak and hole	1.455 and -0.979 $eÅ^{-3}$

Table G: Crystal data and structure refinement for C11

Notes: Largest peaks in EDM close to fluorines, but not a clear case of site disorder in the CF_3 group. No disorder modelled. Slight smearing of electron density may be due to some libration.

Ag(1)-O(7)	2.355(3)	Ag(1)-O(3)	2.602(3)
Ag(1)-O(2)	2.619(3)	Ag(1)-O(6)	2.680(3)
Ag(1)-O(5)	2.733(3)	Ag(1)-O(4)	2.736(3)
Ag(1)-O(1)	2.771(3)	S(1)-O(8)	1.436(3)
S(1)-O(9)	1.440(3)	S(1)-O(7)	1.440(3)
S(1)-C(13)	1.821(5)	F(1)-C(13)	1.289(6)
F(2)-C(13)	1.369(6)	F(3)-C(13)	1.340(5)
O(1)-C(1)	1.422(5)	O(1)-C(12)	1.428(5)
O(2)-C(2)	1.411(5)	O(2)-C(3)	1.425(5)
O(3)-C(4)	1.410(6)	O(3)-C(5)	1.462(6)
O(4)-C(6)	1.413(6)	O(4)-C(7)	1.459(6)
O(5)-C(8)	1.427(5)	O(5)-C(9)	1.447(5)
O(6)-C(10)	1.424(5)	O(6)-C(11)	1.428(4)
C(1)-C(2)	1.501(6)	C(3)-C(4)	1.481(6)
C(5)-C(6)	1.436(8)	C(7)-C(8)	1.479(7)
C(9)-C(10)	1.497(6)	C(11)-C(12)	1.503(5)
O(7)-Ag(1)-O(3)	114.95(12)	O(7)-Ag(1)-O(2)	98.78(10)
O(3)-Ag(1)-O(2)	63.37(10)	O(7)-Ag(1)-O(6)	79.64(9)
O(3)-Ag(1)-O(6)	164.87(10)	O(2)-Ag(1)-O(6)	120.51(9)
O(7)-Ag(1)-O(5)	108.50(11)	O(3)-Ag(1)-O(5)	107.66(10)
O(2)-Ag(1)-O(5)	152.24(9)	O(6)-Ag(1)-O(5)	61.62(8)
O(7)-Ag(1)-O(4)	87.16(10)	O(3)-Ag(1)-O(4)	64.13(11)
O(2)-Ag(1)-O(4)	124.33(9)	O(6)-Ag(1)-O(4)	115.03(9)
O(5)-Ag(1)-O(4)	63.58(9)	O(7)-Ag(1)-O(1)	86.87(9)
O(3)-Ag(1)-O(1)	122.21(10)	O(2)-Ag(1)-O(1)	60.64(8)
O(6)-Ag(1)-O(1)	59.89(8)	O(5)-Ag(1)-O(1)	114.82(8)
O(4)-Ag(1)-O(1)	172.83(9)	O(8)-S(1)-O(9)	115.48(19)
O(8)-S(1)-O(7)	113.4(2)	O(9)-S(1)-O(7)	115.57(18)
O(8)-S(1)-C(13)	103.5(2)	O(9)-S(1)-C(13)	104.62(19)
O(7)-S(1)-C(13)	102.0(2)	C(1)-O(1)-C(12)	111.9(3)
C(1)-O(1)-Ag(1)	111.6(2)	C(12)-O(1)-Ag(1)	111.0(2)
C(2)-O(2)-C(3)	112.8(3)	C(2)-O(2)-Ag(1)	121.5(2)
C(3)-O(2)-Ag(1)	116.0(2)	C(4)-O(3)-C(5)	108.1(4)
C(4)-O(3)-Ag(1)	114.1(3)	C(5)-O(3)-Ag(1)	111.1(3)
C(6)-O(4)-C(7)	112.2(4)	C(6)-O(4)-Ag(1)	110.1(3)
C(7)-O(4)-Ag(1)	112.2(2)	C(8)-O(5)-C(9)	113.3(3)
C(8)-O(5)-Ag(1)	114.4(2)	C(9)-O(5)-Ag(1)	106.3(2)
C(10)-O(6)-C(11)	112.7(3)	C(10)-O(6)-Ag(1)	118.5(2)
C(11)-O(6)-Ag(1)	121.6(2)	S(1)-O(7)-Ag(1)	124.45(17)
O(1)-C(1)-C(2)	107.0(3)	O(2)-C(2)-C(1)	108.1(4)
O(2)-C(3)-C(4)	107.5(4)	O(3)-C(4)-C(3)	109.4(4)
C(6)-C(5)-O(3)	109.8(4)	O(4)-C(6)-C(5)	107.6(4)
O(4)-C(7)-C(8)	113.2(4)	O(5)-C(8)-C(7)	110.3(4)
O(5)-C(9)-C(10)	106.7(4)	O(6)-C(10)-C(9)	107.5(3)
O(6)-C(11)-C(12)	107.4(3)	O(1)-C(12)-C(11)	106.9(3)
F(1)-C(13)-F(3)	108.8(5)	F(1)-C(13)-F(2)	108.0(4)
F(3)-C(13)-F(2)	105.5(4)	F(1)-C(13)-S(1)	113.1(3)
F(3)-C(13)-S(1)	111.9(3)	F(2)-C(13)-S(1)	109.2(4)

Table H: Bond lengths [Å] and angles [°] for C11

X-RAY CRYSTALLOGRAPHIC DATA ON [Ag(benzo-18-crown-6)(OTf)], C13, (K00BJB4/M.WISEMAN)

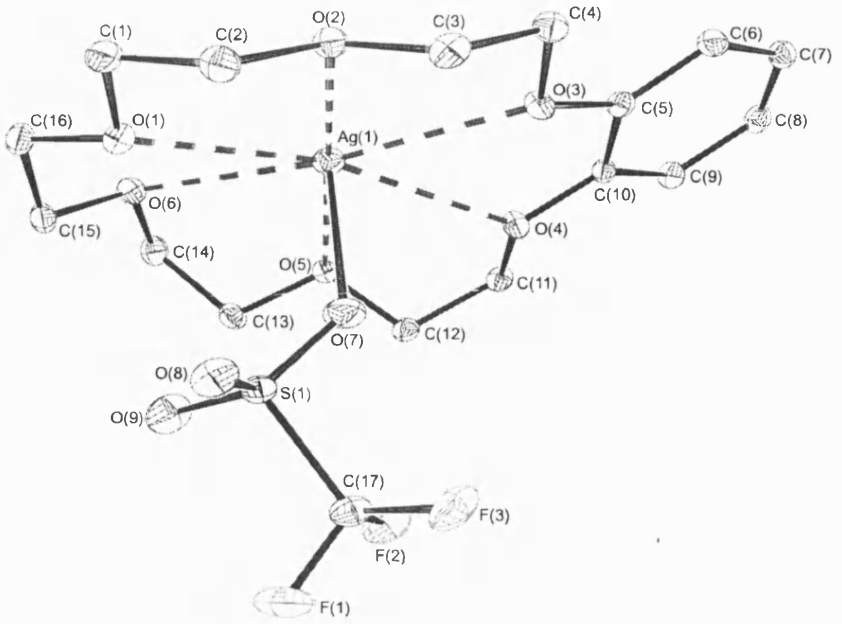

Figure E: Molecular structure of C13

Identification code	**C13** (k00bjb4/M.Wiseman)
Empirical formula	$C_{17}H_{24}AgF_3O_9S$
Formula weight	569.29
Temperature	170(2) K
Wavelength	0.71070 Å
Crystal system	Monoclinic
Space group	$P2_1/n$
Unit cell dimensions	a = 8.99700(10)Å α = 90°
	b = 12.7660(2)Å β = 97.3560(5)°
	c = 18.4690(3)Å δ = 90°
Volume	2103.81(5) $Å^3$
Z	4
Density (calculated)	1.797 Mg/m^3
Absorption coefficient	1.131 mm^{-1}
F(000)	1152
Crystal size	0.20 x 0.20 x 0.15 mm
Theta range for data collection	3.74 to 27.87 °.
Index ranges	-11<=h<=11; -16<=k<=16; -24<=l<=24
Reflections collected	30351
Independent reflections	5001 [R(int) = 0.0334]
Reflections observed (>2σ)	4476
Absorption correction	Multiscan
Max. and min. transmission	0.8487 and 0.8054
Refinement method	Full-matrix least-squares on F^2
Data / restraints / parameters	5001 / 0 / 281
Goodness-of-fit on F^2	0.611
Final R indices [I>2σ(I)]	R_1 = 0.0241 wR_2 = 0.0710
R indices (all data)	R_1 = 0.0284 wR_2 = 0.0782
Largest diff. peak and hole	0.604 and -0.576 $e.Å^{-3}$

Table I: Crystal data and structure refinement for C13

Ag(1)-O(7)	2.4189(17)	Ag(1)-C(7)#1	2.618(2)
S(1)-O(8)	1.4326(15)	S(1)-O(9)	1.4368(15)
S(1)-O(7)	1.4415(16)	S(1)-C(17)	1.832(2)
F(1)-C(17)	1.327(3)	F(2)-C(17)	1.333(2)

F(3)-C(17)	1.328(2)	O(1)-C(1)	1.423(2)
O(1)-C(16)	1.427(2)	O(2)-C(3)	1.421(2)
O(2)-C(2)	1.430(2)	O(3)-C(5)	1.372(2)
O(3)-C(4)	1.436(2)	O(4)-C(10)	1.370(2)
O(4)-C(11)	1.432(2)	O(5)-C(12)	1.424(2)
O(5)-C(13)	1.426(2)	O(6)-C(14)	1.423(3)
O(6)-C(15)	1.423(2)	C(1)-C(2)	1.499(3)
C(3)-C(4)	1.502(3)	C(5)-C(6)	1.379(2)
C(5)-C(10)	1.409(2)	C(6)-C(7)	1.404(3)
C(7)-C(8)	1.382(3)	C(7)-Ag(1)#1	2.618(2)
C(8)-C(9)	1.405(3)	C(9)-C(10)	1.386(2)
C(11)-C(12)	1.502(3)	C(13)-C(14)	1.510(3)
C(15)-C(16)	1.501(3)		
O(7)-Ag(1)-C(7)#1	166.44(7)	O(8)-S(1)-O(9)	115.76(10)
O(8)-S(1)-O(7)	114.75(11)	O(9)-S(1)-O(7)	115.17(11)
O(8)-S(1)-C(17)	103.74(9)	O(9)-S(1)-C(17)	102.57(9)
O(7)-S(1)-C(17)	102.11(9)	C(1)-O(1)-C(16)	111.48(15)
C(3)-O(2)-C(2)	110.39(15)	C(5)-O(3)-C(4)	117.01(14)
C(10)-O(4)-C(11)	116.37(14)	C(12)-O(5)-C(13)	111.35(14)
C(14)-O(6)-C(15)	114.12(15)	S(1)-O(7)-Ag(1)	135.06(10)
O(1)-C(1)-C(2)	108.10(16)	O(2)-C(2)-C(1)	108.67(16)
O(2)-C(3)-C(4)	109.63(15)	O(3)-C(4)-C(3)	107.57(15)
O(3)-C(5)-C(6)	125.11(16)	O(3)-C(5)-C(10)	114.99(15)
C(6)-C(5)-C(10)	119.88(16)	C(5)-C(6)-C(7)	120.05(17)
C(8)-C(7)-C(6)	119.98(17)	C(8)-C(7)-Ag(1)#1	83.73(12)
C(6)-C(7)-Ag(1)#1	112.68(13)	C(7)-C(8)-C(9)	120.41(17)
C(10)-C(9)-C(8)	119.38(17)	O(4)-C(10)-C(9)	124.67(16)
O(4)-C(10)-C(5)	115.04(15)	C(9)-C(10)-C(5)	120.29(16)
O(4)-C(11)-C(12)	107.95(14)	O(5)-C(12)-C(11)	108.37(14)
O(5)-C(13)-C(14)	107.63(16)	O(6)-C(14)-C(13)	112.20(16)
O(6)-C(15)-C(16)	107.79(15)	O(1)-C(16)-C(15)	108.36(15)
F(1)-C(17)-F(3)	107.18(18)	F(1)-C(17)-F(2)	107.40(17)
F(3)-C(17)-F(2)	107.38(17)	F(1)-C(17)-S(1)	111.11(14)
F(3)-C(17)-S(1)	112.14(14)	F(2)-C(17)-S(1)	111.38(14)

Table J: Bond lengths [Å] and angles [°] for C13

Symmetry transformations used to generate equivalent atoms:
#1 -x+1,-y+1,-z

X-RAY CRYSTALLOGRAPHIC DATA ON {[Ag(dibenzo-18-crown-6)(OH$_2$)]$^+$[OTf].DCM}, C15, (K00BJB7/M.WISEMAN)

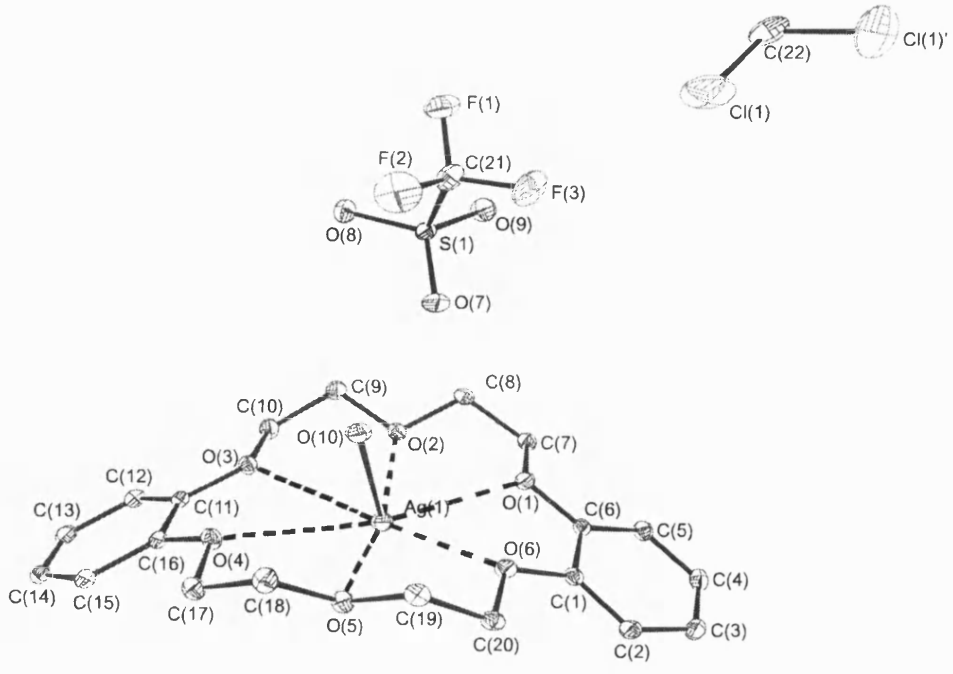

Figure F: Molecular structure of C15

Identification code	**C15** (k00bjb7)
Empirical formula	C21.50 H27 Ag Cl F3 O10 S
Formula weight	677.81
Temperature	150(2) K
Wavelength	0.71070 Å
Crystal system	Monoclinic
Space group	C2/c
Unit cell dimensions	a = 27.4760(4)Å α = 90°
	b = 13.7760(2)Å β = 97.4630(6)°
	c = 14.0470(2)Å δ = 90°
Volume	5271.88(13) Å^3
Z	8
Density (calculated)	1.708 Mg/m^3
Absorption coefficient	1.019 mm^{-1}
F(000)	2744
Crystal size	0.15 x 0.15 x 0.15 mm
Theta range for data collection	3.70 to 27.47 °.
Index ranges	0 =h =35; -17 =k =17; -18 =l =18
Reflections collected	29052
Independent reflections	5969 [R(int) = 0.0413]
Reflections observed (2σ)	5586
Absorption correction	Multiscan
Max. and min. transmission	0.8622 and 0.8622
Refinement method	Full-matrix least-squares on F^2
Data / restraints / parameters	5969 / 3 / 351
Goodness-of-fit on F^2	1.087
Final R indices [I 2σ(I)]	R_1 = 0.0356 wR_2 = 0.0744
R indices (all data)	R_1 = 0.0405 wR_2 = 0.0761
Largest diff. peak and hole	0.518 and -0.645 e.Å^{-3}

Table K: Table 1. Crystal data and structure refinement for C15

Ag(1)-O(10)	2.3291(19)	Ag(1)-C(3) 1	2.437(2)
Ag(1)-O(6)	2.5658(17)	Ag(1)-C(4) 1	2.684(2)
S(1)-O(9)	1.4339(19)	S(1)-O(8)	1.4370(19)
S(1)-O(7)	1.4461(19)	S(1)-C(21)	1.825(3)
F(1)-C(21)	1.337(3)	F(2)-C(21)	1.322(3)
F(3)-C(21)	1.326(3)	Cl(1)-C(22)	1.752(3)
O(1)-C(6)	1.367(3)	O(1)-C(7)	1.438(3)
O(2)-C(8)	1.428(3)	O(2)-C(9)	1.430(3)
O(3)-C(11)	1.372(3)	O(3)-C(10)	1.437(3)
O(4)-C(16)	1.374(3)	O(4)-C(17)	1.432(3)
O(5)-C(18)	1.426(3)	O(5)-C(19)	1.431(3)
O(6)-C(1)	1.373(3)	O(6)-C(20)	1.437(3)
C(1)-C(2)	1.379(3)	C(1)-C(6)	1.413(3)
C(2)-C(3)	1.408(4)	C(3)-C(4)	1.385(4)
C(3)-Ag(1) 1	2.437(2)	C(4)-C(5)	1.400(4)
C(4)-Ag(1) 1	2.684(2)	C(5)-C(6)	1.382(3)
C(7)-C(8)	1.498(3)	C(9)-C(10)	1.503(3)
C(11)-C(12)	1.384(3)	C(11)-C(16)	1.404(3)
C(12)-C(13)	1.404(4)	C(13)-C(14)	1.379(4)
C(14)-C(15)	1.394(4)	C(15)-C(16)	1.392(3)
C(17)-C(18)	1.497(4)	C(19)-C(20)	1.498(3)
C(22)-Cl(1) 2	1.752(3)		
O(10)-Ag(1)-C(3)	159.28(8)	O(10)-Ag(1)-O(6)	92.08(6)
C(3)-Ag(1)-O(6)	107.55(7)	O(10)-Ag(1)-C(4)	145.61(7)
C(3)-Ag(1)-C(4) 1	30.90(8)	O(6)-Ag(1)-C(4)	92.28(6)
O(9)-S(1)-O(8)	115.94(12)	O(9)-S(1)-O(7)	114.22(12)
O(8)-S(1)-O(7)	115.28(12)	O(9)-S(1)-C(21)	103.22(13)
O(8)-S(1)-C(21)	103.08(12)	O(7)-S(1)-C(21)	102.45(13)
C(6)-O(1)-C(7)	116.61(17)	C(8)-O(2)-C(9)	110.71(18)
C(11)-O(3)-C(10)	116.42(18)	C(16)-O(4)-C(17)	116.75(18)
C(18)-O(5)-C(19)	110.75(18)	C(1)-O(6)-C(20)	116.89(18)
C(1)-O(6)-Ag(1)	118.90(13)	C(20)-O(6)-Ag(1)	116.14(13)
O(6)-C(1)-C(2)	124.7(2)	O(6)-C(1)-C(6)	115.0(2)
C(2)-C(1)-C(6)	120.3(2)	C(1)-C(2)-C(3)	119.7(2)
C(4)-C(3)-C(2)	119.8(2)	C(4)-C(3)-Ag(1)	84.45(15)
C(2)-C(3)-Ag(1)	105.30(16)	C(3)-C(4)-C(5)	120.5(2)
C(3)-C(4)-Ag(1)	64.66(14)	C(5)-C(4)-Ag(1)	114.79(16)
C(6)-C(5)-C(4)	119.8(2)	O(1)-C(6)-C(5)	125.1(2)
O(1)-C(6)-C(1)	115.05(19)	C(5)-C(6)-C(1)	119.9(2)
O(1)-C(7)-C(8)	108.16(18)	O(2)-C(8)-C(7)	109.45(19)
O(2)-C(9)-C(10)	108.8(2)	O(3)-C(10)-C(9)	108.1(2)
O(3)-C(11)-C(12)	125.0(2)	O(3)-C(11)-C(16)	115.0(2)
C(12)-C(11)-C(16)	120.0(2)	C(11)-C(12)-C(13)	119.7(2)
C(14)-C(13)-C(12)	120.3(2)	C(13)-C(14)-C(15)	120.3(2)
C(16)-C(15)-C(14)	119.8(2)	O(4)-C(16)-C(15)	124.8(2)
O(4)-C(16)-C(11)	115.3(2)	C(15)-C(16)-C(11)	119.9(2)
O(4)-C(17)-C(18)	108.32(19)	O(5)-C(18)-C(17)	109.00(19)
O(5)-C(19)-C(20)	109.31(19)	O(6)-C(20)-C(19)	107.92(19)
F(2)-C(21)-F(3)	107.8(2)	F(2)-C(21)-F(1)	107.0(2)
F(3)-C(21)-F(1)	106.9(3)	F(2)-C(21)-S(1)	111.7(2)
F(3)-C(21)-S(1)	111.43(19)	F(1)-C(21)-S(1)	111.69(19)
Cl(1)-C(22)-Cl(1)	112.7(3)		

Table L: Bond lengths [Å] and angles [°] for C15

Symmetry transformations used to generate equivalent atoms:

1 -x,-y+1,-z

2 -x,y,-z+3/2

REFERENCES:

[1] G.M. Sheldrick; *Acta Cryst.*, **A46**, 467 (1990)

[2] G.M. Sheldrick, SHELXL, a computer program for crystal structure refinement, University of Göttingen (1993)

[3] P. McArdle, *J.Appl.Cryst.*, **28**, 65 (1995)

APPENDIX 2: X-RAY CRYSTALLOGRAPHIC DATA ON COMPOUNDS G1, G2, P1 AND P4

Summary:

This Appendix contains X-ray crystallographic data on the complexes discussed in Chapter 3. Crystal and structure refinement data and selected bond lengths and angles, are included for all four compounds for completeness. Notes are also included for compounds **G1a**, **G2a** and **P1.** Hydrogen co-ordinates, isotropic displacement parameters and tables of anisotropic temperature factors for each compound are available as supplementary information on request from the Department of Chemistry.

For identification each compound has two labels as noted in appendix 1. Thus for example **G1a** is also **99BJB3.** The label **G1a** is used throughout this thesis to identify $[AuSC_6H_4\text{-}p\text{-}CMe_3]_{10}.0.8C_6H_5OC_2H_5$. The second label follows the convention used by the departmental crystallography unit to identify samples from different research groups.

All data given in the subsequent tables are followed by the calculated standard deviation based on the assumption that the data collected will follow the "normal distribution model". For example in **G1** the Au(1)-S(10) separation is 2.342(4) Å, the standard deviation, σ, is noted for the last decimal place, i.e. 0.004 Å. Using the normal distribution approximation the "true" value could be within the range of the average separation $\pm 3\sigma$.

CONTENTS

X-RAY CRYSTALLOGRAPHIC DATA ON:

$[AuSC_6H_4\text{-}p\text{-}CMe_3]_{10}.0.8C_6H_5OC_2H_5$	**G1a**
$[AuSC_6H_4\text{-}o\text{-}CMe_3]_{12}.2C_6H_5OC_2H_5$	**G2a**
$[Au(PPh_3)(SC_6H_4\text{-}p\text{-}CMe_3)]$	**P1**
$[Au(PPh_3)(SC_6H_4\text{-}o\text{-}CF_3)]$	**P4**

X-RAY CRYSTALLOGRAPHIC DATA ON $[AuSC_6H_5$-p-$CMe_3]_{10}$, G1a, (99BJB3/M.WISEMAN)

A crystal of approximate dimensions 0.2 x 0.2 x 0.2 mm was used for data collection.

Crystal data: $C_{100}H_{130}Au_{10}S_{10}$ $0.8(C_8H_{10}O)$, M = 3720.03, Triclinic , a = 16.641(3), b = 17.274(4), c = 22.703(6) Å , α = 109.45(2), β = 93.40(2), γ = 93.41(2)°, U = 6121.1(24) Å^3, space group P-1(No.2), Z = 2, D_c = 2.018 gcm^{-3}, μ(Mo-K_α) = 12.143 mm^{-1}, F(000) = 3466. Crystallographic measurements were made at 293(2)° K on a CAD4 automatic four-circle diffractometer in the range 2.09<θ<24.97°. Data (21482 reflections) were corrected for Lorentz and polarization and also for absorption[1]. (Max. and Min absorption corrections; 1.000, 0.342 respectively).

The core of the cluster molecule (1 per asymmetric unit) in this structure was seen to consist of 2 intertwining 'cartwheels', each composed of 5 sulphur and 5 gold atoms in an alternating pattern, with a further gold atom at the hub of the wheel. Each of these sulphur atoms is bonded in turn, to 1 p-^{t}butyl benzene moiety. The asymmetric unit is completed by the presence of a disordered solvent entity (0.8 molecules of ethoxy benzene).

Refinement of this structure was relatively straightforward. In the final least squares cycles all atoms in the cluster were allowed to vibrate anisotropically. All phenyl groups were treated as rigid hexagons. Restraints were imposed on the thermal parameters on the organic functionality containing carbons C71-C80, due to anomolously large thermal vibration in one half of the phenyl ring. Moreover, interatomic distances in this fragment were restrained to be the same as those in the C11-C20 entity. As the ethoxy group in the solvent fragment could not be located reliably, it was not included in the refinement while the 6 partial carbon atoms in the solvent were refined isotropically. Hydrogen atoms were included at calculated positions where relevant except in the solvent moiety.

The solution of the structure (SHELX86)[2] and refinement (SHELX93)[3] converged to a conventional [i.e. based on 12502 F^2 data with $Fo>4\sigma(Fo)$] $R1$ = 0.0531 and $wR2$ = 0.1072. Goodness of fit = 0.941. The max. and min. residual densities were 1.347 and -0.794 eÅ^{-3} respectively. The asymmetric unit (shown in Fig. A and B), along with the labelling scheme used was produced using ORTEX[4]. Crystal data and structure refinement, bond distances and angles are given in Tables A, and B.

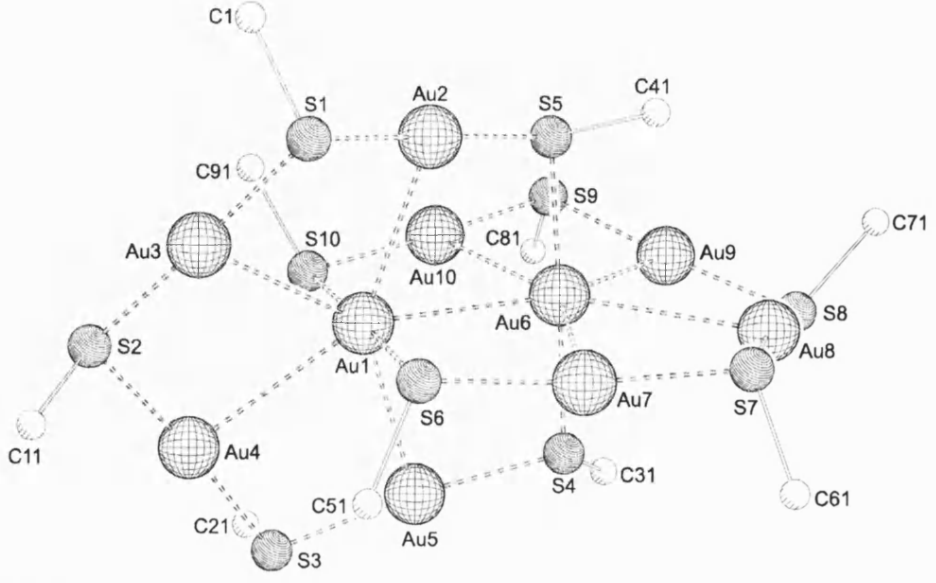

Figure A: $Au_{10}S_{10}C_{10}$ core of G1a

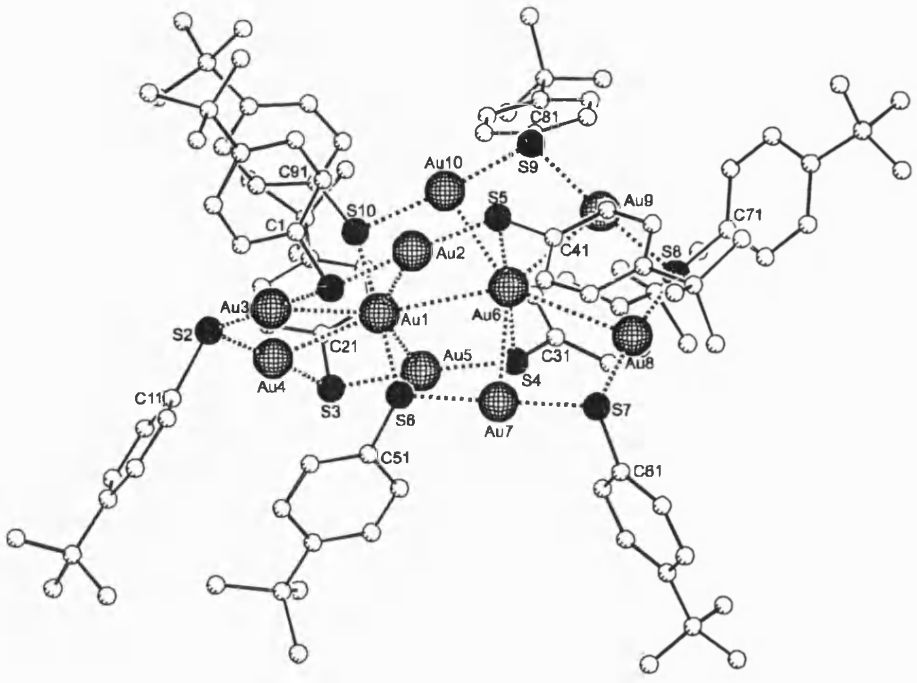

Figure B: Full structure of G1a

Identification code	**G1a** (99bjb3/M.Wiseman)
Empirical formula	$C_{100}H_{130}Au_{10}S_{10}$ 0.8($C_8H_{10}O$)
Formula weight	3720.03
Temperature	293(2) K
Wavelength	0.71069 Å
Crystal system	Triclinic
Space group	P-1 (No.2)
Unit cell dimensions	a = 16.641(3)Å α = 109.45(2)°
	b = 17.274(4)Å β = 93.40(2)°
	c = 22.703(6)Å γ = 93.41(2)°
Volume	6121(2) $Å^3$
Z	2
Density (calculated)	2.018 Mg/m^3
Absorption coefficient	12.143 mm^{-1}
F(000)	3466
Crystal size	0.2 x 0.2 x 0.2 mm
Theta range for data collection	2.09 to 24.97 °.
Index ranges	-19<=h<=19; -20<=k<=19; 0<=l<=26
Reflections collected	21482
Independent reflections	21482 [R(int) = 0.0000]
Absorption correction	DIFABS
Max. and min. transmission	1.000 and 0.342
Refinement method	Full-matrix least-squares on F^2
Data / restraints / parameters	21470 / 84 / 1005
Goodness-of-fit on F^2	0.941
Final R indices [I>2σ(I)]	R1 = 0.0531 wR2 = 0.1072
R indices (all data)	R1 = 0.1072 wR2 = 0.1257
Largest diff. peak and hole	1.347 and -0.794 $eÅ^{-3}$
Weighting scheme	calc $w=1/[\sigma^2(Fo^2)+(0.0591P)^2+0.0000P]$ where $P=(Fo^2+2Fc^2)/3$
Extinction coefficient	0.00016(2)
Extinction expression	$Fc^*=kFc[1+0.001xFc^2\lambda^3/\sin(2\theta)]^{-1/4}$

Table A: Crystal data and structure refinement for G1a.

Au(1)-S(10)	2.342(4)	C(4)-C(7)	1.55(2)
Au(1)-S(6)	2.343(3)	C(7)-C(8)	1.35(3)
Au(1)-Au(2)	2.9735(9)	C(7)-C(9)	1.50(3)
Au(1)-Au(5)	2.9840(10)	C(7)-C(10)	1.58(3)
Au(1)-Au(3)	3.0338(11)	C(14)-C(17)	1.53(2)
Au(1)-Au(6)	3.0462(11)	C(17)-C(20)	1.45(2)
Au(1)-Au(4)	3.1182(11)	C(17)-C(18)	1.48(2)
Au(2)-S(1)	2.294(4)	C(17)-C(19)	1.53(2)
Au(2)-S(5)	2.313(4)	C(24)-C(27)	1.50(2)
Au(3)-S(2)	2.296(4)	C(27)-C(29)	1.43(3)
Au(3)-S(1)	2.302(4)	C(27)-C(30)	1.45(3)
Au(4)-S(3)	2.301(4)	C(27)-C(28)	1.57(3)
Au(4)-S(2)	2.304(4)	C(34)-C(37)	1.51(2)
Au(5)-S(3)	2.294(4)	C(37)-C(38)	1.40(4)
Au(5)-S(4)	2.303(4)	C(37)-C(39)	1.42(3)
Au(6)-S(5)	2.343(4)	C(37)-C(40)	1.50(3)
Au(6)-S(4)	2.343(4)	C(44)-C(47)	1.55(2)
Au(6)-Au(10)	3.0452(10)	C(47)-C(48)	1.53(3)
Au(6)-Au(9)	3.0501(12)	C(47)-C(49)	1.56(3)
Au(6)-Au(7)	3.0996(12)	C(47)-C(50)	1.47(4)
Au(6)-Au(8)	3.1234(11)	C(57)-C(59)	1.47(2)
Au(7)-S(6)	2.299(4)	C(57)-C(58)	1.53(2)
Au(7)-S(7)	2.306(4)	C(57)-C(60)	1.57(3)
Au(8)-S(8)	2.299(4)	C(64)-C(67)	1.54(2)
Au(8)-S(7)	2.313(4)	C(67)-C(68)	1.42(3)
Au(9)-S(9)	2.289(4)	C(67)-C(69)	1.47(3)
Au(9)-S(8)	2.299(4)	C(67)-C(70)	1.59(3)
Au(10)-S(10)	2.294(4)	C(74)-C(77)	1.54(2)
Au(10)-S(9)	2.297(4)	C(77)-C(80)	1.45(3)
S(1)-C(1)	1.794(8)	C(77)-C(78)	1.45(3)
S(2)-C(11)	1.807(8)	C(77)-C(79)	1.52(3)
S(3)-C(21)	1.823(9)	C(84)-C(87)	1.57(2)
S(4)-C(31)	1.773(7)	C(87)-C(88)	1.43(3)
S(5)-C(41)	1.778(8)	C(87)-C(90)	1.46(3)
S(6)-C(51)	1.798(8)	C(87)-C(89)	1.50(4)
S(7)-C(61)	1.790(8)	C(94)-C(97)	1.60(2)
S(8)-C(71)	1.804(12)	C(97)-C(99)	1.53(3)
S(9)-C(81)	1.800(8)	C(97)-C(100)	1.54(3)
S(10)-C(91)	1.771(8)	C(97)-C(98)	1.56(3)
S(10)-Au(1)-S(6)	178.01(13)	C(21)-S(3)-Au(5)	105.3(4)
S(10)-Au(1)-Au(2)	99.07(10)	C(21)-S(3)-Au(4)	106.0(4)
S(6)-Au(1)-Au(2)	81.53(9)	Au(5)-S(3)-Au(4)	100.2(2)
S(10)-Au(1)-Au(5)	87.25(9)	C(31)-S(4)-Au(5)	105.5(3)
S(6)-Au(1)-Au(5)	93.30(8)	C(31)-S(4)-Au(6)	110.4(4)
Au(2)-Au(1)-Au(5)	146.35(3)	Au(5)-S(4)-Au(6)	103.36(14)
S(10)-Au(1)-Au(3)	95.73(9)	C(41)-S(5)-Au(2)	105.8(4)
S(6)-Au(1)-Au(3)	82.61(8)	C(41)-S(5)-Au(6)	103.3(4)
Au(2)-Au(1)-Au(3)	73.41(3)	Au(2)-S(5)-Au(6)	99.5(2)
Au(5)-Au(1)-Au(3)	139.20(3)	C(51)-S(6)-Au(7)	112.3(3)
S(10)-Au(1)-Au(6)	92.86(10)	C(51)-S(6)-Au(1)	103.2(3)
S(6)-Au(1)-Au(6)	89.12(9)	Au(7)-S(6)-Au(1)	107.26(14)
Au(2)-Au(1)-Au(6)	72.32(3)	C(61)-S(7)-Au(7)	104.6(4)
Au(5)-Au(1)-Au(6)	74.39(3)	C(61)-S(7)-Au(8)	101.9(4)
Au(3)-Au(1)-Au(6)	145.56(3)	Au(7)-S(7)-Au(8)	100.58(14)
S(10)-Au(1)-Au(4)	77.34(10)	C(71)-S(8)-Au(9)	105.4(7)
S(6)-Au(1)-Au(4)	101.04(9)	C(71)-S(8)-Au(8)	106.9(7)
Au(2)-Au(1)-Au(4)	143.12(3)	Au(9)-S(8)-Au(8)	102.0(2)

Au(5)-Au(1)-Au(4)	70.53(3)	C(81)-S(9)-Au(9)	108.1(4)
Au(6)-Au(1)-Au(4)	143.89(3)	C(81)-S(9)-Au(10)	106.4(4)
S(1)-Au(2)-S(5)	175.89(13)	Au(9)-S(9)-Au(10)	103.7(2)
S(1)-Au(2)-Au(1)	89.19(10)	C(91)-S(10)-Au(10)	106.7(4)
S(5)-Au(2)-Au(1)	92.10(9)	C(91)-S(10)-Au(1)	106.7(3)
S(2)-Au(3)-S(1)	177.46(14)	Au(10)-S(10)-Au(1)	101.17(14)
S(2)-Au(3)-Au(1)	94.60(9)	C(2)-C(1)-S(1)	122.7(7)
Au(3)-Au(1)-Au(4)	70.52(3)	C(6)-C(1)-S(1)	117.1(7)
S(1)-Au(3)-Au(1)	87.58(9)	C(5)-C(4)-C(7)	119.3(12)
S(3)-Au(4)-S(2)	175.19(14)	C(3)-C(4)-C(7)	120.7(12)
S(3)-Au(4)-Au(1)	92.58(10)	C(8)-C(7)-C(9)	110(2)
S(2)-Au(4)-Au(1)	92.23(10)	C(8)-C(7)-C(4)	114(2)
S(3)-Au(5)-S(4)	173.67(13)	C(9)-C(7)-C(4)	109(2)
S(3)-Au(5)-Au(1)	96.28(10)	C(8)-C(7)-C(10)	110(2)
S(4)-Au(5)-Au(1)	89.52(9)	C(9)-C(7)-C(10)	106(2)
S(5)-Au(6)-S(4)	175.46(13)	C(4)-C(7)-C(10)	108(2)
S(5)-Au(6)-Au(10)	80.42(9)	C(12)-C(11)-S(2)	121.6(6)
S(4)-Au(6)-Au(10)	101.83(9)	C(16)-C(11)-S(2)	118.3(6)
S(5)-Au(6)-Au(1)	89.70(10)	C(15)-C(14)-C(17)	121.3(10)
S(4)-Au(6)-Au(1)	87.29(9)	C(13)-C(14)-C(17)	118.7(10)
Au(10)-Au(6)-Au(1)	72.04(3)	C(20)-C(17)-C(18)	113(2)
S(5)-Au(6)-Au(9)	91.47(10)	C(20)-C(17)-C(14)	111.5(14)
S(4)-Au(6)-Au(9)	92.97(9)	C(18)-C(17)-C(14)	110.3(14)
Au(10)-Au(6)-Au(9)	72.56(3)	C(20)-C(17)-C(19)	107(2)
Au(1)-Au(6)-Au(9)	143.86(3)	C(18)-C(17)-C(19)	103(2)
S(5)-Au(6)-Au(7)	99.83(9)	C(14)-C(17)-C(19)	112.2(14)
S(4)-Au(6)-Au(7)	76.11(9)	C(22)-C(21)-S(3)	120.1(8)
Au(10)-Au(6)-Au(7)	146.94(3)	C(26)-C(21)-S(3)	119.7(8)
Au(1)-Au(6)-Au(7)	74.90(3)	C(23)-C(24)-C(27)	122(2)
Au(9)-Au(6)-Au(7)	140.05(3)	C(25)-C(24)-C(27)	119(2)
S(5)-Au(6)-Au(8)	99.90(9)	C(29)-C(27)-C(30)	120(3)
S(4)-Au(6)-Au(8)	80.70(9)	C(29)-C(27)-C(24)	108(2)
Au(10)-Au(6)-Au(8)	143.27(3)	C(30)-C(27)-C(24)	116(2)
Au(1)-Au(6)-Au(8)	144.32(3)	C(29)-C(27)-C(28)	105(3)
Au(9)-Au(6)-Au(8)	70.71(3)	C(30)-C(27)-C(28)	96(2)
Au(7)-Au(6)-Au(8)	69.64(3)	C(24)-C(27)-C(28)	110(2)
S(6)-Au(7)-S(7)	172.52(12)	C(32)-C(31)-S(4)	122.5(5)
S(6)-Au(7)-Au(6)	88.62(9)	C(36)-C(31)-S(4)	117.4(5)
S(7)-Au(7)-Au(6)	94.41(10)	C(35)-C(34)-C(37)	118.8(11)
S(8)-Au(8)-S(7)	172.6(2)	C(33)-C(34)-C(37)	121.2(11)
S(8)-Au(8)-Au(6)	91.83(11)	C(38)-C(37)-C(39)	108(3)
S(7)-Au(8)-Au(6)	93.66(10)	C(38)-C(37)-C(40)	104(3)
S(9)-Au(9)-S(8)	175.2(2)	C(39)-C(37)-C(40)	107(2)
S(9)-Au(9)-Au(6)	90.82(11)	C(38)-C(37)-C(34)	112(2)
S(8)-Au(9)-Au(6)	93.73(11)	C(39)-C(37)-C(34)	113(2)
S(10)-Au(10)-S(9)	175.35(14)	C(40)-C(37)-C(34)	114(2)
S(10)-Au(10)-Au(6)	93.85(9)	C(42)-C(41)-S(5)	117.8(6)
S(9)-Au(10)-Au(6)	90.78(10)	C(46)-C(41)-S(5)	122.2(6)
C(1)-S(1)-Au(2)	110.1(4)	C(45)-C(44)-C(47)	120.3(12)
C(1)-S(1)-Au(3)	107.3(4)	C(43)-C(44)-C(47)	119.6(12)
Au(2)-S(1)-Au(3)	102.74(14)	C(48)-C(47)-C(49)	103(2)
C(11)-S(2)-Au(3)	108.4(4)	C(48)-C(47)-C(50)	107(2)
C(11)-S(2)-Au(4)	102.9(3)	C(49)-C(47)-C(50)	117(3)
C(95)-C(94)-C(97)	117.3(13)	C(48)-C(47)-C(44)	111(2)
C(93)-C(94)-C(97)	122.6(14)	C(49)-C(47)-C(44)	107(2)
C(99)-C(97)-C(100)	112(2)	C(50)-C(47)-C(44)	112(2)
C(99)-C(97)-C(98)	111(2)	C(52)-C(51)-S(6)	124.1(5)
C(100)-C(97)-C(98)	110(2)	C(56)-C(51)-S(6)	115.9(5)
C(99)-C(97)-C(94)	109(2)	C(55)-C(54)-C(57)	120.4(8)

C(100)-C(97)-C(94)	106(2)	C(53)-C(54)-C(57)	119.6(8)
C(98)-C(97)-C(94)	109(2)	C(59)-C(57)-C(58)	105(2)
C(73)-C(74)-C(77)	117.8(13)	C(59)-C(57)-C(54)	112.6(14)
C(75)-C(74)-C(77)	121.9(13)	C(58)-C(57)-C(54)	112.4(13)
C(80)-C(77)-C(78)	114(3)	C(59)-C(57)-C(60)	108(2)
C(80)-C(77)-C(79)	105(2)	C(58)-C(57)-C(60)	109(2)
C(78)-C(77)-C(79)	105(2)	C(54)-C(57)-C(60)	109.5(13)
C(80)-C(77)-C(74)	110(2)	C(62)-C(61)-S(7)	117.0(6)
C(78)-C(77)-C(74)	112(2)	C(66)-C(61)-S(7)	122.8(6)
C(79)-C(77)-C(74)	112(2)	C(63)-C(64)-C(67)	122.4(10)
C(82)-C(81)-S(9)	117.8(7)	C(65)-C(64)-C(67)	117.5(10)
C(86)-C(81)-S(9)	121.5(7)	C(68)-C(67)-C(69)	111(2)
C(83)-C(84)-C(87)	118.3(12)	C(68)-C(67)-C(64)	113(2)
C(85)-C(84)-C(87)	121.7(12)	C(69)-C(67)-C(64)	115(2)
C(88)-C(87)-C(90)	110(3)	C(68)-C(67)-C(70)	99(2)
C(88)-C(87)-C(89)	105(3)	C(69)-C(67)-C(70)	107(2)
C(90)-C(87)-C(89)	116(3)	C(64)-C(67)-C(70)	110(2)
C(88)-C(87)-C(84)	114(2)	C(72)-C(71)-S(8)	118.7(11)
C(90)-C(87)-C(84)	111(2)	C(76)-C(71)-S(8)	121.2(11)
C(89)-C(87)-C(84)	102(2)	C(92)-C(91)-S(10)	124.0(7)
Au(3)-S(2)-Au(4)	101.10(14)	C(96)-C(91)-S(10)	116.0(7)

Table B: Bond lengths [Å] and angles [°] for **G1a**

X-RAY CRYSTALLOGRAPHIC DATA ON $[AuSC_6H_5\text{-}o\text{-}CMe_3]_{12}$. $2.0(C_6H_5OC_2H_5)$ G2a, (99BJB6/M.WISEMAN/R.T.)

A crystal of approximate dimensions 0.2 x 0.2 x 0.2 mm was used for data collection.

Crystal data: $C_{120}H_{156}Au_{12}S_{12}\ 2.0(C_6H_5OC_2H_5)$, M = 4591.09, Monoclinic , a = 18.108(2), b = 26.621(6), c = 30.256(4) Å , α = 90, β = 99.10(3), γ = 90°, U = 14401.3(41) Å^3, space group $P2_1/n$, Z = 4, D_c = 2.117 gcm^{-3}, μ(Mo-K_α) = 12.391 mm^{-1}, F(000) = 8592. Crystallographic measurements were made at 293(2)° K on a CAD4 automatic four-circle diffractometer in the range $2.05<\theta<24.97°$. Data (25275 reflections) were corrected for 32% decay in the X–ray beam, Lorentz and polarization and also for absorption.[1] (Max. and Min absorption corrections; 1.000, 0.370 respectively).

In the final least squares cycles all atoms were allowed to vibrate anisotropically. The thermal displacement parameters of each block of atoms within the pendant organic moieties were restrained with effective standard deviations to have the same Uij components. Phenyl rings were treated as rigid hexagons. Hydrogen atoms were included at calculated positions where relevant.

The solution of the structure (SHELX86)[2] and refinement (SHELX93)[3] converged to a conventional [i.e. based on 10238 F^2 data with $Fo>4\sigma(Fo)$] $R1$ = 0.0813 and $wR2$ = 0.1281. Goodness of fit = 0.875. The max. and min. residual densities were 1.815 and -1.768 eÅ^{-3} respectively. The asymmetric unit (shown in Fig C), along with the labelling scheme used was produced using ORTEX.[4] Crystal data and structure refinement, bond distances and angles are given in Tables C and D respectively.

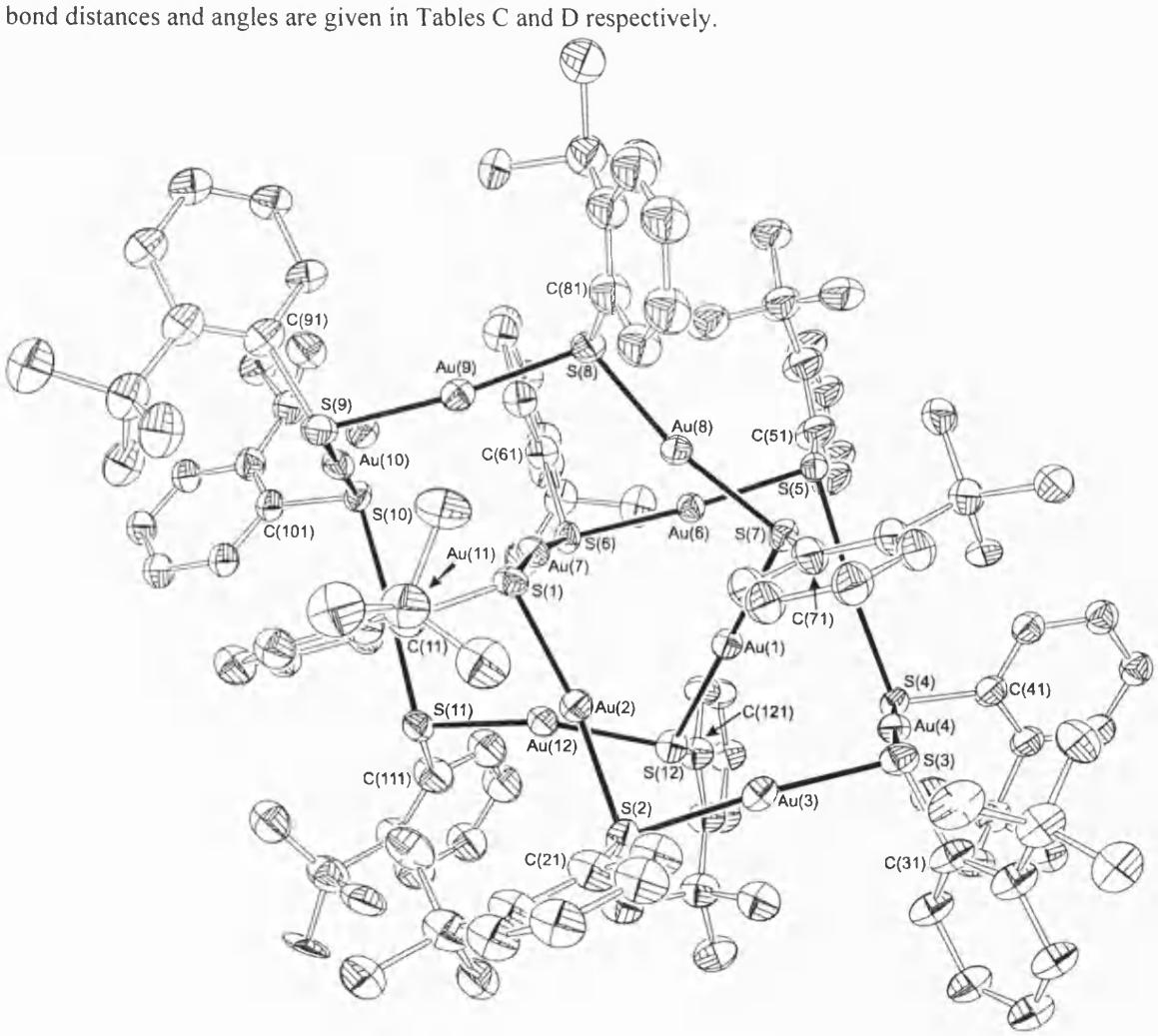

Figure C: Full Structure of G2a

Identification code	**G2a** (99bjb6/m.wiseman/r.t.)
Empirical formula	$C_{136}H_{176}Au_{12}O_2S_{12}$
Formula weight	4591.09
Temperature	293(2) K
Wavelength	0.71069 Å
Crystal system	Monoclinic
Space group	P21/n
Unit cell dimensions	a = 18.108(2)Å α = 90°
	b = 26.621(6)Å β = 99.10(3)°
	c = 30.256(4)Å γ = 90°
Volume	14401(4) $Å^3$
Z	4
Density (calculated)	2.117 Mg/m^3
Absorption coefficient	12.391 mm^{-1}
F(000)	8592
Crystal size	0.2 x 0.2 x 0.2 mm
Theta range for data collection	2.05 to 24.97 °.
Index ranges	-21<=h<=21; 0<=k<=31; 0<=l<=35
Reflections collected	25275
Independent reflections	25275 [R(int) = 0.0000]
Absorption correction	DIFABS
Max. and min. transmission	1.000 and 0.370
Refinement method	Full-matrix least-squares on F^2
Data / restraints / parameters	25275 / 774 / 1314
Goodness-of-fit on F^2	0.875
Final R indices [I>2σ(I)]	R1 = 0.0813 wR2 = 0.1281
R indices (all data)	R1 = 0.1991 wR2 = 0.1536
Largest diff. peak and hole	1.815 and -1.768 $eÅ^{-3}$
Weighting scheme	calc $w=1/[\sigma^2(Fo^2)+(0.0570P)^2+0.0000P]$ where $P=(Fo^2+2Fc^2)/3$

Table C: Crystal data and structure refinement for G2a

Au(1)-S(12)	2.300(5)	C(17)-C(20)	1.54(3)
Au(1)-S(7)	2.325(5)	C(26)-C(27)	1.52(3)
Au(1)-Au(6)	3.191(2)	C(27)-C(30)	1.56(3)
Au(1)-Au(4)	3.1993(14)	C(27)-C(28)	1.57(3)
Au(1)-Au(3)	3.256(2)	C(27)-C(29)	1.58(3)
Au(1)-Au(5)	3.277(2)	C(36)-C(37)	1.52(3)
Au(1)-Au(2)	3.3172(14)	C(37)-C(39)	1.49(3)
Au(2)-S(2)	2.301(6)	C(37)-C(38)	1.52(3)
Au(2)-S(1)	2.318(5)	C(37)-C(40)	1.54(3)
Au(2)-Au(12)	3.1649(14)	C(16)-C(17)	1.54(3)
Au(2)-Au(3)	3.299(2)	C(17)-C(18)	1.52(3)
Au(3)-S(3)	2.287(6)	C(17)-C(19)	1.53(3)
Au(3)-S(2)	2.315(6)	C(147)-C(148)	1.46(5)
Au(3)-Au(4)	3.376(2)	C(46)-C(47)	1.62(2)
Au(4)-S(3)	2.300(7)	C(47)-C(48)	1.52(3)
Au(4)-S(4)	2.312(7)	C(47)-C(49)	1.53(3)
Au(4)-Au(5)	3.282(2)	C(47)-C(50)	1.56(3)
Au(5)-S(5)	2.310(6)	C(56)-C(57)	1.56(3)
Au(5)-S(4)	2.310(5)	C(57)-C(58)	1.55(3)
Au(5)-Au(6)	3.2064(14)	C(57)-C(59)	1.57(4)
Au(6)-S(5)	2.307(5)	C(57)-C(60)	1.57(3)
Au(6)-S(6)	2.310(5)	C(66)-C(67)	1.57(3)
Au(6)-Au(8)	3.2058(14)	C(67)-C(69)	1.51(3)
Au(7)-S(6)	2.307(6)	C(67)-C(70)	1.53(3)
Au(7)-S(1)	2.321(6)	C(67)-C(68)	1.58(3)
Au(7)-Au(12)	3.2068(14)	C(76)-C(77)	1.60(3)

Au(7)-Au(8)	3.2282(14)	C(77)-C(80)	1.48(3)
Au(7)-Au(9)	3.3348(14)	C(77)-C(79)	1.52(3)
Au(8)-S(7)	2.297(5)	C(77)-C(78)	1.58(3)
Au(8)-S(8)	2.309(5)	C(86)-C(87)	1.52(3)
Au(9)-S(8)	2.308(6)	C(87)-C(89)	1.52(3)
Au(9)-S(9)	2.324(6)	C(87)-C(88)	1.55(3)
Au(9)-Au(10)	3.325(2)	C(87)-C(90)	1.58(3)
Au(10)-S(9)	2.298(7)	C(96)-C(97)	1.63(3)
Au(10)-S(10)	2.301(6)	C(97)-C(98)	1.48(3)
Au(10)-Au(11)	3.1878(14)	C(97)-C(99)	1.52(3)
Au(11)-S(11)	2.287(6)	C(97)-C(100)	1.57(3)
Au(11)-S(10)	2.289(6)	C(106)-C(107)	1.51(3)
Au(12)-S(11)	2.300(6)	C(107)-C(109)	1.53(3)
Au(12)-S(12)	2.316(6)	C(107)-C(108)	1.55(3)
S(1)-C(11)	1.790(11)	C(107)-C(110)	1.56(3)
S(2)-C(21)	1.779(13)	C(116)-C(117)	1.57(3)
S(3)-C(31)	1.786(11)	C(117)-C(120)	1.50(3)
S(4)-C(41)	1.789(10)	C(117)-C(118)	1.53(3)
S(5)-C(51)	1.80(2)	C(117)-C(119)	1.55(4)
S(6)-C(61)	1.819(12)	C(126)-C(127)	1.53(3)
S(7)-C(71)	1.788(13)	C(127)-C(128)	1.53(3)
S(8)-C(81)	1.784(13)	C(127)-C(130)	1.57(3)
S(9)-C(91)	1.813(11)	C(127)-C(129)	1.58(3)
S(10)-C(101)	1.795(11)	C(131)-O(1)	1.34(3)
S(11)-C(111)	1.783(13)	C(137)-O(1)	1.38(4)
S(12)-C(121)	1.808(12)	C(137)-C(138)	1.56(5)
O(2)-C(147)	1.40(5)	C(141)-O(2)	1.26(4)
S(12)-Au(1)-S(7)	178.1(2)	C(111)-S(11)-Au(11)	107.4(7)
S(12)-Au(1)-Au(6)	106.7(2)	C(111)-S(11)-Au(12)	99.1(6)
S(7)-Au(1)-Au(6)	74.1(2)	Au(11)-S(11)-Au(12)	105.4(2)
S(12)-Au(1)-Au(4)	88.14(14)	C(121)-S(12)-Au(1)	115.8(6)
S(7)-Au(1)-Au(4)	92.98(14)	C(121)-S(12)-Au(12)	102.0(5)
Au(6)-Au(1)-Au(4)	120.30(4)	Au(1)-S(12)-Au(12)	105.2(2)
S(12)-Au(1)-Au(3)	74.8(2)	Au(11)-S(10)-Au(10)	88.0(2)
S(7)-Au(1)-Au(3)	104.4(2)	C(12)-C(11)-S(1)	116.6(10)
Au(6)-Au(1)-Au(3)	176.18(4)	C(16)-C(11)-S(1)	123.3(10)
Au(4)-Au(1)-Au(3)	63.05(3)	C(15)-C(16)-C(17)	117(2)
S(12)-Au(1)-Au(5)	104.14(14)	C(11)-C(16)-C(17)	123(2)
S(7)-Au(1)-Au(5)	77.7(2)	C(18)-C(17)-C(19)	103(3)
Au(6)-Au(1)-Au(5)	59.41(4)	C(18)-C(17)-C(16)	114(2)
Au(4)-Au(1)-Au(5)	60.89(3)	C(19)-C(17)-C(16)	113(2)
Au(3)-Au(1)-Au(5)	123.93(4)	C(18)-C(17)-C(20)	109(2)
S(12)-Au(1)-Au(2)	73.21(14)	C(19)-C(17)-C(20)	106(2)
S(7)-Au(1)-Au(2)	104.9(2)	C(16)-C(17)-C(20)	113(2)
Au(6)-Au(1)-Au(2)	116.55(4)	C(22)-C(21)-S(2)	115.7(11)
Au(4)-Au(1)-Au(2)	123.08(4)	C(26)-C(21)-S(2)	124.3(11)
Au(3)-Au(1)-Au(2)	60.24(4)	C(23)-C(22)-C(21)	120.0
Au(5)-Au(1)-Au(2)	174.68(4)	C(25)-C(26)-C(27)	114(2)
S(2)-Au(2)-S(1)	166.4(2)	C(21)-C(26)-C(27)	126(2)
S(2)-Au(2)-Au(12)	92.6(2)	C(26)-C(27)-C(30)	115(2)
S(1)-Au(2)-Au(12)	96.8(2)	C(26)-C(27)-C(28)	114(2)
S(2)-Au(2)-Au(3)	44.56(14)	C(30)-C(27)-C(28)	107(2)
S(1)-Au(2)-Au(3)	141.55(14)	C(26)-C(27)-C(29)	111(2)
Au(12)-Au(2)-Au(3)	100.91(4)	C(30)-C(27)-C(29)	104(2)
S(2)-Au(2)-Au(1)	95.16(14)	C(28)-C(27)-C(29)	105(2)
S(1)-Au(2)-Au(1)	97.40(14)	C(32)-C(31)-C(36)	120.0
Au(12)-Au(2)-Au(1)	68.85(4)	C(32)-C(31)-S(3)	114.8(10)
Au(3)-Au(2)-Au(1)	58.96(3)	C(36)-C(31)-S(3)	125.2(10)

S(3)-Au(3)-S(2)	175.4(2)	C(35)-C(36)-C(37)	118(2)
S(3)-Au(3)-Au(1)	88.1(2)	C(31)-C(36)-C(37)	122(2)
S(2)-Au(3)-Au(1)	96.5(2)	C(39)-C(37)-C(38)	111(2)
S(3)-Au(3)-Au(2)	139.6(2)	C(39)-C(37)-C(36)	111(2)
S(2)-Au(3)-Au(2)	44.2(2)	C(38)-C(37)-C(36)	112(2)
Au(1)-Au(3)-Au(2)	60.79(3)	C(39)-C(37)-C(40)	105(2)
S(3)-Au(3)-Au(4)	42.8(2)	C(38)-C(37)-C(40)	106(2)
S(2)-Au(3)-Au(4)	140.4(2)	C(36)-C(37)-C(40)	112(2)
Au(1)-Au(3)-Au(4)	57.65(3)	C(42)-C(41)-S(4)	117.0(8)
Au(2)-Au(3)-Au(4)	118.25(4)	C(46)-C(41)-S(4)	123.0(8)
S(3)-Au(4)-S(4)	177.9(2)	C(45)-C(46)-C(47)	116.1(12)
S(3)-Au(4)-Au(1)	89.2(2)	C(41)-C(46)-C(47)	123.9(12)
S(4)-Au(4)-Au(1)	92.83(14)	C(48)-C(47)-C(49)	108(2)
S(3)-Au(4)-Au(5)	136.51(14)	C(48)-C(47)-C(50)	108(2)
S(4)-Au(4)-Au(5)	44.74(14)	C(49)-C(47)-C(50)	115(2)
Au(1)-Au(4)-Au(5)	60.73(3)	C(48)-C(47)-C(46)	110(2)
S(3)-Au(4)-Au(3)	42.5(2)	C(49)-C(47)-C(46)	110(2)
S(4)-Au(4)-Au(3)	139.33(14)	C(50)-C(47)-C(46)	107(2)
Au(1)-Au(4)-Au(3)	59.30(3)	C(52)-C(51)-S(5)	116.6(12)
Au(5)-Au(4)-Au(3)	120.02(4)	C(56)-C(51)-S(5)	123.3(12)
S(5)-Au(5)-S(4)	176.3(2)	C(55)-C(56)-C(57)	115(2)
S(5)-Au(5)-Au(6)	45.97(13)	C(51)-C(56)-C(57)	125(2)
S(4)-Au(5)-Au(6)	137.55(14)	C(58)-C(57)-C(56)	110(2)
S(5)-Au(5)-Au(1)	92.48(14)	C(58)-C(57)-C(59)	108(3)
Au(6)-Au(5)-Au(1)	58.96(3)	C(56)-C(57)-C(59)	113(2)
S(5)-Au(5)-Au(4)	136.7(2)	C(58)-C(57)-C(60)	107(2)
S(4)-Au(5)-Au(1)	90.9(2)	C(56)-C(57)-C(60)	112(2)
S(4)-Au(5)-Au(4)	44.8(2)	C(59)-C(57)-C(60)	108(2)
Au(6)-Au(5)-Au(4)	117.33(4)	C(62)-C(61)-S(6)	115.4(10)
Au(1)-Au(5)-Au(4)	58.38(4)	C(66)-C(61)-S(6)	124.5(10)
S(5)-Au(6)-S(6)	168.9(2)	C(65)-C(66)-C(67)	117.1(14)
S(5)-Au(6)-Au(1)	94.8(2)	C(61)-C(66)-C(67)	122.8(14)
S(6)-Au(6)-Au(1)	95.4(2)	C(69)-C(67)-C(70)	110(2)
S(5)-Au(6)-Au(8)	90.2(2)	C(69)-C(67)-C(68)	108(2)
S(6)-Au(6)-Au(8)	97.4(2)	C(70)-C(67)-C(68)	104(2)
Au(1)-Au(6)-Au(8)	69.46(3)	C(69)-C(67)-C(66)	116(2)
S(5)-Au(6)-Au(5)	46.06(14)	C(70)-C(67)-C(66)	108(2)
S(6)-Au(6)-Au(5)	137.71(14)	C(68)-C(67)-C(66)	112(2)
Au(1)-Au(6)-Au(5)	61.63(3)	C(72)-C(71)-S(7)	118.2(10)
Au(8)-Au(6)-Au(5)	105.37(4)	C(76)-C(71)-S(7)	121.8(10)
S(6)-Au(7)-S(1)	171.0(2)	C(75)-C(76)-C(77)	116.5(14)
S(6)-Au(7)-Au(12)	79.01(14)	C(71)-C(76)-C(77)	123.5(14)
S(1)-Au(7)-Au(12)	95.62(13)	C(80)-C(77)-C(79)	106(2)
S(6)-Au(7)-Au(8)	96.88(13)	C(80)-C(77)-C(78)	106(2)
S(1)-Au(7)-Au(8)	80.55(13)	C(79)-C(77)-C(78)	111(2)
Au(12)-Au(7)-Au(8)	127.00(4)	C(80)-C(77)-C(76)	112(2)
S(6)-Au(7)-Au(9)	116.34(14)	C(79)-C(77)-C(76)	110(2)
S(1)-Au(7)-Au(9)	70.93(13)	C(78)-C(77)-C(76)	111(2)
Au(12)-Au(7)-Au(9)	157.91(4)	C(82)-C(81)-S(8)	114.3(11)
Au(8)-Au(7)-Au(9)	69.41(3)	C(86)-C(81)-S(8)	125.7(11)
S(7)-Au(8)-S(8)	168.4(2)	C(85)-C(86)-C(87)	118(2)
S(7)-Au(8)-Au(6)	74.1(2)	C(81)-C(86)-C(87)	122(2)
S(8)-Au(8)-Au(6)	112.6(2)	C(89)-C(87)-C(86)	118(2)
S(7)-Au(8)-Au(7)	102.61(14)	C(89)-C(87)-C(88)	113(3)
S(8)-Au(8)-Au(7)	88.93(14)	C(86)-C(87)-C(88)	108(2)
Au(6)-Au(8)-Au(7)	64.00(3)	C(89)-C(87)-C(90)	108(2)
S(8)-Au(9)-S(9)	172.6(2)	C(86)-C(87)-C(90)	108(2)
S(8)-Au(9)-Au(10)	134.4(2)	C(88)-C(87)-C(90)	100(2)
S(9)-Au(9)-Au(10)	43.7(2)	C(92)-C(91)-S(9)	117.0(10)

S(8)-Au(9)-Au(7)	86.39(13)	C(96)-C(91)-S(9)	122.8(10)
S(9)-Au(9)-Au(7)	98.18(13)	C(95)-C(96)-C(97)	118.9(14)
Au(10)-Au(9)-Au(7)	69.69(3)	C(91)-C(96)-C(97)	121.1(14)
S(9)-Au(10)-S(10)	178.2(2)	C(98)-C(97)-C(99)	114(3)
S(9)-Au(10)-Au(11)	133.0(2)	C(98)-C(97)-C(100)	110(2)
S(10)-Au(10)-Au(11)	45.9(2)	C(99)-C(97)-C(100)	103(2)
S(9)-Au(10)-Au(9)	44.3(2)	C(98)-C(97)-C(96)	111(2)
S(10)-Au(10)-Au(9)	134.22(14)	C(99)-C(97)-C(96)	111(2)
Au(11)-Au(10)-Au(9)	117.11(4)	C(100)-C(97)-C(96)	108(2)
S(11)-Au(11)-S(10)	176.9(2)	C(102)-C(101)-S(10)	116.7(10)
S(11)-Au(11)-Au(10)	131.9(2)	C(106)-C(101)-S(10)	123.3(10)
S(10)-Au(11)-Au(10)	46.2(2)	C(105)-C(106)-C(107)	113(2)
S(11)-Au(12)-S(12)	162.8(2)	C(101)-C(106)-C(107)	127(2)
S(11)-Au(12)-Au(2)	116.3(2)	C(106)-C(107)-C(109)	111(2)
S(12)-Au(12)-Au(2)	76.2(2)	C(106)-C(107)-C(108)	109(2)
S(11)-Au(12)-Au(7)	94.84(14)	C(109)-C(107)-C(108)	108(2)
S(12)-Au(12)-Au(7)	101.52(13)	C(106)-C(107)-C(110)	118(2)
Au(2)-Au(12)-Au(7)	64.32(3)	C(109)-C(107)-C(110)	106(2)
C(11)-S(1)-Au(2)	98.7(5)	C(108)-C(107)-C(110)	105(2)
C(11)-S(1)-Au(7)	110.6(6)	C(112)-C(111)-S(11)	115.3(10)
Au(2)-S(1)-Au(7)	93.9(2)	C(116)-C(111)-S(11)	124.5(10)
C(21)-S(2)-Au(2)	101.9(6)	C(115)-C(116)-C(117)	116(2)
C(21)-S(2)-Au(3)	107.2(7)	C(111)-C(116)-C(117)	125(2)
Au(2)-S(2)-Au(3)	91.2(2)	C(120)-C(117)-C(118)	115(2)
C(31)-S(3)-Au(3)	103.3(5)	C(120)-C(117)-C(119)	107(3)
C(31)-S(3)-Au(4)	106.9(6)	C(118)-C(117)-C(119)	104(3)
Au(3)-S(3)-Au(4)	94.8(2)	C(120)-C(117)-C(116)	112(2)
C(41)-S(4)-Au(5)	105.0(5)	C(118)-C(117)-C(116)	113(2)
C(41)-S(4)-Au(4)	105.7(6)	C(119)-C(117)-C(116)	105(2)
Au(5)-S(4)-Au(4)	90.5(2)	C(122)-C(121)-S(12)	116.8(9)
C(51)-S(5)-Au(6)	102.7(6)	C(126)-C(121)-S(12)	123.2(10)
C(51)-S(5)-Au(5)	107.4(7)	C(125)-C(126)-C(127)	116.8(13)
Au(6)-S(5)-Au(5)	88.0(2)	C(121)-C(126)-C(127)	123.2(13)
C(61)-S(6)-Au(7)	113.5(6)	C(126)-C(127)-C(128)	113(2)
C(61)-S(6)-Au(6)	96.6(5)	C(126)-C(127)-C(130)	112(2)
Au(7)-S(6)-Au(6)	95.2(2)	C(128)-C(127)-C(130)	109(2)
C(71)-S(7)-Au(8)	104.2(5)	C(126)-C(127)-C(129)	113(2)
C(71)-S(7)-Au(1)	111.0(6)	C(128)-C(127)-C(129)	106(2)
Au(8)-S(7)-Au(1)	104.1(2)	C(130)-C(127)-C(129)	105(2)
C(81)-S(8)-Au(9)	107.4(6)	O(1)-C(131)-C(132)	113(3)
C(81)-S(8)-Au(8)	103.9(6)	O(1)-C(131)-C(136)	127(3)
Au(9)-S(8)-Au(8)	108.1(2)	O(1)-C(137)-C(138)	107(3)
C(91)-S(9)-Au(10)	105.0(6)	C(131)-O(1)-C(137)	118(3)
C(91)-S(9)-Au(9)	104.5(6)	O(2)-C(141)-C(142)	113(3)
Au(10)-S(9)-Au(9)	92.0(2)	O(2)-C(141)-C(146)	127(3)
C(101)-S(10)-Au(11)	106.9(6)	C(141)-O(2)-C(147)	121(4)
C(101)-S(10)-Au(10)	108.6(5)	O(2)-C(147)-C(148)	113(5)

Table D: Bond lengths [Å] and angles [°] for G2a

X-RAY CRYSTALLOGRAPHIC DATA ON [Au(SC$_6$H$_4$-p-CMe$_3$)(PPh$_3$)], P1, (99BJB4 / M.WISEMAN / R.T.)

A crystal of approximate dimensions 0.2 x 0.2 x 0.2 mm was used for data collection.

Crystal data: $C_{28}H_{28}$ Au P S, M = 624.50, Triclinic , a = 8.353(2), b = 11.969(3), c = 13.582(4) Å , α = 109.82(2), β = 103.50(2), γ = 93.43(2)°, U = 1227.7(6) Å^3, space group P-1(No.2), Z = 2, D_c = 1.689 gcm^{-3}, μ(Mo-K_α) = 6.155 mm^{-1}, F(000) = 612. Crystallographic measurements were made at 293(2)° K on a CAD4 automatic four-circle diffractometer in the range 2.54<θ<24.99°. Data (4840 reflections) were corrected for Lorentz and polarisation but not for absorption.

In the final least squares cycles all atoms were allowed to vibrate anisotropically. Hydrogen atoms were included at calculated positions where relevant.

The solution of the structure (SHELX86)[2] and refinement (SHELX93)[3] converged to a conventional [i.e. based on 3926 F^2 data with $Fo>4\sigma(Fo)$] $R1$ = 0.0343 and $wR2$ = 0.0842. Goodness of fit = 1.090. The max. and min. residual densities were 1.756 and -2.168 eÅ^{-3} respectively. The asymmetric unit (shown in Fig D), along with the labelling scheme used was produced using ORTEX[4]. Crystal data and structure refinement, bond distances and angles are given in Tables E, and F. Tables of anisotropic temperature factors are available as supplementary data.

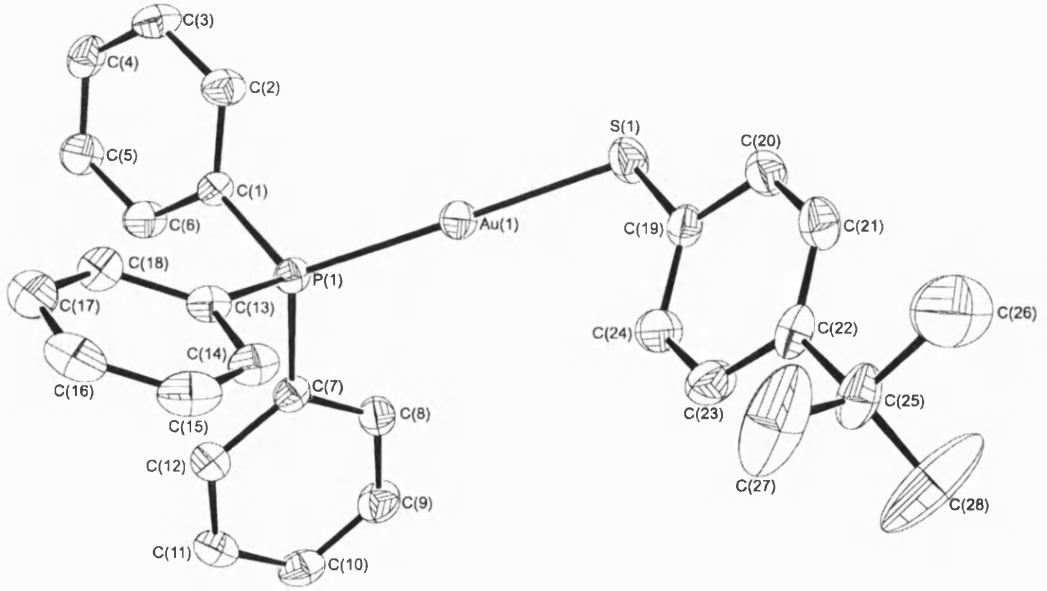

Figure D: Molecular structure of P1.

Identification code	**P1** (99bjb4 / M.Wiseman / R.T.)
Empirical formula	$C_{28}H_{28}$ Au P S
Formula weight	624.50
Temperature	293(2) K
Wavelength	0.71069 Å
Crystal system	Triclinic
Space group	P-1(No.2)
Unit cell dimensions	a = 8.353(2)Å α = 109.82(2)°
	b = 11.969(3)Å β = 103.50(2)°
	c = 13.582(4)Å γ = 93.43(2)°
Volume	1227.7(6) Å^3
Z	2
Density (calculated)	1.689 Mg/m^3
Absorption coefficient	6.155 mm^{-1}

F(000)	612
Crystal size	0.2 x 0.2 x 0.2 mm
Theta range for data collection	2.54 to 24.99 °.
Index ranges	0<=h<=9; -14<=k<=14; -16<=l<=15
Reflections collected	4840
Independent reflections	4306 [R(int) = 0.0128]
Refinement method	Full-matrix least-squares on F^2
Data / restraints / parameters	4301 / 0 / 284
Goodness-of-fit on F^2	1.090
Final R indices [I>2σ(I)]	R1 = 0.0343 wR2 = 0.0842
R indices (all data)	R1 = 0.0384 wR2 = 0.0873
Largest diff. peak and hole	1.756 and -2.168 eÅ^{-3}
Weighting scheme	calc $w=1/[\sigma^2(Fo^2)+(0.0645P)^2+0.0000P]$ where $P=(Fo^2+2Fc^2)/3$
Extinction coefficient	0.0001(5)
Extinction expression	$Fc^*=kFc[1+0.001xFc^2\lambda^3/\sin(2\theta)]^{-1/4}$

Table E: Crystal data and structure refinement for P1

Au(1)-P(1)	2.2575(13)	C(11)-C(12)	1.380(7)
Au(1)-S(1)	2.287(2)	C(13)-C(14)	1.385(7)
P(1)-C(1)	1.809(5)	C(13)-C(18)	1.388(7)
P(1)-C(13)	1.820(5)	C(14)-C(15)	1.372(9)
P(1)-C(7)	1.820(5)	C(15)-C(16)	1.389(10)
S(1)-C(19)	1.764(6)	C(16)-C(17)	1.376(9)
C(1)-C(2)	1.382(7)	C(17)-C(18)	1.374(8)
C(1)-C(6)	1.388(7)	C(19)-C(24)	1.389(8)
C(2)-C(3)	1.390(8)	C(19)-C(20)	1.389(8)
C(3)-C(4)	1.371(8)	C(20)-C(21)	1.387(8)
C(4)-C(5)	1.370(8)	C(21)-C(22)	1.376(9)
C(5)-C(6)	1.380(8)	C(22)-C(23)	1.387(9)
C(7)-C(12)	1.386(7)	C(22)-C(25)	1.541(8)
C(7)-C(8)	1.393(7)	C(23)-C(24)	1.374(8)
C(8)-C(9)	1.380(8)	C(25)-C(28)	1.422(11)
C(9)-C(10)	1.365(8)	C(25)-C(27)	1.445(11)
C(10)-C(11)	1.385(8)	C(25)-C(26)	1.606(12)
P(1)-Au(1)-S(1)	177.79(4)	C(9)-C(10)-C(11)	119.1(5)
C(1)-P(1)-C(13)	104.4(2)	C(12)-C(11)-C(10)	120.5(5)
C(1)-P(1)-C(7)	107.3(2)	C(11)-C(12)-C(7)	120.5(5)
C(13)-P(1)-C(7)	103.3(2)	C(14)-C(13)-C(18)	119.1(5)
C(1)-P(1)-Au(1)	114.6(2)	C(14)-C(13)-P(1)	118.4(4)
C(13)-P(1)-Au(1)	113.4(2)	C(18)-C(13)-P(1)	122.5(4)
C(7)-P(1)-Au(1)	112.9(2)	C(15)-C(14)-C(13)	120.5(6)
C(19)-S(1)-Au(1)	106.2(2)	C(14)-C(15)-C(16)	120.0(6)
C(2)-C(1)-C(6)	119.0(4)	C(17)-C(16)-C(15)	119.7(6)
C(2)-C(1)-P(1)	118.0(4)	C(18)-C(17)-C(16)	120.3(6)
C(6)-C(1)-P(1)	122.8(4)	C(17)-C(18)-C(13)	120.3(5)
C(1)-C(2)-C(3)	119.8(5)	C(24)-C(19)-C(20)	117.1(5)
C(4)-C(3)-C(2)	120.3(5)	C(24)-C(19)-S(1)	124.7(4)
C(3)-C(4)-C(5)	120.2(5)	C(20)-C(19)-S(1)	118.2(4)
C(4)-C(5)-C(6)	120.0(5)	C(21)-C(20)-C(19)	120.8(5)
C(1)-C(6)-C(5)	120.6(5)	C(22)-C(21)-C(20)	122.6(5)
C(12)-C(7)-C(8)	118.8(5)	C(21)-C(22)-C(23)	115.8(5)
C(12)-C(7)-P(1)	122.4(4)	C(21)-C(22)-C(25)	123.1(6)
C(8)-C(7)-P(1)	118.7(4)	C(23)-C(22)-C(25)	121.1(6)
C(9)-C(8)-C(7)	119.9(5)	C(24)-C(23)-C(22)	122.9(6)
C(10)-C(9)-C(8)	121.3(5)	C(23)-C(24)-C(19)	120.9(6)
C(28)-C(25)-C(27)	121.4(10)	C(28)-C(25)-C(26)	105.3(9)

C(28)-C(25)-C(22)	110.2(6)	C(27)-C(25)-C(26)	98.0(9)
C(27)-C(25)-C(22)	110.4(6)	C(22)-C(25)-C(26)	110.4(7)

Table F:Bond lengths [Å] and angles [°] for P1

X-RAY CRYSTALLOGRAPHIC DATA ON [Au(SC$_6$H$_4$-o-CF$_3$)(PPh$_3$)], P4, (k00bjb3)

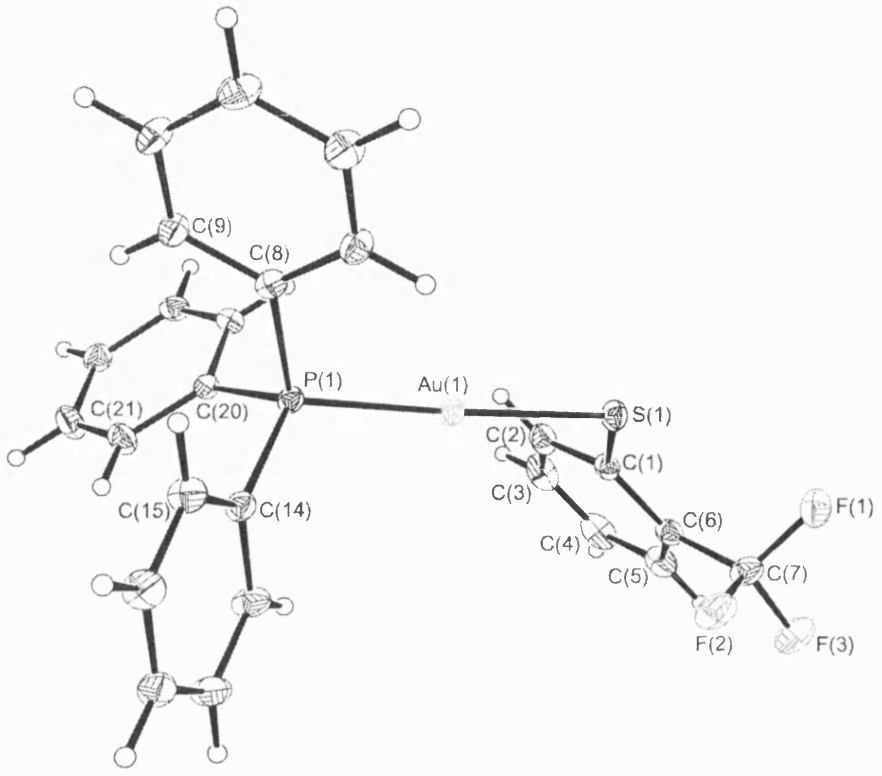

Figure E: Molecular structure of P4

Identification code	**P4** (k00bjb3)
Empirical formula	$C_{25}H_{19}AuF_3PS$
Formula weight	636.40
Temperature	170(2) K
Wavelength	0.71070 Å
Crystal system	Triclinic
Space group	P-1
Unit cell dimensions	a = 9.7590(1)Å α = 103.3560(9)°
	b = 9.9000(1)Å β = 109.7900(9)°
	c = 12.9250(2)Å δ = 91.595(1)°
Volume	1135.51(2) Å^3
Z	2
Density (calculated)	1.861 Mg/m^3
Absorption coefficient	6.675 mm^{-1}
F(000)	612
Crystal size	0.20 x 0.10 x 0.10 mm
Theta range for data collection	3.57 to 27.47°.
Index ranges	-12<=h<=12; -12<=k<=12; -16<=l<=16
Reflections collected	27460
Independent reflections	5192 [R(int) = 0.0723]
Reflections observed (>2σ)	4983
Absorption correction	Semi-empirical from equivalents

Max. and min. transmission	1.314, 0.813
Refinement method	Full-matrix least-squares on F^2
Goodness-of-fit on F^2	0.876
Final R indices [I>2σ(I)]	$R_1 = 0.0247$ $wR_2 = 0.0660$
R indices (all data)	$R_1 = 0.0261$ $wR_2 = 0.0674$
Largest diff. peak and hole	1.266 and -1.242 e.Å^{-3}

Table G: Crystal data and structure refinement for P4

Au(1)-P(1)	2.2607(8)	C(8)-C(13)	1.393(4)
Au(1)-S(1)	2.3006(8)	C(9)-C(10)	1.384(5)
S(1)-C(1)	1.776(3)	C(10)-C(11)	1.381(5)
P(1)-C(20)	1.814(3)	C(11)-C(12)	1.387(5)
P(1)-C(14)	1.819(3)	C(12)-C(13)	1.382(5)
P(1)-C(8)	1.820(3)	C(14)-C(15)	1.390(4)
F(1)-C(7)	1.346(4)	C(14)-C(19)	1.398(4)
F(2)-C(7)	1.345(4)	C(15)-C(16)	1.395(5)
F(3)-C(7)	1.342(4)	C(16)-C(17)	1.376(5)
C(1)-C(2)	1.394(4)	C(17)-C(18)	1.383(5)
C(1)-C(6)	1.416(4)	C(18)-C(19)	1.390(5)
C(2)-C(3)	1.391(6)	C(20)-C(21)	1.388(4)
C(3)-C(4)	1.377(7)	C(20)-C(25)	1.394(4)
C(4)-C(5)	1.379(6)	C(21)-C(22)	1.394(5)
C(5)-C(6)	1.387(5)	C(22)-C(23)	1.387(5)
C(6)-C(7)	1.498(5)	C(23)-C(24)	1.380(5)
C(8)-C(9)	1.392(4)	C(24)-C(25)	1.390(4)
P(1)-Au(1)-S(1)	173.18(3)	C(9)-C(8)-C(13)	119.6(3)
C(1)-S(1)-Au(1)	105.5(1)	C(9)-C(8)-P(1)	121.8(2)
C(20)-P(1)-C(14)	106.7(1)	C(13)-C(8)-P(1)	118.6(2)
C(20)-P(1)-C(8)	115.9(1)	C(10)-C(9)-C(8)	119.8(3)
C(14)-P(1)-C(8)	105.1(1)	C(11)-C(10)-C(9)	120.6(3)
C(20)-P(1)-Au(1)	114.0(1)	C(10)-C(11)-C(12)	119.7(3)
C(14)-P(1)-Au(1)	115.1(1)	C(13)-C(12)-C(11)	120.2(3)
C(8)-P(1)-Au(1)	110.2(1)	C(12)-C(13)-C(8)	120.1(3)
C(2)-C(1)-C(6)	117.7(3)	C(15)-C(14)-C(19)	119.5(3)
C(2)-C(1)-S(1)	120.5(3)	C(15)-C(14)-P(1)	121.6(2)
C(6)-C(1)-S(1)	121.8(2)	C(19)-C(14)-P(1)	118.9(2)
C(3)-C(2)-C(1)	120.9(4)	C(14)-C(15)-C(16)	119.8(3)
C(4)-C(3)-C(2)	120.8(4)	C(17)-C(16)-C(15)	120.2(3)
C(3)-C(4)-C(5)	119.2(3)	C(16)-C(17)-C(18)	120.5(3)
C(4)-C(5)-C(6)	121.1(4)	C(17)-C(18)-C(19)	119.7(3)
C(5)-C(6)-C(1)	120.3(3)	C(18)-C(19)-C(14)	120.2(3)
C(5)-C(6)-C(7)	118.4(3)	C(21)-C(20)-C(25)	119.3(3)
C(1)-C(6)-C(7)	121.3(3)	C(21)-C(20)-P(1)	123.5(2)
F(3)-C(7)-F(2)	105.7(3)	C(25)-C(20)-P(1)	117.2(2)
F(3)-C(7)-F(1)	105.6(3)	C(20)-C(21)-C(22)	119.8(3)
F(2)-C(7)-F(1)	106.3(3)	C(23)-C(22)-C(21)	120.6(3)
F(3)-C(7)-C(6)	112.4(3)	C(24)-C(23)-C(22)	119.8(3)
F(2)-C(7)-C(6)	113.6(3)	C(23)-C(24)-C(25)	119.9(3)
F(1)-C(7)-C(6)	112.6(3)	C(24)-C(25)-C(20)	120.6(3)

Table H: Bond lengths [Å] and angles [°] for P4

REFERENCES

[1] N. Walker, D. Stuart, *Acta Cryst.*, **A39**, 158 (1983)

[2] G.M. Sheldrick, *Acta Cryst.*, **A46**, 467 (1990)

[3] G.M. Sheldrick, SHELXL, a computer program for crystal structure refinement, University of Göttingen (1993)

[4] P. McArdle, *J.Appl.Cryst.*, **28**, 65 (1995)

APPENDIX 3: PUBLICATIONS AND PRESENTATIONS

Summary

This Appendix contains papers that have been published or submitted for publication during the course of this Ph.D. Also included is the Editors' Choice section of Science Magazine that highlighted our studies. A note of presentations made during the same period is also included.

Publications

- **Homoleptic Gold Thiolate Catenanes:**

  M.R. Wiseman, P.A. Marsh, P.T. Bishop, B.J. Brisdon, M.F. Mahon, *J. Am. Chem. Soc.*, **122**, 12598 (2000)

- **Fine Gold Rings:**

  G. Chin (editor), **Editors' Choice**, *Science Magazine*, **290**, 2213 (2000)

Publication submitted:

- **Complexes of 18-crown-6 Derivatives with Silver(I) Nitrate and Triflate**

  M.R Wiseman, B.J Brisdon, M.F. Mahon and P. Bishop, *J. Chem. Soc., Dalton Trans.*.

  Abstract:
  Reaction between $AgNO_3$ and $AgOSO_2CF_3$ and 18-crown-6, benzo-18-crown-6 and dibenzo-18-crown-6 in tetrahydrofuran affords 1:1 complexes. X-ray structure determinations on $[Ag(18\text{-crown-}6)(OSO_2CF_3)]$, **1**, $[Ag(\text{benzo-}18\text{-crown-}6)(OSO_2CF_3)]$, **3**, and $[Ag(\text{dibenzo-}18\text{-crown-}6)(H_2O)][OSO_2CF_3].0.5CH_2Cl_2$, **7**, revealed that silver is co-ordinated to all six oxygen atoms of the crown-ethers with Ag-O separations in the range 2.566(2) – 2.991(3) Å, together with a monodentate triflate or water ligand approximately orthoginal to the plane of the crown. In both **3** and **7** a peripheral arene ring of the ligand causes dimerisation of the metal centres through two asymmetric Ag-C bonds of between 2.437(2) and 2.822(2) Å.

Presentations given:

- **Gold Rings: Homoleptic Gold Thiolate Catenanes,**
  M.R. Wiseman, B.J. Brisdon, M.F. Mahon, P.T. Bishop, P.A. Marsh, Comprehensive Inorganic Chemistry II, Texas A & M University, USA, March 12-15, 2000

- **Silver Crowns and Gold Rings,**
  M.R. Wiseman, Royal Society of Chemistry, Dalton Division South West Regional Meeting, Cardiff University, April 13, 2000

- **Crown-Ether Complexes of Silver(I) Triflate,**
  M.R. Wiseman, B.J. Brisdon, M.F. Mahon, Royal Society of Chemistry, Dalton Division South West Regional Meeting, University of Bristol, April 19, 2001

Homoleptic Gold Thiolate Catenanes

Matthew R. Wiseman,† Patsy A. Marsh,‡ Peter T. Bishop,‡ Brian J. Brisdon,*,† and Mary F. Mahon†

Department of Chemistry, University of Bath Bath BA2 7AY, UK
Johnson Matthey Technology Centre Sonning Common, Reading RG4 9NH, UK

Received March 30, 2000

One of the most interesting features in the chemistry of gold is the subtle effects of weak Au···Au interactions on both the solid-state structural diversity and physical characteristics of Au(I) complexes.[1] Closed-shell attractions in these compounds are typically in the range 7−11 kcal/mol for each Au···Au bond,[2] which is of the same order of magnitude as the strength of a typical hydrogen bond. As a result both the type and extent of aggregation in many gold compounds are determined by the subtle interplay between various types of weak intermolecular interactions.[3] We recently showed[3b] that in the thiolate derivatives [Au(PPh$_3$)(SCR$_2$COOH)], association through H-bonding only (R = Me), and secondary Au···S interactions plus H-bonding (R = H), is preferred over dimerization through Au···Au attractions as found in [Au(PPh$_3$)(SCH$_3$)][4] and other phosphine-containing thiolate analogues.[5] In a search for new examples of gold compounds in which reinforcement of more than one type of weak interaction can occur, we have expanded our structural studies to include homoleptic gold thiolates. This class of molecules was chosen since the crystal structures of the three homoleptic gold thiolates which have been determined to date[6−8] all exhibit ring formation involving Au−S interactions only,[9] whereas alkanethiolate anions are capable of binding two or three [Au(PR$_3$)]$^+$ ions to afford species which contain Au···Au interactions.[4]

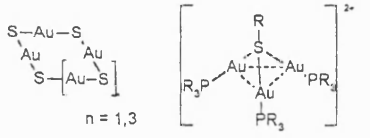

We now report the first two examples in gold chemistry where Au−S interactions, complemented and reinforced by multi Au···Au interactions, produce novel examples of inorganic [2]-catenanes. The only previous known examples[10] of gold catenanes are provided by its acetylide derivatives.

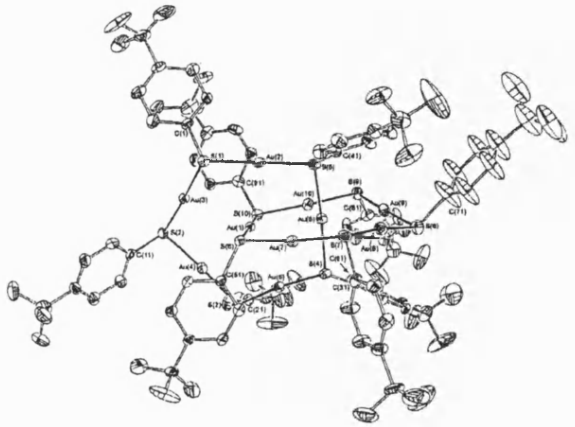

Figure 1. Thermal elipsoid plot (20% probability for clarity) of **1.** Ranges of bond lengths and angles are: Au−S, 2.289(4)−2.343(3); S−C, 1.771(8)−1.823(9) Å; Au−S−Au, 99.5(2)−107.26(14); S−Au−S, 172.52(12)−178.01(13)°.

The complexes [{Au(SC$_6$H$_4$-*p*-CMe$_3$)}$_{10}$], **1**, and [{Au(SC$_6$H$_4$-*o*-CMe$_3$)}$_{12}$], **2**, were prepared in over 90% yields by the reaction of the appropriate *tert*-butylthiophenol dissolved in xylene with an aqueous solution of [AuCl(C$_2$H$_5$SC$_2$H$_4$OH)].[11] Recrystallization of **1** from ethoxybenzene and **2** from xylene/acetonitrile yielded crystals suitable for structure determinations.[12,13] Compound **1** has been synthesized previously by a slightly different procedure,[14] but its structure was not determined. The structures of **1** and the Au$_{10}$S$_{10}$ and Au$_{12}$S$_{12}$ cores of **1** and **2** are illustrated in Figures 1−3, respectively.

The core of **1** consists of two interpenetrating pentagons defined by five S atoms and five Au atoms arranged in an alternating pattern about the periphery, with a sixth Au atom at each pentagon center. The maximum rms deviations of the central Au atoms from the least-squares planes containing gold atoms around the periphery of each pentagon are 0.068 and 0.180 Å, respectively, and the interplanar angle is 79°. The total of nine close Au···Au contacts (Table 1) which involve Au(1) and Au(6) atoms average 3.05 Å, with much longer Au···Au separations (average = 3.59 Å) occurring around the periphery of each pentagon. All four Au(1)/Au(6)−S bond lengths are 2.343(3) Å, while the remaining 16 Au−S separations lie within the narrow range 2.289(4)−2.313(4) Å. It appears that in **1** the Au−S bond lengths involving the central atoms are affected by multiple Au···Au interactions. The structure of this unique core can be readily rationalized by

* Author for correspondence: Telephone: 01225 826517. Fax: 01225 826231. E-mail: B. J.Brisdon@bath.ac.uk.
† University of Bath.
‡ Johnson Matthey Technology Centre.

(1) For recent reviews see: (a) Schmidbaur, H. *Chem. Soc. Rev.* **1995**, 391. (b) Mingos, D. M. P. *J. Chem. Soc., Dalton Trans.* **1996**, 561. (c) Schmidbaur, H., Ed. *Gold. Progress in Chemistry, Biochemistry and Technology*; Wiley: New York, 1999.

(2) (a) Schmidbaur, H.; Graf, W.; Müller, G. *Angew. Chem., Int. Ed. Engl.* **1988**, *27*, 417. (b) Harwell, D. E.; Mortimer, M. D.; Knobler, C. B.; Anet, F. A. L.; Hawthorne, M. F. *J. Am. Chem. Soc.* **1996**, *118*, 2679. (c) Tang, S. S.; Chang, C.-P.; Lin, I. J. B.; Liou, L.-S.; Wang, J.-C. *Inorg. Chem.* **1997**, *36*, 2294.

(3) (a) Schneider, W.; Bauer, A.; Schmidbaur, H. *Organometallics* **1996**, *15*, 5445. (b) Bishop, P., Marsh, P. A.; Brisdon, A. K.; Brisdon, B. J.; Mahon, M. F. *J. Chem. Soc., Dalton Trans.* **1998**, 675. (c) Jones, P. G.; Ahrens, B. *New J. Chem.* **1998**, *10*, 1041. (d) Tzeng, B.-C.; Schier, A.; Schmidbaur, H. *Inorg. Chem.* **1999**, *38*, 3978. (e) Ahrens, B.; Jones, P. G.; Fischer, A. K. *Eur. J. Inorg. Chem.* **1999**, 1103.

(4) (a) Sladek, A.; Angermaier, K.; Schmidbaur, H. *J. Chem. Soc., Chem. Commun.* **1996**, 1959. (b) Tzeng, B.-C.; Chan, C.-K.; Cheung, K.-K.; Che, C.-M.; Peng, S.-M. *J. Chem. Soc., Chem. Commun.* **1997**, 135.

(5) (a) Nakamoto, M.; Hiller, W.; Schmidbaur, H. *Chem. Ber.* **1993**, *126*, 605. (b) Fackler, J. P., Jr.; Staples, R. J.; Elduque, A.; Grant, T. *Acta Crystallogr., Sect. C* **1994**, *50*, 520.

(6) Schroter, I.; Strähle, J. *Chem. Ber.* **1991**, *124*, 2161.

(7) Bonasia, P. J.; Gindleberger, D. E.; Arnold, J. *Inorg. Chem.* **1993**, *32*, 5126.

(8) Wojnowski, W.; Becker, B.; Sassmannhausen, J.; Peters, E. M.; Peters, K.; Von Schnering, H. G. *Z. Anorg. Allg. Chem.* **1994**, *620*, 1417.

(9) Gold thiomalate, Na$_2$CsAu$_2$(L)(LH), where L = [O$_2$CCH$_2$CH(S)CO$_2$]$^{3-}$, although not strictly a homoleptic thiolate contains two interpenetrating −Au−S− helices in which the closest approach of pairs of Au atoms are 3.485(2) and 3.227(5) Å. See: Bau, R. *J. Am. Chem. Soc.* **1998**, *120*, 9380.

(10) (a) Mingos, D. M. P.; Yau, J.; Menzer, S.; Williams, D. J. *Angew. Chem., Int. Ed. Engl.* **1995**, *34*, 1894. (b) McArdle, C. P. Irwin, M. J.; Jennings, M. C.; Puddephatt, R. J. *Angew. Chem., Int. Ed.* **1999**, *38*, 3376.

(11) Complexes **1** and **2** were prepared in a two-phase reaction between aqueous [AuCl(EtSC$_2$H$_4$OH)] and the appropriate *tert*-butylthiophenol dissolved in xylene. Procedural details and analytical data are contained in the Supporting Information.

(12) Crystals of **1**·[0.8(C$_8$ H$_{10}$ O)] from ethoxybenzene are triclinic (*P*-1) with a = 16.641(3) Å, b = 17.274(4) Å, c = 22.703(6) Å, α = 109.45(2)°, β = 93.40(2)°, γ = 93.41(2)°, V = 6121.1(24) Å^3, D_c = 2.018 gcm^{-3}, Z = 2. Details are available in the Supporting Information.

(13) Crystals of **2** from xylene are monoclinic ($P2_1/n$), a = 18.108(2) Å, b = 26.621(6) Å, c = 30.256(4) Å, β = 99.10(3)°, V = 14401.3(41) Å^3, D_c = 2.117 gcm^{-3}, Z = 4. Details are available in the Supporting Information.

(14) Al−Sa'ady, A. K. H.; Moss, K.; McAuliffe, C. A.; Parish, R. V. *J. Chem. Soc., Dalton Trans.* **1984**, 1609.

10.1021/ja0011156 CCC: $19.00
Published on Web 12/02/2000

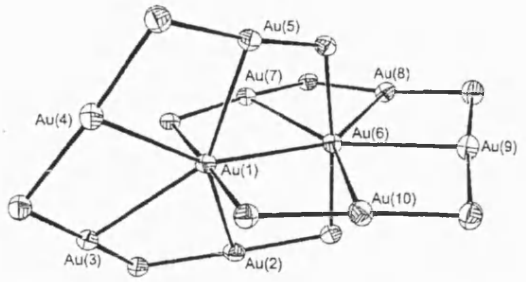

Figure 2. The $Au_{10}S_{10}$ core of **1** showing the two interpenetrating Au_5S_5 pentagons and all Au···Au interactions less than 3.15 Å.

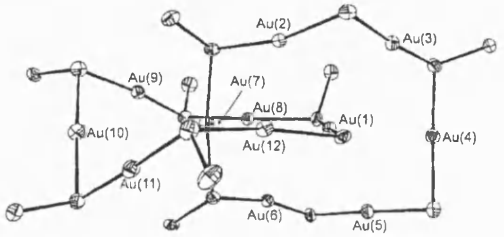

Figure 3. The $Au_{12}S_{12}$ core of **2** showing only eight alpha C atoms of the phenyl rings for clarity. Ranges of bond lengths and angles are: Au–S, 2.287(6)–2.435(5); S–C, 1.779(13)–1.819(12) Å; Au–S–Au, 88.0(2)–108.1(2); S–Au–S, 162.8(2)–178.2(2)°.

Table 1. Au···Au Separations in **1** and **2** less than 3.32 Å

compound **1**		compound **2**	
Au–Au	/Å	Au–Au	/Å
1–2	2.97	1–3	3.25
1–3	3.03	1–4	3.20
1–4	3.12	1–5	3.27
1–5	2.98	1–6	3.19
6–1	3.05	2–3	3.30
6–7	3.10	2–12	3.16
6–8	3.12	4–5	3.28
6–9	3.05	5–6	3.21
6–10	3.05	6–8	3.21
		7–8	3.22
		7–12	3.21
		10–11	3.19

consideration of the structural parameters found in many other thiolates.[15] The normal linear coordination about Au atoms combined with Au–S separations of 2.30 Å and an angular Au–S–Au arrangement averaging 105° defines a planar pentagon of side 4.6 Å. These geometric constraints maximize the number of stabilizing Au···Au contacts possible for an in-plane Au located at the center of the ring and impose a value of 3.0 Å for each Au···Au "spoke" in the pentagonal cartwheel.

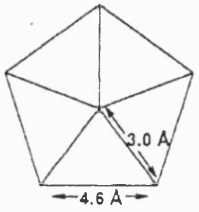

The central core of **2** can also be described as a [2]catenane, but neither of the two interpenetrating hexagons, each defined by a total of 12 alternating S and Au atoms, is planar. The near linear S–Au–S arrangement with Au–S separations in the range 2.287(6)–2.325(5) (average 2.30 Å) persists in both hexagonal units, but Au···Au contacts between the central gold atoms in each ring, Au(1) and Au(7), and those on the periphery vary widely (3.19–3.69 Å), and as such are in the same range as Au···Au contacts between gold atoms around the periphery. Buckling in the second ring permits just two relatively short transannular Au···Au contacts [Au(2)···Au(12), 3.16; Au(6)···Au(8), 3.21 Å]. All Au···Au contacts less than twice the Bondi van der Waals radius of gold[16] are listed in Table 1. It is evident from packing considerations that the bulky *tert*-butyl substituent in the ortho position of the arene ring prevents the formation of a structural analogue of **1**. There are no secondary Au···S interactions of significance in either **1** or **2**.

The weakness of a single aurophilic interaction generally results in its complete disruption on dissolution, but occasionally an equilibrium is observed between associated and dissociated species.[17] The room-temperature proton NMR spectrum of **1** in noncoordinating organic solvents contains three sets of methyl and aromatic resonances in the ratio 1:2:2. This is in keeping with the inequivalence of the ligands on the periphery of interlinked pentagons as in the core of the solid. At low temperatures line broadening is followed by band splitting at −90 °C as ligand motion is restricted. We have confirmed previous findings[14] that at elevated temperatures single sets of methyl and aromatic resonances are observed, but we have been unable to determine whether the core remains intact under these conditions. Preliminary mass spectral studies using low resolution FAB revealed a complex fragmentation pattern in which $[Au_xS_y(SC_6H_4\text{-}p\text{-}CMe_3)_z)]^+$ species, $x = 5$ or 6, $y = 0–2$, $z = 5$ predominate, but which also includes higher cluster species including $[Au_{11}S_2(SC_6H_4\text{-}p\text{-}CMe_3)_9]^+$. The proton NMR spectrum of **2** is far more complex than that of **1**, and it is both temperature- and solvent-dependent, with evidence of more than one species being present in solution at ambient temperatures.

Complete dissociation of both **1** and **2** is readily effected by chemical reactions involving soft donors. Thus, in the presence of triphenylphosphine **1** forms $[Au(PPh_3)SC_6H_4\text{-}p\text{-}CMe_3]$, **3**, in almost quantitative yield. According to X-ray crystallography[18] the individual molecules have the normal quasi-linear coordination at gold with a Au–S–C bond angle of 106.6(2)°. There are no short intermolecular Au···Au or Au···S contacts present.

In summary, the electronic and structural preferences evident in many coordination complexes of Au(I) are perfectly combined in the [2]catenane structure found for the $Au_{10}S_{10}$ core of **1**. Unlike [2]catenanes which have been the subject of much recent interest[19] and are either entirely or largely organic based, there is a unique "spoke" system in both rings of **1** consisting of a total of nine Au···Au interactions which imparts structural stability.

Acknowledgment. We thank the Engineering and Physical Sciences Research Council (EPSRC) for support. We also wish to acknowledge the use of the EPSRC's National Mass Spectrometry and Chemical Database Services at Swansea and Daresbury, UK, respectively.

Supporting Information Available: Synthetic and analytical data on compounds **1** and **2**. Tables of crystallographic data including diffractometer data and refinement data, final coordinates, bond lengths, bond angles, and anisotropic displacement parameters for molecular species **1** and **2** (PDF). This material is available free of charge via the Internet at http://pubs.acs.org.

JA0011156

(15) A survey of entries in EPSRC's Chemical Database revealed an average Au–S–Au bond angle of 91° for Au(I)–thiolate derivatives containing the Au–S–Au linkage and 95° (range 105.4–82.9°) for the same angle in homoleptic Au(I)–thiolates. See The United Kingdom Chemical Database Service, Fletcher, D. A.; McMeeking, R. F.; Parkin, D. *Chem. Inf. Comput. Sci.* **1996**, *36*, 746

(16) Bondi, A. *J. Phys. Chem.* **1964**, *68*, 441

(17) Narayanaswamy, R.; Young, M. A.; Parkhurst, E.; Oullette, M.; Kerr, M. E.; Ho, D. M.; Elder, R. C.; Bruce, A. E.; Bruce, M. R. M. *Inorg. Chem.* **1993**, *32*, 2506.

(18) Crystals of **3** from xylene/acetonitrile are triclinic ($P\text{-}1$), $a = 8.353(2)$ Å, $b = 11.969(3)$ Å, $c = 13.582(4)$ Å, $\alpha = 109.82(2)°$, $\beta = 103.50(2)°$, $\gamma = 93.43(2)°$, $V = 1227.7(6)$ Å^3, $D_c = 1.689$ gcm^{-3}, $Z = 2$. Full details of the structure will be published elsewhere.

(19) Stoddart, J. F.; Raymo, F. M. *Chem. Rev.* **1999**, *99*, 1643.; Fujita, M. *Acc. Chem. Res.* **1999**, *32*, 53.; Fujita, M.; Ogura, K. *Coord. Chem. Rev.* **1996**, *148*, 249.

CHEMISTRY

Fine Golden Rings

Catenanes are interlinked molecular rings. They are usually fully or mostly organic, and sophisticated versions may have future applications in molecular electronics. Gold-based catenanes have been reported, but in those structures the gold atoms were linked with organic bridges; direct gold-gold interactions were not significant. Wiseman *et al.* have synthesized unusual catenanes that have fully inorganic rings made of alternating gold and sulfur atoms, a ten-membered ring in one case and twelve in another. A large organic ligand is attached to each of the sulfur atoms. Weak gold-gold interactions, both between atoms in the same ring and between atoms in different rings, contribute to stabilization of the catenanes. — JU

J. Am. Chem. Soc., in press.

Fine Gold Rings: G. Chin (editor), **Editors' Choice**, *Science Magazine,* **290**, 2213 (2000)